Exploring the regeneration potential of salivary glands using organoids as a model

Rocchi, Cecilia

DOI:
10.33612/diss.168896082

Exploring the Regeneration Potential of Salivary Glands using Organoids as a Model

Cecilia Rocchi

Rocchi, C.

Exploring the Regeneration Potential of Salivary Glands using Organoids as a Model

PhD dissertation, University of Groningen, The Netherlands

Cover Design: Emily Fong.
www.emilyfongstudio.com

Printed by Ipskamp Printing, Enschede, The Netherlands (www.ipskampprinting.nl)

university of groningen

Exploring the regeneration potential of salivary glands using organoids as a model

PhD thesis

to obtain the degree of PhD at the
University of Groningen
on the authority of the
Rector Magnificus Prof. C. Wijmenga
and in accordance with
the decision by the College of Deans.

This thesis will be defended in public on

Wednesday 26 May 2021 at 14.30 hours

by

Cecilia Rocchi

born on 29 July 1985
in Reggio Emilia, Italy

Supervisor
Prof. R.P. Coppes

Co-supervisors
Dr. R.P. van Os
Dr. L. Barazzuol

Assessment Committee
Prof. G. de Haan
Prof. C. Ovitt
Prof. M. Verheij

Alla mia mamma e al mio papà

Paranymphs

Peter Nagle
Marianne van der Zwaag

TABLE OF CONTENTS

CHAPTER 1

GENERAL INTRODUCTION & OUTLINE OF THE THESIS

GENERAL INTRODUCTION AND OUTLINE OF THE THESIS

Salivary gland dysfunction occurs when a large number of acinar cells, the functional secretory units of the gland, have been irreversibly damaged. This may occur as consequence of radiotherapy treatment (RT) for head and neck cancer and can be further aggravated by radiation-induced alterations of the tissue environment, such as disruption of the parasympathetic innervation[1,2], senescence[3,4] changes in extracellular matrix composition[5-7] and a depletion of potential stem/progenitor cells[8]. The progressive decline of the salivary gland epithelium, due to the often unavoidable inclusion of the salivary gland within the irradiation field, leaves 40% of head and neck cancer survivors facing the challenges of the significant morbidities of radiation treatment, including irreversible hyposalivation, that will lead to the onset of xerostomia, which drastically decreases their quality of life[9].

Although several clinical studies have provided evidence that partial recovery of saliva production can occur in patients treated with intensity-modulated radiation therapy (IMRT)[10], indicative of the potential for endogenous tissue repair following RT, the mechanisms behind adult salivary gland regeneration potential are still unknown. Recent retrospective studies have shown that while healthy human acinar cells are able to divide and act as a cell source for the slow turnover maintenance of the secretory unit, radiation treatment drastically reduces this source of cell replacement[11], indicating that other cell types might be responsible for the regeneration of the damaged gland. The currently limited knowledge of the extrinsic and intrinsic factors that regulate salivary gland homeostasis and regeneration after damage has so far curtailed the application into the clinic of regenerative strategies, such as reactivation of endogenous repair programs or transplantation of stem/progenitor cells to replace the lost tissue. Therefore, the majority of currently available treatments are primarily palliative solutions, such as saliva substitutes, which aim to temporarily alleviate the discomfort of the symptoms[12].

Adult organs, including the salivary glands, maintain their function through the ability of resident adult stem/progenitor-like cells to preserve a correct balance between self-renewal and differentiation. While fast turnover tissues, such as intestine, skin and hair follicles, rely on the homeostatic activity of their resident stem cells, facilitating significant advances in understanding their renewal potential, slow turnover tissues, such as salivary glands, primarily rely on the activity of tissue resident stem-like cells upon injury. This makes the identification of the intrinsic and extrinsic factors involved in the regeneration processes within slow turnover tissues more challenging and leaving no consensus within the field as to the nature of the key players[13].

Over the past 10-15 years, the use of conditional and inducible lineage tracing mouse models opened up the possibility to temporally control the expression of putative molecular switches

within the salivary gland epithelium. This strategy allowed researchers to map cell fate as well as to compare cell expression patterns during homeostasis and regeneration. Recent work has defined that while lineage restricted progenitor cells seem to be the cellular source involved in the maintenance of the different salivary gland compartments during homeostasis[1,14,15], plasticity mechanisms, more than a dedicated stem cell population seems to be involved in salivary gland regeneration in a context-specific manner[16,17].

While mouse *in vivo* experiments have helped to elucidate cell dynamics during salivary gland homeostasis and regeneration, and shed light on several progenitor populations within the mouse salivary gland[1,14,15], their limited translational potential to humans[18] has raised the need for new approaches to study regeneration processes in human salivary glands. Therefore, to understand the dynamics of human salivary gland stem/progenitor cells during homeostasis and regeneration, it is necessary to use strategies that will allow characterization and test functionality of adult salivary gland stem cells, and eventually allow for the quantitative analysis of the contribution of each cell type to the regeneration of damaged tissue (and homeostasis).

The establishment of adult stem cell-based organoids has allowed the modelling of regenerative processes for several organs[19] including salivary glands[18,20,21]. Organoids are defined as 3D structures derived from adult tissues stem cells, iPSCs or ESCs capable of self-renewal and self-organization through cell sorting and spatially restricted lineage commitment, and have features resembling the counterpart *in vivo* tissue[22,23]. The ability to generate salivary gland organoids depends on the isolated population of cells and on the niche factors that allow on one hand to keep cells in their stem-like state, and on the other hand drive differentiation of progenitor-like cells into specialized salivary gland secretory cells.

The work described in this thesis uses organoid systems as a regenerative model to investigate mouse and human salivary gland stem/progenitor-like cells as well as the niche signaling pathways that might be involved in controlling cell fate and explores their potential use for autologous transplantation in patients suffering from RT-induced hyposalivation.

Chapter 2: reviews the literature focusing on how recent advances in stem cells biology and changes in adult stem cell definition have influenced salivary gland biology defining a new regenerative landscape.

Chapter 3: discusses the complexity of the salivary gland stem cell niche focusing on elucidating the effect of the Wnt/B catenin signaling pathway on the regenerative potential of salivary gland stem/progenitor cells. It also introduces the uses of organoids to dissect/manipulate the salivary gland niche, as well as new parameters to evaluate functionality of stem/progenitor cells and their potential use in regenerative therapies.

Chapter 4: provides evidence that Yes-Associated-Protein (YAP) acts as a sensor of tissue integrity during salivary gland regeneration thereby regulating stem cell self-renewal both in

mouse and human-derived salivary gland cells. It also introduces a potential YAP activation-based pharmacological strategy to improve the radiation response of human salivary gland-derived cells that if validated in an *in vivo* system could open up new treatment opportunities to rescue the radiation-induced hyposalivation phenotype.

Chapter 5: demonstrates that perturbation of salivary gland homeostasis leads to changes in the basal autophagy flux and it describes how the dynamic of these changes varies between the different compartments of the gland. Finally, it demonstrates that a constant fuel of the autophagy machinery is necessary to maintain the self-renewal ability of salivary gland-derived cells.

Chapter 6: describes the application of a gene network co-expression framework on stem-like cell-enriched and differentiated human salivary gland-derived organoid cultures to obtain a "holistic view" of the molecular mechanisms that might drive salivary gland regeneration. Probing the transcriptomic landscape of salivary gland organoids identified potential novel mechanisms of salivary gland renewal.

Chapter 7: describes the development of a GMP-compliant protocol that allows the isolation and expansion of human-derived salivary gland cells. Furthermore, it demonstrates the safety and feasibility of the first organoid-based cell therapy to potentially rescue radiation-induced hyposalivation in head and neck cancer patients.

Chapter 8: summarizes the findings of this thesis, puts them in a general perspective and discusses their potential impact in basic stem cell research and ultimately the translation towards the development of a therapeutic intervention for radiation-induced hyposalivation

REFERENCES

1 Emmerson, E., May, A. J., Berthoin, L., Cruz-Pacheco, N., Nathan, S., Mattingly, A. J. *et al.* Salivary glands regenerate after radiation injury through SOX2-mediated secretory cell replacement. *EMBO Mol Med* **10**, doi:10.15252/emmm.201708051 (2018).

2 Emmerson, E., May, A. J., Nathan, S., Cruz-Pacheco, N., Lizama, C. O., Maliskova, L. *et al.* SOX2 regulates acinar cell development in the salivary gland. *Elife* **6**, doi:10.7554/eLife.26620 (2017).

3 Marmary, Y., Adar, R., Gaska, S., Wygoda, A., Maly, A., Cohen, J. *et al.* Radiation-Induced Loss of Salivary Gland Function Is Driven by Cellular Senescence and Prevented by IL6 Modulation. *Cancer Res* **76**, 1170-1180, doi:10.1158/0008-5472.CAN-15-1671 (2016).

4 Peng, X., Wu, Y., Brouwer, U., van Vliet, T., Wang, B., Demaria, M. *et al.* Cellular senescence contributes to radiation-induced hyposalivation by affecting the stem/progenitor cell niche. *Cell Death Dis* **11**, 854, doi:10.1038/s41419-020-03074-9 (2020).

5 Coppes, R. P., Zeilstra, L. J., Kampinga, H. H. & Konings, A. W. Early to late sparing of radiation damage to the parotid gland by adrenergic and muscarinic receptor agonists. *Br J Cancer* **85**, 1055-1063, doi:10.1054/bjoc.2001.2038 (2001).

6 Hakim, S. G., Ribbat, J., Berndt, A., Richter, P., Kosmehl, H., Benedek, G. A. *et al.* Expression of Wnt-1, TGF-beta and related cell-cell adhesion components following radiotherapy in salivary glands of patients with manifested radiogenic xerostomia. *Radiother Oncol* **101**, 93-99, doi:10.1016/j.radonc.2011.07.032 (2011).

7 Yarnold, J. & Brotons, M. C. Pathogenetic mechanisms in radiation fibrosis. *Radiother Oncol* **97**, 149-161, doi:10.1016/j.radonc.2010.09.002 (2010).

8 Vissink, A., van Luijk, P., Langendijk, J. A. & Coppes, R. P. Current ideas to reduce or salvage radiation damage to salivary glands. *Oral Dis* **21**, e1-10, doi:10.1111/odi.12222 (2015).

9 Tsai, W. L., Huang, T. L., Liao, K. C., Chuang, H. C., Lin, Y. T., Lee, T. F. *et al.* Impact of late toxicities on quality of life for survivors of nasopharyngeal carcinoma. *BMC Cancer* **14**, 856, doi:10.1186/1471-2407-14-856 (2014).

10 Gujral, D. M. & Nutting, C. M. Patterns of failure, treatment outcomes and late toxicities of head and neck cancer in the current era of IMRT. *Oral Oncol* **86**, 225-233, doi:10.1016/j.oraloncology.2018.09.011 (2018).

11 Luitje, M. E., Israel, A. K., Cummings, M. A., Giampoli, E. J., Allen, P. D., Newlands, S. D. *et al.* Long-Term Maintenance of Acinar Cells in Human Submandibular Glands After Radiation Therapy. *Int J Radiat Oncol Biol Phys*, doi:10.1016/j.ijrobp.2020.10.037 (2020).

12 Rocchi, C. & Emmerson, E. Mouth-Watering Results: Clinical Need, Current Approaches, and Future Directions for Salivary Gland Regeneration. *Trends Mol Med* **26**, 649-669, doi:10.1016/j.molmed.2020.03.009 (2020).

13 Rocchi, C., Barazzuol, L. & Coppes, R. P. The evolving definition of salivary gland stem cells. *NPJ Regen Med* **6**, 4, doi:10.1038/s41536-020-00115-x (2021).

14 Aure, M. H., Konieczny, S. F. & Ovitt, C. E. Salivary gland homeostasis is maintained through acinar cell self-duplication. *Dev Cell* **33**, 231-237, doi:10.1016/j.devcel.2015.02.013 (2015).

15 May, A. J., Cruz-Pacheco, N., Emmerson, E., Gaylord, E. A., Seidel, K., Nathan, S. *et al.* Diverse progenitor cells preserve salivary gland ductal architecture after radiation-induced damage. *Development* **145**, doi:10.1242/dev.166363 (2018).
16 Ninche, N., Kwak, M. & Ghazizadeh, S. Diverse epithelial cell populations contribute to the regeneration of secretory units in injured salivary glands. *Development* **147**, doi:10.1242/dev.192807 (2020).
17 Weng, P. L., Aure, M. H., Maruyama, T. & Ovitt, C. E. Limited Regeneration of Adult Salivary Glands after Severe Injury Involves Cellular Plasticity. *Cell Rep* **24**, 1464-1470 e1463, doi:10.1016/j.celrep.2018.07.016 (2018).
18 Pringle, S., Maimets, M., van der Zwaag, M., Stokman, M. A., van Gosliga, D., Zwart, E. *et al.* Human Salivary Gland Stem Cells Functionally Restore Radiation Damaged Salivary Glands. *Stem Cells* **34**, 640-652, doi:10.1002/stem.2278 (2016).
19 Huch, M. & Koo, B. K. Modeling mouse and human development using organoid cultures. *Development* **142**, 3113-3125, doi:10.1242/dev.118570 (2015).
20 Maimets, M., Rocchi, C., Bron, R., Pringle, S., Kuipers, J., Giepmans, B. N. *et al.* Long-Term In Vitro Expansion of Salivary Gland Stem Cells Driven by Wnt Signals. *Stem Cell Reports* **6**, 150-162, doi:10.1016/j.stemcr.2015.11.009 (2016).
21 Nanduri, L. S., Baanstra, M., Faber, H., Rocchi, C., Zwart, E., de Haan, G. *et al.* Purification and ex vivo expansion of fully functional salivary gland stem cells. *Stem Cell Reports* **3**, 957-964, doi:10.1016/j.stemcr.2014.09.015 (2014).
22 Clevers, H. Modeling Development and Disease with Organoids. *Cell* **165**, 1586-1597, doi:10.1016/j.cell.2016.05.082 (2016).
23 Lancaster, M. A. & Knoblich, J. A. Organogenesis in a dish: modeling development and disease using organoid technologies. *Science* **345**, 1247125, doi:10.1126/science.1247125 (2014).

CHAPTER 2

THE EVOLVING DEFINITION OF SALIVARY GLAND STEM CELLS

Rocchi C., Barazzuol L., Coppes RP.

Npj Nature Regenerative Medicine 2021;6(4)

ABSTRACT

Dysfunction of the salivary gland and irreversible hyposalivation are the main side-effects of radiotherapy treatment for head and neck cancer leading to a drastic decrease of the quality of life of the patients. Approaches aimed at regenerating damaged salivary glands have been proposed as means to provide long-term restoration of tissue function in affected patients. In studies to elucidate salivary gland regenerative mechanisms, more and more evidence suggests that salivary gland stem/progenitor cell behaviour, like many other adult tissues, does not follow that of the hard-wired professional stem cells of the hematopoietic system.

In this review, we provide evidence showing that several cell types within the salivary gland epithelium can serve as stem/progenitor-like cells. While these cell populations seem to function mostly as lineage-restricted progenitors during homeostasis, we indicate that upon damage specific plasticity mechanisms might be activated to take part in regeneration of the tissue. In light of these insights, we provide an overview of how recent developments in the adult stem cell research field are changing our thinking of the definition of salivary gland stem cells and their potential plasticity upon damage. These new perspectives may have important implications on the development of new therapeutic approaches to rescue radiation-induced hyposalivation.

INTRODUCTION

Adult salivary glands, like every other tissue and organ in our body, preserve their functionality by maintaining homeostasis, a balance between cell death and cell replacement, which is strictly regulated by adult resident stem/progenitor cells capable of self-renewal and differentiation into mature tissue lineages. Although the function of salivary glands is not a necessity for human survival, the dysfunction of this organ due to radiotherapy treatment of head and neck cancer, leads to long-lasting detrimental side effects. Such side-effects, which include difficulties swallowing (dysphagia), eating and speaking, an accelerated tooth decay and dental caries as well as an increase in fungal and bacterial infections of the oral cavity, can drastically reduce the quality of life of patients [1-4].

Consistent with the need for new therapeutic approaches that will provide long-term solutions to restore salivary gland function and together with the knowledge that radiotherapy treatment leads to a loss of regenerative potential [3,5], there has been an increased focus on identifying the stem/progenitor cell populations and the niche signaling pathways that regulate their behavior during tissue homeostasis and regeneration [6-9].

In this review, we address the challenge of identifying resident adult stem cells, as well as the role they play within the salivary gland during homeostasis and regeneration. Initially presenting salivary gland stem/progenitor cells within the context of the quiescent, multipotent "traditional" stem cell definition, we highlight questions within the field and provide evidence of how recent developments in the adult stem cell research field are changing the perception and quest for identifying salivary gland stem cells from a strictly phenotype-based approach to a more functional approach.

Classical stem cell definition: the hard-wired dogma of the hematopoietic stem cell as template for all other stem cells

Initial attempts to identify stem cells in a relative unexplored tissue, such as the salivary gland, have historically relied on the "stem cell dogma" based on the well characterized multipotent hematopoietic stem cell system (HSCs) [10]. The rarity, the quiescent state and the ability of HSCs to asymmetrically divide are characteristics that served as a template for all studies aiming to characterize adult stem cells in most mammalian tissues. These characteristics guarantee, on one hand, the "self-renewal and long-lived permanence" of the tissue, and on the other hand, ensure a unidirectional differentiation of well characterized progenitors along the hierarchical tree until final differentiation is reached [11,12].

However, can we apply this template based on the only non-solid fast turnover tissue in our body (the hematopoietic system) to solid tissues that differ in size, morphology, physiology, constitution, function and stressors to which they are exposed to during life? Starting from the HSC point of view, the simplest definition of a stem cell in adult mammalian tissue is a slow-

cycling cell that, under homeostatic conditions, limits the number of consecutive divisions to minimize DNA replication errors. In this view, the differentiated cells of a given tissue are derived from transient amplifying progenitors rather than directly from the “primitive” stem cells sitting at the apex of the hierarchical tree. Cells with a low proliferative activity are experimentally defined by the ability to retain chromatin labels, such as 3H-thymidine, Bromodeoxyuridine (BrdU) and histone-GFP fusion protein (H2B-GFP), for an extended period of time and are therefore termed label retaining cells (LRCs).

While retention of nuclear labels essentially defines the proliferative history of cells, studies based on long-term pulse-chase experiments and on the repair of radiation-induced damage in epidermis and intestine [13-15] showed that LRCs were spatially segregated in these tissues. This led to the proposal that cell cycle characteristics and spatial organization of these cells could describe their identities: slow cycling cells are stem cells (located in the basal layer, in a protected position) and fast cycling cells represent the transient amplifying cells that terminally differentiate after a finite number of divisions following a unidirectional stream starting from the basal layer [14,16,17]. Although the search for novel stem cells based on quiescence is complicated, also considering the fact that the majority of adult cells are not dividing, studies on LRCs (and therefore defining the quiescent state as a “stem cell trait”) were successfully applied in the quest to uncover adult stem cells in several tissues, such as the hair follicle [18], skin (reviewed in [19]), sweat glands [20,21], teeth [22], pancreas [23] and intestine [24].

Similar to liver, prostate and lung, the salivary gland belongs to a group of tissues in our bodies with a relatively slow turnover (>60 days) [25]. These tissues increase proliferation in response to damage, in order to replace the lost cells, to then go back to their low-level maintenance when homeostasis is restored.

The quest for salivary gland stem cells

Salivary glands are composed of two types of secretory acinar cells surrounded by myoepithelial cells that help the secretion of the mucous or serous fluid into the ductal network through which saliva reaches the oral cavity (Figure 1) [26-28].

During salivary gland homeostasis a single administration of 3H-thymidine labeled intercalated ducts and to a lower extent acinar cells and granulated ducts [29]. Over time the number of labeled intercalated ductal cells decreased, while the number of labeled acinar and granulated ductal cells increased, potentially identifying the intercalated ductal cells as candidates for transient amplifying (T/A) progenitor cells [29-31]. Although the intercalated duct seems to be recognized as the T/A compartment in salivary glands agreeing with the unidirectionality of the differentiation stream proposed based on the model of HSCs, the identity of the multipotent cell that occupies the apex of the salivary gland stem cell hierarchy tree remains unknown.

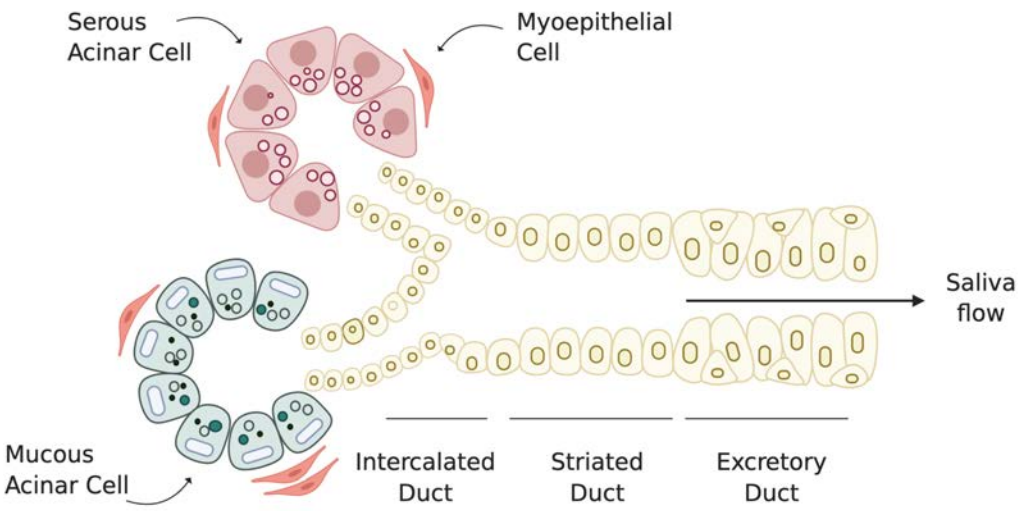

Figure 1 : Schematic representation of a generic salivary gland structure. The salivary gland epithelium is composed of two types of saliva producing cell types, serous acinar cells and mucous acinar cells. Myoepithelial cells surrounding the acinar unit aids the expulsion of saliva from acinar cells into the ductal network, composed of intercalated, striated and excretory ducts, through which saliva is modified and transported to the oral cavity. (Figure created with BioRender.com)

While LRC studies in adult salivary gland show a scattered distribution of LRCs throughout the parenchyma, and co-expression of putative salivary gland progenitor cell markers [32], these studies only focus on the gland in homeostatic situations and do not consider the limitations that arise using a label retaining approach. LRC studies are unable to discriminate between potential quiescent stem/progenitor cells and other cell types which are cycling slowly at the moment of the pulse or differentiated cells that have ceased dividing, and thus potentially generate false positives. In order to address the nature and regenerative potential of LRCs, a label retaining approach should be combined with an injury model to verify whether the number of LRCs stays the same or decreases; the percentage of proliferating LRCs and whether these proliferating LRCs (if present) contribute to salivary gland regeneration in a multipotent way, giving rise to both acinar and ductal cells. Currently, label retaining approaches applied to adult salivary glands, have resulted in being neither sensitive enough, nor specific enough [32], for the identification of salivary gland stem/progenitor cells and it is therefore not possible to conclude, based on their spatial localization and cycling characteristics, whether salivary gland LRCs are (or are not) stem cells.

The recent use of genetic lineage tracing models in salivary gland, have provided new insights into the nature and properties of adult tissue progenitor cells. Tracing of adult acinar cell markers or markers for acinar progenitors, such as Mist1, Pip and Sox2 revealed that homeostasis of the acinar compartment can be achieved via self-duplication of acinar cells or the replacement of mature acinar cells by immature acinar progenitor cells [33-35] without the contribution of a more primitive adult stem cell population. Keratin-14 (K14), Keratin-5 (K5) and

Kit all mark different cell types within the ductal compartment and act as lineage-restricted progenitors to maintain the ductal compartment during homeostasis [36-38].Moreover, lineage tracing for the myoepithelial marker Acta2 (alpha-smooth muscle actin) proves that myoepithelial cells are maintained through self-duplication [36]. In contrast to adult homeostasis, stem/progenitor cells identified during embryonic development are more multipotent and less lineage restricted. For example, K5 and Sox2 are co-expressed throughout cells of the oral epithelium prior to salivary gland development [39] and mark a population of cells that give rise to all epithelial cells of the submandibular and the sublingual glands [40,41]. However, this multipotent cell population becomes restricted to cells of the ductal and acinar lineages, respectively, as development progresses [34,36]. This evidence points to the transition from a multipotent state during development to distinct, unipotent salivary gland proliferative units (SPUs) in adulthood, that provide lineage-restricted support to their compartment of origin in homeostatic conditions (Figure 2). In contrast to HSCs, these cells are relatively abundant, they are not quiescent, they mostly seem to divide symmetrically and their persistence in the tissue is subjected to stochastic events. Therefore, when comparing salivary gland stem/progenitor cells to the paradigm of the HSCs, we have to face the reality that so far, we do not know where or, more importantly, if a multipotent "professional" quiescent stem cell exists within the salivary glands. Could it then be, that salivary glands do not contain such stem cell types, but rely entirely on the proliferative capacity of the three main differentiated cell types: acinar, ductal and myoepithelial cells, and could this be explained by the tissue's development?

Tissues with a fast turnover, such as epidermis or intestine, contain cells with a lifetime of days or weeks, and while they are more easily exposed to insult because of their proximity to the external environment, their natural morphology allows a fast disposal route of cell debris: a direct interface with the outside world [42]. Lineage tracing studies and statistical analysis in fast turnover tissues, such as the testis [43], intestine [44,45], esophagus [46] and glandular stomach [47], revealed that each of these tissues are devoid of slow cycling stem cells, which are central to the dogma of the HSCs. In contrast, they appear to possess a pool of equipotent proliferating stem-like cells (clones), which are capable of giving rise to all differentiated cell lineages in the tissue. All these equally potent stem-like cells compete with each other for niche space and their long-term permanence in the niche will depend solely on stochastic events [48,49], similar to what is described as the neutral theory of molecular evolution in population genetics [50]. In adult tissues, the heterogeneity of the niche structures, the niche size, and the variety and spatial distribution of the signals released from the niche in relation to stem-like cell location, could drive stochastic cell fate decisions. Hence, following a neutral drift dynamic, only certain clones persist in the niche. All other clones are displaced and pushed away from stem cell promoting factors by their actively dividing neighbors, are exposed to differentiation factors and ultimately

are cleared into the external environment [45,49,51,52] (Figure 3A). This continuous process of rapid division and disposal of unwanted/used or damaged cells mostly by cell extrusion shapes these tissues, constantly maintaining the appropriate balance for a correct tissue homeostasis [53].

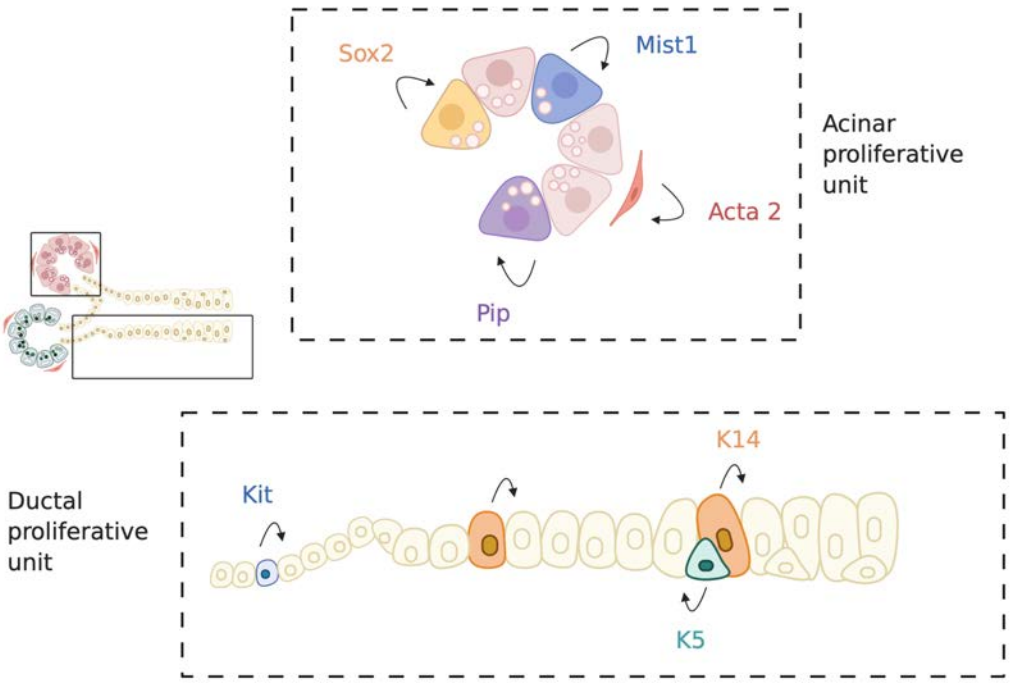

Figure 2: Salivary gland homeostasis seems to be achieved via self-duplication of lineage-restricted progenitor cells. Salivary glands are suggested to be structured in salivary gland proliferative units (SPUs), respectively the acinar and the ductal proliferative units. Each unit contains multiple lineage-restricted progenitor cells which, under normal homeostatic conditions, are able to self-duplicate and replace the lost cells within the unit. (Figure created with BioRender.com)

On the other hand, when tissues with a slow turnover, such as the salivary gland, liver, lung or prostate, are considered, one could hypothesise that the cellular density of these tissues, the heterogeneity of the epithelial composition throughout the tissue, as well as the absence of a direct external environmental interface, could evolutionarily explain the potential "absence" of a single and spatially segregated, quiescent multipotent stem cell population, as well as the presence of multiple populations of proliferative stem/progenitor-like cells, in these tissues. While a quiescent multipotent stem cell population spatially segregated in the tissue (for example in the basal layer of the main excretory ducts) may result in an inefficient short-term regeneration strategy due to the physical distance imposed by the branched morphogenesis of the tissue, other strategies such as plasticity of differentiated cells could account for rapid tissue repair [54]. The absence of a direct disposal route could be the reason why these slow turnover organs invested in a long-term maintenance approach, where the balance between new cells and the clearance of senescent cells and cellular debris could potentially require more sophisticated routes, like resident macrophages [55]. This could involve for example

efferocytosis, potentially performed by tissue resident “professional” (macrophages, dendritic cells) or “non-professional” (epithelial cells) phagocytes, or autophagy [56] (Figure 3B).

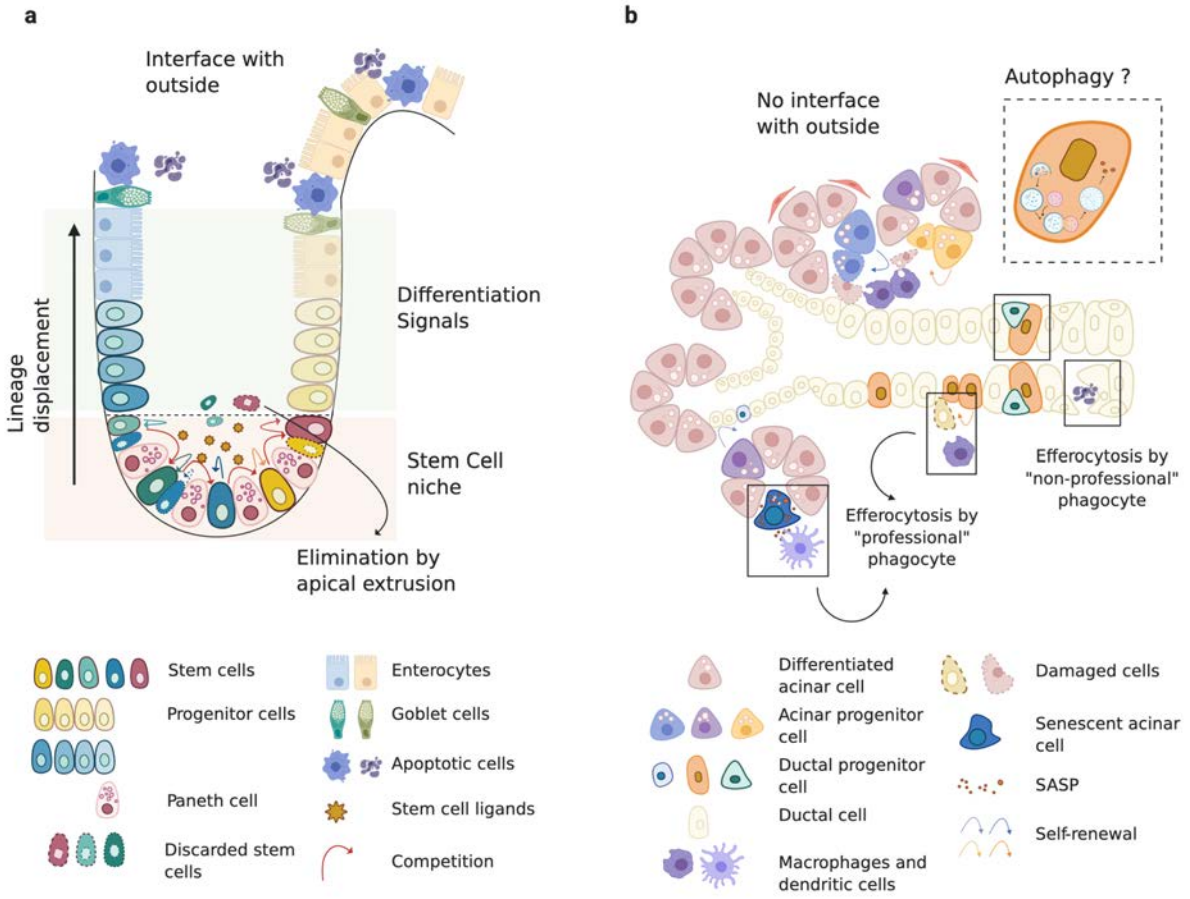

Figure 3: Tissue anatomy and niche size determine the regenerative strategy adopted by different tissues. Adult stem cells in fast turnover epithelial tissues, such as the intestine (A), are subjected to neutral competition for limited stem cell promoting factors and niche space. Only cells that have the capacity to receive stem cell promoting factors will remain stem cells, the others will be eliminated by extrusion from the niche or via lineage displacement in the outer space. In a slow turnover tissue, such as the salivary gland (B), the high cellular density, as well as the branching structure, of the tissue could explain the absence of a “professional” stem-like cell and explain instead the presence of lineage-restricted progenitors. The absence of a direct opening for disposal of damaged/unwanted cells could force salivary glands to use alternative slower clearance routes, such as autophagy or tissue resident immune cells. (Figure created with BioRender.com.)

Regenerative cells: "the usual suspects" or "shape-shifters"?

Despite its slow turnover and the current lack of proof for the existence of a multipotent stem cell, studies on salivary gland damage have revealed a great regenerative potential of the gland, which varies depending on the type of damage inflicted. Upon ligation of the main salivary gland excretory duct, the acinar parenchyma is drastically reduced [33]. Lineage tracing studies revealed that, following removal of the ligation, the few remaining acinar cells in the damaged gland, re-enter the cell cycle and begin cell division without de-differentiating to a stem-like state, and subsequently drive regeneration of the gland. Within 7 to 14 days the acinar tissue of the gland is completely restored [33]. While mild and reversible damage to the gland, such as the described ligation-induce damage, appear to be rescued in a lineage-restricted manner, an alternative repair mechanism seems to come into play when broader stressors, such as radiation, irreversibly damage the whole salivary gland parenchyma.

Despite the beneficial effect of targeted tumor treatment, radiotherapy for head and neck cancers, often inflicts damage to the surrounding healthy salivary gland tissue (which is often unavoidably included in the irradiation field) causing severe complications for surviving patients [57] . Analysis of clinical data to investigate the dose-volume response in salivary gland function revealed that up to 40 Gy fractionated radiation (tumor dose 60-75 Gy in 1.8-2.0 Gy fractions five days a week, over 5-7 weeks) salivary glands may maintain a partial regenerative capability [58-61]. While it is important to take the dose, the volume and the effect of a single dose compared to a fractionated radiation schedule into consideration when looking at a regenerative response, murine models have been widely used to study and describe the kinetics of the salivary gland radiation-damage response [62]. A single dose of 15 Gy of X-rays, delivered locally to the glands, induces a slow and progressive decline of the acinar cell unit that culminates 90 days post local rat salivary gland irradiation [60,63] and seems to resemble best the clinical dose response [64]. Recent lineage tracing studies in mice indicated that at 30 days following doses of 10 -15 Gy γ-rays irradiation, when little acinar cell loss has occurred, acinar and ductal cells activate "a first regeneration response", similar to the one described for ligation-induced damage, which can be described as a lineage-restricted regeneration response: acinar cells give rise to acinar cells [34], while ductal cells remain restricted to replacing ductal cells [36,65]. This phase can be described as a "mild-damage phase", considering that the parenchyma of the gland is still intact [63]. The question remains as to what extent this specific "first regenerative response" occurs after higher doses when fewer remaining cells are capable of division. The subsequent 60 days can be described instead as a "severe-damage phase": only a few clusters of isolated acinar cells are present in the gland, while no major changes are evident in the ductal compartment [66]. Upon such conditions, Weng et al [65] provided proof for an *in vivo* response involving ductal cell plasticity. By tracing the lineage of two distinct ductal cell populations (expressing K5 and Axin2; shown in Figure 4 A, B), they

demonstrated that 90 days post 15 Gy γ-ray irradiation ductal cells rather than “a professional” stem cell population were responsible for a “second regeneration response” attempting to replace the severely compromised acinar cell compartment. Recent fate-mapping analysis upon unilateral ligation of the main excretory duct showed a remarkable plasticity of the ductal ($K14^+$ and $cKit^+$) and myoepithelial cells (SMA^+) to replenish the lost secretory acinar compartment. While $K14^+$ cells activate a multipotency program able to give rise to both acinar and ductal cell lineages, the main contribution to acinar cell replacement seems to take place via dedifferentiation of both myoepithelial cells and $cKit^+$ cells into a common bipotent progenitor cell that gives rise to $cKit^+$ cells and differentiate into acinar secretory cells [67] (Figure 4B). Recent studies revealed that it is not only ductal cells which can acquire a multipotent stem-like state, but also acinar cells have been suggested to respond to ligation-induced injury by undergoing acinar-to-ductal metaplasia [68]. Similar to the response known to be required for the survival of pancreatic acinar cells subjected to stress [69]. It would be of interest to address if, like pancreatic acinar cells, also salivary gland acinar cells possess a “protective plasticity”, the ability to re-acquire the secretory phenotype once the damage is resolved [68,69] (Figure 4B). While there have been only a few studies that reported the plasticity of the salivary gland epithelium during *in vivo* regeneration, which seems to be dependent on the type and severity of injury, radiation or ligation, this phenomenon can be recapitulated *in vitro*. Clonal organoids derived from single cell-sorted salivary gland ductal epithelial cells ($EpCAM^+$, Epithelial Cell Adhesion Molecule marker, or $CD24^+/CD29^+$) exhibit the capacity to proliferate and give rise to organoids containing the three major cell types present in the salivary gland when cultured in Matrigel® [8,70]. The ability of these, thought to be post-mitotic fate-restricted, cells to re-enter the cell cycle is an indication that with the appropriate signaling factors they can acquire the potential to revert to a multipotent stem-like cell state. While lineage tracing studies would be needed to confirm *in vitro* (and *in vivo*) plasticity mechanisms of $EpCAM^+$ cells, we could speculate that plasticity of these cells could occur via the activation of a “revival” cell [71], a rare, non-regenerative cell during homeostasis that upon damage can activate a transient expansion program to reconstitute the progenitor/multipotent cell pool responsible for the generation of the salivary gland lineages, similar to the transdifferentiation process recently described for SMA+ and cKit+ cells [67].

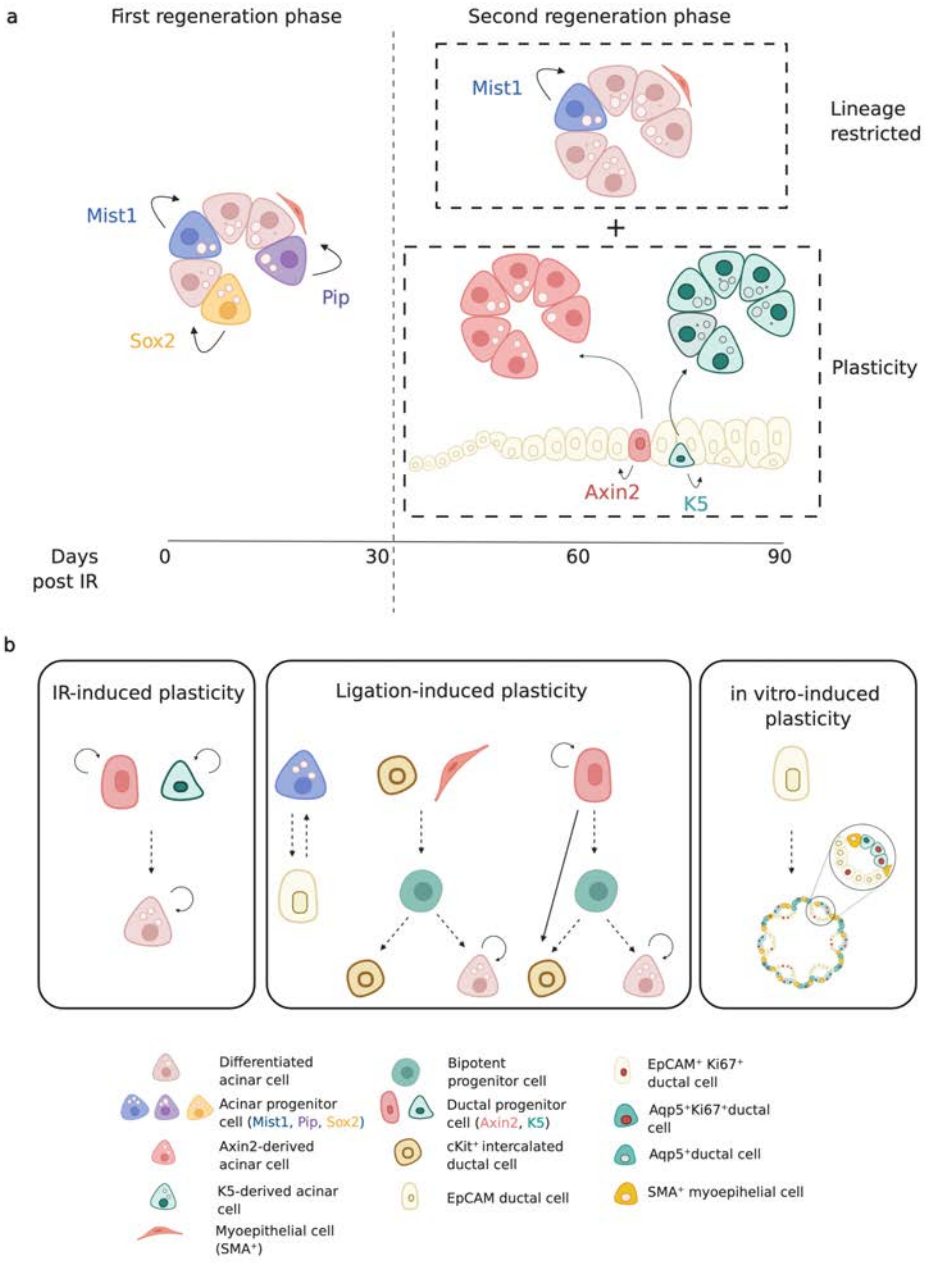

Figure 4: Mechanisms of plasticity after damage in salivary glands. (A) Salivary gland regeneration phases after radiation-induced damage. Upon radiation-damage a first regeneration phase seems to be characterized by a lineage-restricted response defined by the self-duplication ability of acinar cells (Mist1 and Pip) into acinar cells as well as the replacement of acinar cells driven by immature acinar progenitor-like cells (Sox2), that within the first 30 days post-irradiation are able to maintain the integrity of the acinar cell compartment. The second regeneration phase, marked by an extensive loss of acinar cells, seems to rely on the plasticity properties of the ductal cells (Axin2 and K5) that are able to give rise to new acinar cells. (B) In the context of tissue damage, salivary gland progenitor cells exhibit plasticity. Depending on the type of injury inflicted, salivary gland cells show different damage-induced plasticity: irradiation-induced plasticity; ligation-induced plasticity and *in vitro* induced plasticity (giving rise to an organized 3D system formed by different cell types named organoid). (Figure created with BioRender.com)

Salivary gland organoids and niche signaling

The development of salivary organoid cultures has increased the knowledge of how to control and characterize the behavior of salivary gland-derived cells, such as the ability to proliferate and to differentiate into distinct lineages in terms of marker expression and at a molecular level [8,70]. The optimization of culture conditions [8] and the 3D support of an extracellular matrix [70], as well as an increased effort to reproduce *in vitro* the biochemical signals produced by the native microenvironment [72], contributed to their huge expansion potential that has opened up the possibility for using salivary gland-derived organoids as a source for cell therapies. Transplantation of salivary gland organoid-derived cells into irradiated murine salivary gland resulted in engraftment, viability, and long-term survival of the transplanted cells into the host. Selection, expansion and transplantation of salivary gland stem/progenitor cells based on molecular markers taken from well characterized stem cell systems, such as that of the mammary gland (CD24/CD29)[73], indicated their ability to rescue the irradiation-induced hyposalivation up to 50% compared to non-transplanted irradiated animals [70]. In salivary gland the CD24 and CD29 markers label all the ductal cells in the gland, although with different expression intensities between cells [70], raising the possibility that a population of cells with stem-like characteristics could be hidden under the umbrella of a mature lineage.

While the niche signaling that regulates homeostasis in the adult gland remains poorly understood, lineage tracing studies of Axin2-Cre Wnt-responsive cells have shown restricted Wnt activity in the ductal compartment [65]. Moreover, basal EpCAM+ ductal cells co-express nuclear β-catenin, an intracellular signal transducer in the Wnt signaling pathway, most abundantly in the excretory ducts [8]. Organoid culturing of EpCAM+ ductal cells showed an unprecedented expansion and multipotent potential upon Wnt3a and R-spondin stimulation. Wnt-derived organoids facilitated the engraftment and repopulation of irradiated salivary glands upon transplantation and restored 80% of the saliva secretion [8]. Contrary to the long-standing belief that we should be searching for stem cells based on the phenotypic identity of the cells, recovery in saliva production obtained with unselected Wnt-stimulated cells suggests that we should look at the functionality of the cells in terms of their ability to replace damaged tissue instead of surface markers [74]. It could be possible that rather than the identity of the cells transplanted, the signals they are exposed to are responsible for their *in vitro* and *in vivo* regenerative potential. Alternatively, it has been suggested that, beside the niche signalling the cells are exposed to and that are responsible for their activation, transplanted activated cells could be a potential source of paracrine factors [75-77] , such as cytokines, growth factors, or extracellular vesicles, that could contribute indirectly to the final therapeutic benefit of cell transplantation [78].Taken together these findings showed that as the stem cell field evolves, dogmas and definitions are becoming outdated and most mammalian adult tissues, including the salivary glands, do not follow the traditional HSC paradigm. Instead, it seems that they

display more plasticity that was previously believed, with the response of the tissue depending on the type and intensity of the damage.

Future directions and therapeutic perspectives

While in fast turnover tissues, such as the intestine, stem cell function can be distributed over a large population of cycling cells that compete for niche space, slow turnover epithelial tissues appear to adopt a different repair strategy. In the salivary glands as well as in the pancreas [79-81] and liver [82], stem cell function may be executed through the plasticity of previously thought to be terminally differentiated cells. Plasticity in the salivary gland could involve a switch in cellular identity from one differentiated cell to another type of differentiated cell as described upon ligation injury. Alternatively, it could be executed by "revival" cells, being rare terminally differentiated cells activated upon injury that are able to replace the progenitor cell pool responsible for the regeneration of the damaged tissue. This is suggested to occur in the second regeneration phase of irradiated salivary gland, upon unilateral ligation of the main duct and potentially during organoid culture, similarly to what has been observed in the liver and intestine [71,82]. A change in stem cell definition and the phenomenon of plasticity, bring questions regarding the meaning of what is always referred as terminal differentiation. What was once described as a unidirectional process along a hierarchical tree towards a final state, appears now as a dynamic process where several steps along the route may be reversible. Every nucleated cell in our body possesses the same genetic information and therefore the potential to change phenotype. Could we then argue that more than nature, here meant to be a fixed set of genes or specific surface markers, it is nurture that will define the state of cells with regards to their ability to execute stem cell function, and replenish lost or damaged tissue? How should we then characterize the regeneration process of an adult tissue, such as the salivary glands, where the stem cell hierarchy is unknown and where plasticity more than phenotypic characteristics could be responsible?

In vivo lineage tracing studies have so far shed some light on salivary gland cell fate decisions during homeostasis and regeneration in model organisms such as mice. However, these types of genetic manipulations are not feasible in the study of human tissue regeneration processes. While the expression of murine cell markers could be used as a starting point to explore the regeneration ability of the human salivary gland, it has been shown that those markers are either not expressed, or are not equally potent, in human tissue [1]. Culturing of unselected human salivary gland-derived cells as organoids and the transplantation of these cells into locally irradiated salivary glands exploits the regenerative potential of these cells [75].

New, broader and unbiased approaches, which do not require prior knowledge of genes and markers expressed by a cell of interest, are therefore needed to unravel cellular lineage relationships during adult salivary gland tissue regeneration as well to investigate the niche

signals responsible for lineage conversion of both murine and human salivary gland cells. While the niche of two species may differ, xeno-transplantation remains the closest available model to study the functionality and fate of salivary gland-derived cells. However, achieving single cell resolution to identify the regenerative potential of a specific cell type might be complicated. A combination of organoid culture and heritable DNA barcodes, introduced at a single cell level and read using next generation sequencing, could allow one to perform clonal analysis and lineage tree reconstruction, identifying the potency of salivary gland derived cells, without the need for a starting identity. The advancement of single cell RNA sequencing, the principle of which is based on the assumption that cells that are genetically closely related have similar transcriptomes, and their algorithm of analysis could be of used in salivary gland regeneration studies to capture cellular lineage relationships as well as to probe cellular composition and dynamics of the niche under different conditions.

Recent evidence has shown that environmental changes can induce epigenetic modifications of chromatin that can alter stem/progenitor cell behavior providing the plasticity necessary to adapt to the changing environment [83]. Currently, there is very little knowledge on the salivary gland epigenetic landscape. How it is set, maintained, and regulated in terms of DNA methylation, histone modification and chromatin remodelling via pioneer transcription factors during salivary gland development and regeneration remains unknown. These epigenetic events could be responsible for controlling the transcriptomic switches that determine cell-fate decisions, as well as plasticity, of specific cell types during development and regeneration. A deeper understanding of these events in the salivary glands could lead to the identification of specific molecular cell state(s) that could potentially be used for drug targeting to stimulate endogenous regeneration of damaged glands and promote the development of cell plasticity-based regenerative therapy [84]. Furthermore, identifying the underlying epigenetic mechanisms triggered upon injury to induce cell plasticity could allow the further development of epigenetic engineering approaches in cellular model systems, such as salivary gland-derived organoids. This could enhance or potentiate the already proven potential of regenerative therapies to rescue the radiation-induced hyposalivation phenotype.

Each cell in every organ/tissue of the adult body has evolved different cues to meet the tissue-specific requirement, including that of regeneration and repair. From this review, it is apparent that salivary gland stem cells are not embodied in a HSC-like hardwired “professional” stem cell system, but likely are “facultative” stem-like cells [85] that play a role in the regenerative response of the salivary glands. While at present *in vivo* gene therapy approaches provide encouraging results [86,87] in the treatment of salivary gland dysfunction, the characterization of a stem cell-like functional state would open the possibility to combine *ex vivo* stem cells and gene delivery to create an “optimal cell population”. This approach would guarantee both the incorporation of the functional replacement gene(s) into the host DNA and the ability to ensure

that the new information would be permanently part of the new cell population of the tissue, thus avoiding current problems with vector incompatibility, transduction efficiency and short-term gene expression. Looking into the future, taking advantage of computational modelling to integrate multiomics single cell data to understand cell-cell interaction dynamics and the behaviour through time of cell populations within the regenerating salivary gland could be a unique opportunity to unravel cell fate transition in salivary gland tissue regeneration and the pathways by which they are specified. This could lead to the possibility of pharmacologically controlling and/or stabilizing a specific cellular state. Ultimately these approaches could subsequently be used as therapeutic strategy to rescue radiation-induced hyposalivation and improve the quality of life of many thousand head and neck cancer patients.

Acknowledgment

This work was supported by a grant from the Dutch Cancer Society (RUG 2013-5792).

Competing Interest

The authors declare no competing interests.

Author Contributions

C.R. conceived and designed the manuscript and made the figures. L.B. and R.P.C. supervised the development of the manuscript, they critically revised it and approved it for submission.

REFERENCES

1 Pringle, S., Van Os, R. & Coppes, R. P. Concise review: Adult salivary gland stem cells and a potential therapy for xerostomia. *Stem Cells* **31**, 613-619, doi:10.1002/stem.1327 (2013).

2 Tsai, W. L., Huang, T. L., Liao, K. C., Chuang, H. C., Lin, Y. T., Lee, T. F. *et al.* Impact of late toxicities on quality of life for survivors of nasopharyngeal carcinoma. *BMC Cancer* **14**, 856, doi:10.1186/1471-2407-14-856 (2014).

3 van Luijk, P., Pringle, S., Deasy, J. O., Moiseenko, V. V., Faber, H., Hovan, A. *et al.* Sparing the region of the salivary gland containing stem cells preserves saliva production after radiotherapy for head and neck cancer. *Sci Transl Med* **7**, 305ra147, doi:10.1126/scitranslmed.aac4441 (2015).

4 Emmerson, E. & Knox, S. M. Salivary gland stem cells: A review of development, regeneration and cancer. *Genesis* **56**, e23211, doi:10.1002/dvg.23211 (2018).

5 Benderitter, M., Caviggioli, F., Chapel, A., Coppes, R. P., Guha, C., Klinger, M. *et al.* Stem cell therapies for the treatment of radiation-induced normal tissue side effects. *Antioxid Redox Signal* **21**, 338-355, doi:10.1089/ars.2013.5652 (2014).

6 Voog, J. & Jones, D. L. Stem cells and the niche: a dynamic duo. *Cell Stem Cell* **6**, 103-115, doi:10.1016/j.stem.2010.01.011 (2010).

7 Metcalfe, C., Kljavin, N. M., Ybarra, R. & de Sauvage, F. J. Lgr5+ stem cells are indispensable for radiation-induced intestinal regeneration. *Cell Stem Cell* **14**, 149-159, doi:10.1016/j.stem.2013.11.008 (2014).

8 Maimets, M., Rocchi, C., Bron, R., Pringle, S., Kuipers, J., Giepmans, B. N. *et al.* Long-Term In Vitro Expansion of Salivary Gland Stem Cells Driven by Wnt Signals. *Stem Cell Reports* **6**, 150-162, doi:10.1016/j.stemcr.2015.11.009 (2016).

9 Takata, N. & Eiraku, M. Stem cells and genome editing: approaches to tissue regeneration and regenerative medicine. *J Hum Genet* **63**, 165-178, doi:10.1038/s10038-017-0348-0 (2018).

10 Orkin, S. H. & Zon, L. I. Hematopoiesis: an evolving paradigm for stem cell biology. *Cell* **132**, 631-644, doi:10.1016/j.cell.2008.01.025 (2008).

11 Suda, T., Suda, J. & Ogawa, M. Disparate differentiation in mouse hemopoietic colonies derived from paired progenitors. *Proc Natl Acad Sci U S A* **81**, 2520-2524, doi:10.1073/pnas.81.8.2520 (1984).

12 Wilson, A., Laurenti, E., Oser, G., van der Wath, R. C., Blanco-Bose, W., Jaworski, M. *et al.* Hematopoietic stem cells reversibly switch from dormancy to self-renewal during homeostasis and repair. *Cell* **135**, 1118-1129, doi:10.1016/j.cell.2008.10.048 (2008).

13 Mackenzie, I. C. & Bickenbach, J. R. Label-retaining keratinocytes and Langerhans cells in mouse epithelia. *Cell Tissue Res* **242**, 551-556, doi:10.1007/bf00225420 (1985).

14 Potten, C. S. & Morris, R. J. Epithelial stem cells in vivo. *J Cell Sci Suppl* **10**, 45-62, doi:10.1242/jcs.1988.supplement_10.4 (1988).

15 Potten, C. S., Hume, W. J., Reid, P. & Cairns, J. The segregation of DNA in epithelial stem cells. *Cell* **15**, 899-906, doi:10.1016/0092-8674(78)90274-x (1978).

16 Potten, C. S. The epidermal proliferative unit: the possible role of the central basal cell. *Cell Tissue Kinet* **7**, 77-88, doi:10.1111/j.1365-2184.1974.tb00401.x (1974).

17 Braun, K. M. & Watt, F. M. Epidermal label-retaining cells: background and recent applications. *J Investig Dermatol Symp Proc* **9**, 196-201, doi:10.1111/j.1087-0024.2004.09313.x (2004).
18 Cotsarelis, G., Sun, T. T. & Lavker, R. M. Label-retaining cells reside in the bulge area of pilosebaceous unit: implications for follicular stem cells, hair cycle, and skin carcinogenesis. *Cell* **61**, 1329-1337, doi:10.1016/0092-8674(90)90696-c (1990).
19 Terskikh, V. V., Vasiliev, A. V. & Vorotelyak, E. A. Label retaining cells and cutaneous stem cells. *Stem Cell Rev* **8**, 414-425, doi:10.1007/s12015-011-9299-6 (2012).
20 Lu, C. P., Polak, L., Rocha, A. S., Pasolli, H. A., Chen, S. C., Sharma, N. *et al.* Identification of stem cell populations in sweat glands and ducts reveals roles in homeostasis and wound repair. *Cell* **150**, 136-150, doi:10.1016/j.cell.2012.04.045 (2012).
21 Leung, Y., Kandyba, E., Chen, Y. B., Ruffins, S. & Kobielak, K. Label retaining cells (LRCs) with myoepithelial characteristic from the proximal acinar region define stem cells in the sweat gland. *PLoS One* **8**, e74174, doi:10.1371/journal.pone.0074174 (2013).
22 Seidel, K., Ahn, C. P., Lyons, D., Nee, A., Ting, K., Brownell, I. *et al.* Hedgehog signaling regulates the generation of ameloblast progenitors in the continuously growing mouse incisor. *Development (Cambridge, England)* **137**, 3753-3761, doi:10.1242/dev.056358 (2010).
23 Teng, C., Guo, Y., Zhang, H., Zhang, H., Ding, M. & Deng, H. Identification and characterization of label-retaining cells in mouse pancreas. *Differentiation* **75**, 702-712, doi:10.1111/j.1432-0436.2007.00170.x (2007).
24 Buczacki, S. J., Zecchini, H. I., Nicholson, A. M., Russell, R., Vermeulen, L., Kemp, R. *et al.* Intestinal label-retaining cells are secretory precursors expressing Lgr5. *Nature* **495**, 65-69, doi:10.1038/nature11965 (2013).
25 Zajicek, G., Schwartz-Arad, D., Arber, N. & Michaeli, Y. The streaming of the submandibular gland. II: Parenchyma and stroma advance at the same velocity. *Cell Tissue Kinet* **22**, 343-348, doi:10.1111/j.1365-2184.1989.tb00219.x (1989).
26 Amano, O., Mizobe, K., Bando, Y. & Sakiyama, K. Anatomy and histology of rodent and human major salivary glands: -overview of the Japan salivary gland society-sponsored workshop. *Acta Histochem Cytochem* **45**, 241-250, doi:10.1267/ahc.12013 (2012).
27 Martinez-Madrigal, F. & Micheau, C. Histology of the major salivary glands. *Am J Surg Pathol* **13**, 879-899, doi:10.1097/00000478-198910000-00008 (1989).
28 Segawa, A., Shoi, N. & Yamashina, S. [Function of myoepithelial cells in salivary secretion: reevaluation of the expulsion theory]. *Kaibogaku Zasshi* **70**, 330-337 (1995).
29 Yagil, C., Michaeli, Y. & Zajicek, G. Compensatory proliferative response of the rat submandibular salivary gland to unilateral extirpation. *Virchows Arch B Cell Pathol Incl Mol Pathol* **49**, 83-91, doi:10.1007/bf02912087 (1985).
30 Man, Y. G., Ball, W. D., Marchetti, L. & Hand, A. R. Contributions of intercalated duct cells to the normal parenchyma of submandibular glands of adult rats. *Anat Rec* **263**, 202-214, doi:10.1002/ar.1098 (2001).
31 Denny, P. C., Chai, Y., Klauser, D. K. & Denny, P. A. Parenchymal cell proliferation and mechanisms for maintenance of granular duct and acinar cell populations in adult

male mouse submandibular gland. *Anat Rec* **235**, 475-485, doi:10.1002/ar.1092350316 (1993).
32 Chibly, A. M., Querin, L., Harris, Z. & Limesand, K. H. Label-retaining cells in the adult murine salivary glands possess characteristics of adult progenitor cells. *PLoS One* **9**, e107893, doi:10.1371/journal.pone.0107893 (2014).
33 Aure, M. H., Konieczny, S. F. & Ovitt, C. E. Salivary gland homeostasis is maintained through acinar cell self-duplication. *Dev Cell* **33**, 231-237, doi:10.1016/j.devcel.2015.02.013 (2015).
34 Emmerson, E., May, A. J., Berthoin, L., Cruz-Pacheco, N., Nathan, S., Mattingly, A. J. *et al.* Salivary glands regenerate after radiation injury through SOX2-mediated secretory cell replacement. *EMBO Mol Med* **10**, doi:10.15252/emmm.201708051 (2018).
35 Maruyama, E. O., Aure, M. H., Xie, X., Myal, Y., Gan, L. & Ovitt, C. E. Cell-Specific Cre Strains For Genetic Manipulation in Salivary Glands. *PLoS One* **11**, e0146711, doi:10.1371/journal.pone.0146711 (2016).
36 May, A. J., Cruz-Pacheco, N., Emmerson, E., Gaylord, E. A., Seidel, K., Nathan, S. *et al.* Diverse progenitor cells preserve salivary gland ductal architecture after radiation-induced damage. *Development* **145**, doi:10.1242/dev.166363 (2018).
37 Kwak, M. & Ghazizadeh, S. Analysis of histone H2BGFP retention in mouse submandibular gland reveals actively dividing stem cell populations. *Stem Cells Dev* **24**, 565-574, doi:10.1089/scd.2014.0355 (2015).
38 Kwak, M., Ninche, N., Klein, S., Saur, D. & Ghazizadeh, S. c-Kit(+) Cells in Adult Salivary Glands do not Function as Tissue Stem Cells. *Sci Rep* **8**, 14193, doi:10.1038/s41598-018-32557-1 (2018).
39 Lombaert, I. M. A. & Hoffman, M. P. Epithelial stem/progenitor cells in the embryonic mouse submandibular gland. *Front Oral Biol* **14**, 90-106, doi:10.1159/000313709 (2010).
40 Knox, S. M., Lombaert, I. M., Reed, X., Vitale-Cross, L., Gutkind, J. S. & Hoffman, M. P. Parasympathetic innervation maintains epithelial progenitor cells during salivary organogenesis. *Science* **329**, 1645-1647, doi:10.1126/science.1192046 (2010).
41 Emmerson, E., May, A. J., Nathan, S., Cruz-Pacheco, N., Lizama, C. O., Maliskova, L. *et al.* SOX2 regulates acinar cell development in the salivary gland. *Elife* **6**, doi:10.7554/eLife.26620 (2017).
42 Iismaa, S. E., Kaidonis, X., Nicks, A. M., Bogush, N., Kikuchi, K., Naqvi, N. *et al.* Comparative regenerative mechanisms across different mammalian tissues. *NPJ Regen Med* **3**, 6, doi:10.1038/s41536-018-0044-5 (2018).
43 Klein, A. M., Nakagawa, T., Ichikawa, R., Yoshida, S. & Simons, B. D. Mouse germ line stem cells undergo rapid and stochastic turnover. *Cell Stem Cell* **7**, 214-224, doi:10.1016/j.stem.2010.05.017 (2010).
44 Lopez-Garcia, C., Klein, A. M., Simons, B. D. & Winton, D. J. Intestinal stem cell replacement follows a pattern of neutral drift. *Science* **330**, 822-825, doi:10.1126/science.1196236 (2010).
45 Snippert, H. J., van der Flier, L. G., Sato, T., van Es, J. H., van den Born, M., Kroon-Veenboer, C. *et al.* Intestinal crypt homeostasis results from neutral competition between symmetrically dividing Lgr5 stem cells. *Cell* **143**, 134-144, doi:10.1016/j.cell.2010.09.016 (2010).

46 Doupe, D. P., Alcolea, M. P., Roshan, A., Zhang, G., Klein, A. M., Simons, B. D. *et al.* A single progenitor population switches behavior to maintain and repair esophageal epithelium. *Science* **337**, 1091-1093, doi:10.1126/science.1218835 (2012).
47 Leushacke, M., Ng, A., Galle, J., Loeffler, M. & Barker, N. Lgr5(+) gastric stem cells divide symmetrically to effect epithelial homeostasis in the pylorus. *Cell Rep* **5**, 349-356, doi:10.1016/j.celrep.2013.09.025 (2013).
48 Stine, R. R. & Matunis, E. L. Stem cell competition: finding balance in the niche. *Trends Cell Biol* **23**, 357-364, doi:10.1016/j.tcb.2013.03.001 (2013).
49 Klein, A. M. & Simons, B. D. Universal patterns of stem cell fate in cycling adult tissues. *Development* **138**, 3103-3111, doi:10.1242/dev.060103 (2011).
50 Kimura, M. & Weiss, G. H. The Stepping Stone Model of Population Structure and the Decrease of Genetic Correlation with Distance. *Genetics* **49**, 561-576 (1964).
51 Bullen, T. F., Forrest, S., Campbell, F., Dodson, A. R., Hershman, M. J., Pritchard, D. M. *et al.* Characterization of epithelial cell shedding from human small intestine. *Lab Invest* **86**, 1052-1063, doi:10.1038/labinvest.3700464 (2006).
52 Eisenhoffer, G. T., Loftus, P. D., Yoshigi, M., Otsuna, H., Chien, C. B., Morcos, P. A. *et al.* Crowding induces live cell extrusion to maintain homeostatic cell numbers in epithelia. *Nature* **484**, 546-549, doi:10.1038/nature10999 (2012).
53 Ohsawa, S., Vaughen, J. & Igaki, T. Cell Extrusion: A Stress-Responsive Force for Good or Evil in Epithelial Homeostasis. *Dev Cell* **44**, 532, doi:10.1016/j.devcel.2018.02.007 (2018).
54 Kopp, J. L., Grompe, M. & Sander, M. Stem cells versus plasticity in liver and pancreas regeneration. *Nat Cell Biol* **18**, 238-245, doi:10.1038/ncb3309 (2016).
55 Stolp, B., Thelen, F., Ficht, X., Altenburger, L. M., Ruef, N., Inavalli, V. *et al.* Salivary gland macrophages and tissue-resident CD8(+) T cells cooperate for homeostatic organ surveillance. *Sci Immunol* **5**, doi:10.1126/sciimmunol.aaz4371 (2020).
56 Boada-Romero, E., Martinez, J., Heckmann, B. L. & Green, D. R. The clearance of dead cells by efferocytosis. *Nat Rev Mol Cell Biol*, doi:10.1038/s41580-020-0232-1 (2020).
57 Vissink, A., Mitchell, J. B., Baum, B. J., Limesand, K. H., Jensen, S. B., Fox, P. C. *et al.* Clinical management of salivary gland hypofunction and xerostomia in head-and-neck cancer patients: successes and barriers. *Int J Radiat Oncol Biol Phys* **78**, 983-991, doi:10.1016/j.ijrobp.2010.06.052 (2010).
58 Blanco, A. I., Chao, K. S., El Naqa, I., Franklin, G. E., Zakarian, K., Vicic, M. *et al.* Dose-volume modeling of salivary function in patients with head-and-neck cancer receiving radiotherapy. *Int J Radiat Oncol Biol Phys* **62**, 1055-1069, doi:10.1016/j.ijrobp.2004.12.076 (2005).
59 Roesink, J. M., Moerland, M. A., Battermann, J. J., Hordijk, G. J. & Terhaard, C. H. Quantitative dose-volume response analysis of changes in parotid gland function after radiotherapy in the head-and-neck region. *Int J Radiat Oncol Biol Phys* **51**, 938-946, doi:10.1016/s0360-3016(01)01717-5 (2001).
60 Vissink, A., Jansma, J., Spijkervet, F. K., Burlage, F. R. & Coppes, R. P. Oral sequelae of head and neck radiotherapy. *Crit Rev Oral Biol Med* **14**, 199-212, doi:10.1177/154411130301400305 (2003).
61 Dijkema, T., Raaijmakers, C. P., Ten Haken, R. K., Roesink, J. M., Braam, P. M., Houweling, A. C. *et al.* Parotid gland function after radiotherapy: the combined michigan and utrecht experience. *Int J Radiat Oncol Biol Phys* **78**, 449-453, doi:10.1016/j.ijrobp.2009.07.1708 (2010).

62 Barazzuol, L., Coppes, R. P. & van Luijk, P. Prevention and treatment of radiotherapy-induced side effects. *Mol Oncol* **14**, 1538-1554, doi:10.1002/1878-0261.12750 (2020).
63 Coppes, R. P., Zeilstra, L. J., Kampinga, H. H. & Konings, A. W. Early to late sparing of radiation damage to the parotid gland by adrenergic and muscarinic receptor agonists. *Br J Cancer* **85**, 1055-1063, doi:10.1054/bjoc.2001.2038 (2001).
64 Coppes, R. P., Vissink, A. & Konings, A. W. Comparison of radiosensitivity of rat parotid and submandibular glands after different radiation schedules. *Radiother Oncol* **63**, 321-328, doi:10.1016/s0167-8140(02)00129-9 (2002).
65 Weng, P. L., Aure, M. H., Maruyama, T. & Ovitt, C. E. Limited Regeneration of Adult Salivary Glands after Severe Injury Involves Cellular Plasticity. *Cell Rep* **24**, 1464-1470 e1463, doi:10.1016/j.celrep.2018.07.016 (2018).
66 Konings, A. W., Coppes, R. P. & Vissink, A. On the mechanism of salivary gland radiosensitivity. *Int J Radiat Oncol Biol Phys* **62**, 1187-1194, doi:10.1016/j.ijrobp.2004.12.051 (2005).
67 Ninche, N., Kwak, M. & Ghazizadeh, S. Diverse epithelial cell populations contribute to the regeneration of secretory units in injured salivary glands. *Development* **147**, doi:10.1242/dev.192807 (2020).
68 Shubin, A. D., Sharipol, A., Felong, T. J., Weng, P. L., Schutrum, B. E., Joe, D. S. *et al.* Stress or injury induces cellular plasticity in salivary gland acinar cells. *Cell Tissue Res*, doi:10.1007/s00441-019-03157-w (2020).
69 Karki, A., Humphrey, S. E., Steele, R. E., Hess, D. A., Taparowsky, E. J. & Konieczny, S. F. Silencing Mist1 Gene Expression Is Essential for Recovery from Acute Pancreatitis. *PLoS One* **10**, e0145724, doi:10.1371/journal.pone.0145724 (2015).
70 Nanduri, L. S., Baanstra, M., Faber, H., Rocchi, C., Zwart, E., de Haan, G. *et al.* Purification and ex vivo expansion of fully functional salivary gland stem cells. *Stem Cell Reports* **3**, 957-964, doi:10.1016/j.stemcr.2014.09.015 (2014).
71 Ayyaz, A., Kumar, S., Sangiorgi, B., Ghoshal, B., Gosio, J., Ouladan, S. *et al.* Single-cell transcriptomes of the regenerating intestine reveal a revival stem cell. *Nature* **569**, 121-125, doi:10.1038/s41586-019-1154-y (2019).
72 Srinivasan, P. P., Patel, V. N., Liu, S., Harrington, D. A., Hoffman, M. P., Jia, X. *et al.* Primary Salivary Human Stem/Progenitor Cells Undergo Microenvironment-Driven Acinar-Like Differentiation in Hyaluronate Hydrogel Culture. *Stem Cells Transl Med* **6**, 110-120, doi:10.5966/sctm.2016-0083 (2017).
73 Shackleton, M., Vaillant, F., Simpson, K. J., Stingl, J., Smyth, G. K., Asselin-Labat, M. L. *et al.* Generation of a functional mammary gland from a single stem cell. *Nature* **439**, 84-88, doi:10.1038/nature04372 (2006).
74 Clevers, H. & Watt, F. M. Defining Adult Stem Cells by Function, not by Phenotype. *Annu Rev Biochem* **87**, 1015-1027, doi:10.1146/annurev-biochem-062917-012341 (2018).
75 Pringle, S., Maimets, M., van der Zwaag, M., Stokman, M. A., van Gosliga, D., Zwart, E. *et al.* Human Salivary Gland Stem Cells Functionally Restore Radiation Damaged Salivary Glands. *Stem Cells* **34**, 640-652, doi:10.1002/stem.2278 (2016).
76 Weng, P. L., Aure, M. H. & Ovitt, C. E. Concise Review: A Critical Evaluation of Criteria Used to Define Salivary Gland Stem Cells. *Stem Cells* **37**, 1144-1150, doi:10.1002/stem.3046 (2019).
77 Zhao, Q., Zhang, L., Hai, B., Wang, J., Baetge, C. L., Deveau, M. A. *et al.* Transient activation of the Hedgehog-Gli pathway rescues radiotherapy-induced dry mouth via

recovering salivary gland resident macrophages. *Cancer Res*, doi:10.1158/0008-5472.CAN-20-0503 (2020).

78 Ratajczak, M. Z., Kucia, M., Jadczyk, T., Greco, N. J., Wojakowski, W., Tendera, M. *et al.* Pivotal role of paracrine effects in stem cell therapies in regenerative medicine: can we translate stem cell-secreted paracrine factors and microvesicles into better therapeutic strategies? *Leukemia* **26**, 1166-1173, doi:10.1038/leu.2011.389 (2012).

79 Blaine, S. A., Ray, K. C., Anunobi, R., Gannon, M. A., Washington, M. K. & Means, A. L. Adult pancreatic acinar cells give rise to ducts but not endocrine cells in response to growth factor signaling. *Development* **137**, 2289-2296, doi:10.1242/dev.048421 (2010).

80 Pan, F. C., Bankaitis, E. D., Boyer, D., Xu, X., Van de Casteele, M., Magnuson, M. A. *et al.* Spatiotemporal patterns of multipotentiality in Ptf1a-expressing cells during pancreas organogenesis and injury-induced facultative restoration. *Development* **140**, 751-764, doi:10.1242/dev.090159 (2013).

81 Houbracken, I., de Waele, E., Lardon, J., Ling, Z., Heimberg, H., Rooman, I. *et al.* Lineage tracing evidence for transdifferentiation of acinar to duct cells and plasticity of human pancreas. *Gastroenterology* **141**, 731-741, 741 e731-734, doi:10.1053/j.gastro.2011.04.050 (2011).

82 Raven, A., Lu, W. Y., Man, T. Y., Ferreira-Gonzalez, S., O'Duibhir, E., Dwyer, B. J. *et al.* Cholangiocytes act as facultative liver stem cells during impaired hepatocyte regeneration. *Nature* **547**, 350-354, doi:10.1038/nature23015 (2017).

83 Atlasi, Y. & Stunnenberg, H. G. The interplay of epigenetic marks during stem cell differentiation and development. *Nat Rev Genet* **18**, 643-658, doi:10.1038/nrg.2017.57 (2017).

84 Macchi, F. & Sadler, K. C. Unraveling the Epigenetic Basis of Liver Development, Regeneration and Disease. *Trends Genet* **36**, 587-597, doi:10.1016/j.tig.2020.05.002 (2020).

85 Wabik, A. & Jones, P. H. Switching roles: the functional plasticity of adult tissue stem cells. *EMBO J* **34**, 1164-1179, doi:10.15252/embj.201490386 (2015).

86 Baum, B. J., Alevizos, I., Zheng, C., Cotrim, A. P., Liu, S., McCullagh, L. *et al.* Early responses to adenoviral-mediated transfer of the aquaporin-1 cDNA for radiation-induced salivary hypofunction. *Proc Natl Acad Sci U S A* **109**, 19403-19407, doi:10.1073/pnas.1210662109 (2012).

87 Lombaert, I. M. A., Patel, V. N., Jones, C. E., Villier, D. C., Canada, A. E., Moore, M. R. *et al.* CERE-120 Prevents Irradiation-Induced Hypofunction and Restores Immune Homeostasis in Porcine Salivary Glands. *Mol Ther Methods Clin Dev* **18**, 839-855, doi:10.1016/j.omtm.2020.07.016 (2020).

CHAPTER 3

LONG-TERM *IN VITRO* EXPANSION OF SALIVARY GLAND STEM CELLS DRIVEN BY WNT SIGNALS

Maimets, M., Rocchi, C., Bron, R., Pringle, S., Kuipers, J., Giepmans, BNG., Vries, RGJ., Clevers, H., de Haan, G., van Os, R., Coppes, RP.
.

Stem Cell Reports. 2016 Jan 12;6(1):150-62.

SUMMARY

Adult stem cells are the ultimate source for replenishment of salivary gland (SG) tissue. Self-renewal ability of stem cells is dependent on extrinsic niche signals that have not been unraveled for the SG. The ductal compartment in SG has been identified as the location harboring stem cells. Here we report that rare SG ductal EpCAM^{+} cells express nuclear β-catenin indicating active Wnt-signaling. In cell culture experiments, EpCAM^{high} cells respond potently to Wnt signals stimulating self-renewal and long-term expansion of SG organoids, containing all differentiated salivary gland cell types. Conversely, Wnt inhibition ablated long-term organoid cultures. Finally, transplantation of cells pre-treated with Wnt agonists into submandibular glands of irradiated mice successfully and robustly restored saliva secretion and increased the number of functional acini *in vivo*. Collectively, these results identify Wnt signaling as a key driver of adult SG stem cells, allowing extensive *in vitro* expansion, enabling restoration of SG function upon transplantation.

INTRODUCTION

Tissue homeostasis and regeneration are maintained by resident stem cells that have the ability to self-renew and to generate all differentiated lineages that characterize a particular tissue. Self-renewal of stem cells should be achieved by asymmetric cell division to maintain sufficient numbers of stem cells and to allow ample production of mature, functional tissue specific cells. The balance between self-renewal and differentiation is stringently regulated by cell-intrinsic transcriptional programs and extracellular signals originating from a specialized microenvironment – the stem cell niche [1]. Strict cell-extrinsic control is crucial to avoid the continuous self-renewal of stem cells and their possible progression into cancerous cells [2]. An important feature of the stem cell niche model is the limited availability of self-renewing factors due to their local release and short signaling distance [3]. Understanding the nature of these factors and their effect on adult stem cells has been hindered due to the low abundance of stem cells and the limited number of functional assays.

The salivary gland is a useful model for studying adult stem cell maintenance due to the easy accessibility and its extensive regenerative capacity [4-8]. Salivary glands are complex secretory organs which are composed of saliva-producing acinar cells, myoepithelial cells which facilitate the saliva expulsion and ductal cells through which saliva is secreted into the oral cavity [9]. Intermingled with ductal cells reside salivary gland stem cells (SGSCs), which express c-Kit, CD49f, CD133, CD24, CD29 cell surface markers [10-12]. Upon transplantation, SGSCs attenuate radiation-induced hyposalivation [11,12] and improve tissue homeostasis necessary for long-term maintenance of the adult tissue [13]. Although, recently we [14] and others [15] have successfully purified SGSCs able to self-renew and differentiate *in vitro* and *in vivo*, the molecular cues underlying the maintenance of SGSCs and the existence of a specialized stem cell niche are still enigmatic.

The canonical Wnt/β-catenin signaling has been shown to play a crucial role in the maintenance of multiple types of adult stem/progenitor cells [16]. The Wnt target gene *Lgr5* has been identified as a marker of resident stem cells in the small intestine and colon [17], hair follicle [18], stomach [19], kidney [20] and liver [21]. In adult salivary glands, Wnt/β-catenin signaling is weak, but is significantly activated during functional regeneration [22]. Furthermore, concurrent transient activation of Wnt/β-catenin signaling ameliorates irradiation-induced salivary gland dysfunction [23]. Whether Wnt proteins directly control normal salivary gland stem cell maintenance is still not known. In this study, we used a combination of cell culture and *in vivo* transplantation experiments to show that Wnt proteins serve as important self-renewing factors for SGSCs.

RESULTS

EpCAM$^+$ cells in salivary gland ducts co-express β-catenin

In the salivary gland, stem cells have been suggested to reside within the ductal compartment [24,25]. Therefore, a universal marker for ductal cells of adult submandibular gland would allow identification and enrichment of a population containing stem cells. EpCAM (Epithelial cell adhesion molecule) is present on most epithelial cells and has been used as a marker for self-renewing compartments in liver [26,27] and pancreas [28]. To assess the presence of EpCAM in the salivary gland, we stained whole gland sections using immunofluorescence. The expression of EpCAM was detected throughout the whole epithelia of the salivary gland (Figure S1A). However, we encountered most abundant and enhanced expression of EpCAM in the ductal compartment, marking excretory, striated and intercalated ducts (Figure 1A) and low EpCAM expression in acinar cells, which comprise most of the mouse submandibular gland. No background staining was detected in salivary gland sections treated without primary antibody (Figure S1B and D). Interestingly, transcription of EpCAM is activated upon Wnt/β-catenin signaling in other tissues [29]. Therefore, we attempted to determine sites of Wnt-signaling in the salivary gland using β-catenin as a general reporter [30]. Indeed, highest β-catenin expression was observed to be confined to ductal cells (Figure 1B) of the salivary gland while the acinar cells showed low levels of β-catenin. Again, no background staining was detected without primary antibody (Figure S1C and D). Moreover, most cells positive for β-catenin were found to co-express EpCAM (Figure 1C and D). To quantify this, co-localization analysis was performed and Pearson correlation coefficient (PCC) for sub-region of interests (ROIs) were calculated. This revealed the strongest correlation of EpCAM and β-catenin occurring in excretory ducts (Figure 1E, ROI 2) (PCC=0.121644), which were previously suggested to contain the stem cells [9,12]. Interestingly, striated ducts displayed more exclusive EpCAM$^+$ cells (Figure 1E, ROI 1) (PCC=0.032378) while intercalated ducts revealed more exclusive β-catenin expression (Figure 1E, ROI 3) (PCC=0.001784). Importantly, scanning of excretory ducts revealed rare basal cells with nuclear β-catenin expression (Figure 1F, arrows) suggesting an occurrence of active Wnt signaling in these cells. The existence of these rare cells agrees with the low level of cell turnover of the salivary glands [31].

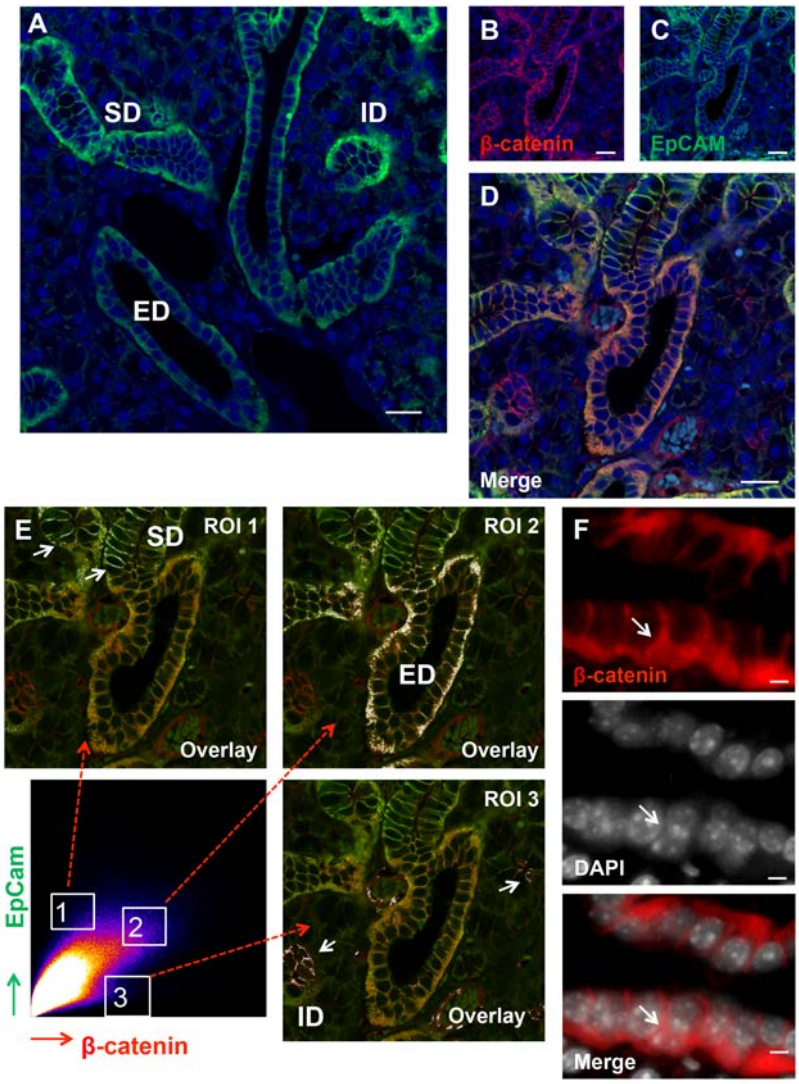

Figure 1: EpCAM expressing ductal cells have the potential to be Wnt activated. (A) Immunofluorescence staining of EpCAM in striated, intercalated and excretory ducts. **(B-D)** β-catenin (red) co-localizes with EpCAM (green) in salivary gland ducts. **(E)** Scattegram of colocalization of EpCAM and β-catenin . Different regions of interests (ROIs) show which pixels (arrows) are included in the analysis. For each pixel in the fluorescent image, the two intensities (green, red) are used as coordinates in the scattergram. Images analyzed with ImageJ „Colocalization_Finder" plugin (Christophe Laummonerie; 2006/08/29: Version 1.2). **(F)** Nuclear localization of β-catenin in rare basal cells (arrow) of excretory ducts. Top: β-catenin; center: DAPI; bottom: overlay. Scale bars 20 µm (A-E) and 5 µm (F)

Recently, Wnt target genes *Lgr5* [17] and *Lgr6* [32] have been identified as markers of stem cells in the intestine/colon and skin respectively. We utilized the LGR5-EGFP [17] and LGR6-EGFP [32] knock-in alleles to determine the expression of LGR5 and LGR6 in the salivary gland. Both receptors are essentially undetectable in the tissue under steady-state conditions (data not shown). This is in line with recent findings in other slow turnover tissues such as liver [21] and pancreas [28] where under homeostatic conditions no expression of LGR5 was detected. These data indicate that EpCAM$^+$ cells in salivary gland excretory ducts co-express β-catenin and therefore could potentially be activated by Wnt-signaling, albeit not through LGR5/6 receptors.

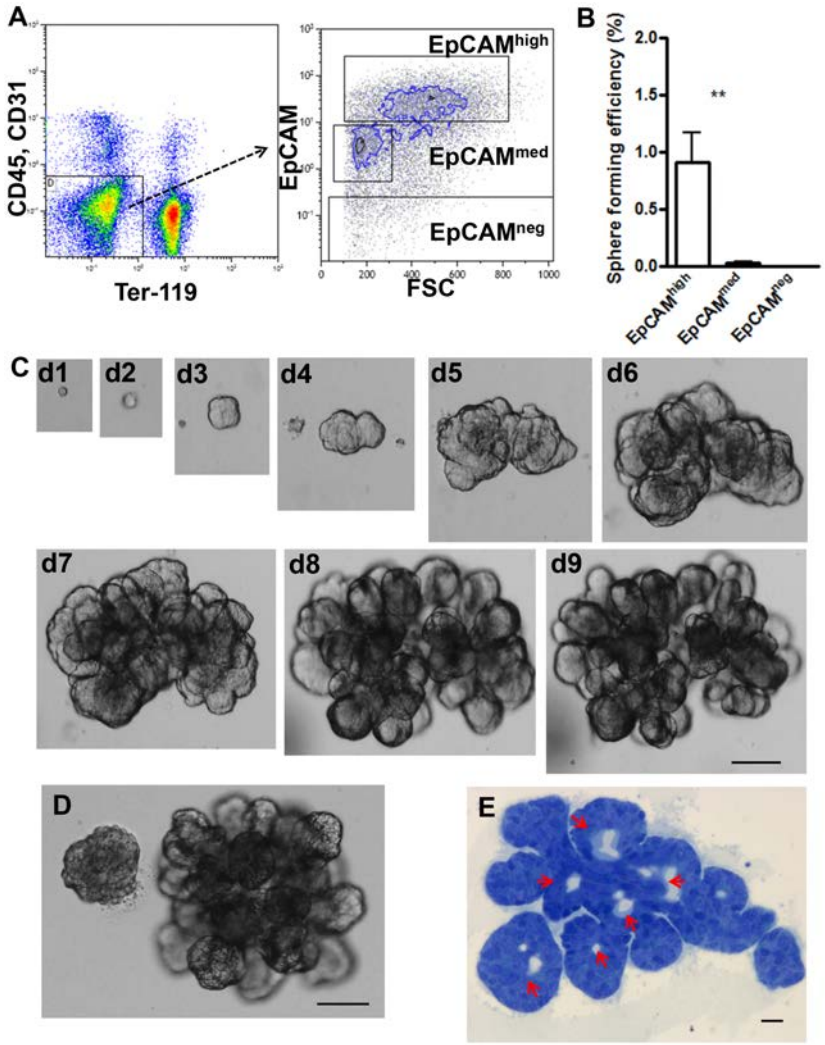

Figure 2: Single EpCAM^{high} cells generate spheres and miniglands. **(A)** Representative fluorescence-activated cell sorting (FACS) gating strategy for the analysis of ductal cells in the salivary gland. Left panel shows the exclusion of lineaege marker-expressing cells. Right panel depicts the distribution of EpCAM^{high}, EpCAM^{med} and EpCAM^{neg} cells in dissociated adult mouse salivary gland. FSC, forward scatter. **(B)** Sphere forming efficiency of EpCAM^{high}, EpCAM^{med}, and EpCAM^{neg} populations (** $p < 0.005$). Data are expressed as the mean of ± SEM of three independent experiments. **(C)** Differential interference contrast image of a growing minigland until 9 days of culture. **(D)** Representative example of a salisphere and a minigland originating from single EpCAM^{high} in 9-day-old culture. **(E)** Toluidine blue staining shows uniform lumen formation throughout minigland (arrows). Scale bars 100 µm (C,D) and 10 µm (E)

EpCAM^{high} cells give rise to secondary salivary gland spheres and miniglands

Based on our observations *in vivo*, we next asked whether Wnt proteins could directly influence EpCAM^{+} salivary gland ductal cells *in vitro* by promoting their sphere-initiating ability. Therefore, salivary glands from adult healthy mice were isolated and digested into single cell suspension. After removing cell clumps, dead cells and debris, we depleted CD45^{+} and TER119^{+} hematopoietic and CD31^{+} endothelial cells (Figure 2A). Subsequently, salivary gland

cells were subdivided into three distinct cell populations: EpCAM^{high}, EpCAM^{med} and EpCAM^{neg} using Fluorescence Activated Cell Sorting (FACS) (Figure 2A). Purified cells were embedded into Matrigel containing enriched medium supplemented with Epidermal Growth Factor (EGF), Fibroblast Growth Factor 2 (FGF2), insulin and Y-27632 [14], to which Wnt3A and Rspo1 were added (WRY medium). Under these conditions, 0.9±0.2% of single cells from the EpCAM^{high} population generated spheres within 24-48 hours (Figure 2B). In contrast, single cells from EpCAM^{med} and EpCAM^{neg} populations were unable to form spheres (<0.05%, Figure 2B). Moreover, only 0.05±0.01% of live, non-marker selected cells and 0.2±0.1% non-sorted cells were capable of generating spheres in WRY medium, further indicating that high EpCAM expression pronouncedly enriches for cells with *in vitro* self-renewing capabilities (Figure S2A). Similarly, to gastric organoid units [19] supplementing the cultures with either Wnt3a or Rspo1 alone lead to the formation of a lower number of spheres (Figure S2B). We did not observe any cell growth in cultures not supplemented with Wnt proteins (Figure S2B) presumably due to the requirement of Wnt-signaling for the initiation of sphere-growth under these conditions.

Interestingly, within 9 days of culture 10.8±1.8% of the spheres formed differentiated organoid-like structures, which we termed miniglands (Figure 2C and S2C). Miniglands underwent extensive budding events during this time frame and were up to 4-6 times bigger than co-cultured salispheres (89.2±1.8%), reaching up to 1 mm in diameter (Figure 2D and S2D) by day 15. Toluidine blue staining of miniglands revealed a lobular structure with evenly distributed lumina (Figure 2E). Moreover, miniglands consisted of differentiated CK18^{+} ductal (Figure 3A, C and S3A), Aqp5^{+} acinar (Figure 3B, C) and SMA-α^{+} myoepithelial cells forming the outer layer of a lobe (Figure 3D and Movie S1), as shown by immunostaining, indicative of retention of differentiation potential of EpCAM^{high} salivary gland stem cells in the presence of Wnt agonists. No background staining was detected in any of the samples treated without primary antibody even with enhancing the lasers of confocal microscope to excessive levels (Figure S3B). Interestingly, ultrastructural analysis of entire miniglands at high resolution with large scale electron microscopy [33] further indicated representation of both, serous acinar (Figure 3E, arrows) and mucous acinar cells (Figure 3E, arrowheads) as recognized by characteristically electron dense and electron pale secretory vesicles, respectively (Movie S2). The basement membrane was lined with myoepithelial cells (Figure 3E, asterisk) distinguished by their elongated shapes. We also observed an abundance of CK5+ cells (Figure 3F), which is considered to be a progenitor cell population in embryonic salivary glands [34]. Taken together, culturing single EpCAM^{high} stem cell *in vitro* in Wnt-inducing conditions gives rise to 3-dimensional structures which a) consist of all salivary gland cell lineages and b) contain large numbers of CK5^{+} putative progenitors.

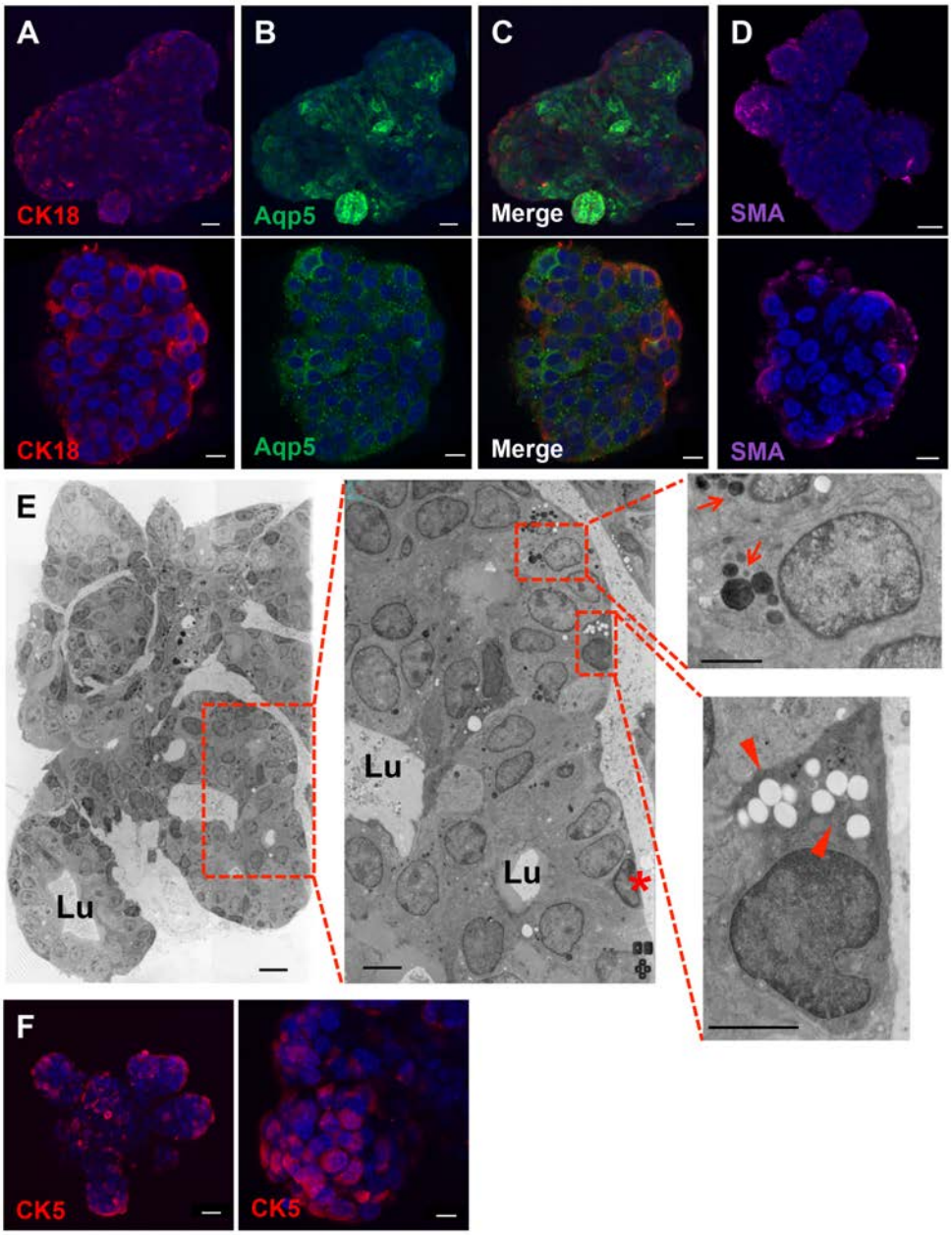

Figure 3: Single-cell derived miniglands acquire fate of salivary gland cells. (A-D), Confocal images (z-stack projection) for salivary gland specific markers (A) CK18 (red, ductal cells), (B) Aqp5 (green, acinar cells), (C) Overlay of CK18 (red) and Aqp5 (green), (D) α-SMA (purple, myoepithelial cells), Counterstain, Hoechst 33342 (blue). **(E)** Electron microscopy demonstrates serous (arrows) and mucous (arrowheads) acinar cells and myoepithelial cells (asterisk). Data accessible: www.nanotomy.org , salivary gland organoid. Lu, lumen. **(F)** Confocal images (z-stack projection) for CK5 (red, embryonic SG progenitor cells). Counterstain, Hoechst 33342 (blue). Scale bars 30 µm (A-D,F upper panel), 10 µm (A-D,F lower panel) and 10 µm, 5 µm and 2 µm (E) left, center and right panel respectively.

Single salivary gland stem cell expansion is Wnt-driven

Recently, we have shown pronounced expansion of SGSCs *in vitro* in the presence of Rho-kinase inhibitor Y-27632 [14], without Wnt agonists. However, this expansion was initiated from liquid cultures enriched for primary sphere forming cells and might involve a paracrine effect of Wnt-stimulation. To test the requirement of the Wnt pathway in this format, salivary glands from adult healthy mice were isolated and digested into dispersed cells, which formed primary salispheres within 3 days (Figure 4A). Next, single cells derived from dissociated primary spheres were embedded in Matrigel supplemented with expansion medium (EM) (Figure 4B) [14] or EM containing a panel of Wnt antagonists: IWR-1-endo (Figure 4D), which stabilizes Axin proteins within the β-catenin destruction complex [35], IWP-2 (Figure 4E), which inactivates Porcn, a protein known to be essential for the production of Wnt ligands [35] and SFRP-1 (Figure 4F), which directly binds to Wnt proteins [36]. Indeed, chemical inhibition of the Wnt pathway by IWR-1 endo compound completely suppressed growth of spheres while treatment of IWP-2 and sFRP1 dramatically reduced the growth of spheres (Figure 4G-H). DMSO treated cells (Figure 4C and G-H) did not have a significant effect on the population doublings or sphere forming efficiency. These data suggest that Wnt-signaling is essential for the initiation of sphere-growth, not only when isolating SGSCs directly from tissue (Figure 2A) but also in cultures enriched for salivary gland stem cells [12,14]. We next reasoned, that if Wnt inhibition leads to a lack of proliferation in salispheres, Wnt activation may lead to an increased proliferation and salisphere forming potential, and as such expansion of the SGSC pool. We tested this by seeding single cells derived from primary salispheres in Matrigel supplemented with WRY medium (Figure 4I). As expected, the presence of Wnt proteins had an enhanced effect on cell proliferation (population doubling 6.5±0.2) (Figure 4N). Furthermore, we observed a significant effect on sphere forming efficiency (15.7±1.1%) (Figure 4O) when compared to EM conditions (population doubling 3.2±0.2; sphere forming efficiency 12.0±1.0%). Disruption of Wnt-pathway by IWR-1-endo (Figure 4K), IWP-2 (Figure 4L) or sFRP1 (Figure 4M) in WRY conditions lead to a reduced cell growth (3.5±0.1; 0.6±0.2; 1.6±0.4 population doublings respectively) (Figure 4N) and weakened sphere forming efficiency (6.3±1.1%; 2.0±0.6; 3.3±1.2 respectively) (Figure 4O), indicative of incomplete inhibition of Wnt-signalling by Wnt antagonists in the presence of Wnt3a and R-spondin1. DMSO exposure (Figure 4J) did not alter cell growth or sphere formation (population doubling 5.9±0.3; sphere forming efficiency 14.3±1.9) (Figure 4N-O) compared to untreated condition. To test the self-renewal capacity of cells cultured in WRY conditions, every consecutive week, organoids were enzymatically digested into single cells and plated with the density of 10.000 cells per well (Figure 4A). The cultures maintained exponential growth for more than 8 months with

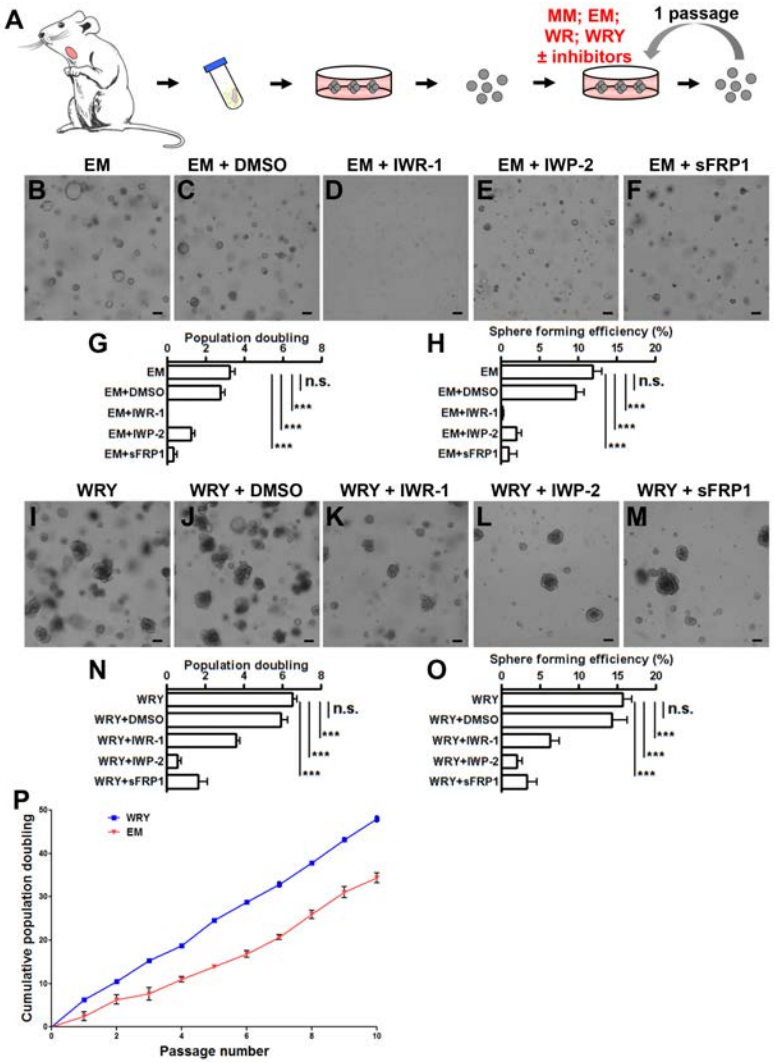

Figure 4: *In vitro* expansion of salivary gland stem cells, **(A)** Scheme showing isolation method of SGSCs and establishment of long-term salivary gland organoid culture. **(B-F)** DIC images of salivary gland organoid cultures grown in enriched medium (EM) (B) [14] in combination with DMSO (C) or Wnt antagonists IWR-1-endo (D), IWP-2 (E), sFRP1 (F). Scale bars 100 µm. **(G-H)**, Population kinetics of salisphere-derived salivary gland organoid cultures during inhibition of Wnt-pathway grown in EM) representing population doubling (G) and sphere forming capability (H). **(I-M)** DIC images of salivary gland organoid cultures grown in WRY medium (I) in combination with DMSO (J) or Wnt antagonists IWR-1-endo (K), IWP-2 (L), sFRP1 (M). Scale bars 100 µm. **(N-O)**, Population kinetics of salisphere-derived salivary gland organoid cultures during inhibition of Wnt-pathway grown in WRY medium representing population doubling (N) and sphere forming capability (O). **(P)** Population dynamics plot of salisphere self-renewal culture (formula in materials and methods). MM, minimal culturing media. WRY, minimal media supplemented with Wnt3a, R-spondin1 and y-27632. Data are expressed as the mean of ± SEM of three independent experiments (panels G,H,N-P). Scale bars 100 µm.

cell doubling times essentially unchanged during the culturing period (Figure 4P, WRY). Furthermore, when compared to our previously published enriched medium (Figure 4P, EM) [14] cells grown in the presence of Wnt agonists displayed an enhanced capacity for stem cell expansion.

We then asked whether the original organoids derived from EpCAM^{high} cells (Figure 2) contain cells capable for self-renewal and therefore give rise to long-term SGSC cultures. To this end, salivary glands from adult healthy mice were isolated and digested into single cell suspension. After removing cell clumps, dead cells and debris, we depleted CD45+ and TER119+ hematopoietic and CD31 endothelial cells (Figure S4A). As before, the cells were divided into three cell populations EpCAM^{high}, EpCAM^{med} and EpCAM^{neg} using FACS (Figure S4B) and embedded into Matrigel containing previously defined WRY-medium. During 10 days of culture, EpCAM^{high} cells generated organoids (Figure S4C, arrows) as shown previously. As expected, single cells from EpCAM^{med} and EpCAM^{neg} populations were unable to form organoids (<0.05%) (Figure S4D-E). Next, organoids intiated from single EpCAM^{high} cells were dissociated and re-plated into Matrigel supplemented with WRY-medium. Within the period of 3 passages (3 weeks) these cultures displayed exponential growth (Figure S4F) similar to cultures initiated from liquid cultures (Figure 4P). Additionally, as cells derived from EpCAM^{high} population were passaged, an increase in the ability to form spheres was observed (Figure S4G), indicative of enrichment in stem/progenitor cells when cultured under Wnt-inducing conditions. This shows that EpCAM^{high} cell population discerned from freshly isolated salivary glands in contrast to EpCAM^{med} and EpCAM^{neg} populations contain cells with self-renewal potential.

In order to assess the suitability of expanded SGSCs for *in vivo* reconstitution experiments we beforehand tested their tumorigenicity and differentiation potential. First, when transplanting 8 x 10e5 passage 13 cells subcutaneously into immunocompromised mice, no tumor formation was detected after 1 year in any of the mice analyzed (n=5) (Figure S5A). Secondly, when embedding passage 18 spheres into our previously published differentiation assay containing Collagen Type IV and Basement Membrane Matrigel (50%:50%) [14] the growth of lobular organoids was observed within 14 days (Figure S5B) suggesting a normal differentiation potential when growing salivary gland cells for multiple passages with WR medium. Therefore, we conclude that passaging SGSCs in Wnt-inducing conditions allows massive expansion of salivary gland stem cell pool.

Transplantation of Wnt-induced cells unprecedentedly rescue irradiation-damaged salivary glands

Based on our *in vitro* observations showing that only EpCAM^{high} cells give rise to secondary structures indicating the presence of stem cells, we finally tested the potential of these cells to rescue radiation-induced hyposalivation *in vivo*. For this purpose ACTB-DsRed (DsRed) mice were used as donor to enable tracing the donor cells after transplantation. First, sphere cultures from DsRed mice were initiated and cultured for 1 or 7 passages in Basement

Membrane Matrigel supplemented with WR media (Figure 5A). Subsequently, cultures were collected, trypsinized into single-cell suspension and

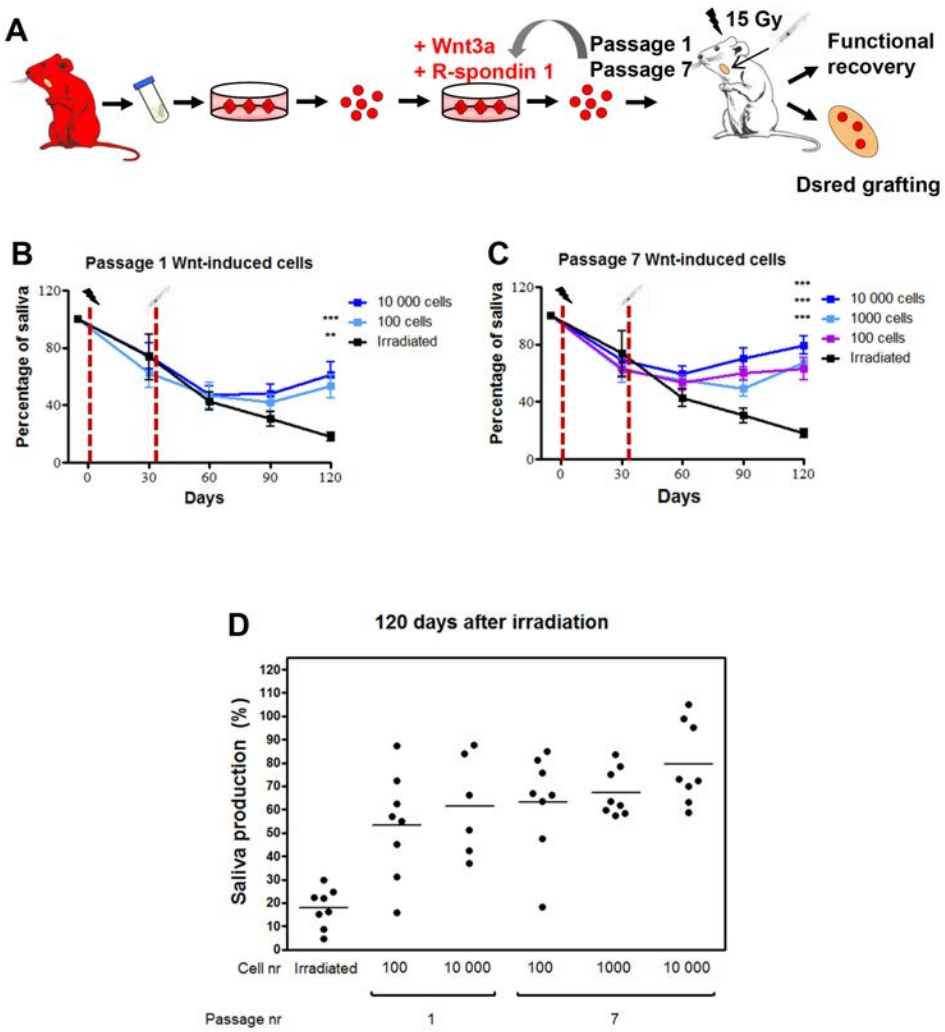

Figure 5: Transplantation of cultured Wnt-induced cells improves function of irradiated salivary gland tissue. **(A)** Scheme representing the transplantation protocol. **(B)** Transplants of 10.000 (blue), 100 (cyan) of passage 1 Wnt-induced cells in time course analysis of relative saliva production in comparison to irradiated control animals (black). Statistical analysis is shown in comparison to irradiated control group (*** p <0.001, ** p < 0.01 at relevant time point). Data are expressed as the mean of ± SEM, n=8 animals per time point. **(C)** Transplants of 10.000 (blue), 1000 (purple), 100 (cyan) of passage 7 Wnt-induced cells in time course analysis of relative saliva production in comparison to irradiated control animals (black). Statistical analysis is shown in comparison to irradiated control group (*** p <0.001, ** p < 0.01 at relevant time point). Data are expressed as the mean of ± SEM, n=8 animals per time point. **(D)** Relative saliva production at 120 days after irradiation in animals transplanted with 100, 10.000 passage 1 or 100, 1000, 10.000 passage 7 Wnt-induced cells per animal. Each data point represents a recipient animal. Note the uniform response of animals transplanted with passage 7 Wnt-induced cells.

transplanted intraglandularly into C57BL/6 recipient mice, which were previously locally irradiated with 15 Gy to the head and neck region [12]. Both glands in each mouse received equal cell numbers, so that a total cell number of 100, 1000 or 10,000 were transplanted per

recipient mouse. The functionality of the transplanted glands was determined by pilocarpine stimulated saliva flow rate as described previously [12]. As expected, 120 days after irradiation, in control animals (irradiated and non-transplanted), saliva production dropped to 17±3% of pre-irradiation values (Figure 5B-D). In contrast, saliva flow of mice transplanted with 100 or 10,000 passage 1 Wnt-induced cells increased significantly to 53±8% and 62±9%, respectively (Figure 5B and D). Furthermore, the transplantation was even more successful in mice transplanted with 100, 1000 or 10.000 passage 7 Wnt-induced cells, reaching levels of 63±8%, 67±3% and 79±6% of pre-irradiation saliva flow, respectively (Figure 5C and D). This indicates that our culturing conditions are optimized for the enrichment in salivary gland stem cell pool with *in vivo* reconstitution ability.

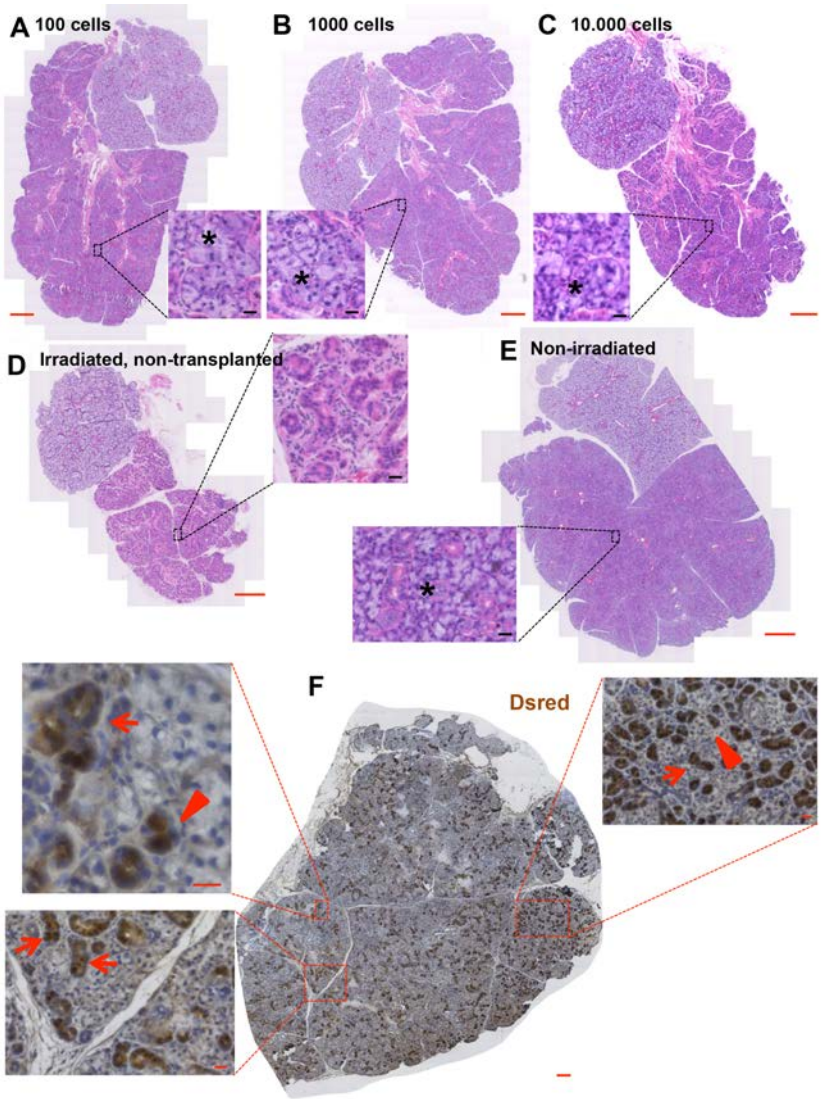

Figure 6: Donor-derived cells regenerate destroyed salivary gland tissue. (A-E), H&E stainings of SG tissue: irradiated and transplanted with 100 (A), 1000 (B) or 10.000 (C) Wnt-induced cells, irradiated control (D) untreated control (E) showing presence of acini (asterisk). **(F)** Immunohistochemical staining for DsRed reveals incorporation of transplanted Wnt-induced cells into donor tissue and formation of ducts (arrows) and acini (arrowheads). Scale bars 100 µm (zoom-out panel) and 20 µm (zoom-in panel).

Recovery of the glandular tissue was further demonstrated by improvement of general morphology (Figure 6A-C) and the re-appearance of functional acinar tissue (Figure 6A-C, asterisk). The histological improvement was observed in all transplanted mice when compared to irradiated controls (Figure 6D), returning to levels close to non-irradiated controls determined by strong increase in acini (Figure 6E). We also analyzed the engraftment of Wnt-induced cells by DsRed staining on serial sections of the entire salivary gland. We found $DsRed^+$ ducts (Figure 6F, arrows) and acini (Figure 6F, arrowheads) incorporated in the tissue, indicating that they were derived from donor cells. No specific staining was detected in C57BL/6 salivary gland sections treated with DsRed antibody (Figure S5A) while most of the cells were positively stained in salivary gland sections of DsRed mice (Figure S5B). We did not observe any sign of tumor growth or dysplastic change in any of the transplanted areas indicating the non-transformed origin of cultured cells. Taken together, these data reveal that culturing SGSCs in Wnt-inducing conditions broadly expands SGSCs with enhanced potential to restore functionality in destroyed submandibular glands. However, with these experiments we cannot sufficiently conclude that Wnt proteins are responsible for restoring the function of irradiated salivary glands *in vivo*.

DISCUSSION

Wnt/β-catenin signaling is involved in many biological processes, including proliferation, differentiation, organogenesis and cell migration [16]. It has been shown previously that combinations of Wnt- and R-spondin proteins support long term cultures of small intestine [37], stomach [19], liver [21] and pancreas [28]. Until now, the role of Wnt signaling on key properties of salivary gland stem cell regulation has remained elusive. In this study, we provide evidence that Wnt proteins are required for salivary gland stem cell self-renewal and robustly promote their long-term expansion in culture. Our study further strengthens the role of Wnt-signaling as a universal self-renewal pathway [38-40].

A lack of stem cell assays in the adult salivary gland field has hindered studies aimed to assess functional properties and/or regenerative potential of putative stem cell populations. Our previous attempts for studying SGSC biology were based on *in vitro* cultures, already enriched for stem/progenitor cells [12,14]. Here we report the development of an optimized culture system for generating salivary gland organoids from primary adult submandibular glands *in vitro,* based on activation of Wnt-signaling. Although in addition to the common transmembrane expression of EpCAM we also detect an unexpected basal localization of the protein in excretory duct cells of the salivary gland, FACS selection for single $EpCAM^{high}$ cells and subsequent culturing in the presence of Wnt-activating proteins efficiently generate three-dimensional salivary gland organoids that closely resemble primary salivary gland tissue.

Recently, Xiao and colleagues [15] successfully isolated and cultured $Lin^{-}CD24^{+}c\text{-}Kit^{+}Sca1^{+}$ salivary gland stem cells as spheres lacking phenotypical hallmark of differentiation - branching morphogenesis. Contrary to this, the organoids presented here underwent series of budding events, until reaching sizes up to 1 mm (supplementary figure 2C). Combined with orthotopic transplantation [41], these findings may open up novel routes to organ replacement regenerative therapy. Using technique reported here we are able to expand salivary gland stem cells, derived from a single animal, to clinically relevant numbers without the use of specific stem cell markers. Previously reported methods have been required to start expansion cultures with cells derived from multiple animals, and used cell surface markers that are mouse specific [15], rendering the expansion protocol less clinically relevant.

Achieving control of cell fate determination in adult tissues is one of the key goals of regenerative medicine. Given the central role of Wnt-mediated cellular responses in stem cell self-renewal we focused our attention on activation as well as inhibition of Wnt-signaling. By using a panel of chemical inhibitors of Wnt pathway we effectively show that Wnt signaling is required for the maintenance of salivary gland stem cell cultures. Although the ability of IWR and IWP compounds to selectively inhibit the Wnt pathway has been characterized elsewhere [35], it is still possible that chemical inhibition causes off target effects. Therefore, in the future it would be of interest to use conditional β-catenin loss-of-function mouse model [42] or CRISPR-Cpf1 genome editing system [43] for the ablation of Wnt-pathway.

Ultimately, this study provides proof of principle that SGSCs cultured under Wnt-inducing conditions can be used for stem-cell therapy to irradiation-damaged epithelium and possibly other cases of salivary gland dysfunction. Remarkably, the transplanted cells adhere and engraft into damaged tissue and contribute to the normal homeostasis of the salivary gland. We report an unprecedented improvement of saliva flow recovery over previously reported methods [11,14,15,44], which could have been achieved by transplantation of heterogeneous pool of cells containing stem, progenitor and differentiated cells present in these cultures. Although translation to the human situation is needed, the current study implies that *in vitro* expansion and transplantation of long-term cultured SGSCs may be a promising option for patients with severe salivary gland hypofunction.

In conclusion, we provide clear evidence that Wnt-signals are necessary for SGSC maintenance *in vitro*. However, this does not exclude the relevance of other pathways in these processes. For example, platelet-derived growth factor receptor signaling, in concert with FGF signaling, has been shown to be essential for proliferation and survival of *ex* vivo cultures of embryonic salivary gland progenitors [45,46]. Furthermore, epidermal growth factors and their receptors are important for embryonic SMG proliferation [34,47]. However, none of these pathways have been exploited to study adult stem cell maintenance *in vitro* to the extent as the Wnt-signaling pathway presented here. We believe that the efficient *in vitro* system

reported here will be of vital use for validating and implementing further studies on adult SGSC biology and for the discovery of novel pathways involved in the salivary gland maintenance and regeneration.

EXPERIMENTAL PROCEDURES

Mice

8–12 week old female C57BL/6 mice were purchased from Harlan. NOD.Cg-*Prkdc*^{scid}*Il2rg*^{tmlWjl}/SzJ, B6.Cg-Tg(ACTB-DsRed*MST)1Nagy/J and B6.129P2-*Lgr5*$^{tm1(cre/ESR1)Cle}$/J animals were bred in the Central Animal Facility of University Medical Centre Groningen. LGR6-EGFP [32] were bred in Hubrecht Institute, University Medical Centre Utrecht. The mice were maintained under conventional conditions and fed *ad libitum* with food pellets (RMH-B, Hope Farms B.V.) and water. All experiments were approved by the Ethical Committee on animal testing of the University of Groningen.

Immunostaining

Mouse salivary glands were 4% formaldehyde fixed (24 hours, RT) and processed for paraffin embedding. Following dehydration, the tissue was embedded in paraffin and sliced into 5 µm sections. The sections were dewaxed, boiled for 8 min in pre-heated 10 mM citric acid retrieval buffer (pH 6.0) containing 0.05 % Tween20, washed thoroughly prior to primary antibody exposure and labeled for the following markers: EpCAM (1:100; [48]), β-catenin (1:100; Transduction laboratories, 610154), DsRed (1:100; BioVision, #3984-100). For fluorescence microscopy Alexa Fluor 488 goat anti-rabbit (Life technologies, A11008) or Alexa Fluor 594 donkey anti-mouse (Life technologies, A21203) conjugates at 1:300 dilution were used as secondary antibodies. Nuclear staining was performed with DAPI (Sigma-Aldrich). Haematoxylin and Eosin staining was performed according to standard protocols. Visualization for bright field microscopy was accomplished by addition of specific secondary biotin carrying antibodies (Dako), an avidin–biotin-horse radish peroxidase complex (ELITE ABC Kit, Vector Laboratories) and the diaminobenzidine (DAB) chromogen. Nuclear staining was performed with hematoxylin.

Cell sorting and single cell salivary gland sphere culture

Salivary glands were harvested from healthy adult mice, mechanically disrupted by gentleMACS Dissociator (Milteny) followed by enzymatic digestion with collagenase type II (0,63 mg/ml; Gibco), hyaluronidase (0,5 mg/ml; Sigma-Aldrich) and $CaCl_2$ (6,25 mM; Sigma-Aldrich). After filtering through 100 µm cell strainer the suspension was dissociated using 0,05% trypsin-EDTA (Gibco) following filtering through 35 µm strainer. Cell pellets were incubated with anti-mouse CD31-PE (eBioscience, 12-0311-82), CD45-PE (Biolegend,

103106), TER-119-PE/Cy7 (Biolegend, 116222) and EpCAM-APC antibody (eBiosciences, 17-5791-80) for 15' on room temperature. After washing thoroughly cells were suspended in a solution containing propidium iodide (PI; 1mg/ml; Sigma-Aldrich), $MgSO_4$ (10 mM; Sigma-Aldrich) and DNase I (50 µg/ml; Sigma-Aldrich). Pulse-width gating excluded cell doublets while dead cells were excluded by gating on PI negative cells. Positive gating was based on the comparison of non-stained and single antibody-stained samples. Sorted cells were embedded in Basement Membrane Matrigel (BD Biosciences) and seeded in 12-well. Cells were cultured in EM [14] or in WRY medium (DMEM:F12 containing Pen/Strep antibiotics (1X; Invitrogen), Glutamax (1X; Invitrogen), N2 (1X; Gibco), EGF (20 ng/ml; Sigma-Aldrich), FGF2 (20 ng/ml; Sigma-Aldrich), insulin (10 µg/ml; Sigma-Aldrich), dexamethasone (1 µM; Sigma-Aldrich), Y-27632 (10 µM; Sigma-Aldrich 10% R-spondin1 conditioned media (provided by C. Kuo) and 50% Wnt3a conditioned media).

Primary salispheres were cultured as published previously [12]. Shortly, cell suspensions were prepared first by mechanical disruption with gentleMACS (Milteny) followed by enzymatic digestion with collagenase type II (0,63 mg/ml; Gibco), hyaluronidase (0,5 mg/ml; Sigma-Aldrich) and $CaCl_2$ (6,25 mM; Sigma-Aldrich). After washing thoroughly cell suspensions were re-suspended in DMEM:F12 medium containing 1X Pen/Strep antibiotics (Invitrogen), Glutamax (1X; Invitrogen), EGF (20 ng/ml; Sigma-Aldrich), FGF-2 (20 ng/ml; Sigma-Aldrich), N2 (1X; Gibco), insulin (10 µg/ml; Sigma-Aldrich) and dexamethasone (1 µM; Sigma-Aldrich), at a density of 400,000 cells per well of a 12-well plate.

Self-renewal assay

3-day salisphere cultures were dispersed to single cell suspensions using 0.05 % trypsin-EDTA (Invitrogen), enumerated and concentration adjusted to 0.4 x 10^6 cells/ml. 25 µl of cell suspension was combined on ice with 50 µl of BM Matrigel and deposited in the center of 12-well tissue culture plates. After solidifying the gels for 20 minutes at 37 °C, gels were covered in minimal medium (MM), expansion medium (EM) [14], WR medium, WRY medium or combinations of EM or WRY medium containing Wnt antagonists IWR-1-endo (20 µM, Cayman Chemical), IWP-2 (1 µM, Merck Millipore) or sFRP1 (20 ng/ml, Peprotech). 7-10 days after seeding, Matrigel was dissolved by incubation with Dispase (1 mg/ml; Sigma) for 1 hour at 37ºC. Spheres released from the gels were processed to a single cell suspension using 0.05 % trypsin EDTA, cell number and sphere number noted, and encapsulation in Matrigel repeated. This cycle was repeated up to 25 times (25 passages). Cell numbers seeded at the start of each passage and harvested at the end were used to calculate the number of population doublings that had occurred, using the following formula, where pd = population doublings and ln = natural log.

$$pd = \frac{ln\,(harvested\ cells\ /\ seeded\ cells)}{ln2}$$

Whole-mount immunostaining

Matrigel in 10-day salisphere culture was dissolved by incubation with Dispase for 1 hour at 37ºC. Released spheres and miniglands were FA fixed for 12 hours at 4ºC, washed thoroughly and labeled for the following markers: Aqp5 (1,5 µg/ml; Alomone Labs, #AQP-005), CK18 (1:100; Abcam, ab668), α-SMA (1:100; Sigma-Aldrich, A2547) and CK5 (1:100; Covance, PRB-160P). Alexa Fluor 488 goat anti-rabbit (Life technologies, A11008) or Alexa Fluor 594 donkey anti-mouse (Life technologies, A21203) conjugates at 1:300 dilution were used as secondary antibodies. Nuclear counterstaining was performed with Hoechst 33258 (Sigma-Aldrich).

Electron microscopy (TEM)

Large scale electron miscroscopic analysis was carried out essentially as described before [33]. 10-day salisphere culture in Matrigel was fixed in 2% glutaraldehyde in 0.1 M sodiumcacodylate buffer for 24 h at 4 °C. After fixation in 1% osmiumtetroxide/1,5% potasiumferrocyanide (2 hr at 4 degree), salispheres were dehydrated using ethanol and embedded in EPON epoxy resin. 60nm sections were cut and contrasted using 2% uranylacetate in methanol followed by Reynolds leadcitrate. Images were taken with a Zeiss Supra55 in STEM mode at 29 KV using an external scan generator (Fibics) yielding mosaics of large area scans at 2 nm pixel resolution. These large scale TIF images were stitched and converted to html files using VE Viewer (Fibics). These html files can be opened using the following link: www.nanotomy.org , Salivary gland organoid. Annotations were done on the original TIFF files using Photoshop.

Irradiation and regeneration assay

The irradiation and regeneration assay employed here was described earlier [12]. Shortly, salivary glands of female C57BL/6 mice were irradiated with a single dose of 15 Gy (Precision X-ray Inc.). 4 weeks after irradiation, mice were anesthetized and SMG was exposed by small incision. As a source of donor cells passage 1 or passage 7 Wnt-induced or not induced salisphere cultures were dissociated into single cell solution, 100, 1000 or 10.000 cells suspended in equal volumes of α-MEM (Gibco) and injected into both submandibular glands of irradiated mice intra-glandular. Saliva was collected for 15 minutes at 30, 60, 90 and 120 days post irradiation.

Image analysis

Immunofluorescence images from tissue sections and images of cultivated cells were acquired with Leica TCS Sp8 confocal microscope. Images of time-lapse experiment were acquired with an Olympus IMT-2 inverted microscope. Immunohistochemical images of tissue sections were acquired with Leica 6000 series microscope or with Tissuegnostics TissueFAXS high throughput fluorescence microscope. Colocalization of 2 proteins were quantified by ImageJ "Colocalization_Finder" plugin (Christophe Laummonerie 2006/08/29: Version 1.2). Immunofluorescence images were reconstructed and analyzed using Imaris (Bitplane) software.

Data analysis

All values are represented as mean ± standard error of the mean (SEM). A 2-way analysis of variance (ANOVA) and Bonferroni post-hoc test with alpha values of 0.05 were applied to the time course analysis of saliva flow. *n* numbers for tested groups are stated in figure legend. All calculations were performed using GraphPad Prism (GraphPad software) software.

Acknowledgements

This work was supported by grants from The Netherlands Organisation for Health Research and Development (ZonMW-Grant nr. 11.600.1023), the Netherlands Institute for Regenerative Medicine (NIRM, Grant No. FES0908), and the Dutch Cancer Society (RUG2013-5792). M.M. has been supported by SA Archimedes DoRa programme. We thank L.S.Y. Nanduri for assistance with transplantation experiments. We thank R.-J. van der Lei, G. Mesander and H. Moes for expert cell sorting assistance. M.M. would like to thank O.K. Jutukas for fruitful discussions. Part of the work has been performed at the UMCG Microscopy and Imaging Centre (UMIC), which is sponsored by NWO-grants 40-00406-98-9021; 175-010-2009-023 and 91111.006. In addition, we thank K. Sjollema for expert assistance in light microscopy and H. van der Want for assistance with analysis of electron microscopy.

Author contributions

M.M. designed and performed experiments, analyzed data, and wrote the manuscript. C.R. performed and co-analyzed cell culture experiments. R.B. performed and analyzed immunostaining experiments. J.K. generated electron microscopy data. S.P.; B.N.G.G commented on and edited the manuscript. R.G.J.V; H.C. and G.d.H provided helpful discussions and edited the manuscript. R.v.O. and R.P.C. designed experiments, supervised the project and wrote the manuscript.

Conflict of interests

H.C. is an inventor of several patents involving the organoid culture system. The remaining authors declare no competing interests.

SUPPLEMENTAL INFORMATION

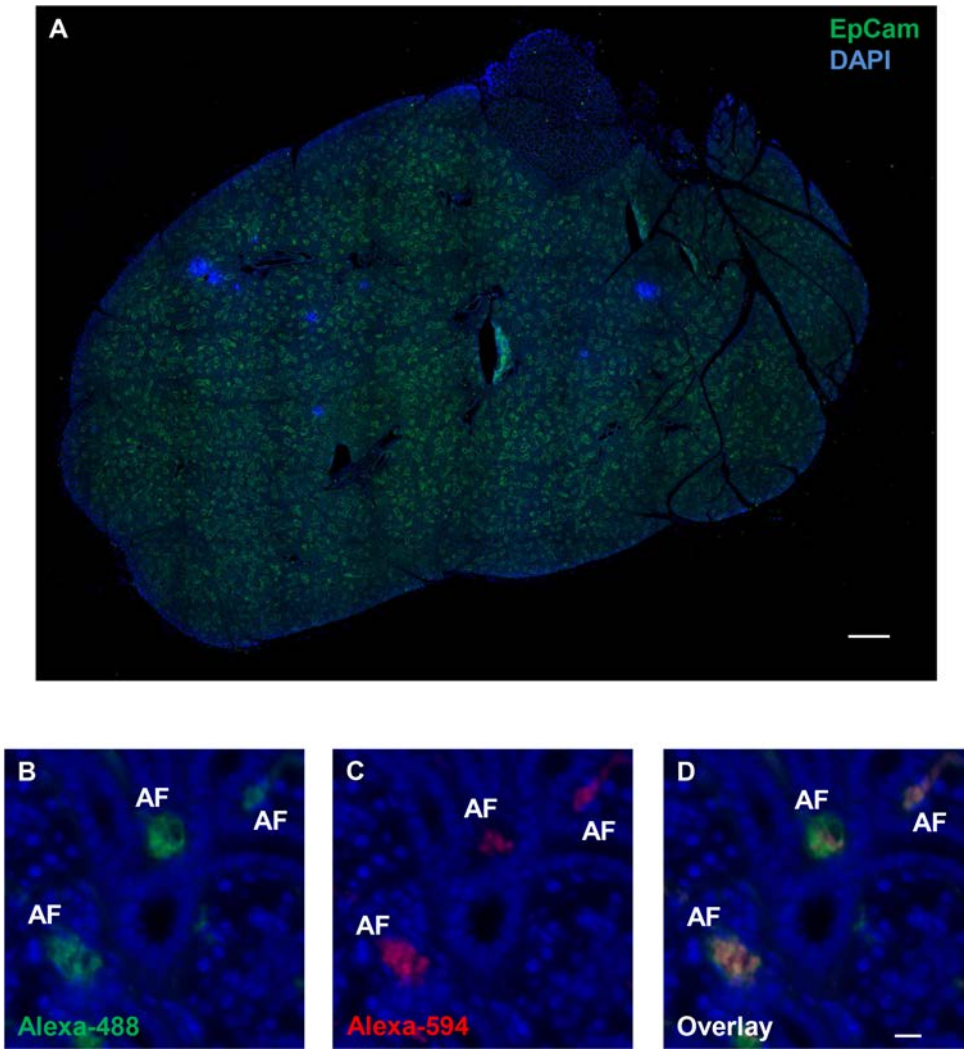

Figure S1: EpCAM expression in whole salivary gland section. (A) Immunostaining showing extensive EpCAM expression throughout the ductal compartment of salivary gland. **(B-D)** Control immunostaining without primary antibody for EpCAM (B), β-catenin (C) and overlay (D). AF – autofluorescence. Scale bars 500 µm **(A)** and 20 µm **(B-D)**.

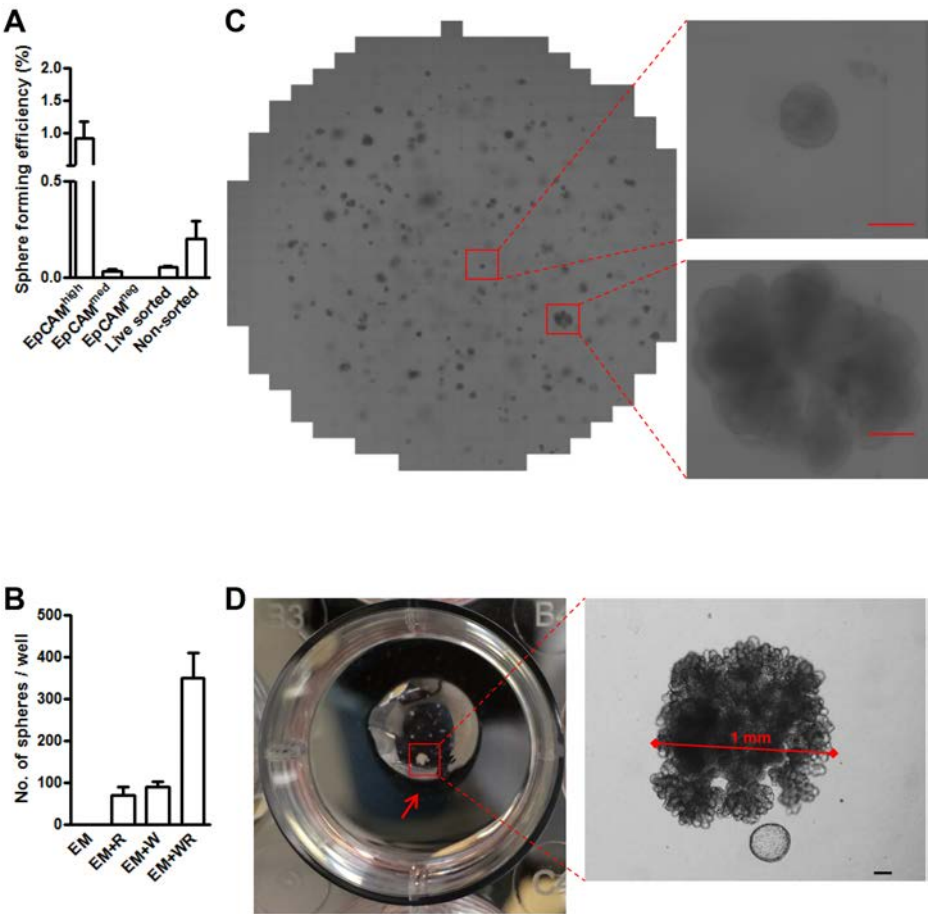

Figure S2: Single EpCAM^{high} cells generate spheres and miniglands. (A) Sphere forming efficiency of EpCAM^{high}, EpCAM^{med}, and EpCAM^{neg} populations compared to live sorted and non-sorted cells. Data are expressed as the mean of ± SEM of three independent experiments. **(B)** Single EpCAM^{high} cells were seeded and supplemented with enriched media (EM) (Nanduri, 2014); EM+R-spondin-1 (EMR); EM+Wnt3a (EMW) and EM+R-spondin-1+Wnt3a (EMWR). Results are shown as mean of ±SEM of 2 independent experiments. **(C)** Representative image of single EpCAM^{high} –derived *in vitro* culture showing a mixture of spheres (upper right) and miniglands (lower right). **(D)** Single EpCAM^{high} cell gives rise to a minigland reaching 1 mm in diameter. Scale bars 100 µm.

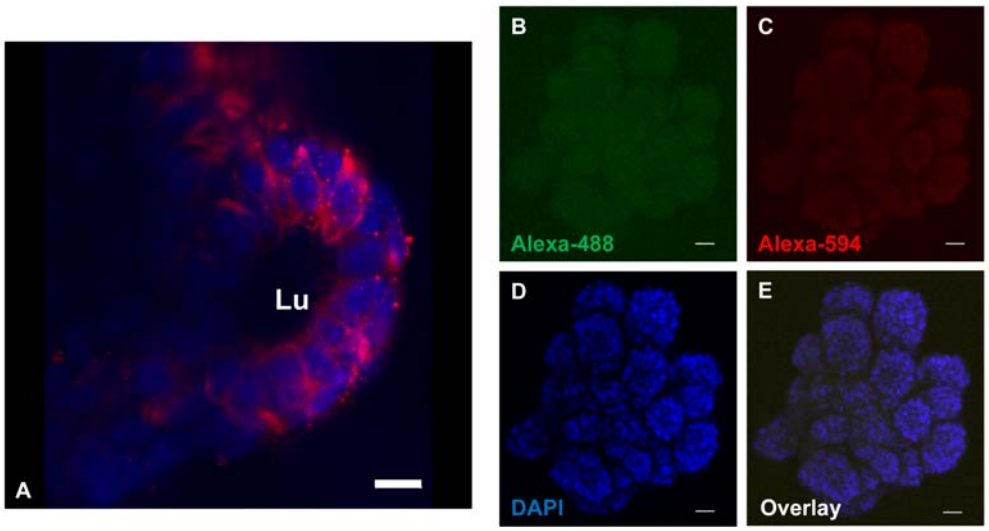

Figure S3: Cellular composition of miniglands. (A) Confocal images (z-stack projection) for ductal marker CK18 (red) depicting duct and lumen (Lu) formation within a minigland. **(B-E)** Control immunostaining without primary antibodies for A488 **(B)**, A594 **(C)**, DAPI **(D)** and overlay **(E)**. Scale bars 10 µm **(A)** and 30 µm **(B-E)**.

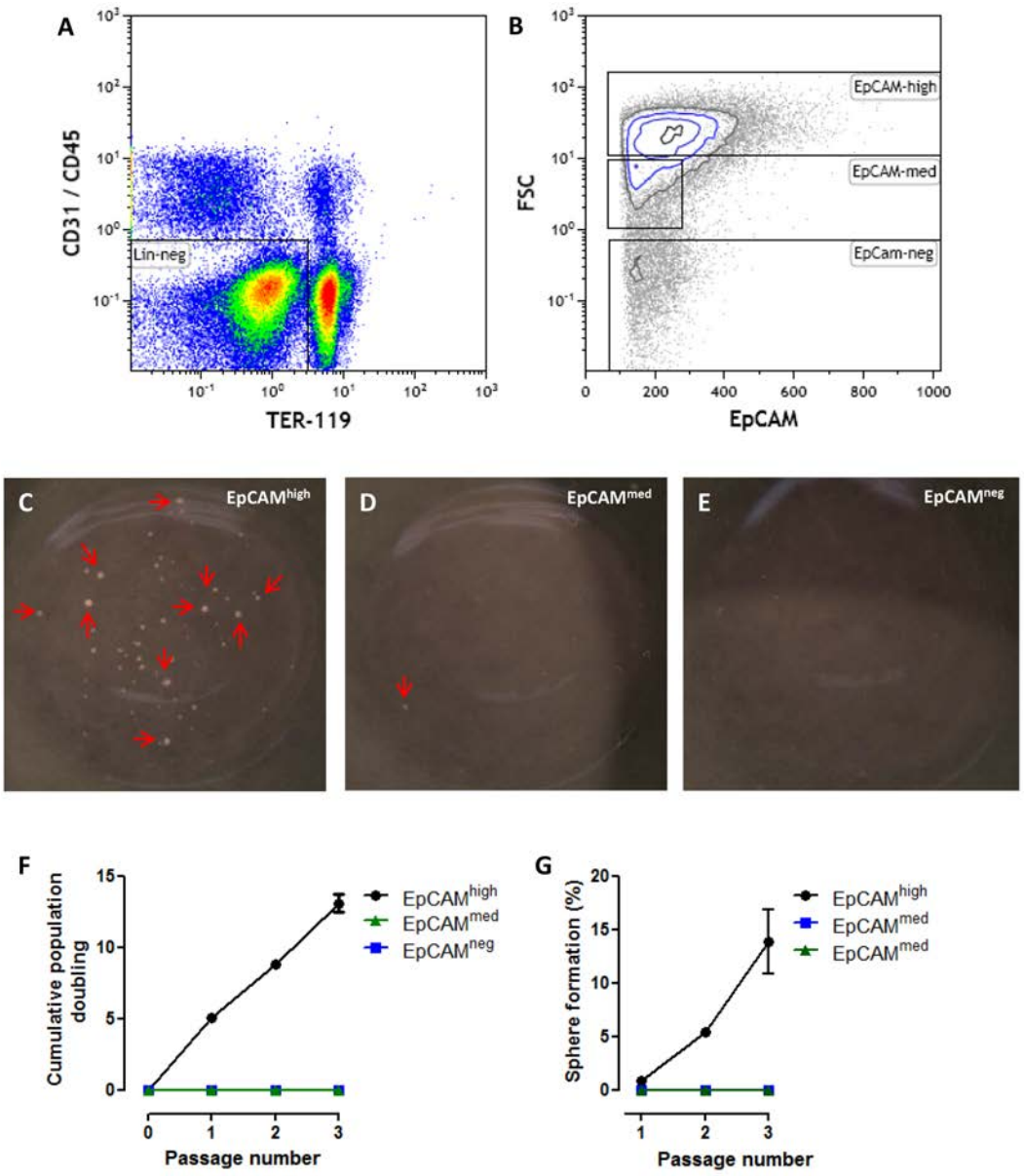

Figure S4: Expansion of EpCAM^{high} cells isolated from salivary gland tissue. (A-B) Representative FACS gating strategy for the analysis of EpCAM expressing cells in the salivary gland. (A) Exclusion of lineaege marker-expressing cells. (B) Distribution of EpCAM^{high}, EpCAM^{med} and EpCAM^{neg} cells in dissociated adult mouse salivary gland. FSC, forward scatter. **(C-E)** Sphere forming efficiency of (C) EpCAM^{high}, (D) EpCAM^{med} and (E) EpCAM^{neg} populations. **(F)** Population dynamics plot of the self-renewal culture of EpCAM^{high} cells. **(G)** Sphere formation kinetics of cultures initiated from EpCAM^{high} cells during serial passaging.

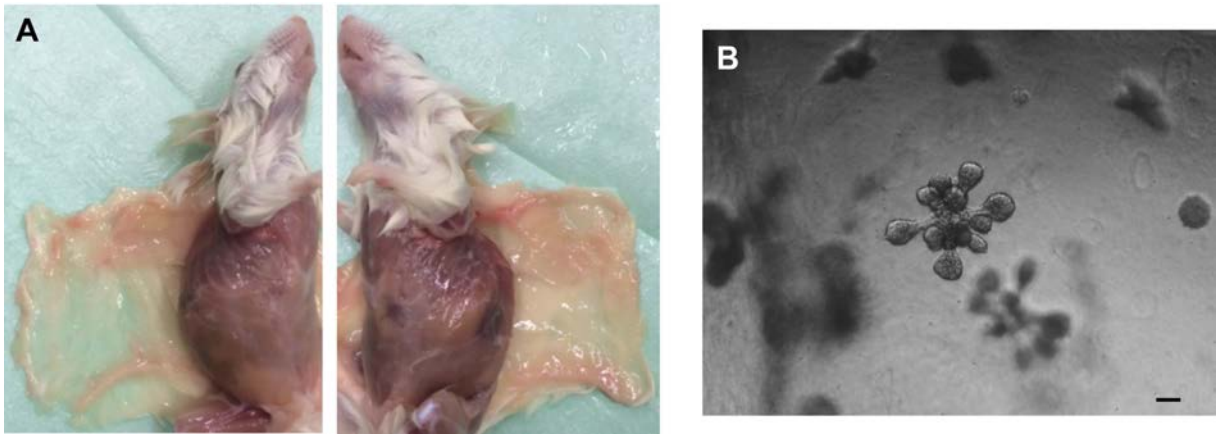

Figure S5: Tumorigenicity and differentiation potential of expanded SGSCs. (A) Transplantation of 800 000 passage 13 Wnt-induced cells sub cutaneously on the side of NSG mice do not show any sign of tumour formation after 1 year follow-up. **(B)** Embedding passage 18 Wnt-induced spheres in matrigel/collagen (Differentiation assay, materials and methods) gives rise to terminally differentiated organoids after 15 days. Scale bar 100 µm.

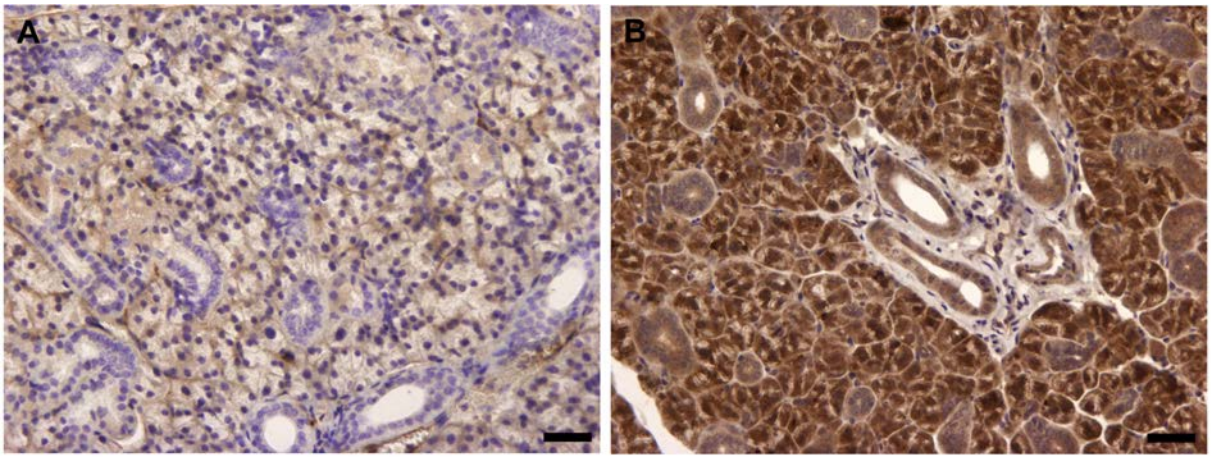

Figure S6: Controls for dsRed staining in transplanted salivary glands. (A) Immunohistochemical staining showing no specific expression of DsRed in the salivary gland of a C57BL/6 mouse. **(B)** Immunohistochemical staining showing extensive DsRed expression throughout the salivary gland of a DsRed mouse. Scale bars 50 µm.

REFERENCES

1 Morrison, S. J. & Spradling, A. C. Stem cells and niches: mechanisms that promote stem cell maintenance throughout life. *Cell* **132**, 598-611, doi:10.1016/j.cell.2008.01.038 (2008).

2 Clarke, M. F. & Fuller, M. Stem cells and cancer: two faces of eve. *Cell* **124**, 1111-1115, doi:10.1016/j.cell.2006.03.011 (2006).

3 Clevers, H., Loh, K. M. & Nusse, R. Stem cell signaling. An integral program for tissue renewal and regeneration: Wnt signaling and stem cell control. *Science* **346**, 1248012, doi:10.1126/science.1248012 (2014).

4 Ball, W. D. Development of the rat salivary glands. 3. Mesenchymal specificity in the morphogenesis of the embryonic submaxillary and sublingual glands of the rat. *The Journal of experimental zoology* **188**, 277-288, doi:10.1002/jez.1401880304 (1974).

5 Denny, P. C., Chai, Y., Klauser, D. K. & Denny, P. A. Parenchymal cell proliferation and mechanisms for maintenance of granular duct and acinar cell populations in adult male mouse submandibular gland. *Anat Rec* **235**, 475-485, doi:10.1002/ar.1092350316 (1993).

6 Denny, P. C., Ball, W. D. & Redman, R. S. Salivary glands: a paradigm for diversity of gland development. *Critical reviews in oral biology and medicine : an official publication of the American Association of Oral Biologists* **8**, 51-75 (1997).

7 Ihrler, S., Zietz, C., Sendelhofert, A., Lang, S., Blasenbreu-Vogt, S. & Lohrs, U. A morphogenetic concept of salivary duct regeneration and metaplasia. *Virchows Archiv : an international journal of pathology* **440**, 519-526, doi:10.1007/s004280100537 (2002).

8 Osailan, S. M., Proctor, G. B., Carpenter, G. H., Paterson, K. L. & McGurk, M. Recovery of rat submandibular salivary gland function following removal of obstruction: a sialometrical and sialochemical study. *International journal of experimental pathology* **87**, 411-423, doi:10.1111/j.1365-2613.2006.00500.x (2006).

9 Pringle, S., Van Os, R. & Coppes, R. P. Concise review: Adult salivary gland stem cells and a potential therapy for xerostomia. *Stem Cells* **31**, 613-619, doi:10.1002/stem.1327 (2013).

10 Hisatomi, Y., Okumura, K., Nakamura, K., Matsumoto, S., Satoh, A., Nagano, K. *et al.* Flow cytometric isolation of endodermal progenitors from mouse salivary gland differentiate into hepatic and pancreatic lineages. *Hepatology* **39**, 667-675, doi:10.1002/hep.20063 (2004).

11 Nanduri, L. S., Maimets, M., Pringle, S. A., van der Zwaag, M., van Os, R. P. & Coppes, R. P. Regeneration of irradiated salivary glands with stem cell marker expressing cells. *Radiother Oncol* **99**, 367-372, doi:10.1016/j.radonc.2011.05.085 (2011).

12 Lombaert, I. M., Brunsting, J. F., Wierenga, P. K., Faber, H., Stokman, M. A., Kok, T. *et al.* Rescue of salivary gland function after stem cell transplantation in irradiated glands. *PLoS One* **3**, e2063, doi:10.1371/journal.pone.0002063 (2008).

13 Nanduri, L. S., Lombaert, I. M., van der Zwaag, M., Faber, H., Brunsting, J. F., van Os, R. P. *et al.* Salisphere derived c-Kit+ cell transplantation restores tissue homeostasis in irradiated salivary gland. *Radiother Oncol* **108**, 458-463, doi:10.1016/j.radonc.2013.05.020 (2013).

14 Nanduri, L. S., Baanstra, M., Faber, H., Rocchi, C., Zwart, E., de Haan, G. *et al.* Purification and ex vivo expansion of fully functional salivary gland stem cells. *Stem Cell Reports* **3**, 957-964, doi:10.1016/j.stemcr.2014.09.015 (2014).

15 Xiao, N., Lin, Y., Cao, H., Sirjani, D., Giaccia, A. J., Koong, A. C. *et al.* Neurotrophic factor GDNF promotes survival of salivary stem cells. *J Clin Invest* **124**, 3364-3377, doi:10.1172/JCI74096 (2014).
16 Clevers, H. & Nusse, R. Wnt/beta-catenin signaling and disease. *Cell* **149**, 1192-1205, doi:10.1016/j.cell.2012.05.012 (2012).
17 Barker, N., van Es, J. H., Kuipers, J., Kujala, P., van den Born, M., Cozijnsen, M. *et al.* Identification of stem cells in small intestine and colon by marker gene Lgr5. *Nature* **449**, 1003-1007, doi:10.1038/nature06196 (2007).
18 Jaks, V., Barker, N., Kasper, M., van Es, J. H., Snippert, H. J., Clevers, H. *et al.* Lgr5 marks cycling, yet long-lived, hair follicle stem cells. *Nature genetics* **40**, 1291-1299, doi:10.1038/ng.239 (2008).
19 Barker, N., Huch, M., Kujala, P., van de Wetering, M., Snippert, H. J., van Es, J. H. *et al.* Lgr5(+ve) stem cells drive self-renewal in the stomach and build long-lived gastric units in vitro. *Cell stem cell* **6**, 25-36, doi:10.1016/j.stem.2009.11.013 (2010).
20 Barker, N., Rookmaaker, M. B., Kujala, P., Ng, A., Leushacke, M., Snippert, H. *et al.* Lgr5(+ve) stem/progenitor cells contribute to nephron formation during kidney development. *Cell reports* **2**, 540-552, doi:10.1016/j.celrep.2012.08.018 (2012).
21 Huch, M., Dorrell, C., Boj, S. F., van Es, J. H., Li, V. S., van de Wetering, M. *et al.* In vitro expansion of single Lgr5+ liver stem cells induced by Wnt-driven regeneration. *Nature* **494**, 247-250, doi:10.1038/nature11826 (2013).
22 Hai, B., Yang, Z., Millar, S. E., Choi, Y. S., Taketo, M. M., Nagy, A. *et al.* Wnt/beta-catenin signaling regulates postnatal development and regeneration of the salivary gland. *Stem cells and development* **19**, 1793-1801, doi:10.1089/scd.2009.0499 (2010).
23 Hai, B., Yang, Z., Shangguan, L., Zhao, Y., Boyer, A. & Liu, F. Concurrent transient activation of Wnt/beta-catenin pathway prevents radiation damage to salivary glands. *Int J Radiat Oncol Biol Phys* **83**, e109-116, doi:10.1016/j.ijrobp.2011.11.062 (2012).
24 Denny, P. C. & Denny, P. A. Dynamics of parenchymal cell division, differentiation, and apoptosis in the young adult female mouse submandibular gland. *The Anatomical record* **254**, 408-417 (1999).
25 Man, Y. G., Ball, W. D., Marchetti, L. & Hand, A. R. Contributions of intercalated duct cells to the normal parenchyma of submandibular glands of adult rats. *The Anatomical record* **263**, 202-214 (2001).
26 Dan, Y. Y., Riehle, K. J., Lazaro, C., Teoh, N., Haque, J., Campbell, J. S. *et al.* Isolation of multipotent progenitor cells from human fetal liver capable of differentiating into liver and mesenchymal lineages. *Proceedings of the National Academy of Sciences of the United States of America* **103**, 9912-9917, doi:10.1073/pnas.0603824103 (2006).
27 Huch, M., Gehart, H., van Boxtel, R., Hamer, K., Blokzijl, F., Verstegen, M. M. *et al.* Long-term culture of genome-stable bipotent stem cells from adult human liver. *Cell* **160**, 299-312, doi:10.1016/j.cell.2014.11.050 (2015).
28 Huch, M., Bonfanti, P., Boj, S. F., Sato, T., Loomans, C. J., van de Wetering, M. *et al.* Unlimited in vitro expansion of adult bi-potent pancreas progenitors through the Lgr5/R-spondin axis. *The EMBO journal* **32**, 2708-2721, doi:10.1038/emboj.2013.204 (2013).

29 Yamashita, T., Budhu, A., Forgues, M. & Wang, X. W. Activation of hepatic stem cell marker EpCAM by Wnt-beta-catenin signaling in hepatocellular carcinoma. *Cancer research* **67**, 10831-10839, doi:10.1158/0008-5472.CAN-07-0908 (2007).
30 Peifer, M., Sweeton, D., Casey, M. & Wieschaus, E. wingless signal and Zeste-white 3 kinase trigger opposing changes in the intracellular distribution of Armadillo. *Development* **120**, 369-380 (1994).
31 Aure, M. H., Konieczny, S. F. & Ovitt, C. E. Salivary gland homeostasis is maintained through acinar cell self-duplication. *Dev Cell* **33**, 231-237, doi:10.1016/j.devcel.2015.02.013 (2015).
32 Snippert, H. J., Haegebarth, A., Kasper, M., Jaks, V., van Es, J. H., Barker, N. *et al.* Lgr6 marks stem cells in the hair follicle that generate all cell lineages of the skin. *Science* **327**, 1385-1389, doi:10.1126/science.1184733 (2010).
33 Sokol, E., Kramer, D., Diercks, G. F., Kuipers, J., Jonkman, M. F., Pas, H. H. *et al.* Large-Scale Electron Microscopy Maps of Patient Skin and Mucosa Provide Insight into Pathogenesis of Blistering Diseases. *The Journal of investigative dermatology*, doi:10.1038/jid.2015.109 (2015).
34 Knox, S. M., Lombaert, I. M., Reed, X., Vitale-Cross, L., Gutkind, J. S. & Hoffman, M. P. Parasympathetic innervation maintains epithelial progenitor cells during salivary organogenesis. *Science* **329**, 1645-1647, doi:10.1126/science.1192046 (2010).
35 Chen, B., Dodge, M. E., Tang, W., Lu, J., Ma, Z., Fan, C. W. *et al.* Small molecule-mediated disruption of Wnt-dependent signaling in tissue regeneration and cancer. *Nature chemical biology* **5**, 100-107, doi:10.1038/nchembio.137 (2009).
36 Finch, P. W., He, X., Kelley, M. J., Uren, A., Schaudies, R. P., Popescu, N. C. *et al.* Purification and molecular cloning of a secreted, Frizzled-related antagonist of Wnt action. *Proceedings of the National Academy of Sciences of the United States of America* **94**, 6770-6775 (1997).
37 Sato, T., Vries, R. G., Snippert, H. J., van de Wetering, M., Barker, N., Stange, D. E. *et al.* Single Lgr5 stem cells build crypt-villus structures in vitro without a mesenchymal niche. *Nature* **459**, 262-265, doi:10.1038/nature07935 (2009).
38 Reya, T., Duncan, A. W., Ailles, L., Domen, J., Scherer, D. C., Willert, K. *et al.* A role for Wnt signalling in self-renewal of haematopoietic stem cells. *Nature* **423**, 409-414, doi:10.1038/nature01593 (2003).
39 Zeng, Y. A. & Nusse, R. Wnt proteins are self-renewal factors for mammary stem cells and promote their long-term expansion in culture. *Cell stem cell* **6**, 568-577, doi:10.1016/j.stem.2010.03.020 (2010).
40 Lim, X., Tan, S. H., Koh, W. L., Chau, R. M., Yan, K. S., Kuo, C. J. *et al.* Interfollicular epidermal stem cells self-renew via autocrine Wnt signaling. *Science* **342**, 1226-1230, doi:10.1126/science.1239730 (2013).
41 Ogawa, M., Oshima, M., Imamura, A., Sekine, Y., Ishida, K., Yamashita, K. *et al.* Functional salivary gland regeneration by transplantation of a bioengineered organ germ. *Nature communications* **4**, 2498, doi:10.1038/ncomms3498 (2013).
42 Huelsken, J., Vogel, R., Erdmann, B., Cotsarelis, G. & Birchmeier, W. beta-Catenin controls hair follicle morphogenesis and stem cell differentiation in the skin. *Cell* **105**, 533-545 (2001).
43 Zetsche, B., Gootenberg, J. S., Abudayyeh, O. O., Slaymaker, I. M., Makarova, K. S., Essletzbichler, P. *et al.* Cpf1 Is a Single RNA-Guided Endonuclease of a Class 2 CRISPR-Cas System. *Cell* **163**, 759-771, doi:10.1016/j.cell.2015.09.038 (2015).

44 Lombaert, I. M., Brunsting, J. F., Wierenga, P. K., Kampinga, H. H., de Haan, G. & Coppes, R. P. Cytokine treatment improves parenchymal and vascular damage of salivary glands after irradiation. *Clin Cancer Res* **14**, 7741-7750, doi:10.1158/1078-0432.CCR-08-1449 (2008).

45 Steinberg, Z., Myers, C., Heim, V. M., Lathrop, C. A., Rebustini, I. T., Stewart, J. S. *et al.* FGFR2b signaling regulates ex vivo submandibular gland epithelial cell proliferation and branching morphogenesis. *Development* **132**, 1223-1234, doi:10.1242/dev.01690 (2005).

46 Yamamoto, S., Fukumoto, E., Yoshizaki, K., Iwamoto, T., Yamada, A., Tanaka, K. *et al.* Platelet-derived growth factor receptor regulates salivary gland morphogenesis via fibroblast growth factor expression. *The Journal of biological chemistry* **283**, 23139-23149, doi:10.1074/jbc.M710308200 (2008).

47 Haara, O., Koivisto, T. & Miettinen, P. J. EGF-receptor regulates salivary gland branching morphogenesis by supporting proliferation and maturation of epithelial cells and survival of mesenchymal cells. *Differentiation; research in biological diversity* **77**, 298-306, doi:10.1016/j.diff.2008.10.006 (2009).

48 Schnell, U., Kuipers, J., Mueller, J. L., Veenstra-Algra, A., Sivagnanam, M. & Giepmans, B. N. Absence of cell-surface EpCAM in congenital tufting enteropathy. *Human molecular genetics* **22**, 2566-2571, doi:10.1093/hmg/ddt105 (2013).

CHAPTER 4

THE HIPPO SIGNALING PATHWAY EFFECTOR YAP REGULATES SALIVARY GLAND REGENERATION AFTER INJURY

Rocchi C., Serrano Martinez P., Jellema - de Bruin A., Baanstra M., Brouwer U., del Angel Zuivre C., Schepers H., van Os R., BarazzuoL L.*, Coppes RP.

Under revision in Science Signalling

ABSTRACT

Adult tissue regeneration involves dynamic cellular processes responsible for restoring tissue integrity. Little is known about how adult salivary gland cells sense and respond to injury. Here, using an *in vivo* injury model and through genetic loss/gain of function approaches in salivary gland-derived organoids, we define a central role for YAP during adult salivary gland regeneration. We show that YAP nuclear activity changes dynamically between homeostasis and regeneration in the salivary gland epithelium. Local injury of the gland triggers a region-specific YAP activation at the regeneration site, characterized by activation of the normally dormant ductal compartment. In a well-defined *in vitro* organoid model, we show that promoting YAP nuclear translocation increases the regenerative ability of human salivary gland-derived cells. Our results point towards a YAP-driven plasticity of the salivary gland ductal compartment during regeneration that could be used to promote *in vivo* regeneration of salivary gland after radiation-induced damage.

INTRODUCTION

Radiotherapy is a major part of the treatment for over 500,000 patients per year that are diagnosed with head and neck cancer worldwide[1]. While radiotherapy treatment significantly increases the survival rate of these patients, the unavoidable inclusion of healthy salivary glands within the radiation field leads to a high probability of developing late radiation toxicity which culminates in the onset of radiation-induced hyposalivation and consequential xerostomia[2-4]. The extent of structural damage and subsequent functional decline of an organ following radiation treatment depends on the cellular radiosensitivity of the given tissue[4]. The salivary gland epithelium is composed of morphologically and functionally distinct cell types and compartments. Similarly to other adult tissue, such as the intestine[5], different compartments of the gland display differential responses, both in terms of kinetics and sensitivity to ionizing radiation[6].

The acinar compartment, the functional unit of the salivary gland, has been shown to be mitotically active, thus playing an important role in the maintenance of adult mouse salivary gland tissue homeostasis[7,8]. Additionally, upon radiation damage, $SOX2^+$ acinar cells show regenerative capacity within the first 30 days post-irradiation[8]. Their regenerative ability, however, appears to be limited and their eventual loss of cell division ability due to radiation-induced damage leads to the loss of the functional acinar compartment[6,8,9]. In contrast, the excretory and striated ductal network compartment, which modifies the saliva composition and directs saliva secretion to the oral cavity, appears to be in a relative quiescent state[10,11]. The slow turnover and the observation that ductal cells show little to no loss of ductal specific marker expression[8] after irradiation may be indicative of a relative resistance to radiation-induced damage, similar to what has been observed for brain cells[12,13].

While some lineage tracing studies in adult mouse salivary glands point towards the existence of mainly progenitor lineage-restricted populations ($K14^+$, $Kit^+/K5^+$) within the ductal compartment[9,14], others point to a possible plasticity of the intercalated and excretory duct compartments in contributing to the regeneration of the functional acinar unit of irradiated glands[15]. However, after high radiation doses these compartments fail to fully regenerate the salivary gland tissue ultimately leading to the functional loss of saliva production[15-17].

Interestingly, we previously showed in both rats and patients, that the radiation dose delivered to the region of the parotid salivary gland containing the main ducts predicts salivary gland dysfunction. This supports the idea of the existence of a stem/progenitor cell population residing in the main ducts and therefore sparing this region has been proposed as a means to preserve saliva production after radiotherapy treatment[18].

Furthermore, *in vitro* 3D culture of salivary gland Wnt-responsive cells showed the ability of $Epcam^{high}$ excretory ductal cells to enter into the cell cycle and give rise to organoids containing terminally differentiated acinar cells, indicating that the appropriate signaling stimulation can

guide the quiescent compartment to an active state able to generate a tissue resembling structure[19]. While Wnt signaling has been shown to drive *in vitro* self-renewal and maintenance of salivary glands, the pathways involved in regeneration of the salivary glands after injury remain poorly understood.

The transcriptional regulator Yes-Associated Protein (YAP) emerged as a key control factor of tissue growth and regeneration in tissue such as intestine, liver and skin[20,21]. YAP transcriptional activity relies on the changes in its nuclear-cytoplasmic localization that is tightly controlled by the Hippo pathway. The Hippo pathway consists of a highly conserved group of serine/threonine kinases that by phosphorylation of YAP at serine 127 determine its cellular localization. The core of the Hippo pathway is composed of MST1 and MST2 kinases which activate the Lats1 and Lats2 kinases to promote YAP phosphorylation. Inactivation of the pathway kinase cascade leads to YAP nuclear translocation and its transcriptional activation by binding to TEA-domain (Tead) family of transcription factors. The ectopic activation of YAP has been shown to promote stem/progenitor cell expansion and to de-differentiate somatic epithelial cells, such as mammary gland and pancreas, to a stem cell state[22] opening important opportunities for regenerative medicine. The ability to increase the stem cell number or transiently activate existing stem cells could be especially important in tissues with a slow turnover or a low regenerative potential, such as the salivary gland[21,23]. YAP function has been examined in the salivary gland and has been implicated in development[24]. Deletion of YAP in the developing salivary gland epithelium leads to severe morphogenesis defects of the glands reflecting compromised epithelial patterning. The inability of YAP-null embryonic salivary gland epithelium to specify ductal progenitors indicates the importance of YAP during the development of salivary glands[24]. However, little is known about where and when YAP is expressed in adult salivary glands[25].

Here we report an essential role of YAP transcriptional activity during homeostasis and regeneration of adult salivary glands after damage. Although YAP has a pivotal role during salivary gland development[24], we show that its activity changes dynamically between homeostasis and regeneration in the adult glands. Upon salivary gland ligation, YAP nuclear expression increases in the ductal compartment at the site of regeneration, supporting the existence of a relatively quiescent stem cell-like population residing in the striated ducts[19]. Using a 3D organoid culture system that has been shown to mimic regeneration[19,26,27], we provide evidence that YAP inactivation diminishes organoid formation efficiency of mouse and human adult salivary gland-derived stem/progenitor cells, while YAP-overexpression promotes stem/progenitor organoid culture expansion. We finally demonstrate that induction of YAP nuclear translocation after irradiation promotes regeneration *in vitro*. Our data further support the idea that regeneration upon severe damage can be mediated by newly activated

ductal cells and that stimulation of YAP nuclear translocation can be used to promote regeneration of radiation-damaged salivary glands.

RESULTS

Increased nuclear YAP expression in salivary gland ductal cells during regeneration

To gain an insight into the role of YAP during adult salivary gland regeneration, an *in vivo* mouse injury model was used to investigate the expression pattern of YAP in adult salivary glands. Both submandibular glands were sutured below the sublingual glands to induce a dynamic regenerative response of the gland. The suture causes the division of the salivary gland into two distinct regions: a lower caudal region of the gland and an upper cranial region (Figure 1A and Supplementary figure 1A and B).

To trace proliferating cells, the mice were subjected to two BrdU injections at 24 and 6 hours prior to sacrifice. Within 14 days of ligation a loss of tissue morphology in the lower caudal region of the gland was evident (Supplementary figure 1B and D). Immunofluorescence staining (IF) showed a pronounced reduction in AQP5 positive acinar cells in the lower caudal region of the gland, while the upper cranial region retained a strong AQP5 expression, indicative of an intact and functional acinar cell compartment (Supplementary figure 1C and D).

Given the pronounced damage that the suture induced to the lower caudal region of the gland, it was next investigated if regeneration was taking place in the upper cranial region of the gland. Interestingly, a significant increase of BrdU positive cells was observed in close proximity to the suture (the regeneration site) (Figure 1B and C and Supplementary figure 1D) compared to the homeostatic area of the gland (distal from the regeneration site) and to the control gland. While the control gland and the homeostatic area of the ligated gland predominantly showed proliferation activity in the intercalated duct and acinar compartments, at the regeneration site proliferation was predominantly in the excretory/striated ductal compartment. These differences in the regenerative response between the cranial and caudal regions of the gland are in accordance with the idea that the ductal compartment contributes to the regeneration of the gland[18].

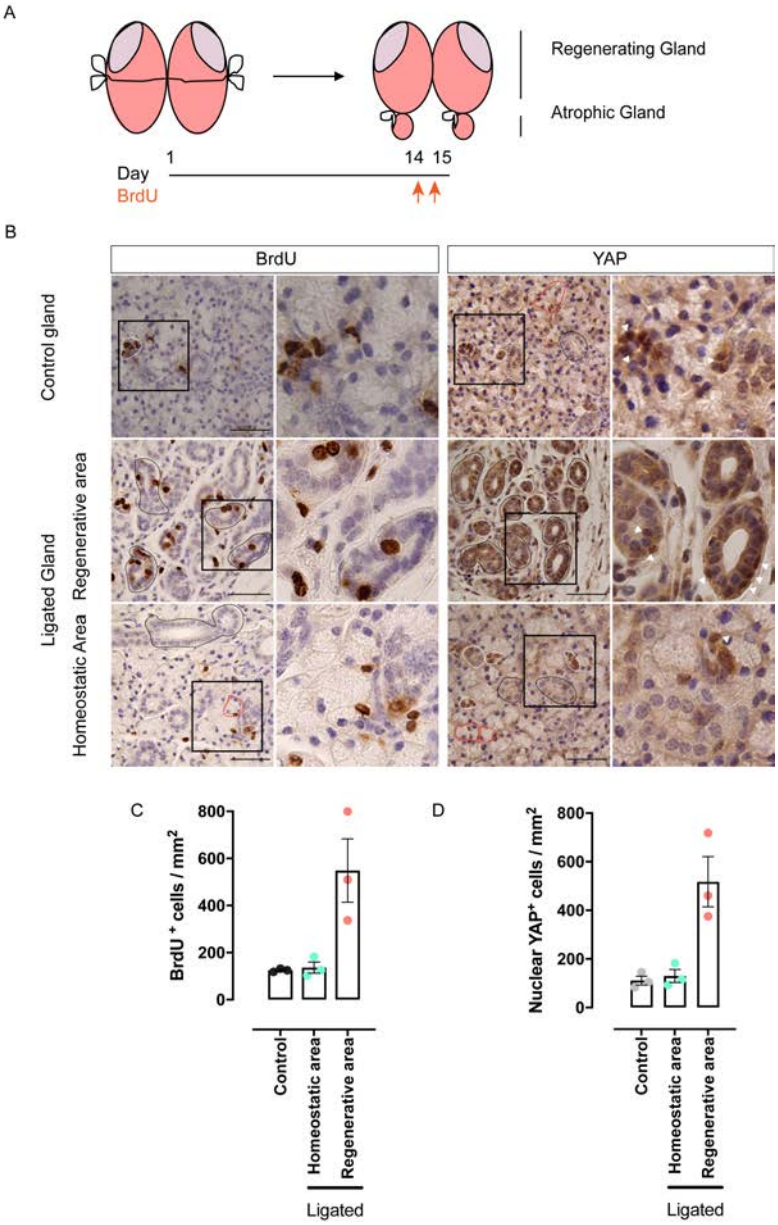

Figure 1: YAP nuclear expression increases in the striated and excretory ductal compartment at the regenerative site of the submandibular gland. (A) Schematic showing the time course of the ligation injury model and BrdU pulses in adult mice. (B) Control and ligated submandibular glands stained at 14 days after ligation for BrdU and total YAP. Intercalated ducts are outlined in white, striated and excretory ducts in black and acinar cells in red. Cells with YAP nuclear localization are indicated by white arrowheads. Scale bars represent 50 μm. (C) Quantification of BrdU positive and (D) nuclear YAP cells per mm^2 of tissue in control homeostatic gland, regenerative and homeostatic areas in ligated gland (see also Supplementary Figure 1B). n=3 for both control glands and ligated glands, were n indicates the number of animals. Each dot represents analysis from a different mouse (n=3). Data are represented as mean ± SEM (C and D). Statistical significance between the three groups was determined using one-way ANOVA ($p<0.05$). *$p<0.05$, **$p<0.01$, ***$p<0.001$, ****$p<0.0001$.

As YAP localization within the cell, nuclear or cytoplasmic, identifies its activity, we examined whether we could observe distinct patterns of YAP protein localization within the ligated

submandibular gland and the control gland. Consecutive submandibular gland sections were analyzed by immunohistochemistry (IHC) against total YAP and BrdU. IHC analysis revealed that YAP expression was predominant in the acinar and intercalated ductal compartments in control salivary glands (Figure 1B), while the excretory ductal compartment, where quiescent stem/progenitor cells have been suggested to reside[19,28], showed a weak cytoplasmic localization of YAP. Interestingly, at two weeks post ligation, IHC of total YAP showed a markedly distinct distribution in the submandibular gland epithelium, with increased nuclear YAP expression in the excretory and striated ductal compartments at the regeneration site and a lower level of nuclear YAP confined predominantly to the acinar intercalated duct compartment in the homeostatic area of the ligated gland (Figure 1B and D and Supplementary figure 1E). The BrdU and YAP expression patterns along the proximal-distal axis of the regeneration site are indicative of a potential dynamic role of YAP during regeneration of the injured gland.

YAP nuclear activity drives mouse salivary gland organoid growth

Given the increased YAP nuclear localization in salivary gland ductal cells during regeneration *in vivo,* we next investigated the function of YAP on self-renewal potential of mouse salivary gland stem/progenitor cells (SGSPCs) as assessed *in vitro* by organoid forming efficiency (OFE). Purified primary ductal cells derived from mouse submandibular glands were seeded in Matrigel and cultured as previously described[19,26]. Treatment with verteporfin (VP), an inhibitor of the YAP-TEAD interaction, at the single cell stage (day 0) completely abrogated organoid formation (Figure 2A-C), whereas drug exposure in 4-day-old organoids led to a collapse of the organoid structure and impairment to form secondary organoids in the next passage (Figure 2D and E; Supplementary figure 2A and B). Similarly, siRNA-mediated YAP knockdown led to a significant decrease of salivary gland OFE (Figure 2F and G). These data suggest an essential role of YAP nuclear activity for SGSPC self-renewal and maintenance. We next reasoned that if inhibition of YAP nuclear activity led to reduced OFE, enhanced YAP nuclear translocation could lead to increased self-renewal potential and expansion of SGSPCs. Indeed, when organoid-derived cells were treated with lysophosphatidic acid (LPA), a compound known to inhibit LATS1/2 kinase activity by modifying cytoskeleton tension[29], simultaneous increase of total YAP protein levels and OFE were observed (Figure 3A-D). To further confirm the importance of YAP nuclear activity in SGSPC self-renewal, we performed siRNA-mediated knock down of LATS1 which resulted in an increased OFE compared to control (Figure 3E-G), further highlighting the importance of Hippo signaling on the activity of SGSPCs.

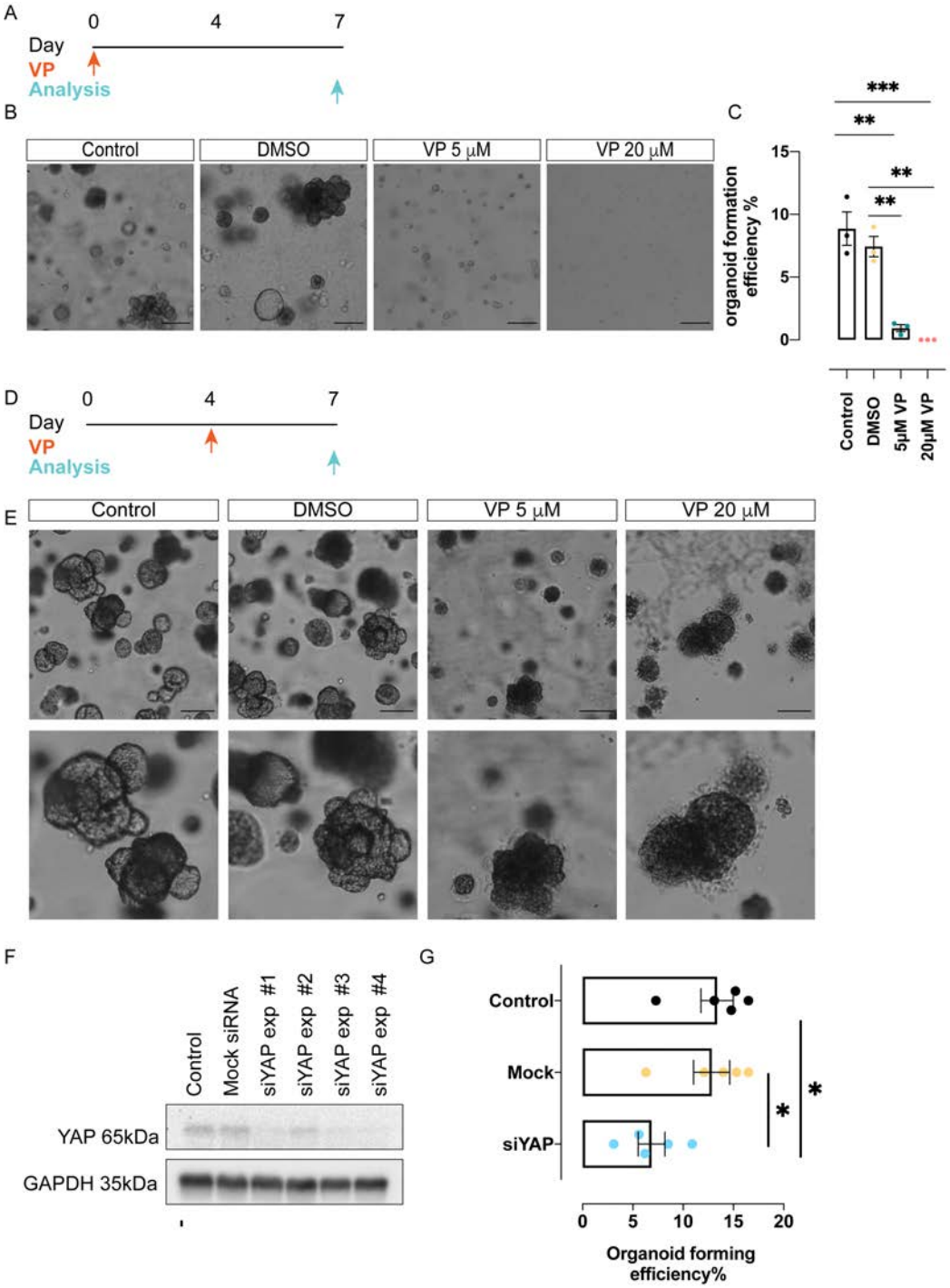

Figure 2: Inhibition of YAP nuclear activity reduces self-renewal ability of mouse adult salivary gland derived stem/progenitor cells. (A)(D) Schematics showing the time course of VP treatment on salivary gland derived organoid culture. (B)(E) Representative images of salivary gland derived organoids treated with DMSO or VP 5 μM and 20 μM respectively from the start of the culture and (B) and from day 4 of culture (E). Scale bar=50 μm. (C) Organoid forming efficiency of mouse salivary gland cells after treatment with VP 5 μM and 20 μM starting at day 0. (F) Western blot analysis of mouse salivary gland organoids showing siYAP knock down efficiency in 4 different experiment (Exp #1 to Exp #4), and (G) their relative ability to form organoids measured as organoid forming efficiency % (OFE%). Mock= scrambled siRNA. Control= no transfection. Data are represented as the mean ± SEM (C)(G). (C)(G) One-way ANOVA was used to test the differences between the groups ($p<0.05$). *$p<0.05$, **$p<0.01$, ***$p<0.001$, ****$p<0.0001$.

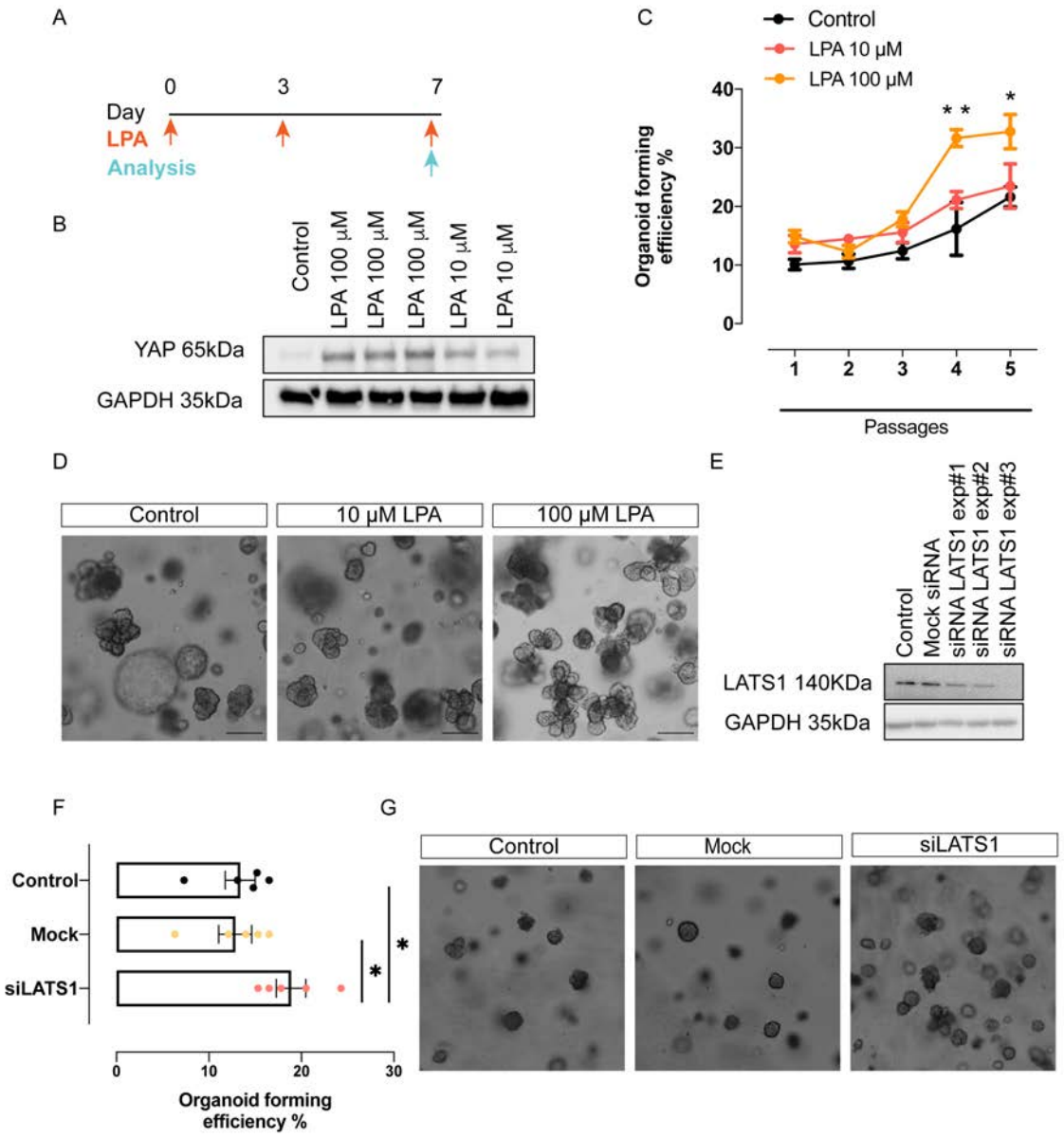

Figure 3: **Stimulation of YAP nuclear translocation increases the ability of salivary gland derived cells to form secondary organoids.** (A) Schematic showing the time line of LPA treatment in salivary gland derived organoid culture. (B) Western blot of lysates from mouse salivary gland derived organoids treated with or without 10 and 100 µM LPA. (C) Organoid formation efficiency of mouse salivary gland derived organoid treated with 10 and 100 µM LPA over 5 passages of culture. (D) Representative pictures of mouse salivary gland organoids at the end of P5 after treatment with 10 and 100 µM LPA. Scale bar=50 µm. (E) Western blot analysis of mouse salivary gland organoids showing siLATS1 knock down efficiency in 3 different experiments (Exp#1 to Exp#3) and (F) their relative ability to form secondary organoids measured as organoid forming efficiency (OFE%). Each dot represents a culture derived from a different mouse (n=4). Mock= scrambled siRNA. Control= no transfection. Data are represented as the mean ± SEM (C)(F). Two-way ANOVA (mixed model) (C); One-way ANOVA (F). *p<0.05, **p<0.01, ***p<0.001, ****p<0.0001.

YAP overexpression in human salivary gland-derived organoids increases stem cell potential

To validate that increased YAP nuclear translocation increases self-renewal ability of SGSPCs, we investigated whether ectopic expression of YAP in salivary gland organoid-derived cells would have similar effects as LPA treatment. We transduced salivary gland organoid-derived cells at the end of passage 1 (P1) with a lentiviral vector encoding for WT YAP-t2A-mCherry[30]. As a control, cells were transduced with an empty lentiviral vector (t2a-mCherry). Transduced cells were cultured for 7 days and, following isolation by fluorescence activated cell sorting for mCherry, plated in Matrigel to assess secondary organoid formation potential (Figure 4A). YAP overexpression was confirmed by western blot analysis of total YAP protein (Figure 4B). Strikingly, YAP overexpressing cells (mCherry+ YAP^{OE}) cultured in EM media gave rise to a significantly higher number of secondary organoids compared to mCherry- and control transduced cells (Supplementary Figure 3A). This difference was maintained for the subsequent 3 passages (Figure 4C and D). We also found that the number of cells and the size of the organoids were significantly increased in YAP^{OE} cells compared to controls (Figure 4E and F). Notably, we observed that overexpression of YAP in human salivary gland-derived organoids cultured in Wnt enriched media (WRYTN) did not support the expansion of the culture to the same extent as in EM media, indicating that YAP and Wnt could have different roles or act at different time during the regeneration process (Supplementary Figure 3B and C). These results indicate that ectopic YAP overexpression promotes stem cell properties in human salivary gland-derived cells. Interestingly, human salivary gland organoids overexpressing YAP cultured in EM media, showed a branched morphology phenotype at the end of P1 which greatly differs from the round shape phenotype of non-overexpressing control organoids and organoids cultured in WRYTN (Supplementary Figure 4A and B). Collectively, several lines of evidence indicate that promoting YAP nuclear translocation increases human SGSPC potential.

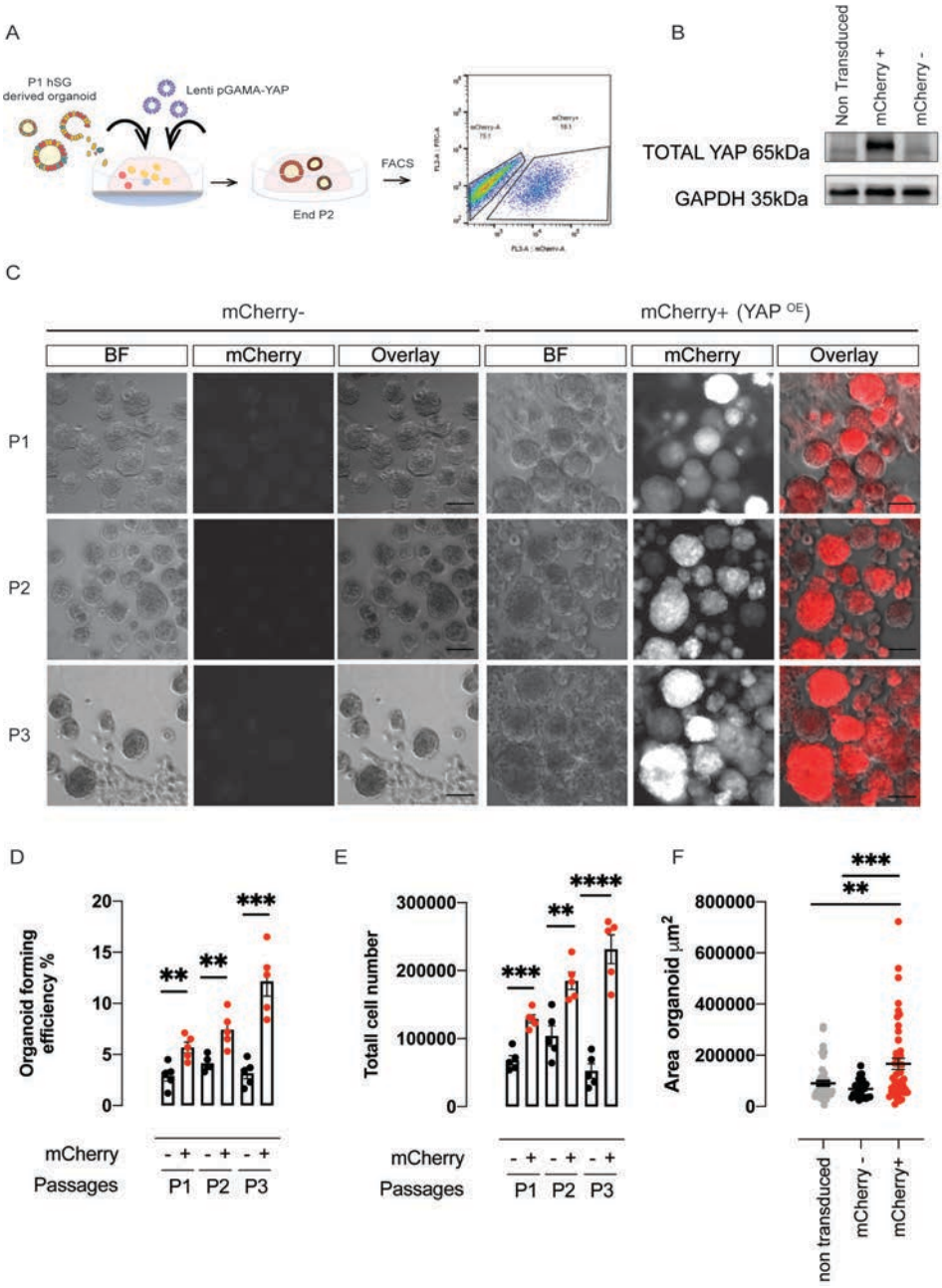

Figure 4: YAP overexpression in human salivary gland derived cells increases their self-renewal potential. (A) Schematic of the experiment performed on human salivary gland (hSG) derived organoids with the lentiviral vector pGAMA-YAP. FACS plot showing the % of mCherry positive cells indicative of the efficiency of transduction. (B) Western blot analysis of lysates derived from hSG transduced organoids showing YAP protein level in non-transduced cells, mCherry- and mCherry+ cells. (C) Representative images and (D) quantification of secondary and tertiary organoids, (E) total cell numbers and (F) area of hSG derived organoid transduced with pGAMA-YAP. Each dot represents a culture derived from a different patient (n=4). Red dots= mCherry+; Black dots= mCherry-. Data are represented as the mean ± SEM (D)(E)(F). One-way ANOVA (D)(E)(F). *p<0.05, **p<0.01, ***p<0.001, ****p<0.0001.

Chemical inhibition of Mst1/2 kinases promotes regeneration of salivary gland organoids after irradiation

The proximal-distal patterning of nuclear YAP from the regeneration site in mouse ligated salivary gland suggests that YAP nuclear activity is required during regeneration. As YAP-overexpression in human SGSPs increases their self-renewal ability, we next investigated whether increased YAP nuclear activity could improve human salivary gland organoid response to irradiation. To increase YAP nuclear translocation upon radiation treatment, we treated human salivary gland organoids with a potent inhibitor of MST1/MST2 kinases (XMU-MP-1), an upstream effector of the Hippo pathway, known to promote liver regeneration after damage[31]. Human SGSP-derived organoids were seeded as single cells in Matrigel and irradiated with 2 and 4 Gy.

Upon irradiation, XMU-MP1-treated cells showed a higher OFE, thus reflecting a higher survival fraction of stem cells after treatment compared to irradiated-only organoids (Figure 5A, Supplementary Figure 5A). Interestingly, the irradiated and XMU-MP1-treated organoids were larger in size than irradiated-only organoids, indicating that after radiation treatment induction of YAP nuclear activity increased proliferation of human SGSPCs and improved the response of human salivary gland organoids to radiation damage (Figure 5B-E). These results indicate that our 3D organoid culture system can be used as a tool to study the underlying signaling pathways responsible for regeneration after radiation-induced damage. It also emphasizes the importance of YAP nuclear translocation as part of the Hippo signaling pathway during regeneration after damage.

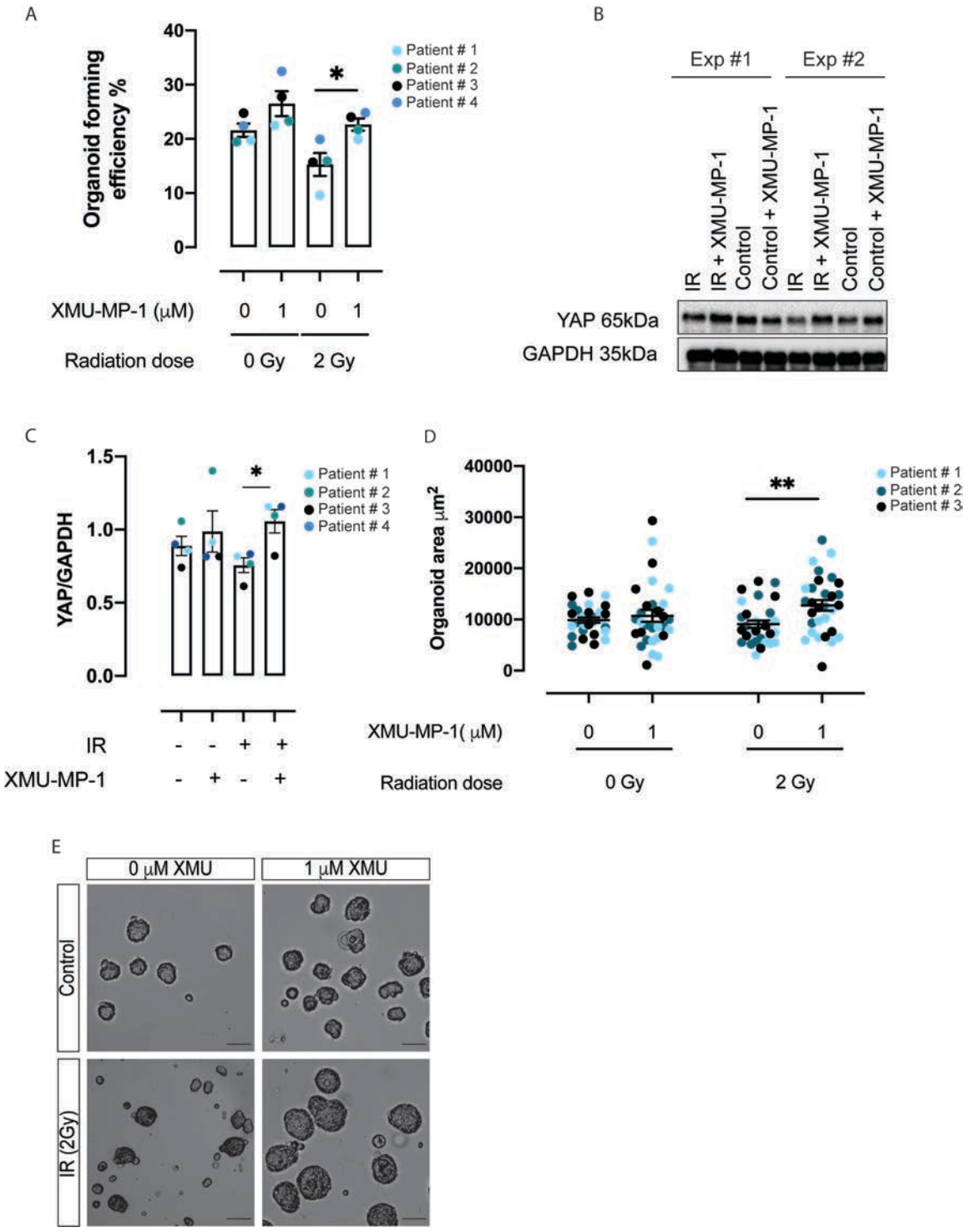

Figure 5: Chemical inhibition of MST1/2 improves salivary gland organoid irradiation response. (A) Organoid forming efficiency and (D) area of hSG derived organoids upon irradiation treatment (2 Gy) and inhibition of MST1/2 kinase by the use of XMU-MP1 (1 μM). Each color represents a culture derived from a different patient (n=4). (B) Western blot analysis of lysates derived from hSG transduced organoids showing changes in total YAP expression upon irradiation and XMU-MP-1 treatment in two different experiments (Exp#1, Exp#2). (C) Quantification of (B). Each color represents a different patient (n=4). (E) Representative images of hSG derived organoid upon irradiation (2 Gy) and XMU-MP-1 (1 μM) treatment. Scale bar=50 μm. Data are represented as the mean ± SEM (A) (C) (D). T-test (C); Two-way ANOVA (mixed model) (A)(C). *p<0.05, **p<0.01, ***p<0.001, ****p<0.0001.

DISCUSSION

Following injury, stem and progenitor cells attempt to re-build both the structural and functional units of the damaged tissue through a tightly controlled process that involves self-renewal and differentiation. While it has been shown that transplantation of SGSPCs can be used to rescue the secretory function of damaged salivary glands[19,26,32,33], the mechanisms of regeneration after injury remain unclear. Here we report that YAP activation is a critical step in the regeneration process of damaged adult salivary glands and modulation of this pathway could be used to increase salivary gland stem cell potential.

We show that during homeostasis salivary glands display low levels of YAP activity, which is confined to the acinar and intercalated ductal compartments known to be involved in the maintenance of the glands[7-9,11,34,35]. After local injury, a dramatic and region-specific increase in nuclear YAP expression was observed at the regeneration site of the ligated gland supporting a role for the Hippo signaling pathway in the response to damage. YAP activation in the normally dormant excretory duct compartment of the salivary gland may point towards the existence in the salivary gland of a 'revival' stem cell population, similar to that seen in the intestine[36], capable of reconstituting the structural and functional unit of the damaged tissue. While differences in regeneration response can be due to the level of damage inflicted to the gland, the ability to regenerate the damaged epithelium by transient YAP activation following ligation-induced damage may indicate that cellular plasticity, rather than a distinct resident population of progenitor cells, might be responsible for the regeneration of the salivary gland after pronounced damage, in contrast to what has been proposed so far in the salivary gland field[8,9].

While future *in vivo* work combining different injury models and lineage tracing could be fundamental to verifying the potential contribution of YAP-activated cells to acinar cell replacement, our *in vitro* data from organoid cultures of salivary gland-derived cells seem to support the regeneration ability of the main striated/excretory ductal cell compartment.

Salivary gland-derived organoid cultures arise from Epcam+ cells of the ductal epithelium compartment[19], known to be quiescent during homeostasis[7]. The ability of these cells to give rise to 3D structures (organoids), which contain all major cell types spatially arranged similarly to the tissue of origin, and to rescue hyposalivation phenotype upon intraglandular transplantation, proves their potential plasticity and regeneration ability. The *in vivo* observations that YAP is involved in salivary gland regeneration are supported by a strong decline in organoid formation efficiency upon YAP knock down. Both promoting YAP nuclear translocation and YAP overexpression showed a pronounced increase in the ability to form secondary and tertiary organoids uncovering a role for YAP in the maintenance of stem/progenitor cells and self-renewal capacity. In agreement with what has recently been shown in intestinal organoids, it is tempting to speculate that salivary gland organoid

development also follows a regenerative model that requires transient YAP activation[27]. Contrary to what was shown in the intestine, but in accordance with the *in vivo* role of YAP in embryonic salivary gland development[24], sustained overexpression of YAP seems to promote the formation of branched organoids. The *in vitro* formation of a branched epithelial ductal network indicates a potential additional function of YAP in patterning and morphogenesis of human adult salivary gland epithelium. While our observation, highlights a role for YAP in directing the expansion and patterning of adult human salivary gland epithelial progenitors, its role in specification and differentiation of salivary gland epithelium is still unknown. Further work is needed to elucidate whether YAP could function as a "gatekeeper" in the salivary gland, marking the boundary between the ductal compartment and the distal acinar compartment, similar to other branching organs[37-39].

Finally, we show that our previously described *in vitro* model can be used to study the regeneration of salivary gland organoids after irradiation, and that stimulating YAP nuclear translocation after irradiation significantly improves the radiation response of human salivary gland-derived cells. Moreover, transient chemical stimulation of YAP nuclear translocation could open new treatment possibilities to promote regeneration or enhance expansion of human SGSPCs *in vitro* for transplantation purposes.

While our study supports the idea of YAP as a sensor of tissue integrity[27] and a key driver in regeneration of both murine and human salivary gland organoids, future studies should elucidate whether modulating YAP levels could induce *in vivo* regeneration, with the aim to use this approach as a regenerative therapy to ameliorate radiation-induced hyposalivation.

METHODS

Mice

Eight to twelve-week-old female C57BL/6 mice were purchased from Envigo. Mice were housed in environmentally controlled rooms, under conventional conditions and fed ad libitum in the Animal Facility of the University Medical Center Groningen. All experiments were performed according to approved institutional animal care and use committee (IACUC) protocols of the University of Groningen (under IVD protocol number 184824-01-001).

Patients

Human non-malignant submandibular gland tissues were obtained from donors after informed consent and Institutional Review Board (IRB) approval during an elective head and neck dissection procedure for the removal of squamous cell carcinoma of the oral cavity at the University Medical Centre Groningen (UMCG) and Medical Centre Leuwaarden (MCL).

Contact for Reagent and Resource Sharing

Further information and requests for resources and reagents should be directed to and will be fulfilled by the corresponding authors, Dr. L. Barazzuol (l.barazzuol@umcg.nl) and Prof. Dr. R.P Coppes (r.p.coppes01@umg.nl).

Mouse submandibular gland ligation

C57BL6 mice were anesthetize with the use of isoflurane. A small incision was made in the neck to visualize the submandibular glands. Each submandibular gland was ligated with the use of (non-dissolvable) wire just below the sublingual gland. Fourteen days later the animals were re-anaesthetized and sacrifice by cervical dislocation. Submandibular glands were isolated, ligation removed and fixed in 4% formaldehyde overnight (ON) at room temperature (RT). Section were used for immunohistochemistry and immunofluorescence (as describe below) to determine the regenerative status of the gland.

Control mice with matching sex and age were subjected to a mock ligation surgery that included isoflurane anesthesia, exposure of the submandibular gland and suture of the incision.

BrdU injection and labelling

To assess proliferation in the ligated submandibular gland as well as the control gland, mice were subjected to two intraperitoneal Bromodeoxyuridine (BrdU; Sigma B5002-1G) injections. BrdU was dissolved in physiologic solution at a concentration of 50 mg/Kg of body weight and injected respectively 24 h and 6 h prior sacrifice. Following BrdU labeling, IHC and quantification was performed as describe below.

Immunohistochemistry and immunofluorescence

All antibodies and reagents used in this study are listed in the Table 1.

Table 1: Antibodies and reagents		
REAGENT or RESOURCE	**Source**	**Identifier**
Antibodies		
Rabbit anti-YAP1	Cell Signaling Technology	#4912
Rat anti-BrdU	Biorad	OBT0030G
Rabbit anti-AQP5	Alomone	AQP-005
Rabbit anti LATS1	Cell Signaling Technology	#9153
Goat anti-rabbit Alexa Fluor 488	Invitrogen	A11008
Donkey anti-mouse Alexa Fluor 594	Invitrogen	A21203
Swine anti-rabbit	Dako	E0431
Polyclonal rabbit anti Rat Immunoglobulins biotinylated	Dako	E0468
Anti -mouse IgG HRP linked	GE healthcare	GENXA931
Anti- rabbit IgG HRP linked	GE healthcare	NA934
Mouse anti-GAPDH	Fitzgerald	
Chemical, Peptides and Recombinant Protein		
1-Oleoyl lysophosphatidic acid sodium salt (LPA)	Tocris- Biotechne	3854
Verteporfin (VP)	Tocris	5305
XMU-MP-1	MedChemExpress	HY-100526
Noggin	Preprotech-Bioconnect	120-10C
A8301	Tocris Bioscience	2939
N2 Supplement	Gibco	17502-048
EGF	Sigma	E9644
FGF2	Preprotech-Bioconnect	100-18B
Dexamethasone	Sigma	d4902-25mg

Insulin	Sigma	I6634-100MG
Y-27632 dihydrochloride Rho-Kinase inhibitor	Bioconnect-Abcam	ab120129
HBSS (Hank's Balanced Salt Solution)	GIBCO	14175-129
BSA (Bovine Serum Albumin)	GIBCO	15260037
Glutamax	ThermoFisher Scientific	35050038
Pen/Strep	Invitrogen	15140-163
DMEM F12 (Dulbecco's modified Eagle's medium: F12)	Gibco/Invitrogen	11320-074
Wnt3a conditioned media	Clvers's lab gift	N/A
R-spondin1 conditioned media	Clvers's lab gift	N/A
Matrigel	Vwr	356235
0.05% Tryosin-EDTA	Invitrogen (Gibco Life Technologies)	25300-096
Dispase	Gibco/Invitrogen	17105-041
Collagenase type II	Gibco/Invitrogen	17101-015
Hyaluronidase	Sigma	H3506-5G
$CaCl_2$	Sigma	C3306 SIGMA
5-Bromo-2′-deoxyuridine (brdu used for mouse injection	Sigma	B5002-1G
FBS (Fetal Bovine Serum)	Greiner	lotnr 11113
DAB (3.3'-diaminobenzide)	Sigma	D4168-50set
DAPI	ThermoFisher Scientific/Pierce	62247
Eukit	Sigma	03989-500 ml
Mounting Medium	DAKO	S3025
Triton X-100	Sigma	X100
Tween-20	Sigma	P1379-500ML

H_2O_2 Peroxidase	Jackson ImmunoResearch Laboratories	011-000-120
Donkey serum	Jackson ImmunoResearch Laboratories	017-000-121
Formaldehyde solution	Sigma	252549-1L
Hematoxylin	Sigma	H3136-25G
TGX Stain-Free™ FastCast™ Acrylamide Kit, 10%	Biorad	1610183
TGX Stain-Free™ FastCast™ Acrylamide Kit, 12%	Biorad	1610185
PEI	Sigma	P3143
Polybrene	Santa Cruz	Sc134220
Lipofectamine 2000	Invitrogen	11668-019
Safil 5/0 polyglycolic acid braided coated absorbable	B. Braun	1048507
Critical Commercial Assay		
Vectastatin® ABC kit	Vector	PK-6100
Experimental Model		
C57BL/6 inbred mice	Envigo	057
Oligonucleotides		
Dharmacon siGENOME siRNA smart pools: YAP1(22601)	Dharmacon	M-046247-01-0005
Dharmacon siGENOME siRNA smart pools: LATS1	Dharmacon	M-063467-01-0005
Dharmacon siGENOME siRNA smart pools: stk3	Dharmacon	M-040440-01-0005 5 nmol
Dharmacon siGENOME siRNA smart pools: stk4	Dharmacon	M-059385-01-0005 5 nmol
pGAMA EMPTY Fw		ctagcgaattctt
pGAMA EMPTY Rev		cgaagaattcg
Recombinant DNA		

psPAX2	Addgene	#12260
pCMV-VSV-G	Addgene	#8454
pGAMA-YAP	Addgene	#74942
p-GAMA-empty	This work	N/A
Software and Algorithms		
Prism 8 (Graphpad Software)		https://www.graphpad.com/scientific-software/prism/
Image J	NIH	https://imagej.nih.gov/ij/

Tissue was isolated and fixed in 4% formaldehyde ON at RT. The tissue was then processed using an automatic tissue processor machine (Leica TP 1020) before standard paraffine embedding. Tissue blocks were sliced in 5 μm section using a rotary microtome (Thermo Fisher HM 340E).

For Light microscopy, sections were dewaxed before heat-activated antigen retrieval using a citric acid buffer containing 0.05% tween 20 (10mM, pH: 6). Section were allowed to cool down for 1h at RT followed by permeabilization on 0,4% Triton X-100 in PBS. For BrdU staining sections were treated with 2,5 M HCl for 25 minutes at RT and neutralized with 0,1 M sodium borate (pH= 8.5) for 5 minutes. Sections were permeabilized in blocking solution (1% BSA, 4% serum and 0.4% Triton X-100 in PBS) and incubate with desired primary antibody ON at 4°C. The day after section were washed thoroughly and quenched in 0.5% H_2O_2 followed by secondary antibody incubation in blocking buffer (1% BSA, 4% donkey serum and 0.4% Triton X-100 in PBS). Vectastatin® ABC kit (Vector labs) was used followed by 3.3'-diaminobenzide (DAB) kit to detect positive staining. Finally, sections were counterstained with Hematoxilin, dehydrated and coverslip mounted using Eukit. Negative controls were generated by omitting primary antibody.

For fluorescence double labelling, heated induced antigen retrieval and DNA denaturation procedure were performed as describe above. Slides were incubated for 1 h at RT in blocking buffer (1% BSA, 4% serum and 0.4% Triton X-100 in PBS) prior incubating in primary antibody solution ON at 4°C. The following day section were washed in PBS 3 times for 10 minutes each, followed by incubation in secondary antibody for 1 h at RT. Finally slides were stained with DAPI (4',6-diamidino-2-phenylindole,dihydrochloride) and mounted using DAKO mounting media. Antibodies used and their final dilutions are as follows: rabbit anti-YAP1 (Cell Signaling), 1:100; rat anti-BrdU (Biorad)1:100; rabbit anti AQP5 (Alomone) 1:200.

Isolation of mouse and human submandibular gland derived cells

Submandibular gland were harvested from healthy adult mice, mechanically digested with the use of gentleMACS dissociator (Milteny) and simultaneously digested in the digestion buffer containing collagenase type II (0.63mg/mL; Gibco), hyaluronidase (0.5 mg/mL, Sigma-Aldrich) and $CaCl_2$ (6.25mM; Sigma-Aldrich) in Hank's Balanced Salt Solution (HBSS) containing 1% bovine serum albumin (BSA; Invitrogen).The digestion procedure was repeated for 2 periods of 30 minutes in a shaking water bath at 37°C. To obtain optimal digestion, both submandibular glands from a single mouse were digested in a 2 mL volume of the digestion buffer. At the end of the digestion, cells were collected by centrifugation at 400 G for 5 minutes and filter through a 100 μm cell strainers (BD Biosciences). The resultant cell suspension was centrifuged at 400 G for 5 minutes and resuspended in Dulbecco's modified Eagle's medium: F12 (DMEM F12) containing Pen/Strep antibiotics (Invitrogen), Glutamax, 20 ng/mL epidermal growth factor (EGF; Sigma Aldrich), 20 ng/mL fibroblast growth factor-2 (Sigma- Aldrich), N2 (Invitrogen), 10 μg/mL insulin (Sigma-Aldrich) and 1 μM dexamethasone (Sigma-Aldrich). Cells were plated at a density of $4x10^4$ cells per well in a 12-well plate and incubate at 37°C and 5% CO_2 for 3 days as floating primary culture.

For human submandibular gland cells isolation, the biopsies collected in the operating room were transferred to the lab in a 50 mL falcon tube containing HBSS 1% BSA on ice. The biopsy was weighted in a sterile petri dish and using a sterile disposable scalpel minced into small pieces. To obtain optimal digestion 20 mg of tissue was processed per 1 mL of digestion buffer volume, with a maximum of 100 mg of tissue per tube. The human biopsies were then processed in the same manner as the mouse tissue.

Self-renewal assay of mouse and human salivary gland derived cells

Three days-old primary spheres were harvested and dispersed to single cells suspension using 0.05% trypsin EDTA (Invitrogen). Single cells were counted and resuspended in culture media at a final concentration of $0.4x10^6$ or $0.8x10^6$ cells per mL. 25 μL of cell suspension was mix on ice with 50 μL of ice cold Matrigel and the 75 μL gel pipetted in the middle of a 12-well plate. After solidifying the Matrigel gels were covered in enriched media (EM; DMEM/F12, pen/strep [1x; Invitrogen], glutamax [1x; Invitrogen], N2 [1x; Gibco], EGF [20ng/mL; Sigma Aldrich], FGF2 [20ng/nL;sigma Aldrich], insulin [10μg/mL;Sigma Aldrich], dexamethasone [1μM; Sigma Aldrich], Y27632 [10μM; Sigma Aldrich] or WRYTN (DMEM/F12, pen/strep [1x; Invitrogen], glutamax [1x; Invitrogen], N2 [1x; Gibco], EGF [20ng/mL; Sigma Aldrich], FGF2 [20ng/nL;sigma Aldrich], insulin [10μg/mL;Sigma Aldrich], dexamethasone [1μM; Sigma Aldrich], noggin[50ng/mL; Preprotech-Bioconnect], A8301[1μM Tocris], Y27632 [10μM; Sigma Aldrich], 10% R-spondin1 conditioned medium and 50 % Wnt3a conditioned medium)

media. One week after seeding (end of the passage), the media was replaced with Dispase enzyme (1 mg/mL in DEMEM F12 at 37°C for 30-45 minutes) to dissolve the gels. All the organoids released from the dissolved gels were processed to single cells using 0.05% trypsin-EDTA treatment to form single cell suspension. Organoids and cell number at the end of the passage were noted and the secondary organoid derived single cells re-seeded in Matrigel to start a new passage. Number of organoids and single cells at the end of each passage were used to calculate Organoid Formation Efficiency percentage (OFE%) and Population Doubling as follows:

$$Organoid\ Formation\ Efficiency\ (OFE\%) = \frac{Number\ of\ Organoid\ harvested\ at\ the\ end\ of\ the\ pasaage}{Number\ of\ single\ cells\ seeded\ at\ the\ beginning\ of\ the\ passage}\ x\ 100$$

$$Population\ Doubling = \frac{\ln(harvestes\ cells/seeded\ cells)}{ln2}$$

Irradiation treatment of mouse salivary gland-derived cells

Photon irradiation of 3-day-old salivary gland derived organoid seeded in Matrigel was performed with ^{137}Cs source (IBL 637 Cesium-137 γ-ray machine) with a dose rate of 0.59 Gy/min.

Drug treatment of mouse and human salivary gland-derived cells

To modulate YAP activity during mouse salivary gland-derived organoid growth, cells were culture in WRY (DMEM/F12, pen/strep [1x; Invitrogen], glutamax [1x; Invitrogen], N2 [1x; Gibco], EGF [20ng/mL; Sigma Aldrich], FGF2 [20ng/nL;sigma Aldrich], insulin [10μg/mL;Sigma Aldrich], dexamethasone [1μM; Sigma Aldrich], Y27632 [10μM; Sigma Aldrich], 10% R-spondin1 conditioned medium and 50 % Wnt3a conditioned medium). For YAP nuclear activity inhibition mouse organoid were culture in WRY containing 5 or 20 μM of Verteporfin. Drug was added at day 0 or at day 4 of culture and media refreshed every 2 days. Control culture were cultured in WRY containing the same % of DMSO. To promote YAP nuclear translocation, lysophosphatidic acid (LPA) was added to mouse organoid culture at a final concentration of 10 or 100 μM from day 0. Media was refreshed every 3 days.

To promote YAP nuclear translocation in human salivary gland-derived organoid culture, single cells were seeded in Matrigel and cultured in WRYTN media. Immediately after irradiation, XMU-MP-1 was added to the wells at a final concentration of 1 or 3μM. Media was changed every 2 days.

siRNA transfection of mouse salivary gland-derived cells

Mouse salivary gland derived-cells were transfected using siGENOME SMART pool siRNAYAP, siRNALATS1 and Non-Targeting siRNA from Dharmacon. Cells were seeded at a density of 1 to $1.5x10^5$ in a 12-well plate and incubated at 37°C and 5% CO_2. The second day transfection was done using Lipofectamine 2000 (Invitrogen) in antibiotic-free medium according to manufacturer instructions. Five hours post transfection media was replaced with EM culture media and cells incubate at 37°C and 5% CO_2. A second round of transfection was performed and 5 h post transfection cells were counted, resuspended in EM culture media at a density $0.8x10^6$ cells/mL and seeded in Matrigel. 72 h from the first transfection cells were harvested to check efficiency of knock down. At the end of the passage organoids and cells were counted to establish the OFE%.

Lentiviral production

$1.5x10^6$ HEK293T cells were plated in poly-L-lysin coated 10 cm dish in DMEM supplemented with 10% FBS, Pen/Strep [1x; Invitrogen], Glutamax [1x; Invitrogen] and incubated ON at 37°C and 5% CO_2. On the next day cells were transfected with 3 μg of p-GAMA YAP (AddGene)[30] or empty p-GAMA 3 μg of the packaging plasmid PAX2, 0.7 μg of envelope plasmid VSV-G and 40 μL of PEI (1 μg/mL) as previously described[40]. On the next day medium was changed to DMEM F12. Two days after transfection the viruses were collected, filtered through a sterile syringe filter with a 0.45 μm pore size and hydrophilic PVDF membrane and frozen in 250 μL aliquots at -80 °C. We have tittered the virus-containing supernatant by transduction of mCherry gene. Viruses were always in the range of $5.0x10^6$ – $7.0x10^6$ transduction unit (TU)/mL.

Lentiviral transduction and cell sorting of human salivary gland-derived cells.

Human salivary gland-derived organoids at the end of passage 1 (P1) were released from Matrigel and dissociated to single cells using 0.05% trypsin-EDTA (Invitrogen). Human salivary gland organoid-derived single cells were counted and resuspended in WRYTN media to a final concentration of $2.5x10^6$ cells per mL. For each 100 μL of cell suspension 250 μL of viral supernatant and polybrene (6 μg/mL) was added. The mixture was divided in 350 μL aliquots in a 24-well plate and incubated ON at 37°C and 5% CO_2. The day after transduction single cells were counted to adjust for dead cells, resuspended in media to a final concentration of $0.8x10^6$ cells per mL and seeded in Matrigel into 12-well plate. The cells were cultured for 7 to 10 days in WRYTN media at 37°C and 5% CO_2. At day 7 (or day 10) Matrigel was dissolved with the use of Dispase enzyme (1 mg/mL), and organoids dispersed to single cells with the use of 0.05% trypsin-EDTA. Cells were washed with 0.2% BSA in PBS and

resuspended in 0.2% BSA with the viability dye (DAPI) in PBS. YAP overexpressing cells were isolated by fluorescence-activated cell sorting for mCherry-positive cells, seeded in Matrigel and cultured in WRYTN for the next 3 passages.

Immunoblot

To monitor endogenous gene responses, mouse and human organoids were harvested and centrifuged pellets homogenized by sonication in 2x Laemnli buffer. Protein concentration of the lysates was determined using Bradford quantification method. Homogenates were then boiled at 99°C for 5 minutes and equal protein amounts were separated with 10 or 12% polyacrylamide gels and transfered to PVDF membranes using Trans Blot Turbo System (Bio-Rad). The membranes were blocked in 5% BSA in PBS-Teween-20 and incubated 1 h at RT. Incubation with primary antibodies was done ON at 4°C following by incubation with HRP-conjugated secondary antibodies. Membranes were developed using ECL reagent (Thermo Fisher Scientific) and the signal was detected using ChemiDoc imager (Biorad). Densiometric analysis of western blots at non-saturated exposure were performed using Image J software and the values normalized against the one of GAPDH loading control. For immunoblots, the following primary antibodies at the indicated dilutions were used: rabbit anti-YAP (Cell Signaling) 1:1000; rabbit anti-LATS1 (Cell Signaling) 1:1000; mouse anti-GAPDH (Fitzgerald) 1:10000.

Quantification of IHC images

Light microscopy images taken at 40x, were quantitatively analysed for BrdU and YAP nuclear expression with the use of ImageJ (NIH) software. Five areas (309.68 μm x 232.26 μm) were chosen within each regenerative and homeostatic area of the ligated and control glands, from 3 biological replicates (n=3). For each replicate three different sections were analysed. To quantify the nuclear localization of BrdU or YAP, for each picture, positive nuclear were manually counted using Image J software and the means of positive nuclear/mm^2 calculated and plotted with the use of GraphPad Prism8.

Statistical Analysis

All statistical analyses in this study were performed using GraphPad Prism8 software (GraphPad, La Jolla, CA, USA). The number of mice, patients or individual organoids analyzed (n), presented error bars (SEM), statistical analysis and p values are all stated in each figure or figure legend.

REFERENCES

1 Siegel, R. L., Miller, K. D. & Jemal, A. Cancer statistics, 2018. *CA Cancer J Clin* **68**, 7-30, doi:10.3322/caac.21442 (2018).

2 Vissink, A., Jansma, J., Spijkervet, F. K., Burlage, F. R. & Coppes, R. P. Oral sequelae of head and neck radiotherapy. *Crit Rev Oral Biol Med* **14**, 199-212, doi:10.1177/154411130301400305 (2003).

3 Grundmann, O., Mitchell, G. C. & Limesand, K. H. Sensitivity of salivary glands to radiation: from animal models to therapies. *J Dent Res* **88**, 894-903, doi:10.1177/0022034509343143 (2009).

4 Barnett, G. C., West, C. M., Dunning, A. M., Elliott, R. M., Coles, C. E., Pharoah, P. D. *et al.* Normal tissue reactions to radiotherapy: towards tailoring treatment dose by genotype. *Nat Rev Cancer* **9**, 134-142, doi:10.1038/nrc2587 (2009).

5 Metcalfe, C., Kljavin, N. M., Ybarra, R. & de Sauvage, F. J. Lgr5+ stem cells are indispensable for radiation-induced intestinal regeneration. *Cell Stem Cell* **14**, 149-159, doi:10.1016/j.stem.2013.11.008 (2014).

6 Konings, A. W., Coppes, R. P. & Vissink, A. On the mechanism of salivary gland radiosensitivity. *Int J Radiat Oncol Biol Phys* **62**, 1187-1194, doi:10.1016/j.ijrobp.2004.12.051 (2005).

7 Aure, M. H., Konieczny, S. F. & Ovitt, C. E. Salivary gland homeostasis is maintained through acinar cell self-duplication. *Dev Cell* **33**, 231-237, doi:10.1016/j.devcel.2015.02.013 (2015).

8 Emmerson, E., May, A. J., Berthoin, L., Cruz-Pacheco, N., Nathan, S., Mattingly, A. J. *et al.* Salivary glands regenerate after radiation injury through SOX2-mediated secretory cell replacement. *EMBO Mol Med* **10**, doi:10.15252/emmm.201708051 (2018).

9 May, A. J., Cruz-Pacheco, N., Emmerson, E., Gaylord, E. A., Seidel, K., Nathan, S. *et al.* Diverse progenitor cells preserve salivary gland ductal architecture after radiation-induced damage. *Development* **145**, doi:10.1242/dev.166363 (2018).

10 Peter, B., Van Waarde, M. A., Vissink, A., s-Gravenmade, E. J. & Konings, A. W. Radiation-induced cell proliferation in the parotid and submandibular glands of the rat. *Radiat Res* **140**, 257-265 (1994).

11 Kimoto, M., Yura, Y., Kishino, M., Toyosawa, S. & Ogawa, Y. Label-retaining cells in the rat submandibular gland. *J Histochem Cytochem* **56**, 15-24, doi:10.1369/jhc.7A7269.2007 (2008).

12 Barazzuol, L., Ju, L. & Jeggo, P. A. A coordinated DNA damage response promotes adult quiescent neural stem cell activation. *PLoS Biol* **15**, e2001264, doi:10.1371/journal.pbio.2001264 (2017).

13 Kalamakis, G., Brune, D., Ravichandran, S., Bolz, J., Fan, W., Ziebell, F. *et al.* Quiescence Modulates Stem Cell Maintenance and Regenerative Capacity in the Aging Brain. *Cell* **176**, 1407-1419 e1414, doi:10.1016/j.cell.2019.01.040 (2019).

14 Kwak, M., Alston, N. & Ghazizadeh, S. Identification of Stem Cells in the Secretory Complex of Salivary Glands. *J Dent Res* **95**, 776-783, doi:10.1177/0022034516634664 (2016).

15 Weng, P. L., Aure, M. H., Maruyama, T. & Ovitt, C. E. Limited Regeneration of Adult Salivary Glands after Severe Injury Involves Cellular Plasticity. *Cell Rep* **24**, 1464-1470 e1463, doi:10.1016/j.celrep.2018.07.016 (2018).

16 Sullivan, C. A., Haddad, R. I., Tishler, R. B., Mahadevan, A. & Krane, J. F. Chemoradiation-induced cell loss in human submandibular glands. *Laryngoscope* **115**, 958-964, doi:10.1097/01.MLG.0000163340.90211.87 (2005).
17 Marmary, Y., Adar, R., Gaska, S., Wygoda, A., Maly, A., Cohen, J. *et al.* Radiation-Induced Loss of Salivary Gland Function Is Driven by Cellular Senescence and Prevented by IL6 Modulation. *Cancer Res* **76**, 1170-1180, doi:10.1158/0008-5472.CAN-15-1671 (2016).
18 van Luijk, P., Pringle, S., Deasy, J. O., Moiseenko, V. V., Faber, H., Hovan, A. *et al.* Sparing the region of the salivary gland containing stem cells preserves saliva production after radiotherapy for head and neck cancer. *Sci Transl Med* **7**, 305ra147, doi:10.1126/scitranslmed.aac4441 (2015).
19 Maimets, M., Rocchi, C., Bron, R., Pringle, S., Kuipers, J., Giepmans, B. N. *et al.* Long-Term In Vitro Expansion of Salivary Gland Stem Cells Driven by Wnt Signals. *Stem Cell Reports* **6**, 150-162, doi:10.1016/j.stemcr.2015.11.009 (2016).
20 Yui, S., Azzolin, L., Maimets, M., Pedersen, M. T., Fordham, R. P., Hansen, S. L. *et al.* YAP/TAZ-Dependent Reprogramming of Colonic Epithelium Links ECM Remodeling to Tissue Regeneration. *Cell Stem Cell* **22**, 35-49 e37, doi:10.1016/j.stem.2017.11.001 (2018).
21 Moya, I. M. & Halder, G. Hippo-YAP/TAZ signalling in organ regeneration and regenerative medicine. *Nat Rev Mol Cell Biol* **20**, 211-226, doi:10.1038/s41580-018-0086-y (2019).
22 Panciera, T., Azzolin, L., Fujimura, A., Di Biagio, D., Frasson, C., Bresolin, S. *et al.* Induction of Expandable Tissue-Specific Stem/Progenitor Cells through Transient Expression of YAP/TAZ. *Cell Stem Cell* **19**, 725-737, doi:10.1016/j.stem.2016.08.009 (2016).
23 Gregorieff, A., Liu, Y., Inanlou, M. R., Khomchuk, Y. & Wrana, J. L. Yap-dependent reprogramming of Lgr5(+) stem cells drives intestinal regeneration and cancer. *Nature* **526**, 715-718, doi:10.1038/nature15382 (2015).
24 Szymaniak, A. D., Mi, R., McCarthy, S. E., Gower, A. C., Reynolds, T. L., Mingueneau, M. *et al.* The Hippo pathway effector YAP is an essential regulator of ductal progenitor patterning in the mouse submandibular gland. *Elife* **6**, doi:10.7554/eLife.23499 (2017).
25 Chibly, A. M., Wong, W. Y., Pier, M., Cheng, H., Mu, Y., Chen, J. *et al.* aPKCzeta-dependent Repression of Yap is Necessary for Functional Restoration of Irradiated Salivary Glands with IGF-1. *Sci Rep* **8**, 6347, doi:10.1038/s41598-018-24678-4 (2018).
26 Nanduri, L. S., Baanstra, M., Faber, H., Rocchi, C., Zwart, E., de Haan, G. *et al.* Purification and ex vivo expansion of fully functional salivary gland stem cells. *Stem Cell Reports* **3**, 957-964, doi:10.1016/j.stemcr.2014.09.015 (2014).
27 Serra, D., Mayr, U., Boni, A., Lukonin, I., Rempfler, M., Challet Meylan, L. *et al.* Self-organization and symmetry breaking in intestinal organoid development. *Nature* **569**, 66-72, doi:10.1038/s41586-019-1146-y (2019).
28 Pringle, S., Van Os, R. & Coppes, R. P. Concise review: Adult salivary gland stem cells and a potential therapy for xerostomia. *Stem Cells* **31**, 613-619, doi:10.1002/stem.1327 (2013).
29 Yu, F. X., Zhao, B., Panupinthu, N., Jewell, J. L., Lian, I., Wang, L. H. *et al.* Regulation of the Hippo-YAP pathway by G-protein-coupled receptor signaling. *Cell* **150**, 780-791, doi:10.1016/j.cell.2012.06.037 (2012).

30 Qin, H., Hejna, M., Liu, Y., Percharde, M., Wossidlo, M., Blouin, L. *et al.* YAP Induces Human Naive Pluripotency. *Cell Rep* **14**, 2301-2312, doi:10.1016/j.celrep.2016.02.036 (2016).
31 Fan, F., He, Z., Kong, L. L., Chen, Q., Yuan, Q., Zhang, S. *et al.* Pharmacological targeting of kinases MST1 and MST2 augments tissue repair and regeneration. *Sci Transl Med* **8**, 352ra108, doi:10.1126/scitranslmed.aaf2304 (2016).
32 Nanduri, L. S., Lombaert, I. M., van der Zwaag, M., Faber, H., Brunsting, J. F., van Os, R. P. *et al.* Salisphere derived c-Kit+ cell transplantation restores tissue homeostasis in irradiated salivary gland. *Radiother Oncol* **108**, 458-463, doi:10.1016/j.radonc.2013.05.020 (2013).
33 Pringle, S., Maimets, M., van der Zwaag, M., Stokman, M. A., van Gosliga, D., Zwart, E. *et al.* Human Salivary Gland Stem Cells Functionally Restore Radiation Damaged Salivary Glands. *Stem Cells* **34**, 640-652, doi:10.1002/stem.2278 (2016).
34 Kim, Y. J., Kwon, H. J., Shinozaki, N., Hashimoto, S., Shimono, M., Cho, S. W. *et al.* Comparative analysis of ABCG2-expressing and label-retaining cells in mouse submandibular gland. *Cell Tissue Res* **334**, 47-53, doi:10.1007/s00441-008-0667-8 (2008).
35 Chibly, A. M., Querin, L., Harris, Z. & Limesand, K. H. Label-retaining cells in the adult murine salivary glands possess characteristics of adult progenitor cells. *PLoS One* **9**, e107893, doi:10.1371/journal.pone.0107893 (2014).
36 Ayyaz, A., Kumar, S., Sangiorgi, B., Ghoshal, B., Gosio, J., Ouladan, S. *et al.* Single-cell transcriptomes of the regenerating intestine reveal a revival stem cell. *Nature* **569**, 121-125, doi:10.1038/s41586-019-1154-y (2019).
37 Mahoney, J. E., Mori, M., Szymaniak, A. D., Varelas, X. & Cardoso, W. V. The hippo pathway effector Yap controls patterning and differentiation of airway epithelial progenitors. *Dev Cell* **30**, 137-150, doi:10.1016/j.devcel.2014.06.003 (2014).
38 Mamidi, A., Prawiro, C., Seymour, P. A., de Lichtenberg, K. H., Jackson, A., Serup, P. *et al.* Mechanosignalling via integrins directs fate decisions of pancreatic progenitors. *Nature* **564**, 114-118, doi:10.1038/s41586-018-0762-2 (2018).
39 Rosado-Olivieri, E. A., Anderson, K., Kenty, J. H. & Melton, D. A. YAP inhibition enhances the differentiation of functional stem cell-derived insulin-producing beta cells. *Nat Commun* **10**, 1464, doi:10.1038/s41467-019-09404-6 (2019).
40 Schepers, H., van Gosliga, D., Wierenga, A. T., Eggen, B. J., Schuringa, J. J. & Vellenga, E. STAT5 is required for long-term maintenance of normal and leukemic human stem/progenitor cells. *Blood* **110**, 2880-2888, doi:10.1182/blood-2006-08-039073 (2007).

ACKNOWLEDGMENTS

This work was supported by grant from the Dutch Cancer Society (RUG 2013-5792).

We would like to thank the maxillofacial surgical team of the University Medical Center Groningen and Medical Center Leeuwarden for providing donor biopsies and Monique Stokman for coordination of the sampling of donor material. We also thank the staff members of the Department of Biomedical Sciences of Cells & Systems of the University Medical Center of Groningen for fruitful discussion of data.

AUTHOR CONTRIBUTIONS

C.R. conceptualized the study, designed and performed the experiments, analyzed and interpreted data, wrote and edited the paper. P.S.M. and U.B. contributed to the animal ligation experiments. A.J.d.B. and M.B. contributed to the mouse and human *in vitro* experiments (culture and FACS). C.d.A.Z. contributed to the mouse *in vitro* experiments. H.S. contributed to the conceptualization of the lentiviral experiments, interpretation of the data as well as manuscript writing. R.v.O. and L.B. contributed to the conceptualization, data analysis and interpretation, as well as the design and manuscript writing. R.P.C. provided financial support, contributed to the conceptualization, data analysis and interpretation as well as the design and manuscript writing.

SUPPLEMENTARY INFORMATION

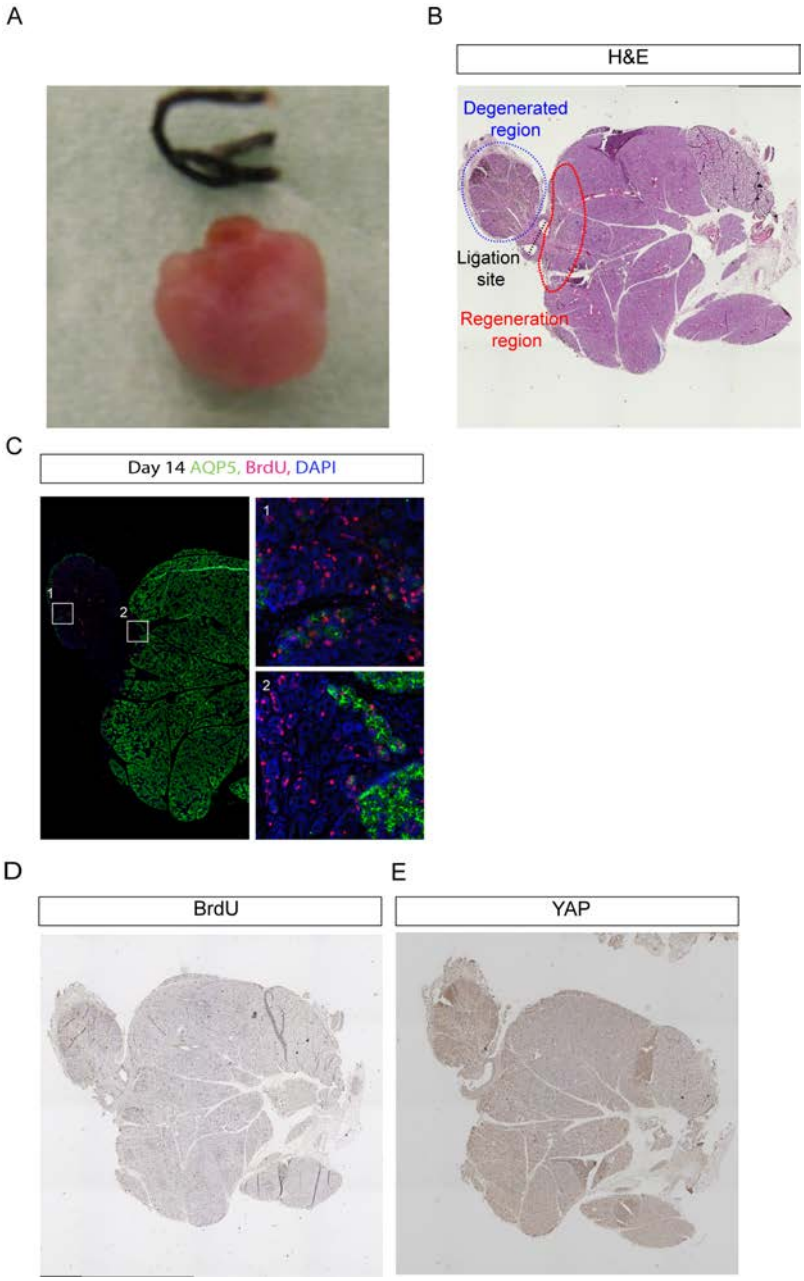

Supplementary Figure 1: YAP nuclear expression increases in the striated and excretory ductal compartment at the regenerative site of the submandibular gland. Relative to Figure 1. (A) Picture showing a mouse salivary gland 14 days after ligation. (B and E) Establishment and characterization of ligated mouse submandibular glands. (B) H&E tile scan showing the ligation site (black dashed line), the degenerative region of the gland (blue dashed line) and the regeneration region of the gland (red dashed line). (C) Immunofluorescent staining of mouse ligated submandibular gland 14 days after ligation. In green aquaporin 5 (AQP5), in red BrdU. White box insets (1 and 2) represent the regions of magnifications. (D) IHC of consecutive paraffine sections showing BrdU and (E) YAP.

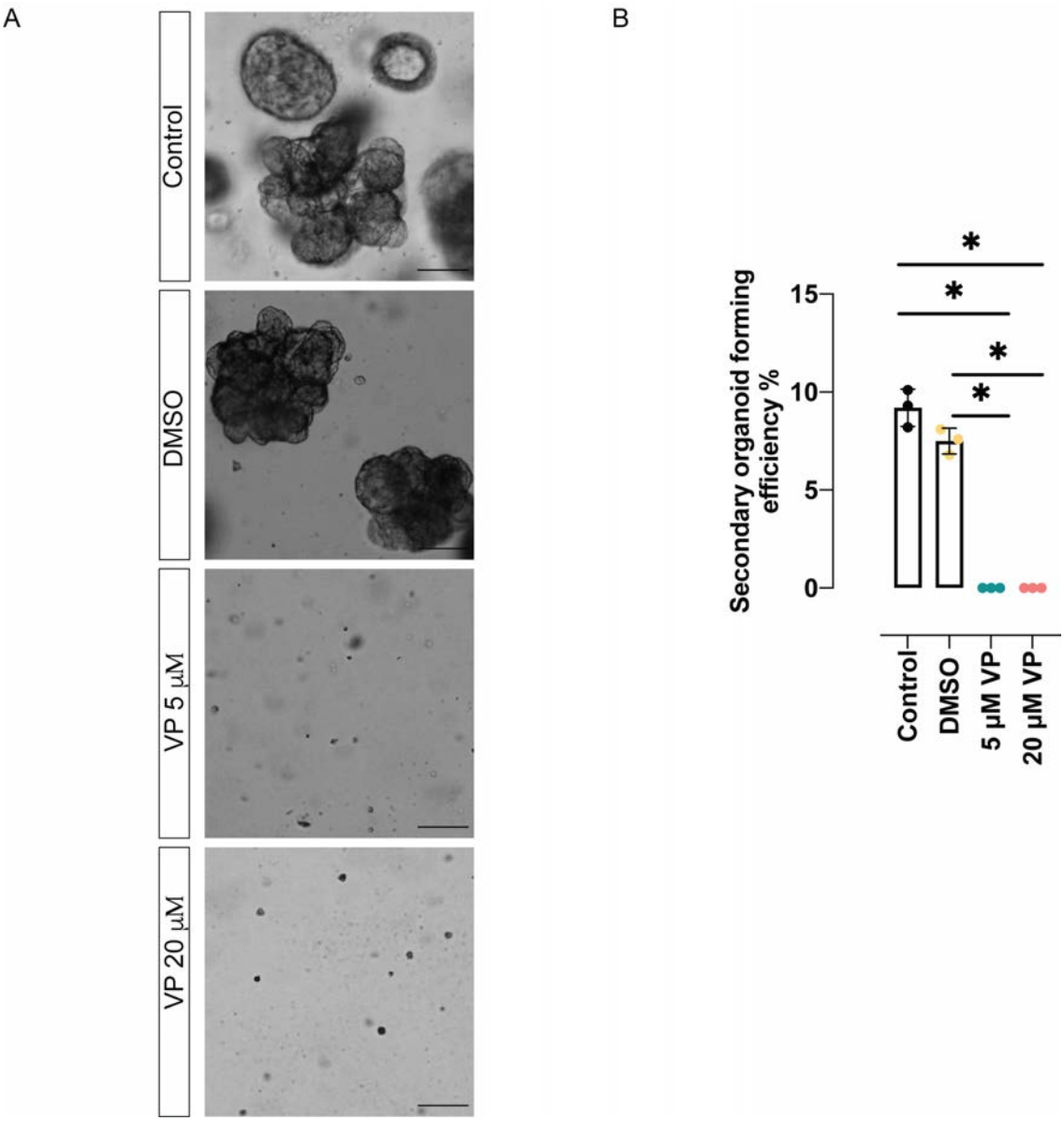

Supplementary Figure 2: Inhibition of YAP nuclear activity inhibits secondary organoid formation. Relative to Figure 2. (A) Representative picture of secondary organoids derived from organoids treated in the previous passage with DMSO, 5 μM VP, 20 μM VP and control. (B) Quantification at the end of the passage of the ability of pretreated cells to form secondary organoids, measured as Organoid forming efficiency OFE%. Data are represented as the mean ± SEM (B). (B) One-way ANOVA *p<0.05, **p<0.01, ***p<0.001, ****p<0.0001.

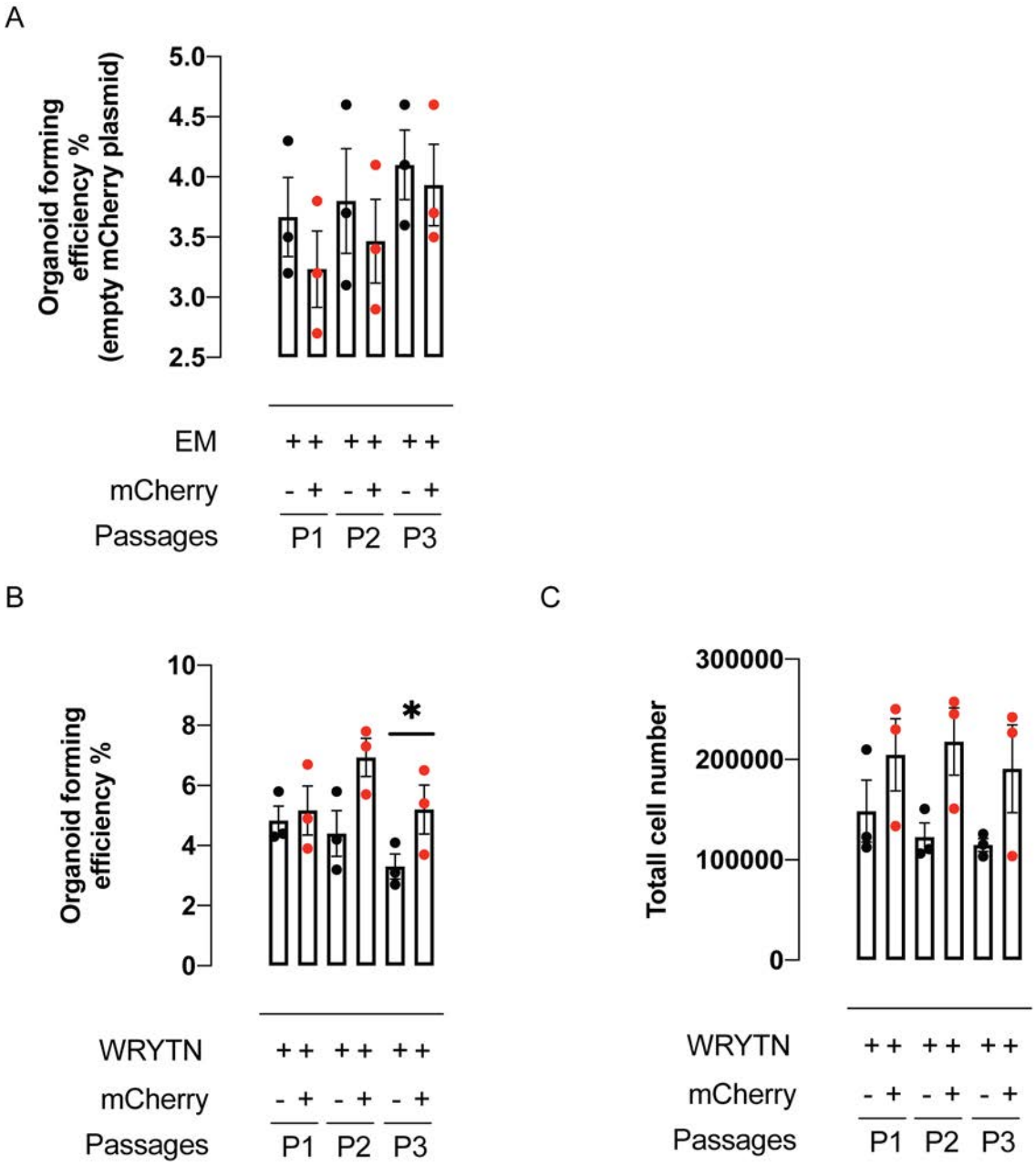

Supplementary Figure 3: YAP overexpression in human salivary gland-derived cells increases their self-renewal potential. Relative to Figure 4. (A) Organoid forming efficiency of human salivary gland cells transduced with empty mCherry plasmid showing no differences in growth between mCherry+ and mCherry-. (B)(C) Quantification of secondary and tertiary organoids (B) and total cell numbers (C) of human salivary gland cells transduced with pGAMA-YAP and cultured in Wnt enriched media (WRYTN). Red dots= mCherry+; Black Dots= mCherry-. Data are represented as the mean ± SEM (A)(B)(C). (B)Two-way ANOVA. *p<0.05, **p<0.01, ***p<0.001, ****p<0.0001.

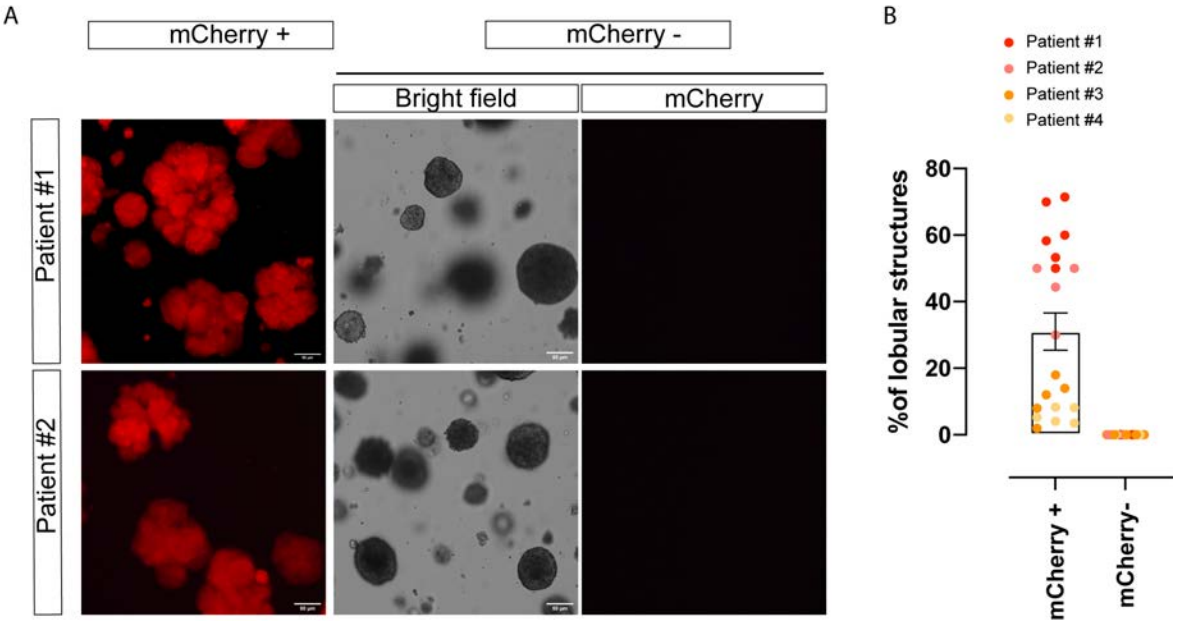

Supplementary Figure 4: YAP overexpression in human salivary gland derived cells promotes branching morphogenesis. Relative to Figure 4. (A) Representative picture of mCherry+ YAP^{OE} overexpressing human salivary gland organoids cultured in EM at the end of passage 1 (P1). YAP^{OE} organoids show branched/lobular phenotype compare to mCherry- derived organoids that show instead a spherical phenotype. (B) Quantification of branched organoids at the end of P1 in 4 different cultures derived from 4 different patients (each color=one patient). % of branched organoids are calculated per well (each dot=1 well).

$$\%\boldsymbol{of\ branched\ organoids} = \frac{\boldsymbol{number\ of\ branched\ organoids\ per\ well}}{\boldsymbol{total\ number\ of\ organoids\ per\ well}} * \mathbf{100}$$

Data are represented as mean ± SEM. (B) T-Test. *p<0.05, **p<0.01, ***p<0.001, ****p<0.0001.

A

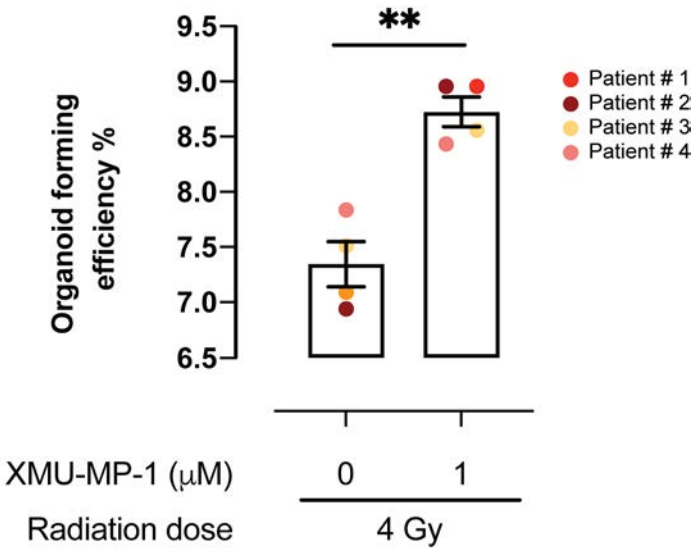

Supplementary Figure 5: Chemical inhibition of MST1/2 kinases improves salivary gland organoid irradiation response. Relative to Figure 5. (A) Organoid forming efficiency of hSG derived cells upon radiation treatment (4 Gy) and inhibition of MST1/2 kinase by the use of XMU-MP1 (1 μM). Each color represents a culture derived from a different patient (n=4). Data are represented as the mean ± SEM. Two-way ANOVA (mixed model). *p<0.05, **p<0.01, ***p<0.001, ****p<0.0001.

CHAPTER 5

AUTOPHAGY INDUCTION DURING STEM CELL ACTIVATION PLAYS A KEY ROLE IN SALIVARY GLAND SELF-RENEWAL

Orhon I., Rocchi C., Villarejo-Zori B., Serrano Martinez P., Baanstra M., Brouwer U., Boya P., Coppes RP.,Reggiorl F.

Accepted in Autophagy

Abstract

Relatively quiescent tissues like salivary glands (SGs) respond to stimuli such as injury to expand, replace and regenerate. Resident stem/progenitor cells are key in this process because, upon activation, they possess the ability to self-renew. Autophagy contributes to and regulates differentiation in adult tissues but an important question is whether this pathway promotes stem cell self-renewal in tissues. We took advantage of a 3D organoid system that allows assessing the self-renewal of mouse SGs stem cells (SGSCs). We found that autophagy in dormant SGSCs has slower flux than self-renewing SGSCs. Importantly, autophagy enhancement upon SGSCs activation is a self-renewal feature in 3D organoid cultures and SGs regenerating *in vivo*. Accordingly, autophagy ablation in SGSCs inhibits self-renewal while pharmacological stimulation promotes self-renewal of mouse and human SGSCs. Thus, autophagy is a key pathway for self-renewal activation in low proliferative adult tissues, and its pharmacological manipulation has the potential to promote tissue regeneration.

Keywords

Salivary glands, stem cells, self-renewal, maintenance, autophagy

Introduction

Stem cells are by definition cells that have the unique capacity of endless self-renewal and differentiation into mature cells, which results in the regeneration of specific cell types and tissues, in both embryos and adults[1]. This ability of self-renewal is a key property for tissue maintenance in adults. Self-renewal of stem cells occurs by an asymmetric cell division into one stem cell and one progenitor cell, which allows to permanently conserve a stem cell pool within a tissue while leading to differentiation of mature tissue-specific and long-lived lineages. There is a delicate balance between self-renewal and differentiation, which is regulated by cell-intrinsic transcriptional programs and extracellular signals from the stem cell surroundings[2]. In adult tissues, stem cells are localized in a specific and often hypoxic microenvironment, usually referred to as stem cell niche, in which they either maintain their quiescent state and preserve their self-renewal capacity or orchestrate tissue reprogramming through cell-cell interactions and extracellular signals. Most tissues with low or no proliferative steady-state properties, such as liver or skeletal muscle, respond to environmental changes, *e.g.*, tissue damage, upon which their stem cells become activated to expand, replace and therefore regenerate the tissue. The change from this quiescent, "dormant" state (naïve, low -activity stem cells) to an "activated" state (primed, proliferating stem cells) for regeneration, is accompanied by a change in both metabolism and gene expression[3,4].

Macroautophagy, hereafter called autophagy, is an evolutionarily conserved, tightly-regulated lysosomal degradative pathway that through the turnover of obsolete and/or damaged proteins and organelles, is crucial to maintain cell homeostasis in steady-state conditions but also in response to various stresses[5]. Autophagy is also playing a central role in cell development and differentiation, through still largely unclear mechanisms[6]. Several studies have initially focused on the role of autophagy in development taking advantage of conditional knockout mice lacking genes essential for autophagy, the so-called *ATG* (*autophagy-related*) genes. Those investigations have shown that in most organs there are no aberrant developmental problems in chronic autophagy deficient models[7], indicating that tissue maintenance upon intrinsic and environmental stresses, may be the primary role of autophagy. Thus, there has

been a research focus and investigations on the physiological role of autophagy on tissue-specific stem cell types such as hematopoietic (HSCs), neuronal (NSCs), mesenchymal (MSCs), cancer (CSCs) stem cells and induced pluripotent stem cells (iPSCs), have revealed that this process contributes to stem cell reprogramming and tissue differentiation[6,8]. The uniqueness of these adult stem cell populations is their multipotency, which is indicated by their ability to self-renew for expansion upon activation and requires strict maintenance of their homeostasis at steady-state. The relationship between tissue self-renewal and autophagy has been investigated so far *in vitro* in muscle stem cells[9], neural stem cells (NSCs)[10], embryonic stem cells (ESCs)[11] and hematopoietic stem cells (HSCs)[12,13], mostly in the context of either the stemness property maintenance or aging cells and their metabolism. *In vitro* studies, however, may have reached conclusions that do not entirely apply *in vivo*, as they lack the cell-cell and cell-matrix interactions that are essential for the establishment of tissue-specific microenvironments and stem cell responses[14,15]. The missing factors might be the presence of other differentiated cell types, signaling molecules, extracellular matrix (ECM) interactions, 3D tissue arrangement and mechanical forces. 3D organoid cultures provide several of these factors, including the 3D arrangement, necessary rigidity, tension and identified soluble niche components[16]. As a result, they represent a well-controlled tool allowing relatively easy experimental manipulation[16].

The recent development of new culturing technologies in 3D organoid systems permits to overcome the limitations of the existing *in vitro* systems and to study the role of autophagy in tissue maintenance and self-renewal in the more physiologically-relevant context of tissue self-organization. Tissue self-renewal has been defined as *the process by which an organ replaces its lost cells*[17] and salivary glands (SGs) are one of the organs capable of rapid regeneration. Despite their slow turnover, studies on damaged adult SGs have highlighted their regeneration potential. For example, acinar cells appear to be replaceable following injury that causes a loss of SGs function[18-20]. Radiation is the main cause of SGs dysfunction as radiotherapy is currently the most effective treatment of patients with head-and-neck cancer. Exposure of healthy SGs to radiation, however, results in a severe progressive loss of SG

acinar unit function leading to irreversible hyposalivation and development of xerostomia, which manifests with dry mouth, tooth decay, oral infection and impaired taste and speech[21]. In this context, stem cell transplantation therapy is considered one of the most promising regenerative strategies along with gene therapy, to permanently restore SGs function[22-24]. Salivary glands stem cells (SGSCs) have been identified and characterized using different expression markers, and the long-term *ex vivo* expansion of SGSCs-derived SGs organoids has also been established for both mouse and patient samples[25-27].

We decided to exploit SGSCs and SGs organoids to develop a system to study the role of autophagy in stem cell maintenance in the context of a tissue, with also the ultimate goal to promote self-renewal of SGs for therapeutic applications. In particular, we have investigated how basal autophagy contributes to the maintenance of SGSCs utilizing a 3D culture system and reveal that dormant SGSCs have a slower basal autophagic flux than the progenitor cells. Autophagy activation in SGSCs is then essential for their self-renewal to generate progenitor cells, and this process can be enhanced pharmacologically. Furthermore, we show that autophagy is also induced in SGSCs in animals upon injury to regenerate the damaged tissue. Altogether, our results uncover a crucial function of autophagy in tissue self-renewal and highlight its therapeutic potential for efficient regeneration upon damage.

Results

Autophagy is essential for continuous SGSCs self-renewal

To study the role of autophagy in the self-renewal of SGs cells, we took advantage of a well-established 3D organoid model of SGSCs[28,29]. Briefly, SGs isolated from mice were mechanically and enzymatically dissociated and cultured to yield organoids that can be passaged as single cells in Matrigel® (Figure 1A). In this 3D organoid system, only single SGSCs seeded in Matrigel® at day 0, will be able to form primary organoids, approximately in 7 days (Figure 1A). Long-term self-renewal potential of SGSCs can then be assessed by isolating single cells from secondary organoids, which are subsequently cultured in Matrigel® and incubated with self-renewal medium for tertiary sphere formation (Figure 1A). This procedure was repeated every 7 days, when the organoids are dissociated into single cells and plated again for the next passage. The self-renewal efficiency of SGSCs at each passage was assessed by determining the organoid forming efficiency (OFE), which represents the percentage of organoids formed from 100 plated cells.

As a first approach to ascertain an eventual role of autophagy in SGSCs self-renewal, we inhibited autophagy in primary SG cells using two common lysosomal inhibitors, bafilomycin (Baf) and chloroquine (CQ), which block the latest steps of autophagy[30]. Single cells derived from primary organoids were incubated separately with these two compounds for 5 h. As expected, these treatments led to the accumulation of the autophagy marker protein LC3-II (lipidated microtubule associated protein 1 light chain 3 alpha) and the autophagy substrate SQSTM1/p62 (sequestrosome 1), which was visualized by either fluorescence microscopy and western blots (Figure S1A and S1B). Subsequently, organoids were dissociated and cultured into secondary organoids in presence of Baf or CQ. SGSCs exposed to these drugs lost their ability to form secondary organoids, suggesting that inhibition of autophagy may negatively affect SGSCs self-renewal (Figure S1C). An identical result was also observed when primary SG cells were treated with wortmannin (data not shown), a compound blocking the early steps of autophagosome biogenesis[30]. As Baf and CQ also inhibit other cellular processes relying on lysosomal functions and could cause SGSCs death that would appear

as an inability to self-renew, we decided to specifically ablate autophagy by knocking down ATG13, a gene regulating the initiation of autophagy[31]. To this aim, cells isolated from SGs were kept in culture for 48 h in presence of scramble or ATG13-targeting siRNAs, before culturing them in Matrigel® to induce organoid formation. Treatment of cells with siRNA targeting ATG13, which resulted in an inhibition of the autophagic flux as expected (Figure S1F), led to a significant reduction of the levels of this protein in the cell population (Figure S1E). Importantly, ATG13-depleted cells displayed a significant and pronounced reduction of their OFE, indicating that autophagy has an important role in the maintenance of the SGSCs to generate into a new lineage, which is critical for self-renewal (Figure 1B-C).

Next, we turned to a knockout model to confirm and study the role of autophagy in SGSCs self-renewal over several passages. Since most of the *ATG* gene knockout mice do not survive the post-birth starvation period[7], we used SGs isolated from *Atg5*$^{-/-}$ embryos at stage E18.5. At this stage, SGs are already post-terminally differentiated into secretory cell types[32]. Freshly isolated embryonic SGs were cultured in Matrigel® for 7 days and treated with or without Baf for 5 h to monitor autophagic flux by assessing the difference in the levels of LC3-II[30]. As expected[7], *Atg5*$^{+/+}$ and *Atg5*$^{+/-}$ organoids showed a functional autophagic flux while the ones derived from *Atg5*$^{-/-}$ embryonic SGs displayed a complete autophagy block, *i.e.*, no LC3-II was formed and SQSTM1 was accumulated also in the absence of Baf (Figure S2B)[30]. Both autophagy competent genotypes, i.e., *Atg5*$^{+/+}$ and *Atg5*$^{+/-}$, had identical self-renewal efficiency as well (Figure 1D). Consistently with the result obtained with lysosomal inhibitors and ATG13 knockdown, SGSCs derived from *Atg5*$^{-/-}$ mice showed a significantly lower self-renewal potential, as well as less and smaller primary organoids, were formed compared to autophagy-competent *Atg5*$^{+/+}$ *and Atg5*$^{+/-}$ cells upon the initial dissociation and culture (Figures 1D and 1E). We followed autophagy competent and incompetent organoids over 5 passages and observed that SGSCs from *Atg5*$^{-/-}$ were completely exhausted by passage 4, while autophagy-capable SGSCs maintained their self-renewal capacity over time (Figure 1D). Cumulative population doublings over 5 passages highlighted that *Atg5*$^{-/-}$ cells, in contrast to autophagy-competent cells, stop expanding after passage 2 in Matrigel® (Figure 1F). The inability of *Atg5*$^{-}$

$^{-/-}$ SGSCs to self-renew was also observed in a WRY medium that robustly stimulates Wnt signaling (data not shown), and thus promotes an increase in organoid formation *in vitro*[27]. Importantly, ANNEXINV and propidium iodide staining for dead cells showed that the inability of *Atg5*$^{-/-}$ SGSCs to produce secondary organoids was not due to cell death as their viability, starting from isolation, *i.e.*, p0, and until exhaustion at passage 4, did not change significantly and was similar to that of *Atg5*$^{+/-}$ and *Atg5*$^{+/+}$ SGSCs (Figure 1G). In contrast, it appears that *Atg5*$^{-/-}$ SGSCs lose their cell division capacity since *Atg5*$^{-/-}$ cells start to accumulate at the S phase through the passages while autophagy competent cells' distribution in G0/G1, S and G2/M phases remain identical (Figure S2C).

Altogether, these data show that functional autophagy is essential for SGSCs maintenance and self-renewal, prior to extrinsic cell differentiation signals.

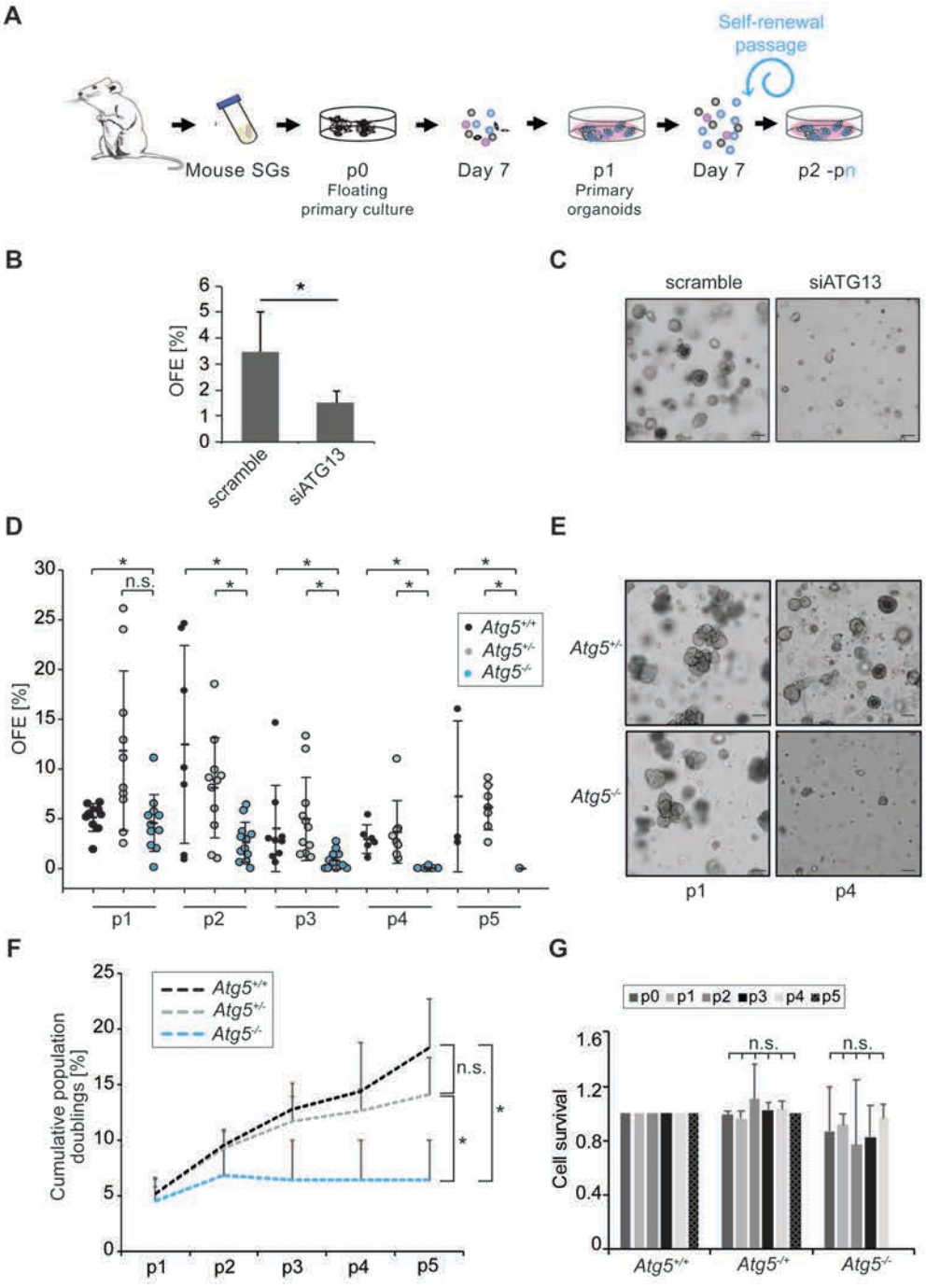

Figure 5: Autophagy is essential for SGSCs self-renewal. (A) Schematic representation of 3D culturing of murine SGSCs for self-renewal analysis. (B) Organoids from SGSCs transfected with either scrambled siRNAs (scramble) or siRNAs targeting ATG13 (siATG13) for 48 h after 7 days in Matrigel®. The percentage of organoid-forming efficiency (OFE) was determined at the end of passage 1 in MM medium as described in Material and Methods. Bars represent the means of 3 independent experiments ± SD. The asterisk annotates a significant difference of $p<0.05$. (C) Brightfield microscope images of organoids from SGSCs transfected as in panel B. (D) OFE of autophagy competent ($Atg5^{+/+}$, $Atg5^{+/-}$) and $Atg5^{-/-}$ 3D cultures over 5 passages (p1 to p5). Each data point represents the measurement of one sample and means ±SD are indicated. Asterisks annotate significant differences of $p<0.05$. (E) Brightfield microscope images of primary organoids from SGSCs derived from $Atg5^{+/-}$ and $Atg5^{-/-}$ embryos at stage E18.5, at the end of passage 1 (p1) and 4 (p4) in the MM medium. (F) Cumulative population doublings of $Atg5^{+/+}$, $Atg5^{+/-}$ and $Atg5^{-/-}$ SGSCs over the 5 passages shown in Figure 1D. Asterisks annotate significant differences of $p<0.05$. (G) Cell survival rates of $Atg5^{+/+}$, $Atg5^{+/-}$ and $Atg5^{-/-}$ SGSCs were determined at the end of 5 passages (p0 to p5) using ANNEXIN V/PI staining and FACS sorting as described in

Material and Methods, and normalized to the cell survival rate of heterozygous Atg5$^{+/+}$ SGSCs. Bars represent the means of 3 independent experiments ±SD. The n.s. abbreviations highlight that there are no significant differences.

Autophagy induction increases SGSCs self-renewal *in vitro*

To directly prove that autophagy induction promotes SGSCs self-renewal, we decided to enhance the flux of this pathway in SGSCs with the expectation of increasing self-renewal efficiency. To this aim, we took advantage of the Tat-BECLIN1 (Tat-BECN1) peptide, which specifically stimulates basal autophagy activity and has been successfully applied to multiple tissues[33]. Tat-BECN1 was added to the single cells during isolation from SGs and kept in the medium during the entire self-renewal assay (Figure 2A). Tat-BECN1 indeed induced the autophagic flux in SGSCs (Figure S3A and S3B). In agreement with our hypothesis, enhancement of basal autophagy stimulated SGSCs self-renewal efficiency over several passages (Figure 2B). Importantly, the organoids formed in presence of Tat-BECN1 showed no morphological alterations in comparison to the control treated cells (Figure 2C), and differentiated structure formation efficiency upon differentiation of SGSCs-derived organoids exposed to Tat-BECN1 was not altered (Figure S3C). These observations highlight the Tat-BECN1 peptide specifically promotes SGSCs self-renewal without affecting differentiation programs. The enhancement in SGSCs self-renewal throughout passages was only maintained when SGSCs were constantly kept in presence of Tat-BECN1 and not when this peptide was applied only during their isolation from SGs (Figures 2D and 2E). In this latter experimental setup, we observed a transient increase in SGSCs self-renewal at passage 2 in the presence of Tat-BECN1, which was not sustained in the subsequent passages during which the peptide was removed, revealing that the increase in SGSCs self-renewal efficiency depends on a sustained autophagic flux and it is not due to a permanent change in SGSCs during their initial isolation from SGs. To prove that this enhancement in SGSCs self-renewal was not caused by an off-target effect of Tat-BECN1, we cultured *Atg5*$^{-/-}$ embryos derived SGSCs in presence of this peptide and observed that autophagy deficient cells did not show any improvement of OFE in contrast to the autophagy-competent genotypes (Figure 2F).

Although murine SGSCs can practically self-renew endlessly in the current 3D culture system, their human counterparts can do it for a limited number of passages, typically 4-5[25]. Therefore, we decided to explore whether autophagy induction by Tat-BECN1 could improve the self-renewal efficiency of human SGSCs as well. The preliminary observation suggests that autophagy stimulation induces OFE efficiency at least in two human samples that we could have access to (Figures S3D and S3E).

Taken together, these results led us to conclude that autophagy stimulation promotes SGSCs self-renewal in mice and human cells.

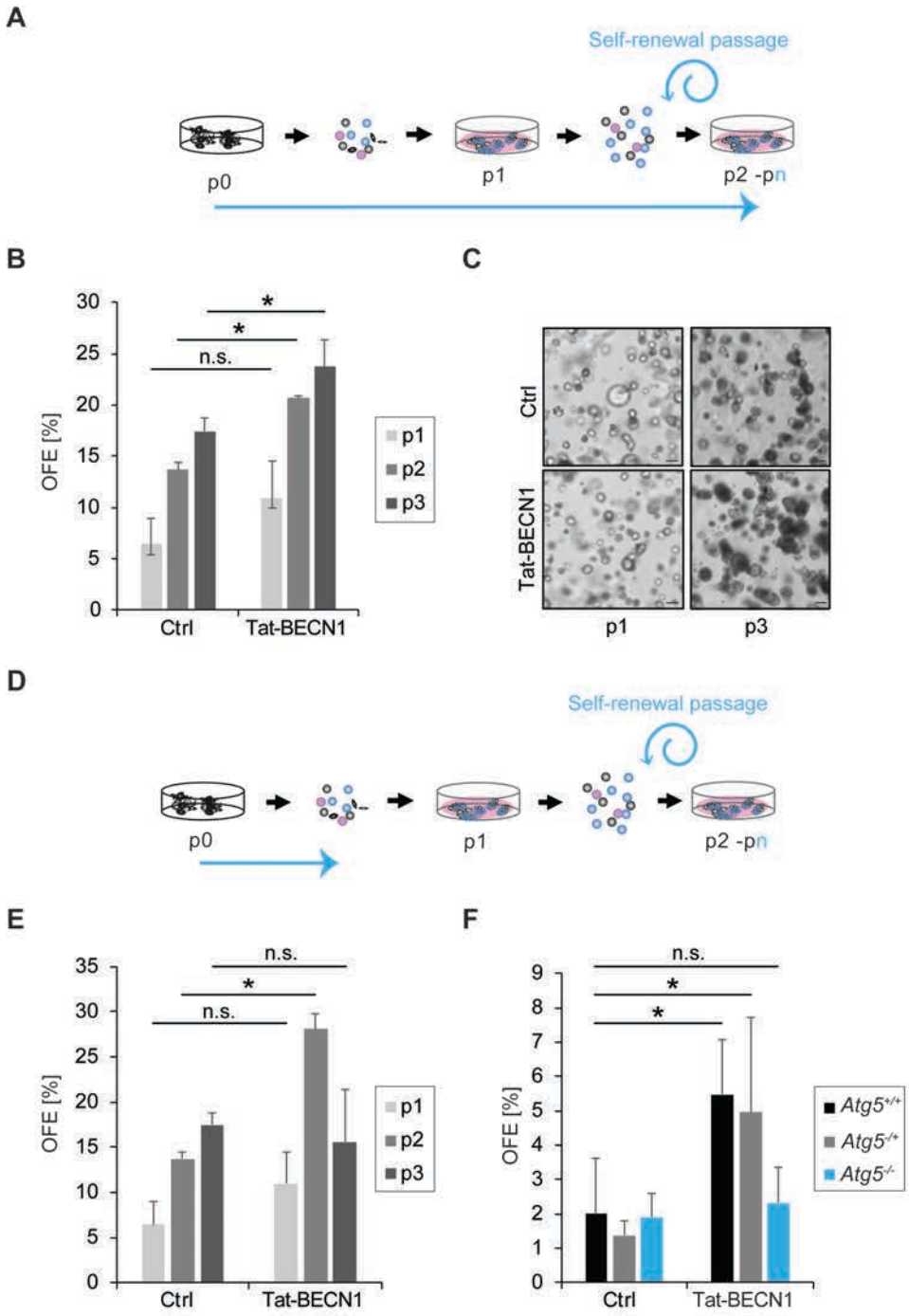

Figure 6: Autophagy induction increases SGSCs self-renewal in vitro. (A) Schematic representation of the experimental setup over 3 passages for the 3D culturing of SGSCs for self-renewal analysis in the continuous presence of Tat-BECN1 in the MM medium. The arrow highlights when Tat-BECN1 was present. (B) OFE of SGSCs treated or not with 50 nM Tat-BECN1 following the experimental setup shown in Figure 3A. Bars represent the means of 3 independent experiments ±SD. Asterisks annotate significant differences of $p<0.05$, while the n.s. abbreviation highlights that there is no significant difference. (C) Brightfield microscope images of organoids from SGSCs treated or not with 50 nM Tat-BECN1, after 7 days in Matrigel® at the end of passage 1 (p1) and 3 (p3). (D) Schematic representation of the experimental setup over 3 passages for the 3D culturing of SGSCs for self-renewal analysis with exposure to Tat-BECN1 treatment only during the initial isolation of single cells from SGs. The arrow highlights when Tat-BECN1 was present. (E) OFE of SGSCs treated or not with 50 nM Tat-BECN1

following the experimental setup shown in Figure 2D. Bars represent the means of 3 independent experiments ±SD. The asterisk annotates a significant difference of $p<0.05$, while the n.s. abbreviation highlights that there is no significant difference. (F) OFE at passage 1 of $Atg5^{+/+}$, $Atg5^{+/-}$ and $Atg5^{-/-}$ SGSCs treated or not with 50 nM Tat-BECN1 following the experimental setup shown in Figure 2A. Bars represent the means of 3 independent experiments ± SD. Asterisks annotate significant differences of $p<0.05$, while the n.s. abbreviation highlights that there is no significant difference.

Autophagy is induced upon SGSCs activation

In adult SG, SGSCs are localized to the SG ducts and they are in a dormant state in the absence of injury. Extracellular stress activates them for self-renewal and differentiation via the production of progenitor cells[27,34]. In contrast, SGSCs are constantly activated in our 3D cultures because they are triggered to proliferate by the enriched medium employed for the self-renewal analysis in Matrigel® (Figure 3A). As a result, it is not possible to distinguish in our 3D culture system whether basal autophagy activity is necessary to maintain dormant SGSCs or whether this pathway is critical for SGSCs self-renewal upon their activation.

To distinguish between these two possibilities, we opted to assess the basal autophagic flux in freshly isolated SGSCs, i.e., at passage 0 (Figure 3A) and to determine whether their basal autophagic flux is lower or higher than in the rest of the tissue. Thus, we isolated SGs ductal-compartment-derived cell populations from the heterogeneous cell composition of SGs by FACS as previously described[26]. More specifically, SGSCs- (cell surface markers $CD29^{hi}$ and $CD24^{hi}$) and SGSCs-derived progenitor- ($CD29^{medium/hi}$ and $CD24^{medium/hi}$) enriched populations were sorted (Figure 3B). Subsequently, we measured the autophagic flux in these two cell populations by western blot while they were cultured in the enriched medium for only 5 h in the absence or the presence of Baf. This experiment revealed that the freshly isolated, SGSCs-enriched population has significantly lower autophagic flux in comparison to the SGSCs progenitor cell-enriched population, which displayed a higher autophagic flux, as observed by the LC3-II accumulation in the presence or the absence of Baf (Figures 3C and 3F). Moreover, SQSTM1 turnover appeared to be reduced in the SGSCs-enriched population, consistently with the notion of a slow autophagic flux (Figure 3C). Finally, and as expected, the SGSCs-enriched population had increased self-renewal efficiency over several passages,

while the SGSCs progenitor-enriched population lost its ability to self-renew over 3 passages (Figure 3E). Importantly, the SGSCs-enriched cell population started to show an enhanced autophagic flux upon activation by expansion in the 3D culture, showing that activation of dormant SGSCs isolated animal tissues is accompanied by an induction of autophagy activity (Figures 3F and S3).

Altogether, these results show that SGSCs derived from the SGs ductal compartments have reduced basal autophagic flux and activation of this flux during expansion correlates with an induction of self-renewal. This observation provides a possible explanation for the relevance of autophagy in SGSCs self-renewal (Figure 1).

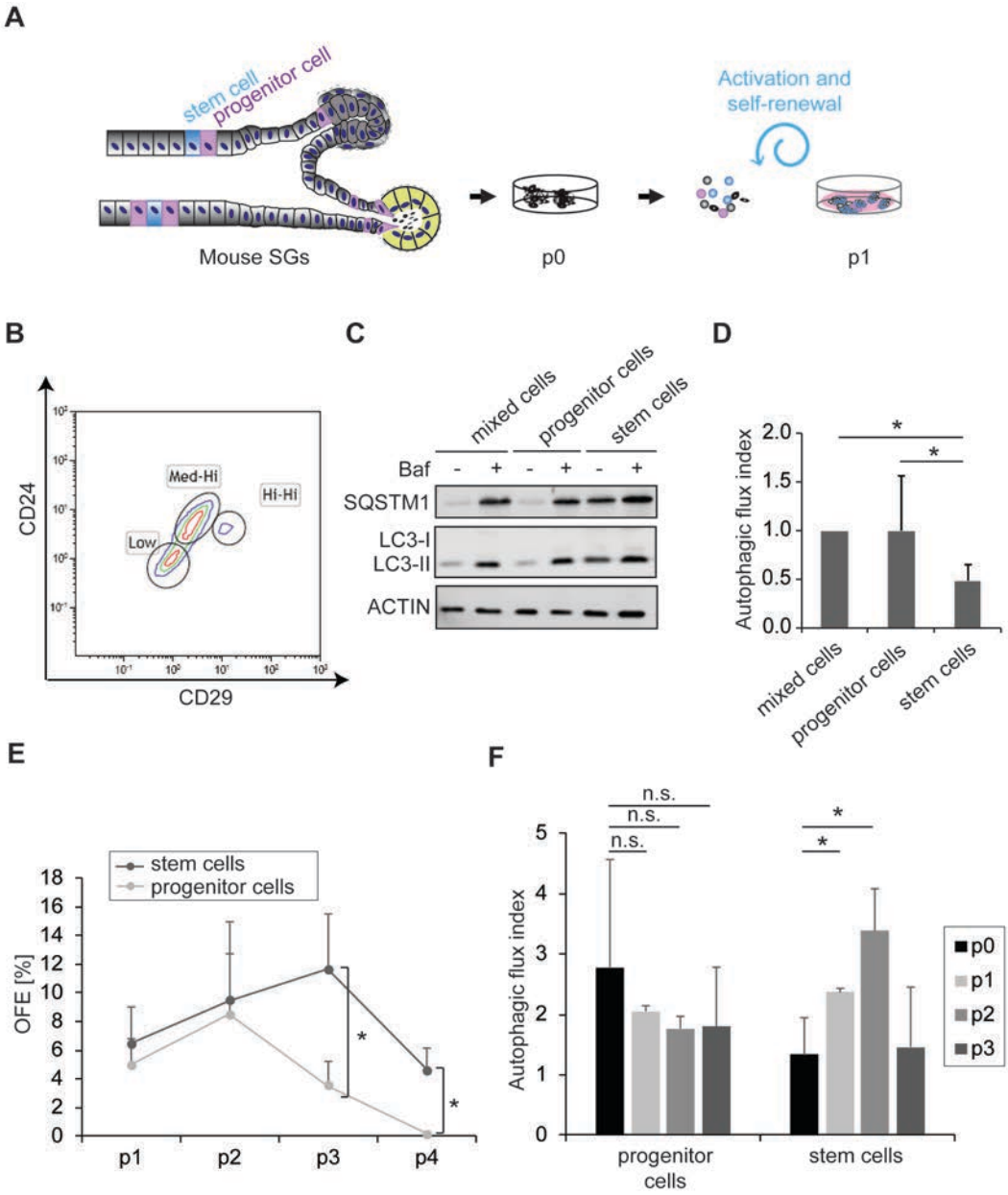

Figure 7: Autophagy is induced upon SGSCs activation. (A) Schematic representation of the duct region of adult SGs and localization of dormant SGSCs and progenitor cells, which are activated in the 3D culture system by the medium embedding the Matrigel®. (B) Representative FACS profiles of SG cells sorted into 2 subpopulations based on the expression levels of the cell surface marker proteins CD29 and CD24. SGSCs are $CD29^{hi/hi}$-and $CD24^{hi/hi}$, while progenitor cells are $CD29^{medium/hi}$ and $CD24^{medium/hi}$. (C) Cells isolated as in Figure 3A were treated or not with 100 nM Baf for 5 h, lysed and proteins examined by western blot using antibodies against SQSTM1 and LC3. ACTIN was used as the loading control. (D) The autophagy flux index in each sample of the experiment shown in Figure 4C was determined by dividing the amount of LC3-II in Baf-treated cells with that in cells not exposed to Baf. Protein levels were normalized to ACTIN, which was used as the loading control. Bars represent the means of 3 independent experiments ±SD and relative to the values of the mixed cell population. Asterisks annotate significant differences of $p<0.05$. (E) The OFE of the samples examined in Figures 3C and 3D was determined for 4 passages and the data points represent the means of 3 independent experiments ±SD. Asterisks annotate significant differences of $p<0.05$ (F) The quantification of the autophagy flux in the mixed, SGSCs progenitor and SGSCs populations analyzed in Figures 3C and S4, was carried out over 3 passages in 3D cell

culture. Bars represent the means of 3 independent experiments ±SD and they are relative to the value measured in each cell population before 3D cell culture, i.e., at p0. Asterisks annotate significant differences of $p<0.05$, while the n.s. abbreviation highlights that there is no significant difference.

Autophagy is induced in regenerating SGs

The results obtained with the 3D culture experiments supported the notion that the basal autophagic flux is slower in dormant SGSCs within SGs, and it is induced upon stimulating proliferation for self-renewal. To address the question whether autophagy is an intrinsic response during SGs regeneration *in vivo*, we took advantage of an *in vivo* injury mouse model for SGs that we recently developed. Briefly, a suture was placed below the sublingual SGs to induce a local injury, which also separates the SGs into a cranial hemisphere and a caudal part that are easily recognizable (Figure 4A). While the caudal part degenerates, the cranial hemisphere undergoes regeneration over a period of 15 days, to reform the complete SGs (Figures 4A and S5). In our experimental setup, animals were sacrificed and SGs examined before the ligation and after 5, 9 and 15 days after ligation, to follow the dynamic process of regeneration. All the mice were also pulsed with 2 bromodeoxyuridine (BrdU) 24 h and 6 h before their sacrifice, to detect proliferating cells through incorporation of this fluorescent nucleotide in newly synthesized DNA. In particular, BrdU labelling is highly suggestive of regeneration and identifies the SGs regions where this process is active. We observed a significant and pronounced increase in the number of cells presenting BrdU-stained nuclei in both acinar and ductal regions of the SGs tissues 5 and 9 days after ligation (Figures 4B and 4C), which showed that SGs were indeed undergoing a process of regeneration as expected. The decrease in BrdU staining 15 days post-ligation, in contrast, revealed that this process was close to termination at that time point (Figures 4B and 4C). In the same tissues, we also examined the distribution of LC3, SQSTM1 and ATG16L1 (autophagy related 16 like 1), another autophagy marker protein[30], by immunofluorescence. Interestingly, we observed that LC3 puncta formation was significantly increased throughout the SGs starting from the 9th day of regeneration in the ducts, while it remained unchanged in the acinar compartments over the 15 days (Figures 4B and 4D). The same results were also obtained with both SQSTM1 and ATG16L1 labelling (Figure S6A). That is, while the number of puncta formed by these two autophagy marker proteins increases in duct regions of the regenerating SGs, their number remained low and constant in the differentiated, acinar compartments (Figure S6A-C).

To prove that the autophagic flux is indeed induced during SGs regeneration, we repeated the SGs ligation experiment and evaluated the levels of LC3 and SQSTM1 in the presence or the absence of hydroxychloroquine (HCQ) (Figure S7A). As expected, the autophagic flux was low at steady state levels in the ductal region (Figure S7B, first column), in agreement with our observations in SGSCs (Figure 3). In contrast, ligation triggered the autophagic flux in the same tissue upon ligation, from day 5, and throughout the regeneration process. We also observed that the number of LC3 puncta per μm^2 in the acinar regions of SGs treated by HCQ was significantly higher than in non-treated SGs, showing that the basal autophagy flux of the acinar region is enhanced as observed in progenitor enriched SG cells (Figure 3). The autophagic flux in acinar regions, however, did not increase significantly upon regeneration triggered by ligation (Figure S7B).

Altogether, these results show that autophagy is induced during SGs regeneration. It is important to note that the increase in the number of LC3 puncta remained throughout the regeneration of the SG tissue until day 15, suggesting that autophagy stimulation is not an immediate stress response in the entire SGs upon tissue damage in our model, but a specific program for a regenerative process that takes place in the ductal region, where stem cells reside (Figure 4C). Together with our previous observations that SGSCs fail to self-renew in the absence of functional autophagy (Figures 1, 2 and 3), these data support the notion that autophagy plays a crucial role during the regeneration process of SGs from dormant SGSCs.

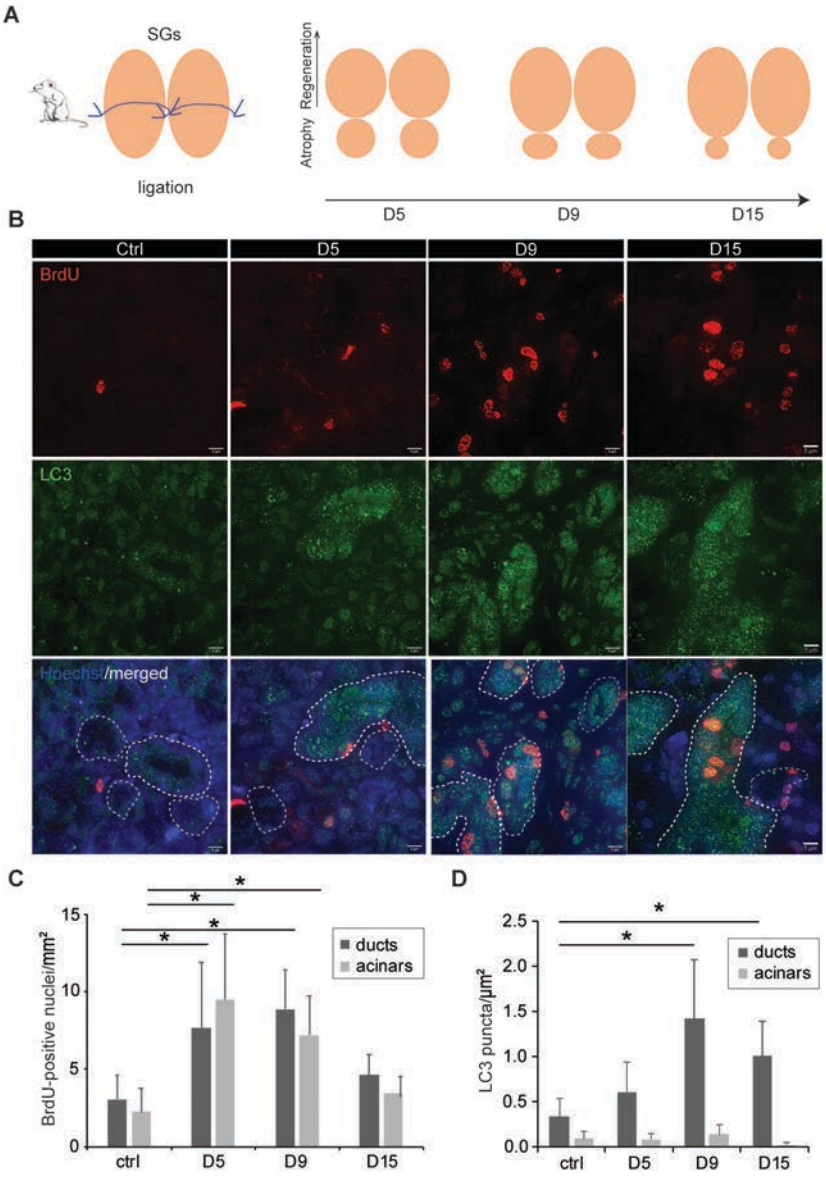

Figure 8: Autophagy is induced in regenerating tissues. (A) Schematic representation of the ligation of mouse SG and the subsequent regeneration process over 15 days. (B) Control SGs, or regenerating SGs at days 5 (d5), 9 (d9) and 15 (d15) post-ligation, were excised from sacrificed animals and processed for immunohistochemistry. Subsequently, 5 µm thick sections were labelled with anti-LC3 and BrdU antibodies. Z-stacks of images separated by 0.2 µm were collected, deconvolved and analyzed as described in Material and Methods. Representative single focal planes are shown. Nuclei are stained with Hoechst. SGs duct regions are delimited by white dash-lines. Scale bars 10 µm. (C) Quantification of BrdU positive nuclei in either duct regions or acinar cell areas (mm^2) in the experiment shown in Figure 4B. (D) Quantification of the LC3 puncta number in either duct regions or acinar cell areas (μm^2), in the experiment shown in Figure 4B. Bars represent the mean numbers ±SD counted at least in 5 randomly selected sections per SGs. Three different control and ligated SGs were analyzed. Asterisks annotate significant differences of $p<0.05$.

Discussion

Stem cells must have the ability to maintain their self-renewal capacity by dividing without differentiating into particular cell lineages via their progeny, to keep their regenerative potential throughout the lifetime of an organism. Autophagy has been shown to be involved in the maintenance and/or differentiation of various stem cells *in vitro*[6,8], but these models lack the morphological and functional organization of a tissue microenvironment. This is particularly important as autophagy activity is locally regulated by the metabolic and oxygenation status, as well as auto- and exocrine factors of the microenvironment[5,35,36]. Our 3D self-renewal model for SGs allows to specifically study this process in a physiologically representative context of a specific tissue. Thus, with our study we have revealed an important role for autophagy in stem cells self-renewal and regeneration within a tissue.

The hematopoietic system is the first tissue to be shown to have a self-renewal ability and that they do this at an extremely high rate to daily replace a large fraction of the circulating blood cells[37]. The experimental systems that allow investigating stemness maintenance and the regenerative capacity of the different HSCs subtypes that generate the various blood cell lineages have led to the finding that autophagy plays a key role in suppression of oxidative phosphorylation (OXPHOS)-driven metabolism[12,38,39]. Specifically, autophagy inhibition leads to an active metabolism in HSCs and a loss of quiescence. A recent study has revealed that the 3D culture of MSCs increases cell viability in comparison to the 2D culture, and this is due to a decrease in ROS production that is mediated by autophagy[40]. Using a murine colitis model, the authors also showed that autophagy induction could be critical to improve MSCs transplantation-based therapies[40]. In tissue with a slower stem cell self-renewal rate such as the nervous system, dormant NSCs display a slower autophagic flux and proteasome activities, in contrast with their activated counterpart[10]. These notions agree with our findings that show that in SGs, which is also a slowly-regenerating tissue, resident stem cells have a low basal autophagy activity than the progenitor cells (Figure 3). To the best of our knowledge, our study is the first one showing that upon injury, the autophagic flux is increased, specifically in ductal compartments, concomitantly with the regeneration process of the SGs *in vivo*

(Figure 4). Moreover, the data obtained using pharmacological modulation of autophagy with Tat-BECN1 suggest that autophagy stimulation could be sufficient to activate stem cell proliferation, in particular, that of SGSCs (Figure 3). This would indicate that the turnover of one or more factors by autophagy could dictate or have an important contribution in the reprogramming necessary to trigger stem cell self-renewal. This hypothesis needs to be further investigated to reach a firm conclusion, as it still cannot be excluded that autophagy induction is a downstream event required for the execution of the stem cell self-renewal rather than having a regulatory function.

One of our most striking findings is that basal autophagy is significantly different between stem and progenitor cells *in vivo* and that SGSCs' basal autophagic flux is significantly increased upon induction of proliferation in both 3D organoid cultures and animals' SGs upon injury (Figures 3, 4 and S4). As reported recently, SGs progenitor cells take an important role in tissue regeneration upon genotoxic damage[34]. Together with our findings that the progenitor cell population behaves significantly different than SGSCs and also that autophagy is induced primarily in the ductal regions where progenitor and stem cells are in close contact[26] upon injury (Figures 4 and S4), the interaction between these cells can be key for an efficient regeneration process. The question of if and how the progenitor and stem cell populations interact to keep a balance between self-renewal and differentiation into acinar cells for a functional recovery needs to be investigated, in particular, because autophagy induction remains local within the ducts during regeneration. These observations assign an important role to basal autophagy in dormant stem cells during tissue homeostasis and cellular reprogramming, which is independent of extracellular stresses.

For the maintenance of resident stem cell functions, the stem cell niche plays an important role in regulating stem cell behavior both during homeostasis and regeneration upon injury. This niche includes cell-to-cell interactions between stem cells and progenitor as and biochemical and biophysical properties of the tissue structure involving the secreted factors, metabolic requirements such as hypoxia etc.[14,41]. Further studies are required to understand the interactions and communication between stem cell and the progenitor cell populations

within SGs, and the functional role of autophagy within their niche upon tissue injury. Mitophagy can have a central role during cell differentiation by regulating the metabolic switch from glycolysis to OXPHOS, due to an increase in energy and metabolite demand during cellular remodeling[42,43]. In the SGs, however, we did not observe a significant difference in mitochondrial mass between dormant SGSCs and the progenitor cells (data not shown). Therefore, we can speculate that activation of autophagy to simulate SGSCs self-renewal does not involve mitochondrial clearance, but further studies are required to determine whether autophagy induction upon SGSCs activation encompasses a selective type of autophagy, mitophagy or another one.

Interestingly, the self-renewal mechanism of skeletal MSCs is regulated by the Notch signaling pathway[44]. A mechanism depending on the SOX2 transcription factor seems to be important for SGs regeneration[34]. In cardiomyocytes as well as other tissues, the Hippo/YAP signaling pathway appears to be an important regulator of regeneration and plasticity[45-47]. All these signaling cascades have been previously reported to be regulated by autophagy[47-49]. As a result, one could imagine that the main role of basal autophagy in SGSCs is to regulate these signaling pathways by selectively degrade one or more of their components. Future studies will need to examine whether autophagy regulates specific signaling pathways for SGSCs self-renewal and tissue regeneration *in vivo*.

Upon radiation treatment for head and neck cancer, the off-target effects of this therapy lead to the damage of saliva producing SGs cells, which in turn results in a lifetime of hyposalivation and co-morbidities. Various systemic diseases such as Sjorgen's syndrome, graft-versus-host disease, HIV infection, may result in irreversible SGs hypofunction and xerostomia as well[50]. Reacquisition of SGs function in these patients principally depends on the regeneration by SGs ductal compartment resident SGSCs as well as by transplantation of autologous adult SGSCs[18,34]. Previously, Morgan-Bathke and colleagues studied the contribution of autophagy in the development of SGs using Atg5f/f;Aqp5-Cre mice model, which results in animals with autophagy-deficient acinar cells[51]. SGs of these mice have normal morphology but acinar cells fail to recover after a 5Gy dose of head-neck irradiation in the absence of autophagy[52].

Interestingly, IGF-1 treatment prior to radiation decreased tissue and function loss, and this beneficial effect depends on autophagy induction, which appears to principally take places in the ducts[52]. These results are consistent with our model that autophagy stimulation in SGSCs concentrating at the ducts is crucial for SGs regeneration. Weng and colleagues have previously shown that mouse duct cells can generate acinar cells upon loss of part of the SGs by radiation[18]. Moreover, we observed in rat and human models that ablation using radiation of the caudal part of parotid SGs, induces regeneration involving the ductal regions in the cranial part of the gland[53]. Our *in vivo* regeneration model, which also ablates the caudal part of SG by suture, supports this finding and adds that the autophagic flux is increased in ductal regions during regeneration after severe injury. However, future studies are needed to translate our results in a clinical setting of patients being treated for head-neck cancer through radiation. Tissue-resident stem cells cultured in the laboratory, as they are capable of self-renewal and differentiate into adult tissues, represent an important approach aiming at future autologous cell transplantation therapies to avoid potential immune reaction[1]. Thus, fundamental knowledge on the role of autophagy in stem cell self-renewal capacity may offer new perspectives on fine-tuning approaches for regenerative medicine. Here, we show that autophagy induction using Tat-BECN1 contributes to an increase in efficiency of mouse and possibly human SGSCs self-renewal through autophagy induction, which may present an important target for therapy. Future studies are required to validate the therapeutic potential of Tat-BECN1 peptide in SGSCs but also other tissue-resident stem cells, as well as other currently available autophagy enhancers such as trehalose, spermidine or resveratrol[54,55].

Our study highlights that autophagy is a key regulatory pathway for SGs self-renewal and more in general for slowly self-renewing tissues. Our 3D culture model offers the unique experimental setup to dissect the precise role of autophagy in this process and decipher both its precise physiological relevance in self-renewal and the regulatory connections. This knowledge could be relevant to develop efficient stem cell therapies that are based on autophagy modulation.

Material and methods

SGs isolation from mice and culture

C57BL/6 mice were purchased from Envigo and housed in environmentally controlled rooms, conventional conditions and fed ad libitum in the Animal Facility of the University Medical Center Groningen. All experiments were performed according to approved institutional animal care and use committee (IACUC) protocols of the University of Groningen (under IVD protocol number 184824-01-001). C57BL/6 mice were purchased from Envigo and housed in environmentally controlled rooms, conventional conditions and fed ad libitum in the Animal Facility of the University Medical Center Groningen and the CIB animal facility. *Atg5*$^{+/-}$ mice[56] were kindly provided by Prof. Noboru Mizushima (Department of Biochemistry and Molecular Biology, Graduate School and Faculty of Medicine, The University of Tokyo). All experiments were performed according to approved institutional animal care and use committee (IACUC) protocols of the University of Groningen (under IVD protocol number 184824-01-001) and the Comunidad de Madrid under the approved protocol (PROEX227/16). Both male and female animals were used in this study. Mice were reared in a barrier-controlled facility (20°C; 12-h light/dark cycle) with *ad libitum* access to food and water. For the maintenance of the colony and obtaining the embryos for the experiments, heterozygous females (*Atg5*$^{+/-}$) have been crossed with heterozygous males (*Atg5*$^{+/-}$), in this way, we guaranteed the obtaining of both *Atg5*$^{-/-}$ embryos and *Atg5*$^{+/+}$ as its direct controls. Animals were crossed and the morning on which the vaginal plug was detected was designated embryonic day (E) 0.5. Animals were euthanized by cervical dislocation and embryos removed by caesarean section. The embryos were staged and then placed in a Petri dish in 1× phosphate-buffered saline (PBS).

Adult submandibular SGs were isolated from 6-8 weeks old female C57BL/6 mice, as previously described[25]. The collected SGs were subjected to mechanical disruption using a gentleMACS dissociator (Miltenyi Biotec), followed by enzymatic digestion in Hank's Balanced Salt Solution (HBSS, Thermofisher Scientific Cat#14175-129) containing 1% BSA (Thermofisher Scientific, Cat#15260037), 0.63 mg/m collagenase II (Thermofisher Scientific, Cat#17101-015), 0.5 mg/ml hyaluronidase (Sigma Aldrich, Cat#H3506) and 50 mM $CaCl_2$ at

37˚C for 30 min. After the digestion, the samples were subjected to centrifugation at 400 g for 5 min and washed with HBSS containing 1% BSA, before a second digestion using the same conditions as above. For a primary culture, the two submandibular SGs from a single mouse were digested in a 2 ml volume. The digested material was filtered through a 100 µm cell strainer (BD Biosciences) and then re-suspended in the minimal medium (MM): 1x Dulbecco's modified Eagle's:F12 medium (Cat#11320-074) containing Pen/Strep antibiotics (Thermofisher Scientific, Cat#15140122), 1x Glutamax (Thermofisher Scientific, Cat#35050061), 20 ng/ml epidermal growth factor (Sigma Aldrich, Cat#E9644), 20 ng/ml fibroblast growth factor-2 (Preprotech-Bioconnect, Cat#100-1813), 1x N-2 Supplement (Gibco, Cat#17502-048), 10 mg/ml insulin (Sigma Aldrich, Cat#I6634-100mg) and 1 mM dexamethasone (Sigma Aldrich, Cat#d4902-25mg)[27], and plated at a density of 400,000 cells per well in a 12-well plate (Sigma Aldrich, Cat# CLS3513-50EA). The primary culture was maintained for 3 days at 37˚C in a 5% CO_2 incubator before proceeding to the self-renewal assay.

For the embryonic SGs isolation, the sacrificed embryos (E18.5) were kept in HBSS containing 1% BSA at 4˚C before dissection of the SGs on ice. From each embryo, one of the SGs was placed in a 6-well plate with 1 ml of HBSS containing 1% BSA, while the other was directly immersed in 4% formaldehyde (Merck, Cat#1.04003.100) in PBS to proceed with the embedding for histochemistry experiments. The isolated SGs in the 6-well plates were subjected to mechanical digestion through numerous successive aspirations by pipetting during the enzymatic digestion in the solution described above, at 37˚C for 5 min. After this treatment, samples were subjected to centrifugation at 400 g for 5 min and washed with HBSS containing 1% BSA. Samples were finally resuspended in the 75 µl of appropriate media, MM or WRY (MM supplemented with 10% R-spondin conditioned media (a kind gift from Hans Clevers, Hubrecht Institute, Utrecht, the Netherlands) and 50% Wnt3a conditioned media (a kind gift from Hans Clevers, Hubrecht Institute, Utrecht, the Netherlands) and mixed with 150 µl of Matrigel® (Vwr, Cat#356235), before splitting them in 3 aliquots of 75 µl, each one of them placed in a different well of a 12-well plate. These primary cultures were maintained at

37˚C in a 5% CO_2 incubator for 7 days, before dispersing them in single cells for the self-renewal assay.

Human SGs

Human non-malignant submandibular SGs tissues were obtained from donors after informed consent and Institutional Review Board (IRB) approval, during an elective head and neck dissection procedure for the removal of squamous cell carcinoma from the oral cavity. Surgical removals were performed at the University Medical Center Groningen and the Medical Centre Leeuwarden. For the isolation of human SGSCs; the biopsies collected in the operating room were transferred to the lab in a 50 mL falcon tube containing HBSS 1% BSA on ice. The biopsy was weighted in a sterile petri dish and using a sterile disposable scalpel minced into small pieces. To obtain optimal digestion 20 mg of tissue was processed per 1 mL of enzymatic digestion buffer (see above) volume, with a maximum of 100 mg of tissue per tube. The human biopsies were then processed in the same manner as the mouse tissue.

Self-renewal assay

Three days old primary SGs cultures were treated with 1 ml of 0.05% trypsin-EDTA (Thermofisher Scientific, Cat#25300-096) at 37˚C for 10-15 min, to generate single cell suspensions and counted to be adjusted to a concentration of 2 x 10^5 cells/ml per well. Then, 25 µl of each cell suspension was combined with 50 µl of Matrigel® on ice before to be deposited at the center of a well in a 12-well culture plate. After solidification at 37˚C for 30 min, the gels were covered with medium, either MM or WRY. Seven days after seeding, the Matrigel® was dissolved by incubation with 1 mg/ml of Dispase (Invitrogen, Cat#17105-041) at 37˚C for 45-60 min. Organoids released from the gels were either counted or processed into single cell suspensions by treating them with 0.05% trypsin-EDTA at 37˚C for 5-10 min. The cell suspensions are quantified for the concentration of 2 x 10^5 cells/ml per well and the seeding procedure in Matrigel® was repeated. This cycle was repeated up to five times, *i.e.*, 5 passages.

At each passage, the self-renewal capacity was determined as established previously[26]. Briefly, the number of organoids was quantified with a brightfield microscope in each well and

the percentage of organoid formation efficiency (OFE) and population doubling was calculated in the following way:

$$\text{OFE [\%]} = \frac{\text{Number of organoids harvested at the end of the passage}}{\text{Number of single cells seeded at the beginning of the passage}} \text{ x } 100$$

$$\text{Population doubling} = \frac{\ln(\text{harvested cells}/\text{seeded cells})}{\ln 2}$$

Mouse submandibular SGs ligation

The *in vivo* injury mouse model for SGs is being described and validated in detail in a manuscript that is in preparation. Briefly, C57BL6 mice were anesthetize with isoflurane before making a small incision in the neck to access the submandibular SGs. Each submandibular SGs was ligated with the use of a non-dissolvable wire, just below the sublingual gland. Suturing of the SGs leads to the appearance of a caudal and a cranial region over time, which can be clearly distinguished morphologically or using the hematoxylin and eosin (H&E) staining, which colors the nuclei and the cytoplasm in histological preparations. The caudal region of the suture results from the loosing of the acinar structures and tissue atrophy, while the cranial region corresponds to the part of the SGs that is regenerating, which also present intact acinar and ductal structures. Five, 9 or 15 days later, the animals were re-anaesthetized and sacrificed by cervical dislocation. The suture was removed, and submandibular SGs were harvested and fixed in 4% formaldehyde overnight at room temperature. Sections were used for immunofluorescence (as described below). Control mice with matching sex and age were subjected to a mock ligation surgery that included isoflurane anesthesia, exposure of the submandibular gland and suture of the incision. To estimate the autophagic flux upon SGs ligation, the experiment was also repeated in animals treated or not with HCQ as follow. HCQ (50 mg/kg) or a saline solution (for the control mice) was administered daily by intraperitoneal injections until sacrifice of the animals 5, 9 or 15 days SGs post-ligation. The sacrifice of the animals and the post-sacrifice treatment of the tissues were done as mentioned above.

To assess cell proliferation in the ligated submandibular SGs as well as in the control SGs, mice were subjected to two intraperitoneal bromodeoxyuridine (BrdU, Sigma Aldrich,

Cat#B5002-1G) injections. BrdU was dissolved in physiologic solution at a concentration of 50 mg/Kg of body weight and injected respectively 24 h and 6 h prior sacrifice. Following BrdU labelling, immunofluorescence and quantification was performed as described below.

Antibodies and other reagents

Primary antibodies for western-blot were against LC3 (Novus Biologicals, Cat#NB600), SQSTM1 (Abcam, Cat#ab56416), ATG13 (Sigma Aldrich, Cat#SAB4200100) and ACTIN (EMD Millipore, Cat#MAB1501). Primary antibodies used for immunofluorescence and immunocytochemistry were against LC3 (MBL, Cat#PM036), SQSTM1 (Progen, Cat#GP62-C), ATG16L1 (Abgent, Cat#AP1817b), AQP5 (Alomone labs, Cat#AQP5-005) and BrdU (Bio-Rad, Cat#MCA2483GA). Fluorescently-labelled antibodies for FACS sorting were against CD31 (CD31-PE, eBioscience, Cat#12-0311-82), CD45 (CD45-PE, Biolegend, Cat#103106), TER-119 (TER119-PE/Cy7, Biolegend, Cat#116222), CD24 (CD24-Pacific Blue, Biolegend, Cat#101820) and CD29 (CD29-FITC, BD Biosciences, Cat#555005). The following secondary antibodies from Thermofisher Scientific were used for the visualization of the primary antibodies: Alexa Fluor 488-conjugated goat anti-mouse (Cat#A-11001), Alexa Fluor 568-conjugated goat anti-mouse (Cat#A-11031) or goat anti-rabbit (Cat#A-11011), Alexa Fluor 647-conjugated goat anti-mouse (Cat#A-21235), and Alexa Fluor 568 conjugated goat anti-Guinea pig (Cat#A-11075).

Hoechst33342 was from Sigma Aldrich (Cat#B2261), Chloroquine (Cat#C6628) was from Sigma Aldrich and bafilomycin A1 was from BioAustralis (Cat#BIA-B1012). Tat-BECLIN1 was from Selleck Chemicals (Cat#S8595), while propidium iodide was from Sigma Aldrich (Cat#P4170).

siRNA transfection of SGSCs

Mouse SGs derived-cells were transfected with 20 pmol of silencing RNAs (siRNAs) against ATG13 (Cat#ON-TARGET plus D-053540) and scrambled (Cat#D-001810-01-05), all from Dharmacon. Briefly, single cells were seeded at a density of 1 to $1.5x10^5$ in a 12-well plate containing MM medium and the transfection was done using Lipofectamine RNAiMAX (Thermofisher Scientific, Cat#3778150). Five h post-transfection, the medium was replaced

with MM medium and cells were incubated at 37°C in 5% CO_2 for an additional 24 h. Then, a second round of transfection was performed as above and 24 h post-transfection, cells were counted, resuspended in MM medium at a density of $0.8x10^6$ cells/ml and seeded in Matrigel®. Cells were harvested 48 h after the first transfection to check the knockdown efficiency of ATG13 by western blot. Moreover, organoids and cells were counted to establish the OFE% at the end of the passage.

Stainings for immunofluorescence and immunohistochemistry analyses

For immunofluorescence staining, cells or organoids were blocked with a solution composed of 0.2% powdered milk (Nutricia, Cat#8712400763004), 2% fetal calf serum (Greiner Bio-One, Cat#758093), 0.1 M glycine, 1% BSA and 0.01% Triton X-100 (Sigma-Aldrich, Cat# 93443), for 30 min at room temperature. Subsequently, they were incubated with the primary antibody in 0.1% BSA in PBS for 1 h at room temperature, washed once with PBS and incubated with the secondary antibody diluted 1:200 in 0.1% BSA in PBS for 30 min at room temperature. The preparation was finally washed with PBS and mounted with ProLong® Gold Antifade Mountant with DAPI (Thermofisher Scientific, Cat# P36931).

For immunohistological staining of tissues, entire SGs were fixed in 4% formaldehyde at room temperature for 24 h and embedded in paraffin wax. Briefly, SGs were dehydrated using a solution with increasing amounts of Ethanol before to be embedded in paraffin and processed into 5 µm sections. The sections were then dewaxed, boiled for 8 min in pre-heated 10 mM citric acid retrieval buffer (pH 6.0) containing either 0.05% Tween (Sigma-Aldrich, Cat#93733) and washed with 1X PBS. Samples were then incubated with 100 mM glycine at room temperature for 15 min, washed once with PBS and blocked with serum of the used secondary antibody diluted 1:200 in 0.04% Triton X-100 in PBS for permeabilization. Subsequently, samples were incubated with the primary antibody diluted in 0.1% Tween in PBS overnight at 4ºC, washed once with PBS and incubated for 1h at room temperature with the secondary antibody in 0.1% Tween in PBS containing 1:100 Hoechst. Preparations were finally mounted with 80% glycerol in PBS and imaged. For BrdU staining, an additional denaturation step was applied after the permeabilization step with 0.04% Triton X-100 in PBS, by incubating the

sections in 2.5 M HCl for 20 min as well as a quenching step for the endogenous peroxide activity prior to the staining with the secondary antibody with 0.5% H_2O_2 for 30 min.

Image acquisition and analysis

Immunohistochemical and immunofluorescence preparations were examined by fluorescence microscopy. Fluorescent signals were collected with a DeltaVision Elite fluorescence microscope (Applied Precision Ltd.) equipped with a CoolSNAP HQ camera (Photometrics). Images were generated by collecting a stack of 20-30 pictures with focal planes 0.20 µm apart using either 60x or 100x objectives, and successive deconvolution using the SoftWoRx software (Applied Precision Ltd.). The quantification of LC3, SQSTM1 or ATG16L1 puncta and BrdU positive nuclei was carried out using the ICY software, while image processing was done using the ImageJ/Fiji software.

Flow cytometry sorting and analyses

For FACS-based cell sorting, after isolation and digestion (see above), SGs were dissociated in 0.05% trypsin-EDTA at 37˚C for 10 min and concentrated by passage through a 35 µm strainer. The resulting cell pellets were subsequently incubated with fluorescent-conjugated antibodies (*i.e.*, CD31-PE, CD45-PE, TER-119-PE/Cy7, CD29-FITC and CD24-PB) in 0.2%BSA in PBS for 15 min at room temperature, washed with 0.02% BSA in PBS and centrifuged at 0.4 g for 5 min. Cell pellets were then resuspended in a solution of 1 mg/ml of propidium iodide (Sigma-Aldrich, Cat#P4170), 10 mM $MgSO_4$ and 50 µg/ml of RNase A (Invitrogen, Cat#8003088), 0.2% BSA in PBS. The CD31-PE, CD45-PE and TER-119-PE/Cy7 were gated to eliminate blood cells from SGs-derived cells, while propidium iodide staining was used to discard dead cells. CD29-FITC- and CD24-PB-positive cells were gated to sort them for further analysis[27]. FACS-based sorting was carried out using a MoFlo XDP Cell Sorter (Beckman Coulter).

SGSCs differentiation into organoids

Matrigel® was diluted 1:1 with ice-cold medium on ice, poured in 96-well plates and incubated at 37˚C for 30 min to coat them. Single cell-derived organoids from the self-renewal assay were collected and quantified to prepare organoid suspensions, which were in a ratio of 25 µl

of media containing 20-30 organoids and 50 µl of Matrigel® per well on ice. 75 µl of the mix was seeded on each well coated with Matrigel® and then incubated at 37˚C for 30 min before adding of 150 µl of MM media supplemented with 50 ng/ml of HGF (Peprotech, Cat#100-39) and 1 µM DAPT (Sigma Aldrich, Cat#D5942). The organoids were cultured at 37˚C in 5% CO_2 for 2 weeks after which the organoids are counted by brightfield microscopy and identified according to their branched morphology[25].

Cell death analysis

After isolation of SGs or culture of SGSCs into organoids, single cells were obtained by dissociation in 0.05% trypsin-EDTA at 37˚C for 10 min, before to be washed with 1% BSA in PBS and concentrated by passage through a 35 µm strainer and centrifugation at 0.4 g for 5 min. The resulting samples were labelled using the FITC Dead Cell Apoptosis Kit (Thermofisher Scientific, Cat#V13242), which contains FITC-conjugated annexin V and propidium iodide to label apoptotic or dead cells, following the manufacturer instructions. Labelled cells were then sorted and examined with a FACS-LSR-II machine (BD Biosciences). The mean fluorescence intensity for 10.000 cells per each condition (determined in forward scatter, FSC, and size scatter, SSC, channels) was determined using the Kaluza Analysis software.

Cell division analysis

Single cells from either isolated SGs or organoids were obtained by dissociation in 0.05% trypsin-EDTA at 37˚C for 10 min before to be washed with 1% BSA in PBS and concentrated by passage through a 35 µm strainer and centrifugation at 0.4 g for 5 min. The resulting samples were fixed in cold 70% ethanol for 30 min, treated with 100 µg/ml ribonuclease (Sigma Aldrich) to ensure that only the DNA is labelled by 50 µg/ml propidium iodide before DNA content quantitation using flow cytometry. Labelled cells were then analyzed with the FACS-LSR-II machine. Both the mean fluorescence intensity for 10.000 cells of each sample (determined in the forward scatter, FSC, and the size scatter, SSC, channels) and the cell count for PI intensity according to cell division phases were determined using the Kaluza Analysis software (Beckman Coulter).

Western-blot analyses

Samples from self-renewal assays were dissolved from Matrigel® by incubation in 1 mg/ml of Dispase (Sigma Aldrich) at 37˚C for 30 min. The dissolved organoids were then collected in ice-cold 0.2 % BSA in PBS and centrifuged at 0.4 g for 5 min at 4 ˚C. Supernatants were discarded and the pellets were frozen at -80˚C. Pellets were subsequently resuspended in 50 μl of Laemmli buffer (4% sodium dodecyl sulphate, 20% glycerol, 10% β-mercaptoethanol, 0.002% bromophenol blue, 0.125 M Tris-HCl, pH6.8) and boiled at 100°C for 10 min. Equal protein amounts were separated by SDS-PAGE and after western blot, proteins were detected using specific antibodies and the Odyssey Imaging System (LI-COR Biosciences). Densitometric values were determined and quantified on western blots at non-saturating exposures using the ImageJ/Fiji software and normalized against the ACTIN loading control.

Statistical Analyses

Data are presented as the mean ± standard deviation (SD) of at least three independent experiments (i.e., biological replicates). Differences between samples and conditions were analyzed using the Student's *t*-test. Statistical significance was set at *p< 0.05.

Acknowledgements

F.R. is supported by Marie Skłodowska-Curie Cofund (713660), Marie Skłodowska-Curie ITN (765912), ALW Open Program (ALWOP.310) and ZonMW VICI (016.130.606) grants. R.C. and C.R. are supported by the Dutch Cancer Society (Grant number 5792 and 12458). Patricia Boya is supported by the Ministerio de Ciencia, Innovación y Universidades (MCIU), the Agencia Estatal de Investigación (AEI), the Fondo Europeo deDesarrollo Regional (FEDER) (PGC2018-098557-B-I00 and a Marie Skłodowska-Curie ITN grant (765912). Idil Orhon is a recipient of a FEBS postdoctoral fellowship and Beatriz Villarejo-Zori of a Fundacion Tatiana Perez de Guzman el Bueno predoctoral fellowhip.

References

1 Clevers, H. STEM CELLS. What is an adult stem cell? *Science* **350**, 1319-1320, doi:10.1126/science.aad7016 (2015).

2 Morrison, S. J. & Spradling, A. C. Stem cells and niches: mechanisms that promote stem cell maintenance throughout life. *Cell* **132**, 598-611, doi:10.1016/j.cell.2008.01.038 (2008).

3 Zhou, W., Choi, M., Margineantu, D., Margaretha, L., Hesson, J., Cavanaugh, C. *et al.* HIF1alpha induced switch from bivalent to exclusively glycolytic metabolism during ESC-to-EpiSC/hESC transition. *EMBO J* **31**, 2103-2116, doi:10.1038/emboj.2012.71 (2012).

4 Kubli, D. A. & Sussman, M. A. Eat, breathe, ROS: controlling stem cell fate through metabolism. *Expert Rev Cardiovasc Ther* **15**, 345-356, doi:10.1080/14779072.2017.1319278 (2017).

5 Boya, P., Reggiori, F. & Codogno, P. Emerging regulation and functions of autophagy. *Nat Cell Biol* **15**, 713-720, doi:10.1038/ncb2788 (2013).

6 Rodolfo, C., Di Bartolomeo, S. & Cecconi, F. Autophagy in stem and progenitor cells. *Cell Mol Life Sci* **73**, 475-496, doi:10.1007/s00018-015-2071-3 (2016).

7 Kuma, A., Komatsu, M. & Mizushima, N. Autophagy-monitoring and autophagy-deficient mice. *Autophagy* **13**, 1619-1628, doi:10.1080/15548627.2017.1343770 (2017).

8 Boya, P., Codogno, P. & Rodriguez-Muela, N. Autophagy in stem cells: repair, remodelling and metabolic reprogramming. *Development* **145**, doi:10.1242/dev.146506 (2018).

9 Garcia-Prat, L., Martinez-Vicente, M., Perdiguero, E., Ortet, L., Rodriguez-Ubreva, J., Rebollo, E. *et al.* Autophagy maintains stemness by preventing senescence. *Nature* **529**, 37-42, doi:10.1038/nature16187 (2016).

10 Leeman, D. S., Hebestreit, K., Ruetz, T., Webb, A. E., McKay, A., Pollina, E. A. *et al.* Lysosome activation clears aggregates and enhances quiescent neural stem cell activation during aging. *Science* **359**, 1277-1283, doi:10.1126/science.aag3048 (2018).

11 Liu, P., Liu, K., Gu, H., Wang, W., Gong, J., Zhu, Y. *et al.* High autophagic flux guards ESC identity through coordinating autophagy machinery gene program by FOXO1. *Cell Death Differ* **24**, 1672-1680, doi:10.1038/cdd.2017.90 (2017).

12 Ho, T. T., Warr, M. R., Adelman, E. R., Lansinger, O. M., Flach, J., Verovskaya, E. V. *et al.* Autophagy maintains the metabolism and function of young and old stem cells. *Nature* **543**, 205-210, doi:10.1038/nature21388 (2017).

13 Salemi, S., Yousefi, S., Constantinescu, M. A., Fey, M. F. & Simon, H. U. Autophagy is required for self-renewal and differentiation of adult human stem cells. *Cell Res* **22**, 432-435, doi:10.1038/cr.2011.200 (2012).

14 Donnelly, H., Salmeron-Sanchez, M. & Dalby, M. J. Designing stem cell niches for differentiation and self-renewal. *J R Soc Interface* **15**, doi:10.1098/rsif.2018.0388 (2018).

15 Yin, X., Mead, B. E., Safaee, H., Langer, R., Karp, J. M. & Levy, O. Engineering Stem Cell Organoids. *Cell Stem Cell* **18**, 25-38, doi:10.1016/j.stem.2015.12.005 (2016).

16 Murrow, L. M., Weber, R. J. & Gartner, Z. J. Dissecting the stem cell niche with organoid models: an engineering-based approach. *Development* **144**, 998-1007, doi:10.1242/dev.140905 (2017).
17 Clevers, H. & Watt, F. M. Defining Adult Stem Cells by Function, not by Phenotype. *Annu Rev Biochem* **87**, 1015-1027, doi:10.1146/annurev-biochem-062917-012341 (2018).
18 Weng, P. L., Aure, M. H., Maruyama, T. & Ovitt, C. E. Limited Regeneration of Adult Salivary Glands after Severe Injury Involves Cellular Plasticity. *Cell Rep* **24**, 1464-1470 e1463, doi:10.1016/j.celrep.2018.07.016 (2018).
19 Luitje, M. E., Israel, A. K., Cummings, M. A., Giampoli, E. J., Allen, P. D., Newlands, S. D. *et al.* Long-Term Maintenance of Acinar Cells in Human Submandibular Glands After Radiation Therapy. *Int J Radiat Oncol Biol Phys* **109**, 1028-1039, doi:10.1016/j.ijrobp.2020.10.037 (2021).
20 Aure, M. H., Konieczny, S. F. & Ovitt, C. E. Salivary gland homeostasis is maintained through acinar cell self-duplication. *Dev Cell* **33**, 231-237, doi:10.1016/j.devcel.2015.02.013 (2015).
21 Vissink, A., Mitchell, J. B., Baum, B. J., Limesand, K. H., Jensen, S. B., Fox, P. C. *et al.* Clinical management of salivary gland hypofunction and xerostomia in head-and-neck cancer patients: successes and barriers. *Int J Radiat Oncol Biol Phys* **78**, 983-991, doi:10.1016/j.ijrobp.2010.06.052 (2010).
22 Lombaert, I., Movahednia, M. M., Adine, C. & Ferreira, J. N. Concise Review: Salivary Gland Regeneration: Therapeutic Approaches from Stem Cells to Tissue Organoids. *Stem Cells* **35**, 97-105, doi:10.1002/stem.2455 (2017).
23 Pringle, S., Van Os, R. & Coppes, R. P. Concise review: Adult salivary gland stem cells and a potential therapy for xerostomia. *Stem Cells* **31**, 613-619, doi:10.1002/stem.1327 (2013).
24 Jensen, S. B., Vissink, A., Limesand, K. H. & Reyland, M. E. Salivary Gland Hypofunction and Xerostomia in Head and Neck Radiation Patients. *J Natl Cancer Inst Monogr* **2019**, doi:10.1093/jncimonographs/lgz016 (2019).
25 Pringle, S., Maimets, M., van der Zwaag, M., Stokman, M. A., van Gosliga, D., Zwart, E. *et al.* Human Salivary Gland Stem Cells Functionally Restore Radiation Damaged Salivary Glands. *Stem Cells* **34**, 640-652, doi:10.1002/stem.2278 (2016).
26 Nanduri, L. S., Maimets, M., Pringle, S. A., van der Zwaag, M., van Os, R. P. & Coppes, R. P. Regeneration of irradiated salivary glands with stem cell marker expressing cells. *Radiother Oncol* **99**, 367-372, doi:10.1016/j.radonc.2011.05.085 (2011).
27 Maimets, M., Rocchi, C., Bron, R., Pringle, S., Kuipers, J., Giepmans, B. N. *et al.* Long-Term In Vitro Expansion of Salivary Gland Stem Cells Driven by Wnt Signals. *Stem Cell Reports* **6**, 150-162, doi:10.1016/j.stemcr.2015.11.009 (2016).
28 Feng, J., van der Zwaag, M., Stokman, M. A., van Os, R. & Coppes, R. P. Isolation and characterization of human salivary gland cells for stem cell transplantation to reduce radiation-induced hyposalivation. *Radiother Oncol* **92**, 466-471, doi:10.1016/j.radonc.2009.06.023 (2009).
29 Pringle, S., Nanduri, L. S., van der Zwaag, M., van Os, R. & Coppes, R. P. Isolation of mouse salivary gland stem cells. *J Vis Exp*, doi:10.3791/2484 (2011).
30 Klionsky, D. J., Abdelmohsen, K., Abe, A., Abedin, M. J., Abeliovich, H., Acevedo Arozena, A. *et al.* Guidelines for the use and interpretation of assays for monitoring

autophagy (3rd edition). *Autophagy* **12**, 1-222, doi:10.1080/15548627.2015.1100356 (2016).
31 Yang, Z. & Klionsky, D. J. Mammalian autophagy: core molecular machinery and signaling regulation. *Curr Opin Cell Biol* **22**, 124-131, doi:10.1016/j.ceb.2009.11.014 (2010).
32 Emmerson, E. & Knox, S. M. Salivary gland stem cells: A review of development, regeneration and cancer. *Genesis* **56**, e23211, doi:10.1002/dvg.23211 (2018).
33 Shoji-Kawata, S., Sumpter, R., Leveno, M., Campbell, G. R., Zou, Z., Kinch, L. *et al.* Identification of a candidate therapeutic autophagy-inducing peptide. *Nature* **494**, 201-206, doi:10.1038/nature11866 (2013).
34 May, A. J., Cruz-Pacheco, N., Emmerson, E., Gaylord, E. A., Seidel, K., Nathan, S. *et al.* Diverse progenitor cells preserve salivary gland ductal architecture after radiation-induced damage. *Development* **145**, doi:10.1242/dev.166363 (2018).
35 Kulkarni, R. S., Bajaj, M. S. & Kale, V. P. Induction and Detection of Autophagy in Aged Hematopoietic Stem Cells by Exposing Them to Microvesicles Secreted by HSC-Supportive Mesenchymal Stromal Cells. *Methods Mol Biol* **1854**, 21-34, doi:10.1007/7651_2018_166 (2019).
36 Kulkarni, A., Dong, A., Kulkarni, V. V., Chen, J., Laxton, O., Anand, A. *et al.* Differential regulation of autophagy during metabolic stress in astrocytes and neurons. *Autophagy* **16**, 1651-1667, doi:10.1080/15548627.2019.1703354 (2020).
37 Kohli, L. & Passegue, E. Surviving change: the metabolic journey of hematopoietic stem cells. *Trends Cell Biol* **24**, 479-487, doi:10.1016/j.tcb.2014.04.001 (2014).
38 Nguyen-McCarty, M. & Klein, P. S. Autophagy is a signature of a signaling network that maintains hematopoietic stem cells. *PLoS One* **12**, e0177054, doi:10.1371/journal.pone.0177054 (2017).
39 Jung, H. E., Shim, Y. R., Oh, J. E., Oh, D. S. & Lee, H. K. The autophagy Protein Atg5 Plays a Crucial Role in the Maintenance and Reconstitution Ability of Hematopoietic Stem Cells. *Immune Netw* **19**, e12, doi:10.4110/in.2019.19.e12 (2019).
40 Regmi, S., Raut, P. K., Pathak, S., Shrestha, P., Park, P. H. & Jeong, J. H. Enhanced viability and function of mesenchymal stromal cell spheroids is mediated via autophagy induction. *Autophagy*, 1-20, doi:10.1080/15548627.2020.1850608 (2020).
41 Pennings, S., Liu, K. J. & Qian, H. The Stem Cell Niche: Interactions between Stem Cells and Their Environment. *Stem Cells Int* **2018**, 4879379, doi:10.1155/2018/4879379 (2018).
42 Esteban-Martinez, L. & Boya, P. BNIP3L/NIX-dependent mitophagy regulates cell differentiation via metabolic reprogramming. *Autophagy* **14**, 915-917, doi:10.1080/15548627.2017.1332567 (2018).
43 Esteban-Martinez, L., Sierra-Filardi, E., McGreal, R. S., Salazar-Roa, M., Marino, G., Seco, E. *et al.* Programmed mitophagy is essential for the glycolytic switch during cell differentiation. *EMBO J* **36**, 1688-1706, doi:10.15252/embj.201695916 (2017).
44 Gopinath, S. D., Webb, A. E., Brunet, A. & Rando, T. A. FOXO3 promotes quiescence in adult muscle stem cells during the process of self-renewal. *Stem Cell Reports* **2**, 414-426, doi:10.1016/j.stemcr.2014.02.002 (2014).
45 Cai, W. F., Wang, L., Liu, G. S., Zhu, P., Paul, C. & Wang, Y. Manipulating the Hippo-Yap signal cascade in stem cells for heart regeneration. *Ann Palliat Med* **5**, 125-134, doi:10.21037/apm.2016.03.03 (2016).

46 Moya, I. M. & Halder, G. Hippo-YAP/TAZ signalling in organ regeneration and regenerative medicine. *Nat Rev Mol Cell Biol* **20**, 211-226, doi:10.1038/s41580-018-0086-y (2019).
47 Totaro, A., Zhuang, Q., Panciera, T., Battilana, G., Azzolin, L., Brumana, G. *et al.* Cell phenotypic plasticity requires autophagic flux driven by YAP/TAZ mechanotransduction. *Proc Natl Acad Sci U S A* **116**, 17848-17857, doi:10.1073/pnas.1908228116 (2019).
48 Wu, X., Fleming, A., Ricketts, T., Pavel, M., Virgin, H., Menzies, F. M. *et al.* Autophagy regulates Notch degradation and modulates stem cell development and neurogenesis. *Nat Commun* **7**, 10533, doi:10.1038/ncomms10533 (2016).
49 Wang, S., Xia, P., Ye, B., Huang, G., Liu, J. & Fan, Z. Transient activation of autophagy via Sox2-mediated suppression of mTOR is an important early step in reprogramming to pluripotency. *Cell Stem Cell* **13**, 617-625, doi:10.1016/j.stem.2013.10.005 (2013).
50 von Bultzingslowen, I., Sollecito, T. P., Fox, P. C., Daniels, T., Jonsson, R., Lockhart, P. B. *et al.* Salivary dysfunction associated with systemic diseases: systematic review and clinical management recommendations. *Oral Surg Oral Med Oral Pathol Oral Radiol Endod* **103 Suppl**, S57 e51-15, doi:10.1016/j.tripleo.2006.11.010 (2007).
51 Morgan-Bathke, M., Lin, H. H., Chibly, A. M., Zhang, W., Sun, X., Chen, C. H. *et al.* Deletion of ATG5 shows a role of autophagy in salivary homeostatic control. *J Dent Res* **92**, 911-917, doi:10.1177/0022034513499350 (2013).
52 Morgan-Bathke, M., Hill, G. A., Harris, Z. I., Lin, H. H., Chibly, A. M., Klein, R. R. *et al.* Autophagy correlates with maintenance of salivary gland function following radiation. *Sci Rep* **4**, 5206, doi:10.1038/srep05206 (2014).
53 van Luijk, P., Pringle, S., Deasy, J. O., Moiseenko, V. V., Faber, H., Hovan, A. *et al.* Sparing the region of the salivary gland containing stem cells preserves saliva production after radiotherapy for head and neck cancer. *Sci Transl Med* **7**, 305ra147, doi:10.1126/scitranslmed.aac4441 (2015).
54 Thellung, S., Corsaro, A., Nizzari, M., Barbieri, F. & Florio, T. Autophagy Activator Drugs: A New Opportunity in Neuroprotection from Misfolded Protein Toxicity. *Int J Mol Sci* **20**, doi:10.3390/ijms20040901 (2019).
55 Towers, C. G. & Thorburn, A. Therapeutic Targeting of Autophagy. *EBioMedicine* **14**, 15-23, doi:10.1016/j.ebiom.2016.10.034 (2016).
56 Kuma, A., Hatano, M., Matsui, M., Yamamoto, A., Nakaya, H., Yoshimori, T. *et al.* The role of autophagy during the early neonatal starvation period. *Nature* **432**, 1032-1036, doi:10.1038/nature03029 (2004).

Supplementary figures

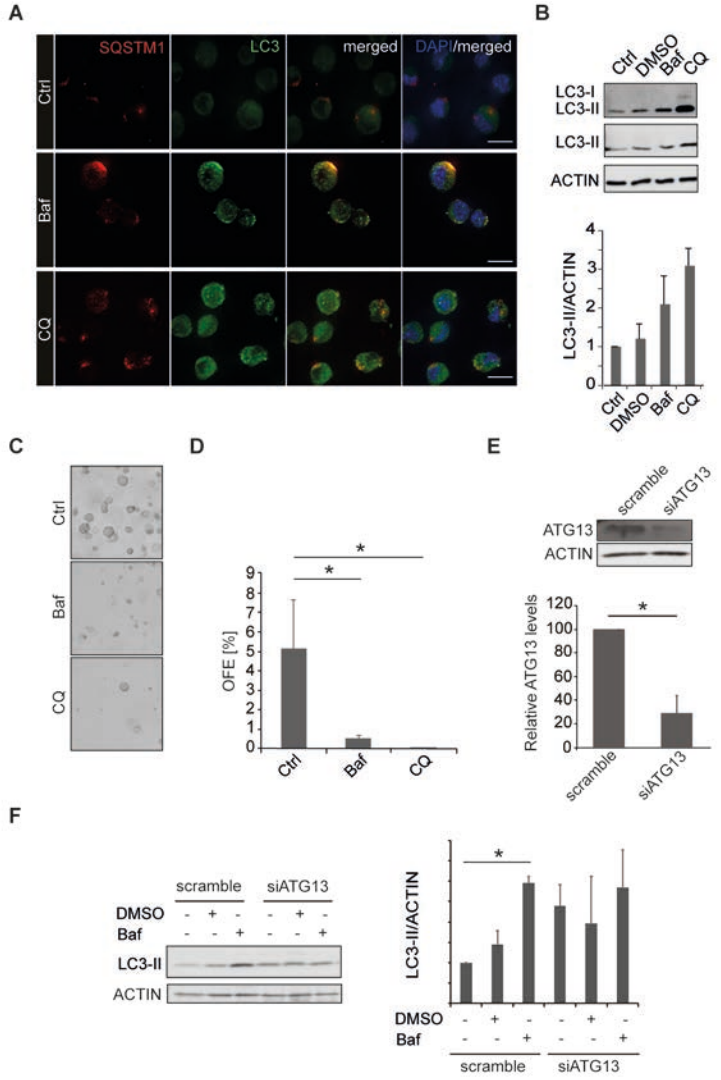

Figure S1: Autophagy inhibition blocks SG organoid formation. (A) Single SGSCs obtained by trypsinization from primary 3D cultures were treated with 100 nm Baf, 100 µM CQ or DMSO for 5h in the MM medium, before to be processed for immunofluorescence with anti-LC3 and anti- SQSTM1 antibodies. Nuclei were stained with Hoechst. Z-stacks of images separated by 0.2 µm were collected, deconvolved and analyzed as described in Material and Methods. A representative Z-projection of combined focal planes is shown. Scale bars 5 µm. (B) Single SGSCs isolated as in panel A were lysed and proteins examined by western blot using antibodies against LC3. ACTIN was used as the loading control. The upper LC3 blot has been overexposed to observe the bands corresponding to LC3-I. The bars represent the levels of LC3 normalized to ACTIN, and relative to the untreated, control single SGSCs. Bars represent the means of 3 experiments ±SD. Asterisks annotate significant differences of $p<0.05$. (C) Brightfield microscope images of secondary organoids obtained from single SGSCs treated with 100 nm Baf, 100 µM CQ or DMSO for 5h, after 7 days in Matrigel®. (D) The OFE of the samples analyzed in panel C was determined at the end of p1. Bars represent the means of 3 experiments ±SD. Asterisks annotate significant differences of $p<0.05$. (E) SGSCs transfected with either scrambled siRNAs (scramble) or siRNAs targeting ATG13 (siATG13) for 48 h, were subjected to western blot analysis with anti-ATG13 antibodies. ACTIN detection served as a loading control. ATG13 protein levels were quantified and normalized to the loading controls and expressed relative to the scramble control. Bars represent the means of 3 independent experiments ± SD. The asterisk annotates a significant difference of $p<0.05$. (F) SGSCs treated as in panel E were incubated with DMSO or 100 nm Baf for 5 h before to be analyzed by western blot using anti-LC3 and anti-ACTIN antibodies. ATG13 protein levels were quantified and normalized to those of ACTIN. A change in the LC3-II/ACTIN ratio upon Baf treatment indicates an autophagic flux, while the absence of a significant difference reveals a block in autophagy [30]. Bars represent the means of 2 independent experiments ± SD.

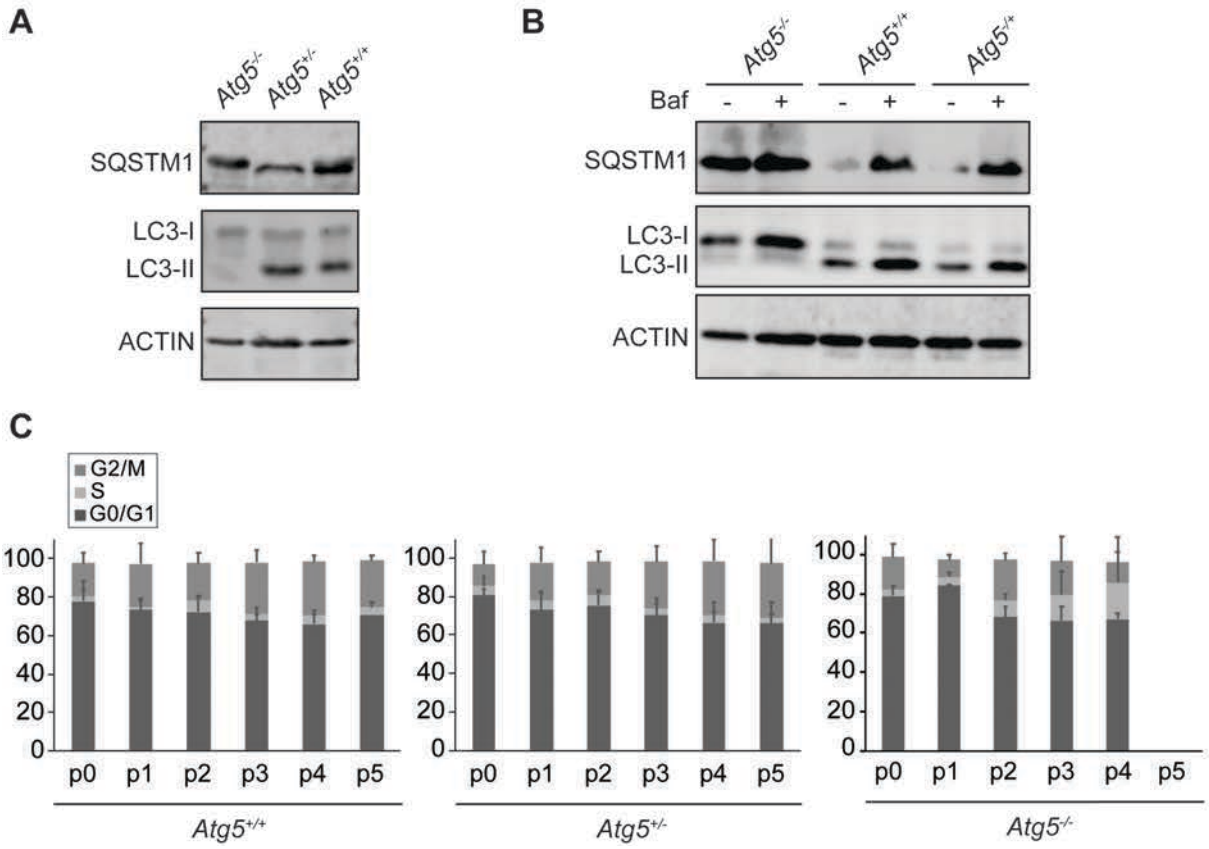

Figure S2: SGs (A) Protein extracts from Atg5$^{+/+}$, Atg5$^{+/-}$ and Atg5$^{-/-}$ SGs from embryos at stage e18.5 were analyzed by western blot using anti-SQSTM1 and anti-LC3 antibodies. ACTIN detection served as a loading control. (B) Passage 1 organoids obtained from embryonic Atg5$^{+/+}$, Atg5$^{+/-}$ or Atg5$^{-/-}$ SG at the embryonal stage E18.5, were treated or not with 100 nm Baf for 5 h, before preparing protein extracts and analyze them by western blot using anti-SQSTM1 and LC3 antibodies. ACTIN detection served as a loading control. (C) Cell cycle analysis of Atg5$^{+/+}$, Atg5$^{+/-}$ and Atg5$^{-/-}$ SGs from p0 to p5 was carried out using propidium iodide staining at the end of each passage, before determining the number of cells in G0/G1, S or G2/M cell cycle phases by flow cytometry.

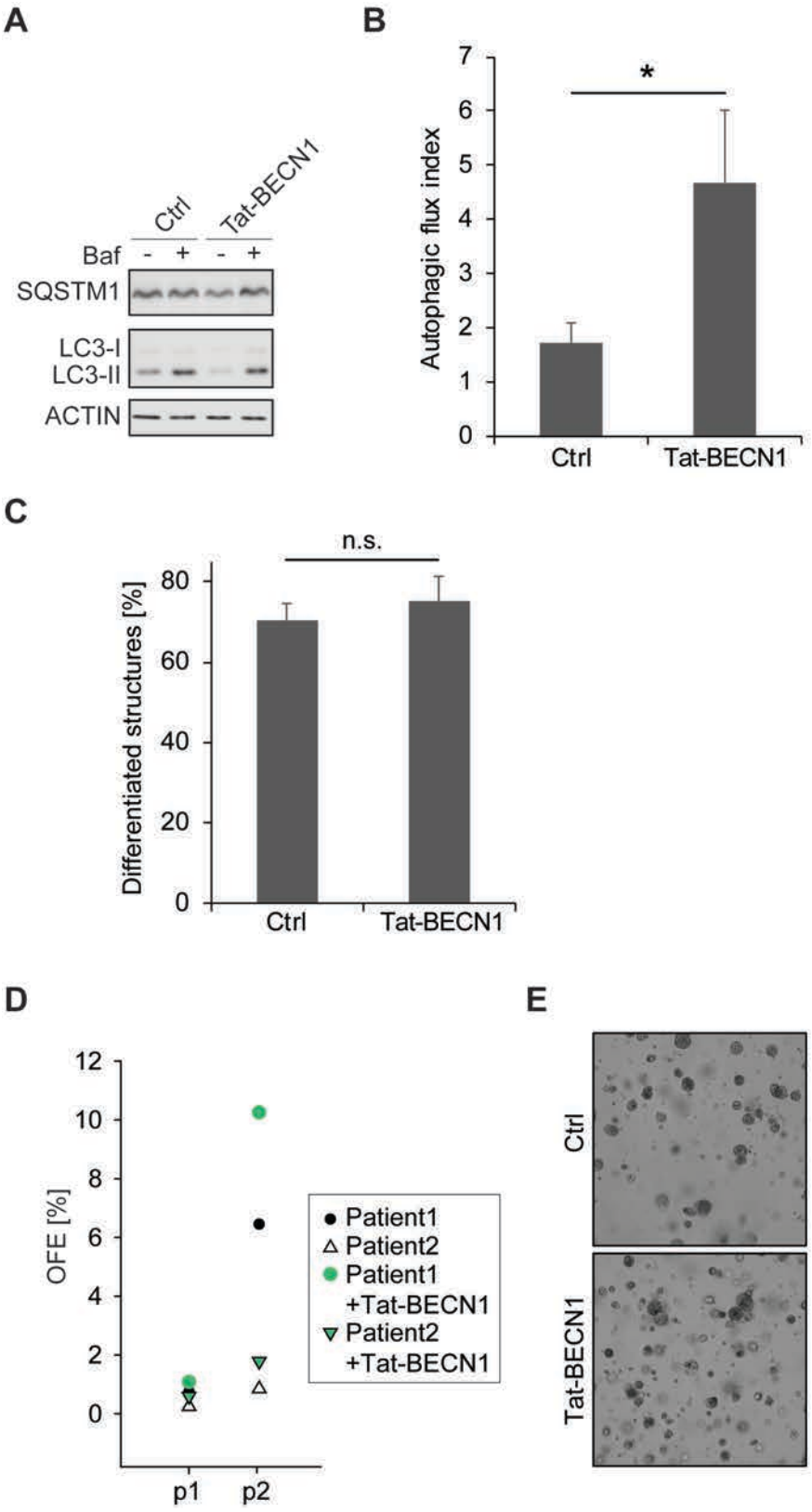

Figure S3: Tat-BECN1 induces autophagic flux in SGSCs. (A) Protein extracts from SGSCs grown in the absence (Ctrl) or the presence of 50 nM Tat-BECN1 and incubated with or without 100 nM Baf for 5 h, were examined by western blot using antibodies against SQSTM1 and LC3. ACTIN was used as the loading control. (B) The autophagy flux index in each sample of panel A was determined by dividing the amounts of LC3-II in Baf-treated cells with that in cells not exposed to Baf. Protein levels were normalized to ACTIN, which was used as the

loading control. Means of 3 independent experiments are normalized to the autophagy flux of control cells ±SD. The asterisk annotates the significant differences of $p<0.05$. (C) Percentage of differentiated structures after differentiation of SGSCs derived organoids treated or not with 50 nM Tat-BECN1. Bars represent the means of 3 experiments ±SD. The n.s. abbreviation highlights that there is no significant difference. (D) The OFE of human 3D SG cultures over 2 passages (p1 to p2), treated or not with 50nM Tat-BECN1 as in Figure 3A. Each data point represents the measurement of one sample. (C) Representative brightfield microscope images of primary organoids from human SGSCs after 7 days in Matrigel®, treated or not with 50nM Tat-BECN1.

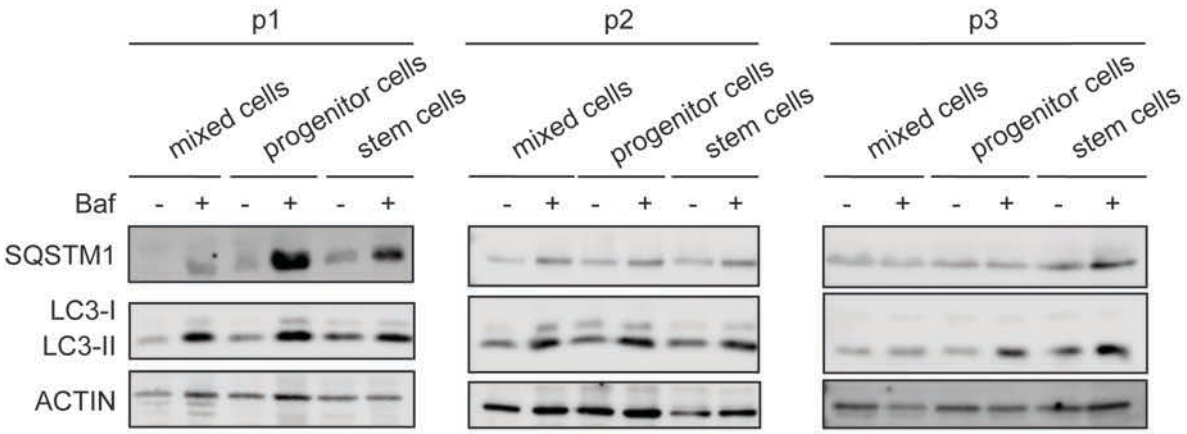

Figure S4: Autophagy flux induction correlates with self-renewal. Mixed cell, SGSCs progenitor ($CD29^{medium/hi}$ and $CD24^{medium/hi}$) and SGSCs ($CD29^{hi/hi}$ and $CD24^{hi/hi}$) populations from passage 1 to 3 (p1-p3) isolated by FACS, were treated or not with 100 nM Baf for 5 h before to be lysed. Protein extracts were subsequently examined by western blot using antibodies against SQSTM1 and LC3. ACTIN was used as the loading control.

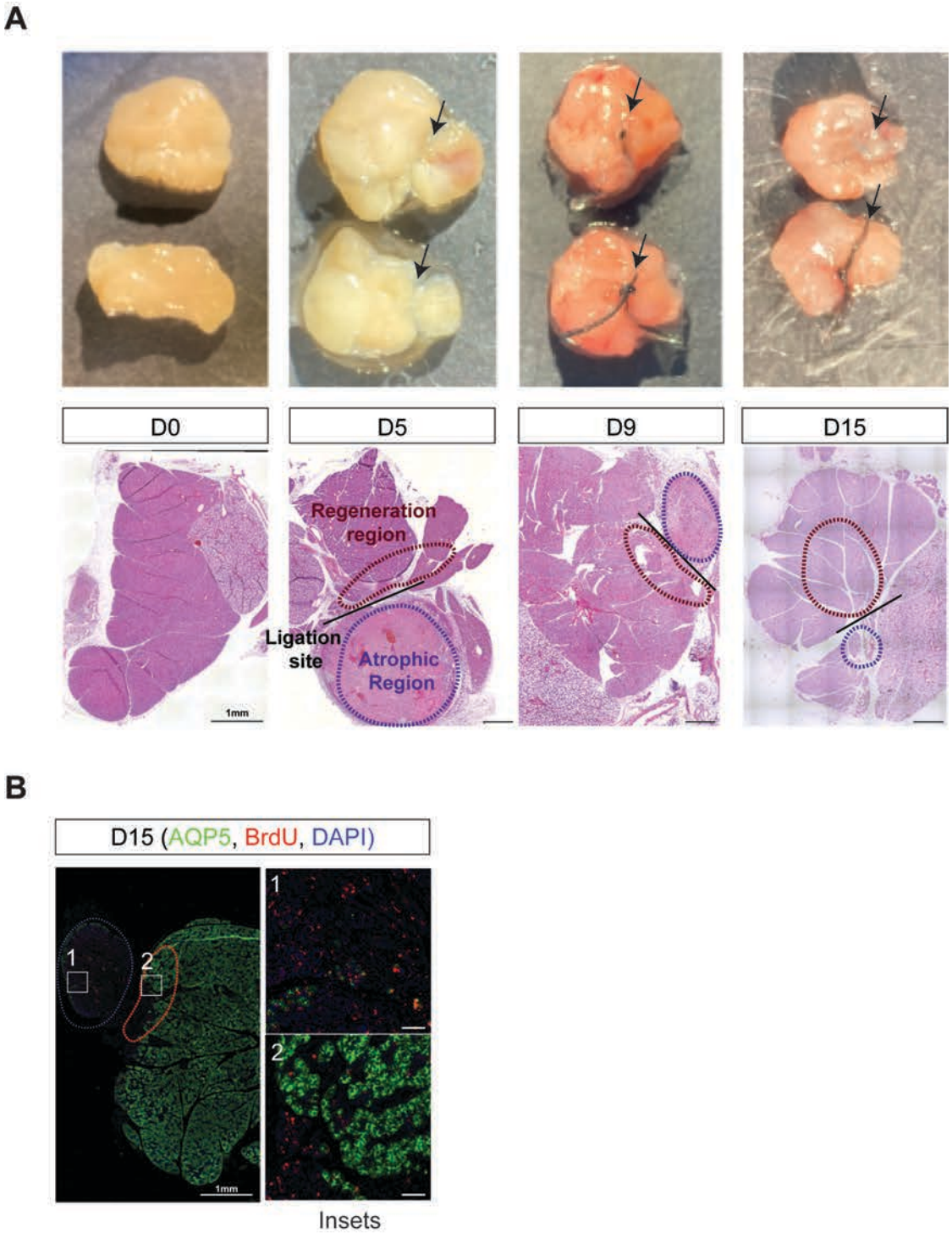

Figure S5: SG ligation induces tissue regeneration. Mouse SGs are ligated to as described in Material and Methods (A) Control and ligated glands are followed over 5, 9 and 15 days post-ligation. Pictures showing examples of removed SGs are shown on the top part of the panel. Ligation sites are indicated by arrowhead. The low part of the panel presents H&E stained immunohistological preparations from the above shown SGs. Atrophic and regenerative regions of each time point are marked with violet and bordau dashed areas. The black lines indicate the ligation sites. Scale bars 1 mm. (B) A representative single plane of regenerative SGs imaged by fluorescence microscopy at 15 days post-ligation is shown. Proliferative regions are labelled with an anti-BrdU antibody, while

differentiated acinar regions are labelled with an anti-AQP5 antibody. Insets show a proliferative (1) or a differentiated acinar (2) region at higher magnification. Cell nuclei are stained with DAPI. Scale bars 10 µm.

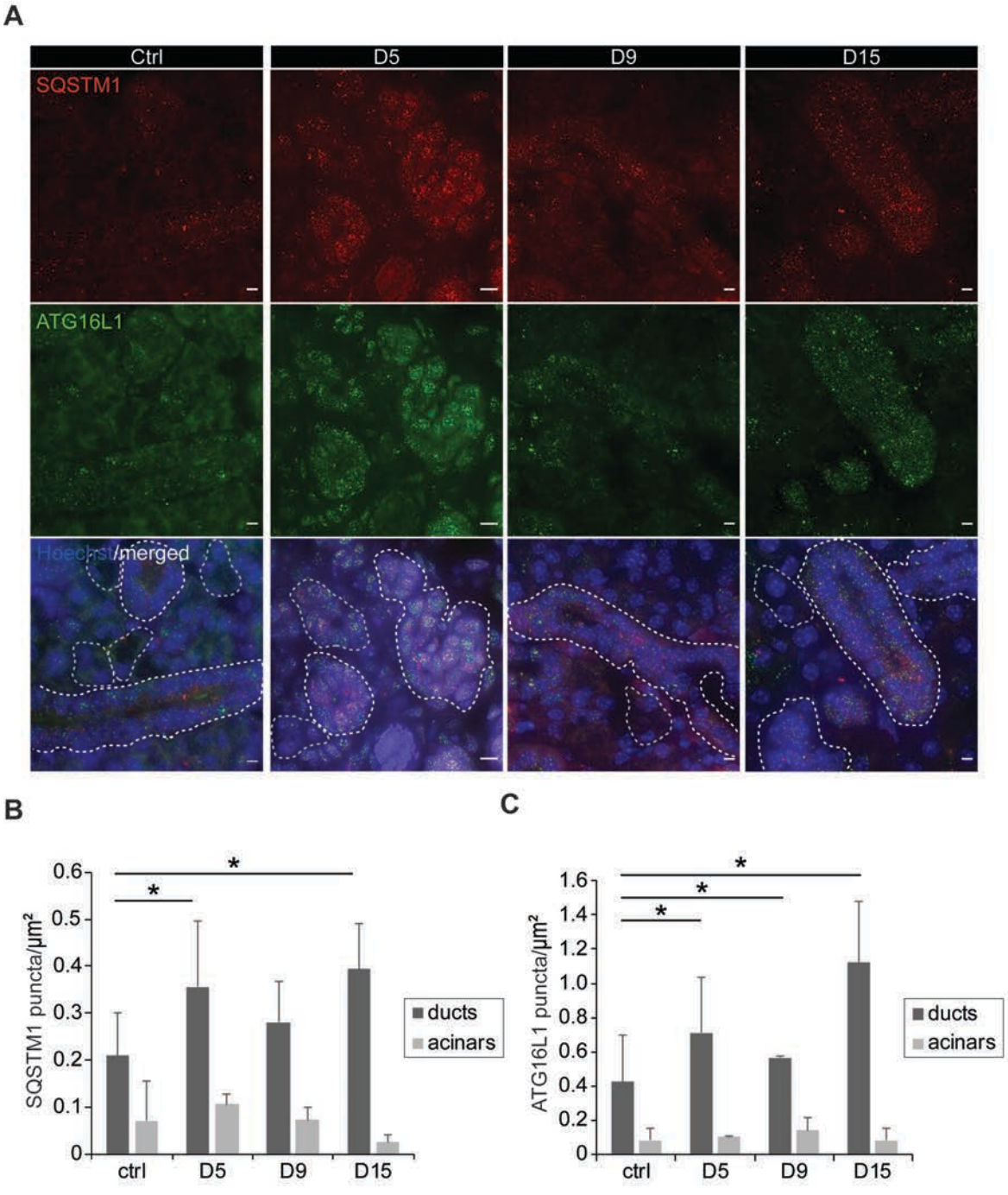

Figure S6: SG ligation-induced tissue regeneration increases autophagy activity. (A) The immunocytochemistry preparations described in Figure 4B were also cut in 5 µm thick sections and label with anti-ATG16L1 and anti-SQSTM1 antibodies. Z-stacks of images separated by 0.2 µm were collected, deconvolved and analyzed as described in Material and Methods. A representative single Z-projection is shown. Nuclei are stained with Hoechst. Ducts are delimitated by white dash-lines. Scale bars 10 µm. (B,C) Quantification of either SQSTM1 (B) or ATG16L1 (C) puncta number in either duct regions or acinar cell areas (μm^2), in the experiment shown in

Figure S5A. Bars represent the mean numbers ±SD counted at least in 5 randomly selected sections per SGs. Three different control and ligated SGs were analyzed. Asterisks annotate significant differences of $p<0.05$.

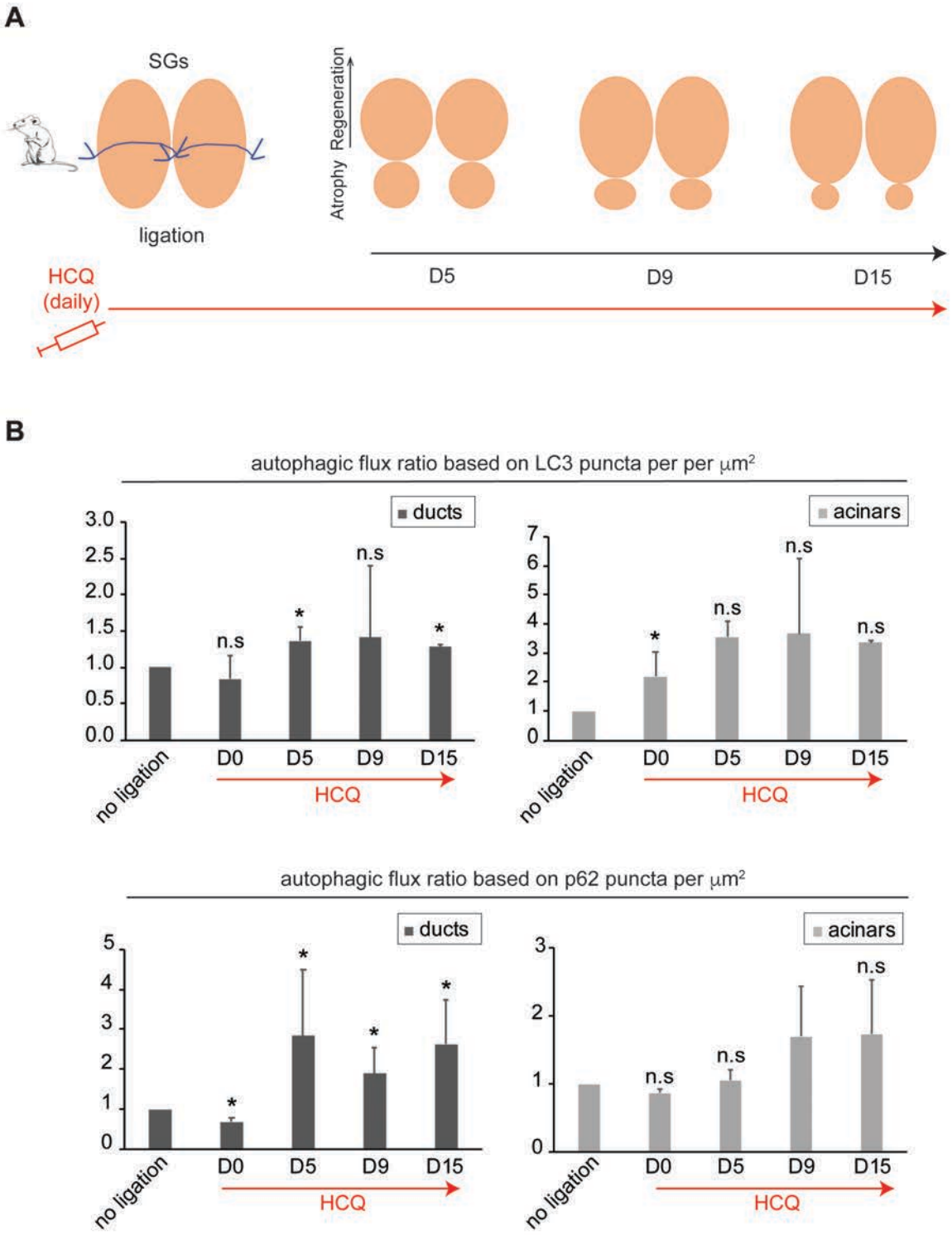

Figure S 7: Autophagy flux is increased in ducts upon ligation-induced SGs regeneration. (A) Schematic representation of the ligation of mouse SGs and the subsequent regeneration process over 15 days upon HCQ

treatment as described in material and methods. (B) Control SGs (no ligation, HCQ-untreated or no ligation, HCQ-treated), or regenerating SGs (ligation, HCQ-untreated or ligation, HCQ-treated) were excised from animals sacrificed at 0 (D0), 5 (D5), 9 (D9) and 15 (d15) days post-ligation, and processed for LC3 and SQSTM1 puncta analysis as in Figure 4B. Subsequently, the average number of LC3 or SQSTM1 puncta per μm^2 was determined in either the duct or acinar cell regions of SGs from animals treated or untreated with HCQ. The autophagic flux index for each condition (day post-ligation, with or without ligation) was then calculated but dividing the number of puncta in the sample treated with HCQ by the number of puncta in the same sample not treated with HCQ. Finally, the autophagic flux index in the ligated SGs was expressed relative to that of the non-ligated SGs. Columns represent the mean numbers $\pm$ SD of at least 3 randomly selected sections per SGs. Three different control mice and 3 different ligated mice were analyzed at each time point. Asterisks annotate significant differences of $p<0.05$.

CHAPTER 6

A MOLECULAR NETWORK-BASED APPROACH REVEALS HUMAN SALIVARY GLAND STEM CELL FEATURES

Rocchi C., Barazzuol L., Boekhoudt J., Jellema- de Bruin A., Baanstra M., Brouwer U., van Os R., Guryev V., Coppes RP.

In preparation

ABSTRACT

The need to restore functionality of salivary gland after irradiation treatment is still unmet. Tissue regenerative strategies could provide opportunities to treat radiation-induced salivary gland dysfunction. However, the molecular processes driving cell fate specification and regulating the balance between regeneration and differentiation are not completely understood. Here we describe the construction and validation of the first molecular network of human salivary gland-derived organoids. Using RNA sequence data obtained from different organoid culture conditions, aimed at enriching for stem cells or functional secretory salivary gland cells, we first build a molecular network based on modules of co-expressed genes. Next, we relate these modules to stem cell traits. This enabled us to identify novel biological processes and specific genes associated with salivary gland regeneration potential and stem-like cell features such as organoid forming ability and long-term self-renewal.

INTRODUCTION

Salivary glands are crucial for maintaining the health of the oral cavity as well as for enabling vital daily activity such as speaking, eating and swallowing [1-3]. Radiotherapy treatment for head and neck cancer, autoimmune diseases like Sjogren's Syndrome as well as natural ageing, all lead to salivary gland dysfunction through progressive degeneration of the secretory acinar cell compartment of the glands [4]. This results in irreversible loss of saliva production and a life time of dry mouth and co-morbidities that drastically decrease the quality of life of the patients affected[5,6]. Despite decades of research, clinically available treatment options for xerostomia patients are palliative, focused on providing short term relief from the symptoms without providing long-term restoration of the gland [4]. Many strategies, including cell therapy [7,8], *in vivo* reactivation of resident stem/progenitor cells [9], restoration of the niche via for example removal of senescence cells [10] and gene therapy[11,12], have been proposed to restore functionality of damaged salivary glands.

While in several organs the identity of tissue specific regenerative cells is known [13], in salivary gland the search for an adult stem cell source possessing the potential to replace acinar cells lost after damage is still ongoing, limiting the potential of regenerative approaches for salivary gland following radiotherapy (Rocchi et al 2020 Npj regenerative medicine, Accepted).

Experiments employing murine cell lineage tracing have allowed major advances in understanding salivary gland epithelial progenitors. However, there is still considerable debate on the nature of the stem/progenitor cells that contribute to tissue homeostasis as well as the mechanisms of regeneration after damage. One model proposes that bipotent murine embryonic salivary gland stem cells (expressing the cytokeratin marker K5) generate ductal and acinar progenitor cells that are postnatally maintained by lineage restricted progenitors. These express the markers K14, Kit/K5 for the ductal cell compartment and SOX2 for the acinar cell compartment [14]. The other model proposes instead a role of plasticity of the salivary gland epithelium in contributing to the functional acinar unit of the irradiated gland[15,16]. We have shown that murine salivary gland-derived epithelial cells from excretory and intercalated ducts can be isolated, grown and expanded *in vitro* as 3D organoids containing differentiated acinar cells and myoepithelial cells [17,18]. These studies suggest that upon activation of proper signaling ductal cells can be directed to give rise to salivary gland tissue-reassembling structures. Transplantation of submandibular salivary gland organoid-derived cells into locally irradiated salivary gland recipient mice allowed 70% rescue of normal total saliva production compared to control-irradiated non-transplanted mice [7,17,18] showing proof-of-principle that regenerative cell therapy approaches could be used for long-term restoration of the damaged salivary gland.

The proven reliability and *in vitro–in vivo* dual usability of salivary gland-derived organoids revealed the potency also of human salivary gland-derived stem/progenitor cells (hSGSPCs)

in rescuing the hyposalivation phenotype when xeno-transplanted into irradiated salivary glands of immunodeficient mice [2]. Although hSGSPCs can be isolated and kept in culture for a number of passages, their potential clinical application is mainly limited by the lack of knowledge regarding the identity of adult hSGSPCs and by the fact that existing culture conditions provide little to no control over their self-renewal and differentiation abilities. While extensive gene expression profiling studies have contributed to the characterization of several adult tissue stem cells and related pathways in homeostatic and disease, adult salivary gland stem cells have not yet been transcriptionally characterized (Rocchi et al 2020, Npj regenerative medicine, Accepted).

Here, we first describe the development of a long-term culture system for human salivary gland derived organoids as well *in vitro* strategies that allow for enrichment of hSGSPCs and differentiation towards more mature salivary gland organoids.

We next hypothesize that RNA sequencing of human salivary gland organoids, enriched for stem cells or differentiated, would enable us to distinguish genes and pathways associated with self-renewal and differentiation of hSGSPCs. We used a network-based gene-weighting approach that allowed the identification of unique groups of co-expressed genes (modules) that represent cellular processes and can be related to the phenotypes of interest [19]. This enabled us to identify genes and gene networks that are directly associated with human salivary gland stem cell related traits. Our findings provide the first set of human salivary gland-derived organoid transcriptomic data and identify molecular pathways which were previously not known to have a pro-regenerative effect in adult salivary glands, such as the fatty acid oxidation pathway. These findings could potentially open new therapeutic strategies for salivary gland dysfunction.

RESULTS

Optimization of human salivary gland culture system

In an attempt to establish a long term human salivary culture system, we adapted our previously established mouse salivary gland culture condition containing Wnt3a, R-spondin and Y-27632 (here called WRY and fully described in the Methods section) [18]. We isolated human salivary gland-derived cells from human submandibular gland biopsies by mechanic and enzymatic digestion, and after 3 days of enrichment in floating culture single cells were seeded in Matrigel (Figure 1A). Organoid formation efficiency (OFE) of single cells obtained from human salivary gland epithelium-derived spheres and cultured in WRY was higher in early passages (P2) compared to those cultured in enriched media (EM) devoid of Wnt3a, R-spondin and Y-27632. However, within 3-4 weeks both culture conditions lost their self-renewal potential, indicating that neither EM nor WRY media was sufficient to promote long-term maintenance of hSGSPCs (Figure 1B and C). Assuming that growth arrest occurred

because of inadequate culture conditions, we next attempted to optimize the culture conditions to increase both the number of stem cell and self-renewal capacity of the stem cells. This was measured as number of passages achievable, by screening various additional growth factors and small molecule modulators under WRY culture condition.

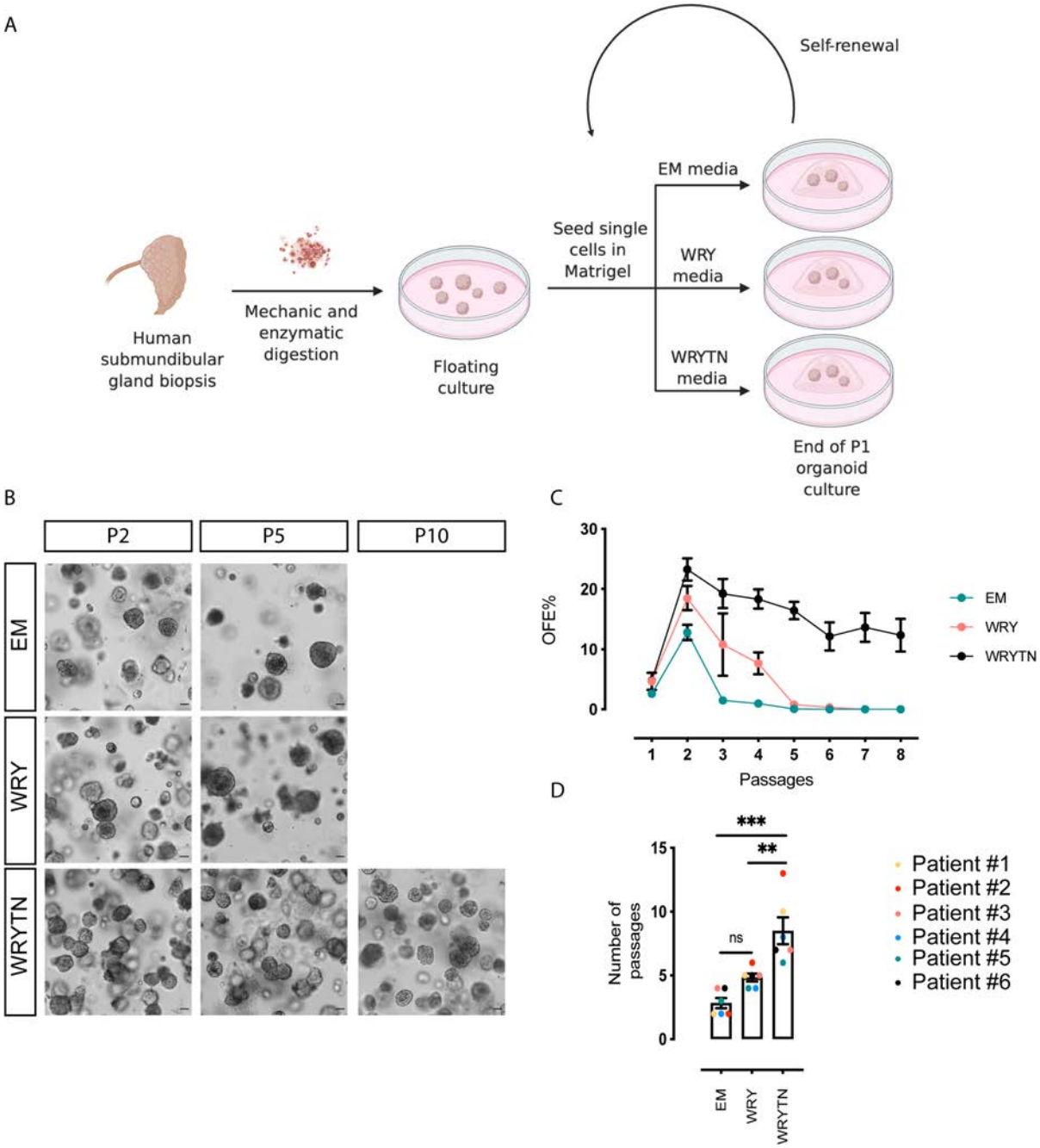

Figure 1: Human-derived submandibular gland organoids can be maintained long-term in culture. A) Schematic representation of the experimental procedure. **B)** Representative brightfield images of human salivary gland-derived organoids grown from single cells seeded in Matrigel® and treated with EM, WRY and WRYTN media at different passages of culture. Scale bar=50 μm **C)** Organoid forming efficiency (OFE) of human-derived salivary gland cells at different passages under the three tested culture conditions (EM, WRY and WRYTN). **D)** Number of passages in culture reached on average under each culture condition. Each color represents a culture

derived from a different patient (n=6). Data are represented as the mean ± SEM (C) and (D). One-way ANOVA (D). *p<0.05, **p<0.01, ***p<0.001, ****p<0.0001.

Although most compounds enhanced self-renewal potential to a certain extent, the combination of two small molecule inhibitors, A83-01 (T; Alk4 inhibitor) and noggin (N; BMP-4 antagonist), synergistically improved both OFE (Figure 1B and C) and long-term culture of hSGSPCs (Supplementary Figure 1B; Figure 1D). This combination allowed culturing up to an average of 8 passages, with a maximum of 12 passages, indicating a maintenance of stem/progenitor cells. Hereafter, we refer to this optimized culture condition as WRYTN.

Combined GSK3B and HDAC inhibition promotes a more primitive and homogeneous salivary gland stem cell organoid culture

In order to obtain a salivary gland stem cell profile in terms of genes and pathways involved in their self-renewal and differentiation, and due to the low yield of stem/progenitor cells in P1, we aimed to further enrich the stem/progenitor cells in subsequent passages. Therefore, we tested the addition of both the GSK3 inhibitor CHIR99021 and the histone deacetylase valproic acid to the WRYTN culture condition. CHIR99021 has previously been shown to promote cell proliferation in epithelial organoids [20,21], while the combination of CHIR99021 and valproic acid promotes Lgr5+ homogeneity in intestinal organoid cultures[22] (Figure 2A). Indeed, also in salivary glands the combined addition of CHIR99021 (3μM) and valproic acid (1mM) (combination now referred to as CV) to the media further enhanced OFE (Figure 2B). To assess whether CV-induced proliferation was due to the enrichment of stem/progenitor cells, we evaluated the potential of treated cells to form secondary and tertiary organoids compared to WRYTN control culture. We observed a significant increase in the ability to form secondary organoids as well as a more active proliferative state of the culture from hSGSPCs that were previously treated with CV compared to untreated WRYTN cultures (Figure 2 B, C, D and E). To further prove that CV treatment leads to a more primitive and undifferentiated stem cell state, we assessed the differentiation potential of CV treated organoids compared to untreated control organoids. To induce differentiation, organoids which had been cultured for 7 days in the presence or absence of CV were re-seeded in Wnt3a-depleted media with the addition of DAPT, an inhibitor of γ-secretase – a key component of the Notch pathway. Removal of Wnt3a and Notch pathway inhibition resulted in clear morphological changes of the organoids derived from the WRYTN control culture conditions (Figure 3B and C), similar to the branching morphogenesis described during embryonic development (Makarenkova et al 2009, Science Signalling). Notably, the continuous presence of CV during differentiation of organoids inhibited changes in organoid morphology, preserved their spherical shape and increased their size, further confirming that CV treatment maintains the cells in a more primitive and

proliferative stem cell state. After withdrawal of CV, organoids regained the ability to differentiate (Figure 3B and C).

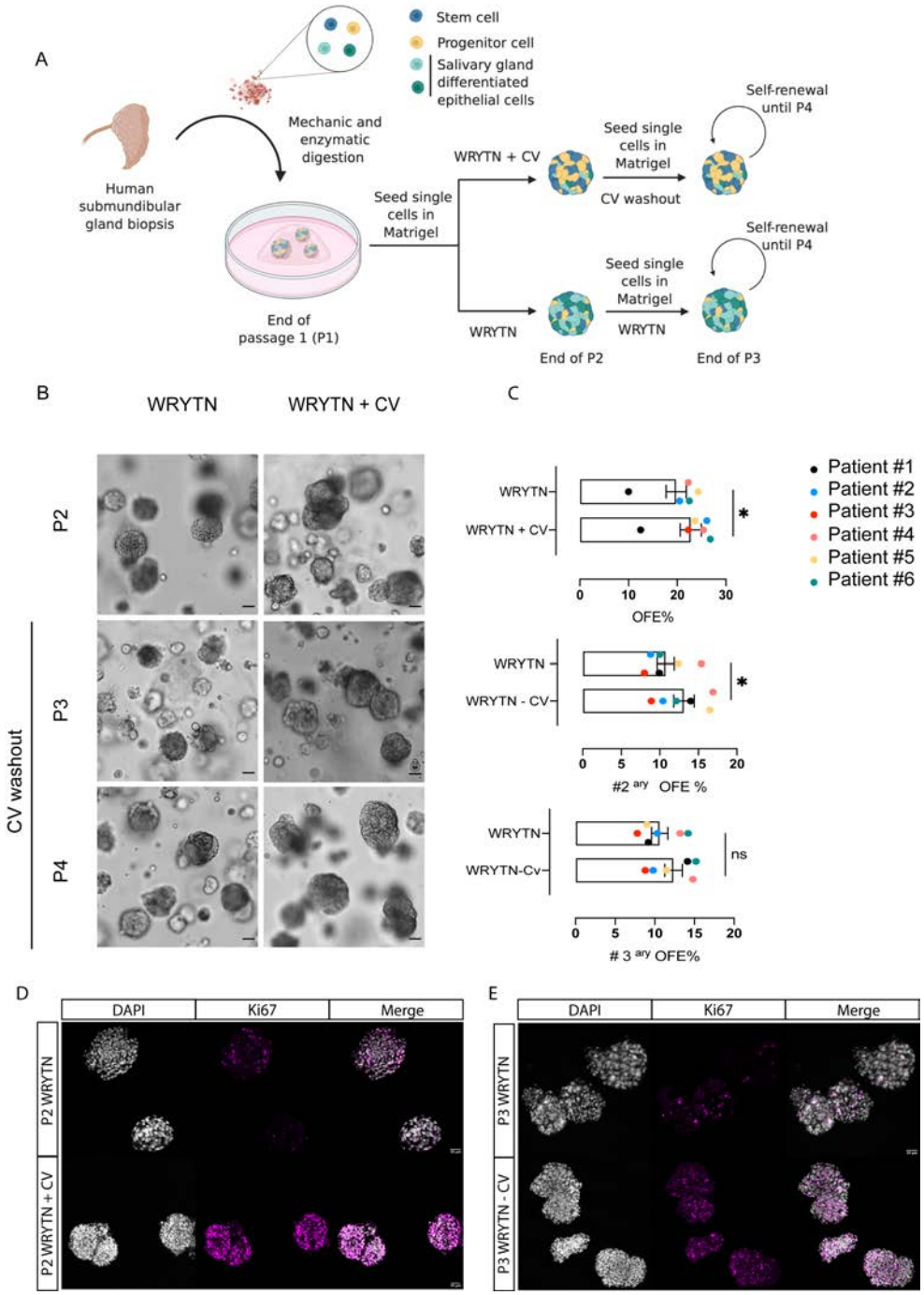

Figure 2: Chir99021 (C) and Valproic Acid (V) treatment increases proliferation and OFE in human salivary gland-derived organoids. A) Schematic drawing of the experimental procedure. Human salivary gland-derived cells were isolated and seeded as single cells in Matrigel®. At the end of the first passage organoids derived from isolated salivary gland-derived cells were trypsinized and re-seeded in Matrigel® and cultured in WRYTN media in presence or absence of CV treatment. At the end of the passage each condition was re-seeded in absence of CV to investigate their ability to form secondary and tertiary organoids. **B)** Representative brightfield images of human salivary gland-derived organoid cultures in WRYTN with or without CV treatment at P2 and after washout (P3 and

P4). Scale bar=50 μm. **C)** Organoid forming efficiency (OFE) of human salivary gland-derived cells at P2 in presence of the treatment, and at P3 and P4 after washout of CV. Each color represents a culture derived from a different patient (n=6). Data are represented as the mean ± SEM (C). One-way ANOVA (C). *p<0.05. **D) and (E)** immunostaining for Dapi (Grey) and ki67 (Magenta) of organoids at P2 and P3. Scale bar=50 μm.

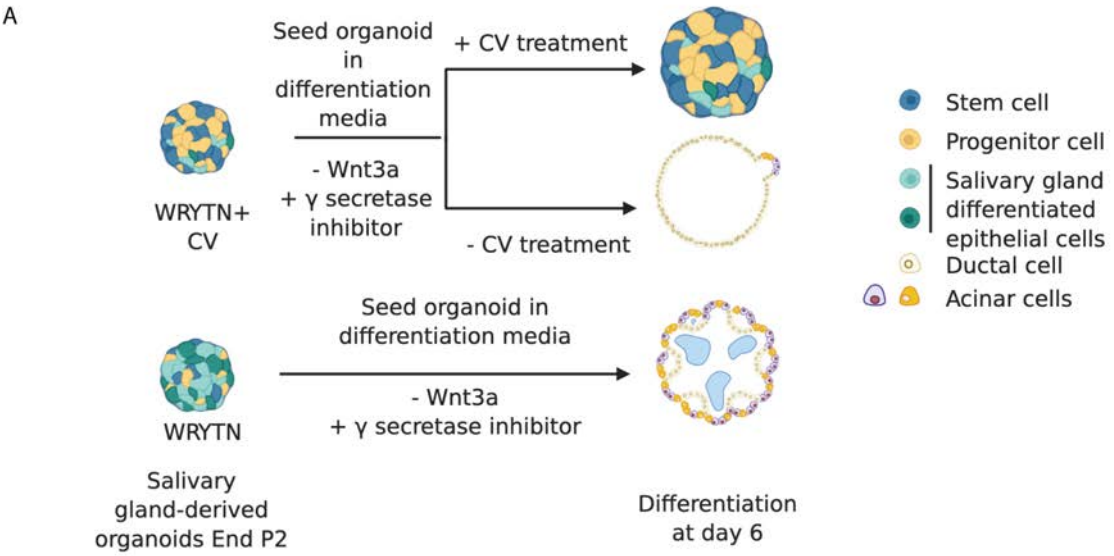

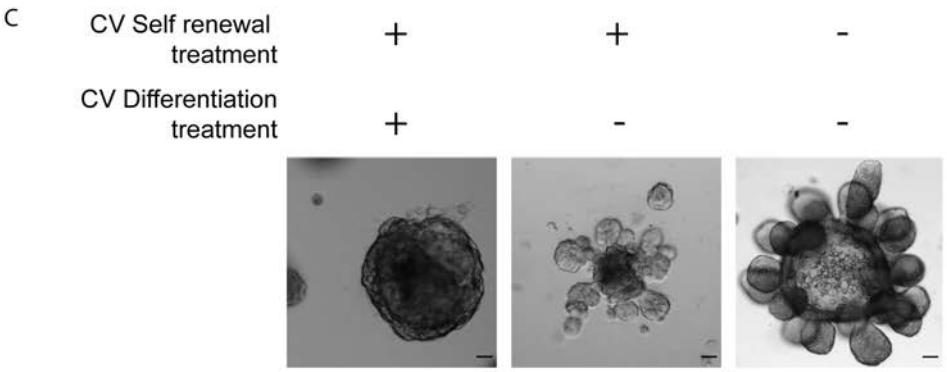

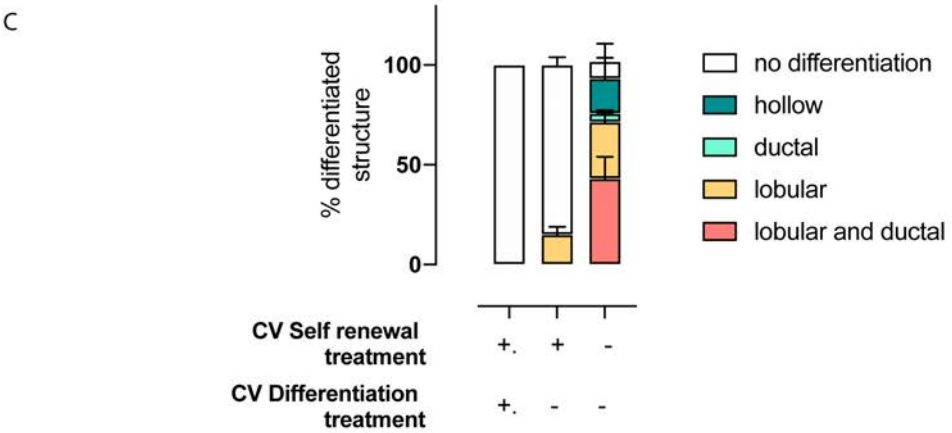

Figure 3: CHIR and Valproic Acid treatment hinders differentiation potential of human salivary gland-derived organoids. A) Schematic representation of the experimental procedure. Organoid cultures in presence or absence of CV treatment at the end of P2 were harvested and seeded in a new gel with and without the CV

treatment in presence of differentiation media. At day 6 of differentiation, the phenotype of the organoids grown from the different conditions were quantified and categorized in different phenotypic category. **B)** Representative brightfield images of human-derived organoids at the end of the differentiation assay. Scale bar=50 μm. **C)** Quantification of the different organoids-phenotypic categories.

These results suggest, in agreement with published data [22,23], that CV treatment of organoids keeps the cells in an undifferentiated state potentially promoting the enrichment for more "primitive" stem/progenitor cells.

Transcriptome analysis of organoids reveals modules of co-expressed genes

To identify a potential signature of hSGSPCs we applied a gene co-expression network analysis (WGCNA) (Zhang B et al, 2005) approach to 10 data sets generated from samples derived from 3 different human salivary gland biopsies (Figure 4A). Six data sets were generated to enable comparison across self-renewal passages of human salivary gland derived organoids cultured in EM and in–WRYTN (at passage P1, P2 and P4). Data set 7 consisted of samples representing human salivary gland-derived organoids enriched in stem cells, which consisted of organoids at P2 cultured in presence of CV (P2 + CV). Data sets 8, 9 and 10 were assembled to compare the differentiation potential of human salivary gland-derived organoids in the presence or absence of CV treatment and after CV withdrawal. Transcriptome profiles of each samples were obtained by [RNA seq methods] and processed for quality control. Principle Component Analysis (PCA) resulted in a consistent segregation of samples (Supplementary Figure 3A) within the different data sets, therefore all samples were included in the analysis. Following data processing, we performed genome-wide gene co-expression analysis [19]. We identified 59 mutually exclusive modules ranging in size between 30 and 700 co-expressed genes hierarchically clustered based on modules eigengenes (MEs) dissimilarity [24] (Figure 4B). Each ME summarizes the characteristic expression pattern of genes that comprise each module. To reveal a consensus transcriptional signature for hSGSPCs, we next assessed the association between each ME and the following phenotypic stem/progenitor cell culture traits: self-renewal and ability to form secondary organoids (OFE), P1 as a more heterogeneous (still unselected) state of the culture and CV treatment as a more primitive (and homogeneous) stem/progenitor cell population. Among the 59 module-trait relationships (Supplementary Figure 3B), three modules (Sienna4, Magenta3 and IndianRed3) showed a positive correlation with OFE and CV treatment indicating that these modules may represent pathways associated with a more primitive stem cell trait, while module Black and Orange, showed a positive correlation with P1 and negative correlations with Sienna4, Magenta3 and IndianRed3 indicating that these modules could represent pathways of a more differentiated trait (Figure 4C).

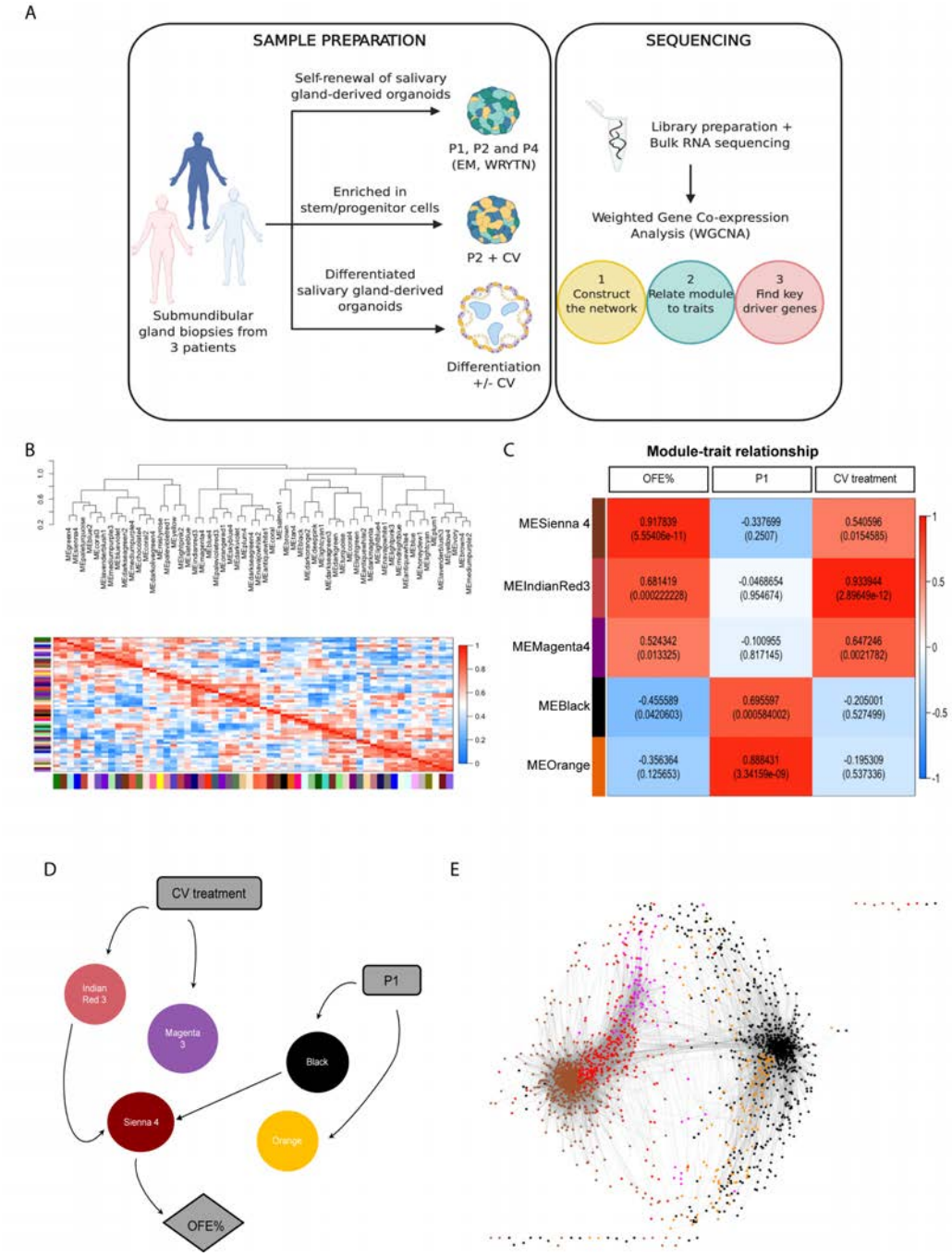

Figure 4: Weighted gene co-expression network analysis of human salivary gland-derived organoids reveals gene co-expression modules. A) Workflow of the strategy used to construct the molecular network. **B)** Structure of the gene co-expression network. Fifty-nine gene co-expression modules were identified and hierarchically cluster based on their module eigengene dissimilarity. **C)** Module-trait association of the module eigengene and culture traits that resemble stem cell features. Each row in the table corresponds to a module and each column to a specific trait. The numbers in the table correspond to the strength of the correlation of the module eigengene and the trait (value= 1 to -1) and the significance of the correlation (P<0.05). The table is colour coded by correlation according to the colour legend. **D)** Directed acyclic graph obtained using Bayesian network structure learning, that represent the relationship between the modules (circles) and the relevant traits (rectangles). **E)** Cytoscape visualization of the complete gene network showing the correlation between each gene within each module and the relation between modules. Each dot represents a gene and each colour represents one of the five

selected modules. The length on the line indicate the strength of the correlation between each gene. The single dots at the top and the bottom of the cytoscape represent genes without any connection in the network.

Subsets of gene co-expression modules correspond to different salivary gland developmental organoid states

We use the intramodular connectivity measure to quantify the similarity between each individual gene within the module and the ME. This is calculated as the Pearson correlation between the expression pattern of a gene and the ME of a module, and quantifies to what extent an individual gene within the module follows the pattern characterized by the ME. This value can be used to identify genes that are the most representative of a module (HUB genes) and that can illustrate a particular cell type or pathway described by that module. In order to understand regulatory loops and dynamic dependency between modules and the stem cell trait, we used a Bayesian network interference approach. A Bayesian network is a probabilistic graphical model where random variables (here being modules and traits) and their conditional dependencies are represented using a directed acyclic graph (DAG)[25]. To limit the network size and focus on more accurate interference, the Bayesian network included: 5 nodes representing trait-associated modules and 3 trait nodes (Figure 4D,E). To determine how the 5 modules (Sienna4, IndianRed3, Magenta3, Orange and Black) represent specific biological processes within salivary gland-derived organoids, we examined the pathway analysis using genes that had a module membership ≥ 0.6 in each module. Module membership indicates how strongly a gene correlates to the module eigengene.

DAVID pathway analysis (https://david.ncifcrf.gov/) revealed a significant enrichment of genes involved in salivary (*P* value = 2.80E-16), pancreatic and gastric secretion indicating a clear glandular transcriptional signature (Figure 5A). This suggests that module Black may represent an acinar progenitor and/or differentiated acinar cells transcriptional signature. Within the 21 genes belonging to the salivary secretion pathway we found mature acinar cells markers, such as *AQP5*, *MUC5B*, *MUC7* and *CHRM3,* as well as defense protein produced by the submandibular gland involved in the innate oral immunity such as Cystatin (*CYS*), and peptide with antimicrobial function such as Histatin (*HIST*). Enzymes, such as lactoperoxidase *(LPO)* or lysozyme *(LYZ)*, are also known to be expressed in adult salivary glands where they contribute to innate salivary gland defense mechanisms[26] (Figure 5B). Interestingly, the cholinergic signaling pathway was one of the pathways most significantly represented in module Black. Cholinergic nerves have been recently reported to play an important role in regulating salivary gland homeostasis and regeneration in adult mouse salivary gland. In mice sublingual gland, cholinergic stimulation acts on Sox2 expressing Chrm3 progenitor cells and activates a Sox2-mediated acinar cell replacement program [9]. Sox2, although not registered

in one of the pathways defined by DAVID, belongs to the module Black with a module membership of 0.6. Taken together these results, particularly the expression profile and high module membership, indicate that the expression signature captured in module Black is specific for acinar cell development. The ability of the cells seeded in P1 to give rise to organoid retaining a secretory profile could indicate that these cells mirror the tissues regeneration process.

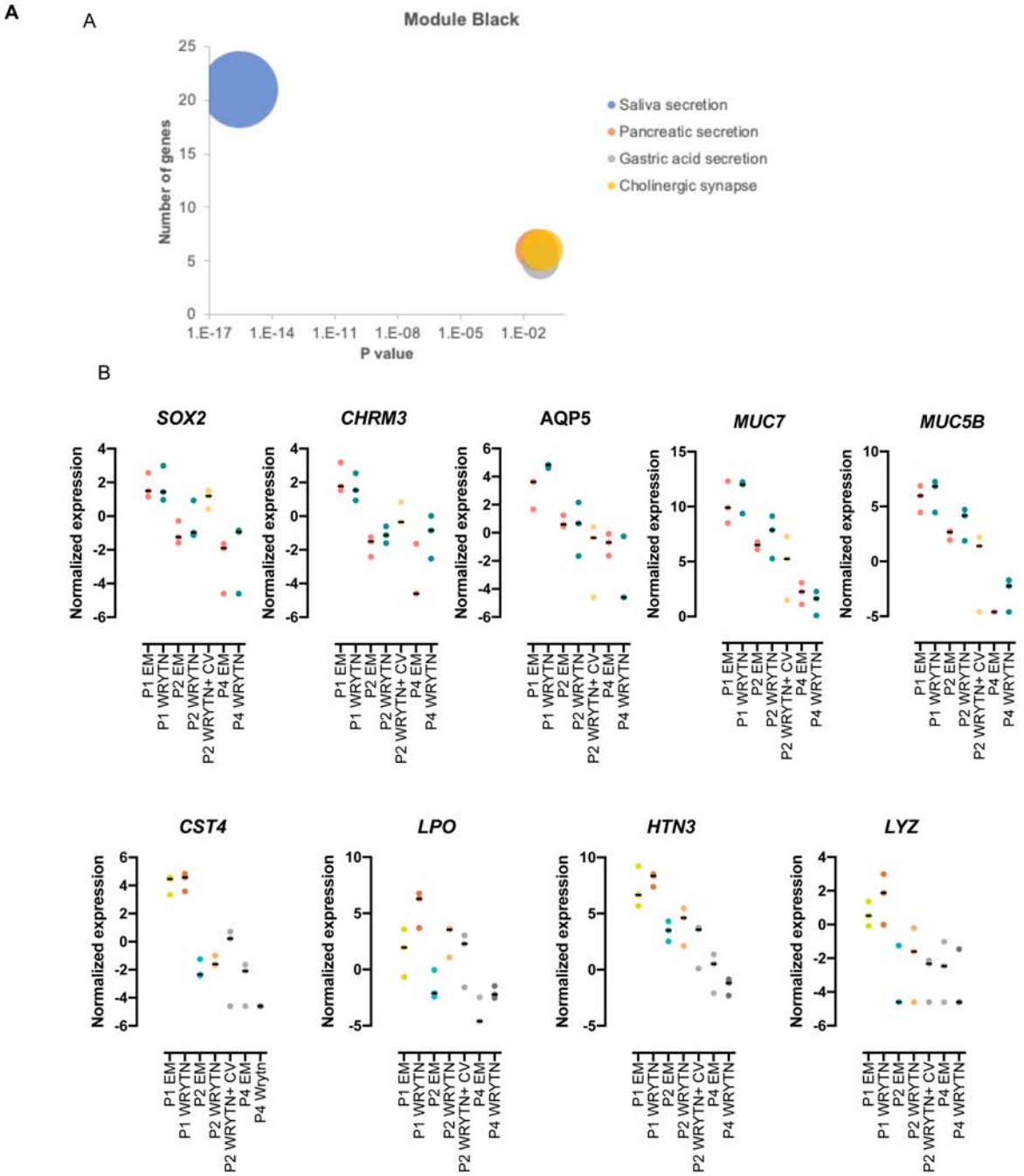

Figure 5: Module Black is representative of acinar development profile. A) Bubble chart representative of the significant pathways obtained by DAVID pathway analysis on MEBlack driver genes (module membership >0,6). Each colour represents a different pathway. The size of the bubble represents the significance of the pathway (P<0.05) and the number of genes enriched in the pathway. **B)** Normalized gene expression of the genes enriched

in the saliva secretion pathway throughout the different culture passages. Each dot represents a single patient. Data are represented as the mean ± SEM.

Module IndianRed describes an enrichment of a pluripotent-like phenotype

The Bayesian network analysis points to IndiaRed3 as the module directly influenced by CV treatment. Considering its high correlation with traits that reassemble a more stem-like cell state (CV treatment and high OFE), and its low correlation with module black, we expected to find in this module pathways that could describe a more stem-like cell/regenerative profile. Pathway analysis revealed that both the Hippo and Wnt pathways were significantly represented in this module for genes known to be involved in stem cells self-renewal (Figure 6 A).

To functionally characterize the role of Wnt signaling in salivary gland stem cells, we assess how pharmacologically inhibition of Wnt pathway in human salivary gland organoids culture influence the ability of salivary gland-derived cells to self-renew. In accordance to what published previously in mouse salivary gland organoids[18], inhibition of the Wnt pathway drastically reduces the self-renewal ability of human salivary gland-derived cells, indicating its fundamental role in the activation and maintenance of salivary gland-derived cells (Supplementary Figure 4A). Notably, treatment with CV induced a "Wnt hyperactivation" phenotype characterize by the upregulation of ligand (*WNT7B*), receptor (*LGR6*), transcription factor of the Wnt pathway (*TCF7*, *LEF1*) and target gene (*AXIN2*). Among the Wnt target gene, *PPARδ*, a peroxisome proliferator activated receptor, nutrient sensor, as well as transcriptional regulator of enzymes involved in lipid metabolism and fatty acid oxidation (FAO), was upregulated in CV treated salivary gland-derived organoids (Figure 6B). We next investigated whether overexpression of *PPARδ,* and potentially stimulation of FAO, in freshly isolated human salivary gland-derived cells, would increase their OFE ability in the absence of CV treatment (Figure 6C). The higher OFE, and total cell number, observed in *PPARδ*-mCherry+ cells compared to their negative counterpart (*PPARδ*-mCherry-) could indicate a role of the lipid metabolism pathway in determining salivary-gland derived cell fate decision (Figure 6 D and E).

When looking at the genes enriched within the Hippo pathway, we saw that CV treatment led to an increased expression of YAP target genes such as *WWC1, PPP2R2B and PP2R2D*, indicating that CV treatment promotes a YAP active state, similar to what has been recently described upon RXRi treatment in the intestinal organoid regenerative signature (Lukonin I et al 2020). Interestingly, module IndianRed3 showed an enrichment for genes involved in the regulation of pluripotent stem cells (P value = 2.7E-2). Interestingly, *PAX6* expression in human-derived salivary gland organoids was similar to the Pax6 expression measured in E18 and 6-week-old mouse submandibular glands [27]. *JARIG2*, a polycomb repressive complex2 (*PRC2*) recruiting protein, has been found to be abundantly expressed in embryonic stem cells as hub component of the pluripotency network[28] involved in the priming of embryonic stem

cells necessary for later stages of development [29]. Together, this data suggests that the different biological processes identified within the IndianRed3 module are integrated to induce and maintain a proliferative, non-differentiated phenotype of salivary gland-derived organoid cells.

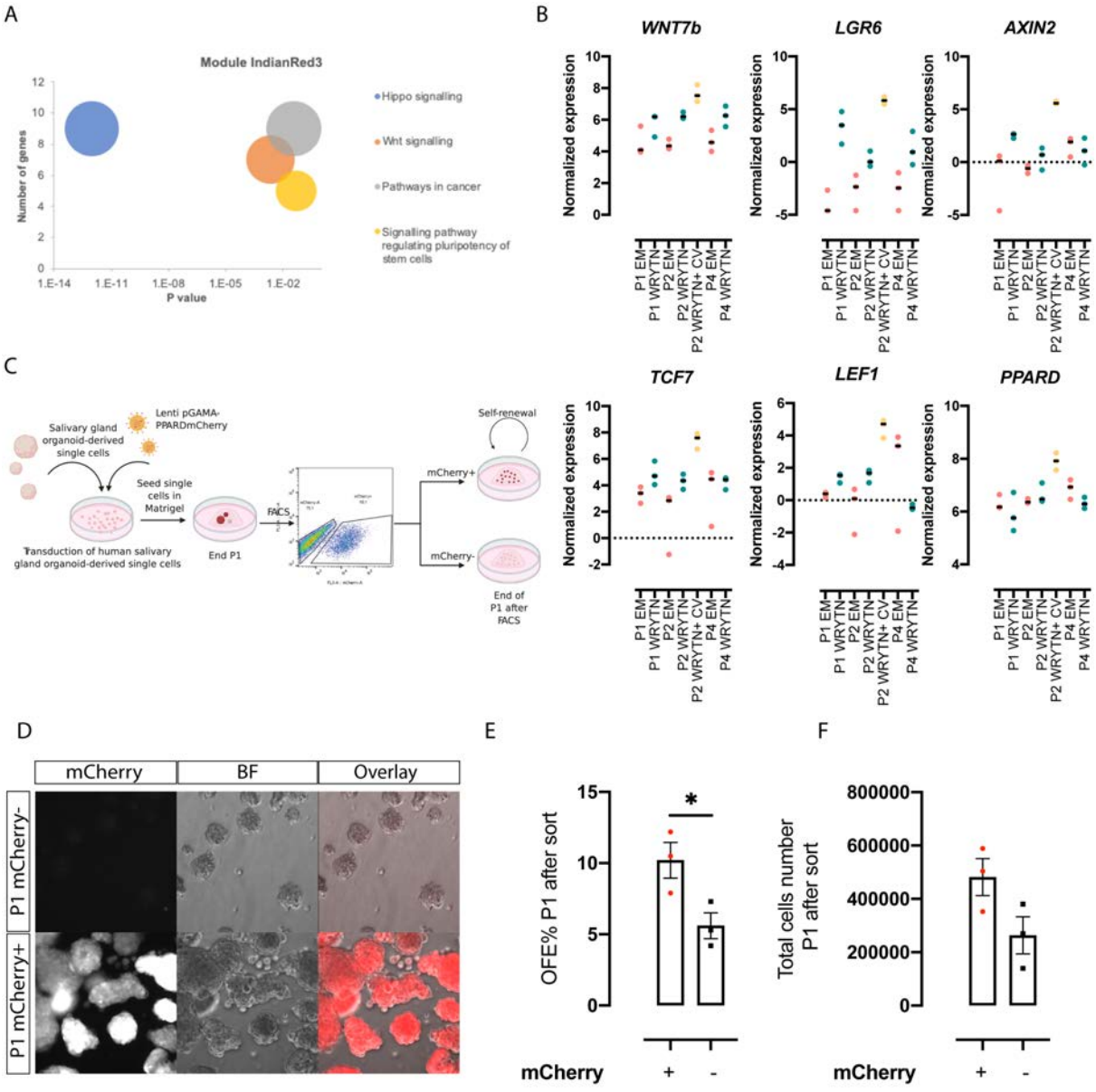

Figure 6: Module IndianRed3 is directly affected by CV treatment and identifies a proliferative, non-differentiated phenotype of salivary gland organoid-derived cell. A) Bubble chart representation of the significant pathways obtained by DAVID pathway analysis on MEIndianRed3 driver genes (module membership >0,6). Each colour represents a different pathway. The size of the bubble represents the significance of the pathway (P<0.05) and the number of genes enriched in the pathway. **B)** Normalized gene expression of the genes enriched in the Hippo and Wnt pathway throughout the different culture passages. Each dot represents a single patient. **C)** Workflow of the lentiviral overexpression experimental procedure used to validate the role of *PPARδ* in human salivary gland-derived cells self-renewal. **D)** Representative images and **(E)** quantification of secondary organoids and **(F)** total number of cells derived from *PPARδ* overexpression cells (mCherry+) compared to control (mCherry-

). Each dot represents a single patient. Data are represented as the mean ± SEM. One-way ANOVA (E)(F). *p<0.05.

A potential transient amplifying (TA) cell signature is associated with long-term self-renewal of human salivary gland-derived cells

We further interrogated the renewal of salivary gland-derived organoids by examining module Sienna4, which based on the Bayesian network analysis was directly linked to the OFE trait. Considering that no enrichment treatment was applied to these cells, this module contains genes that might be responsible for the ability of human salivary gland-derived cells to form organoids over time in culture. Interestingly, the focal adhesion pathway and the hippo pathway were the two pathways highly enriched within the driver genes of module Sienna4, indicating a potential role and interconnection of these pathways in long term maintenance of human salivary gland-derived organoids (Figure 7A). Focal adhesions (FAs) are specialized multiprotein assemblies located within the cells that strongly interact with the extracellular matrix (ECM) and function as dynamic mechanosensor and as upstream regulator of signaling pathways, including the Hippo pathway, in response to environmental changes [30,31].The progressive increase in gene expression of integrin α3 (*ITGα3*), tyrosine kinase *SRC* and the small GTPases *RAC2*, both mediator of FAK signaling, within passages, and their downregulation at P4 EM compared to P4 WRYTN (Figure 7B), could highlight a role of the axis *ITG3-SRC-RAC* in maintaining the ability to form organoids, perhaps via promoting Yap activation in a Lats1/2 independent manner as described in the transient amplifying cells of the mouse incisor[32]. By mining the Human Protein atlas dataset, we found that both *SRC* and *RAC2* were expressed in the basal layer cells of the main striated ducts (Figure 7C). This pattern might suggest that Yap activity via *ITG3-SRC-RAC2* could be stimulated in the basal layer of these cells.

To test if our analysis could enable the identification of potential stem/progenitor cell markers within the salivary gland, we choose *ELOVLI1* (Fatty Acid Elongase 1) which was the first gene within module Sienna4 with high module membership (module membership = 0,853) known to be expressed in salivary gland (Figure 7D). *ELOVL1* is also known to be highly expressed in skin, stomach, lung and kidney and it has been shown to play a central role in the organogenesis of organ depending on high lipid metabolism. Deletion of Elovl1 was found to reduce the expression of genes necessary for bladder epithelium development in zebrafish such as Sox2 and Hb9[33]. Additionally, in mice *ELOVL1* knock out is responsible for the evaporative dry eye phenotype characteristic of aged-induced corneal damage[34]. Here to establish if *ELOVLI1* is expressed in stem/progenitor cells within the salivary gland we first assess its localization within the adult submandibular gland tissue. *ELOVLI1* expression was found mainly in the ductal compartment indicating that the ductal cells might relay on fatty

acid/lipid metabolism (Figure 7E, inset 1 and 2, and F). To test if *ELOVL1* could play a functional role in salivary gland regeneration, we used our organoid culture system as a regenerative model to assess the self-renewal potential of *ELOVL1* overexpressing cells (Figure 7G). We transduced salivary gland-derived cells at the end of P1 with a lentiviral vector encoding for *ELOVL1*-t2A-mCherry and sort for mCherry+ cells one week after transduction. Sorted mCherry+ cells seeded in Matrigel showed higher OFE compared to mCherry- cells indicating, in accordance with the PPARδ finding, that increased fatty acid metabolism can promote the self-renewal of salivary gland-derived cells (Figure 7I and L).

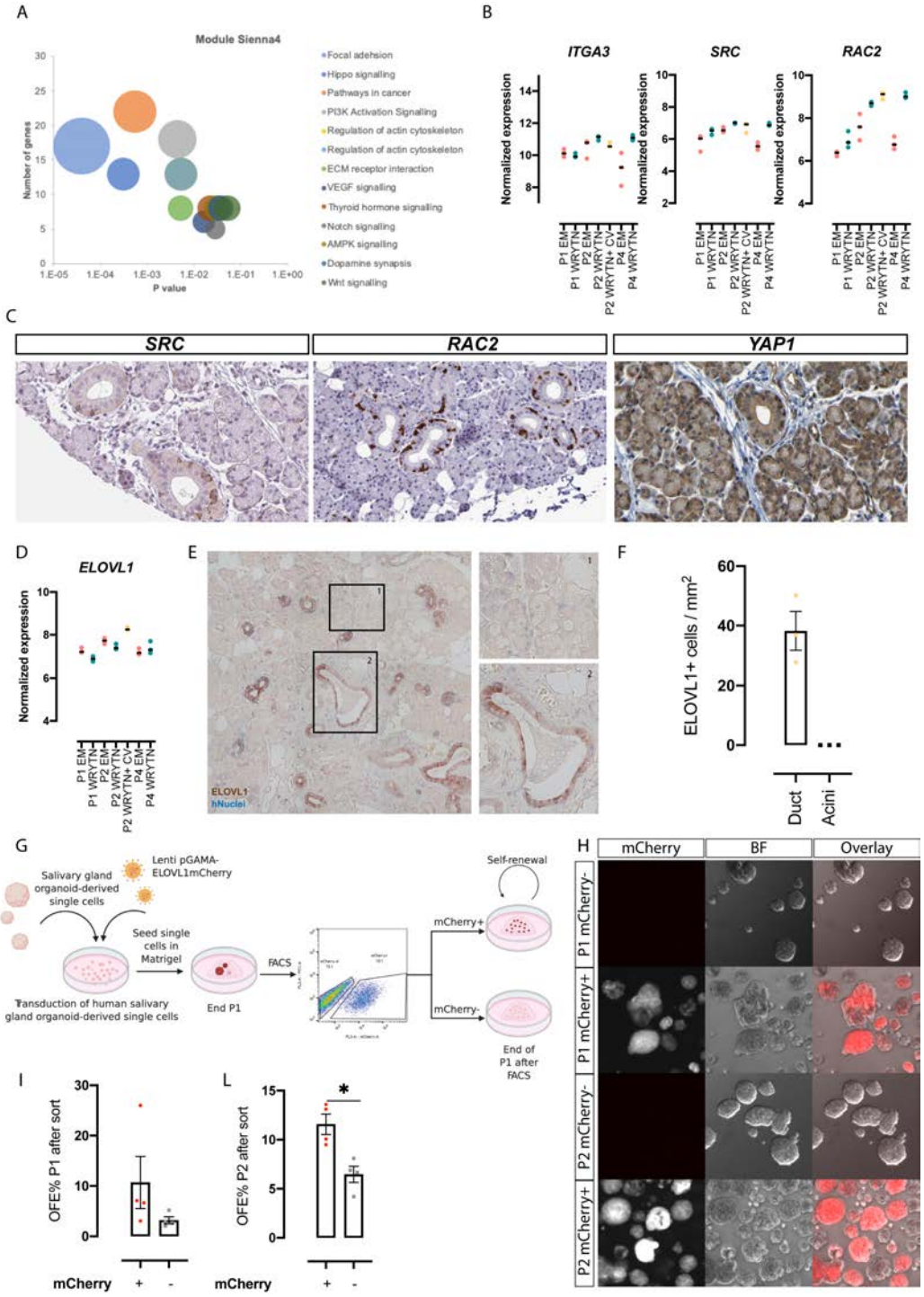

Figure 7: Module Sienna4 genes transcription profile identified an enrichment for potential transient amplifying cells. A) Bubble chart representation of the significant pathways obtained by DAVID pathway analysis on MESienna4 driver genes (module membership >0,6). Each colour represents a different pathway. The size of the bubble represents the significance of the pathway (P<0.05) and the number of genes enriched in the pathway. **B)** Normalized gene expression of the genes enriched in the Focal adhesion pathway. Each dot represents a single patient. **(C)** IHC staining of SCR, Rac2 and YAP1 in human submandibular gland biopsies, showing expression of these protein in the basal layer of the main excretory duct. **D)** Normalized gene expression ELOVL1. Each dot represents a single patient. **E)** ELOVL1 staining in human submandibular gland tissue (Brown) counterstained with hNuclei staining (Blue). Inset 1 shows a region with a main excretory duct positive for ELOVL1. Inset 2 shows acinar cells negative for ELOVL1. **(F)** Quantification of ELOVL1 positive cells per mm^2 of tissue. Patient tissue

biopsies analyzed n=3. **(G)** Workflow of the lentiviral overexpression experimental procedure used to validate the role of *ELOVL1* in human salivary-gland derived cells self-renewal. **H)** Representative images and **(I)** quantification of secondary and **(J)** tertiary organoids derived from ELOVL1 overexpressed cell (mCherry+) compared to control (mCherry-). Data are represented as the mean ± SEM. One-way ANOVA. *p<0.05.

DISCUSSION

In this study we used a gene co-expression analysis approach to identify biological processes and specific genes responsible for the self-renewal and differentiation of human salivary gland-derived cells. The key feature of our approach is the identification of direct molecular-phenotypic stem cell trait relationships which increase the chances of discovering salivary gland specific stem cell associated features. We applied the network analysis to a set of different human-derived salivary gland organoid culture conditions aimed at enriching either for stem cells or for functional secretory salivary gland cells. The framework adopted and our data were able to identify different sets of co-expressed genes that describe biological processes that directly relate to long-term self-renewal and stem cell pluripotency, well separated from those set of genes that instead describe a secretory salivary gland function.

While salivary gland-derived cells have been shown to hold therapeutic potential to treat the irradiation-induced hyposalivation phenotype, little is known about the underlying mechanisms that control their regenerative potential: whether through a direct contribution to replenishing cell loss or due to paracrine effects of the transplanted cells on the surrounding damaged tissue[8,15,35]. The major bottle neck of exploring salivary gland epithelial intrinsic processes *in vivo*, is the slow turnover of the tissue, the current lack of a stem cell marker (or markers) that would allow for the enrichment of a specific cell population by FACS, as well as the emerging view that more than “professional” stem cells, plasticity mechanisms are responsible for the regenerative potential of the glands[15,16] (Rocchi et al 2020, npj Accepted). The recent progress in the organoid field has allowed the growth of slow turnover tissue-derived epithelial cells (mostly non-dividing), including the salivary gland [17,18], by providing niche signaling that coaxes them into an active regenerative state. The possibility to expand salivary gland organoid cultures in a defined medium that allows maintenance of the stem/progenitor pool, as well as differentiation into all salivary gland lineages[18], makes them a perfect tool to tackle this bottle neck. The large quantity of cells derived from organoid cultures allow for the enrichment of rare cell types thereby potentially increasing the resolution of the data generated. Furthermore, the regeneration process mimicked by the development of organoids[36] could enable the investigation of tissue-specific mechanisms that may control tissue renewal, regulation of stem/progenitor cells and cell fate specification.

Isolated salivary gland cells can be induced to form organoids when cultured in Matrigel®. Similar to mouse salivary gland-derived cells[18], in this study, we have shown that human-

derived salivary gland cells are Wnt-responsive and could be stimulated to proliferate, to a certain extent, and form organoids upon exogenous Wnt stimulation. However, in contrast to mouse salivary gland-derived cells, the limited expansion potential of human salivary gland-derived cells, observed under Wnt stimulation, suggested that other pathways might be involved and required for their expansion. Now we have shown that, similar to human liver culture[37], the addition of Tgfβ inhibitor and Noggin to the culture medium allowed the expansion and long term-maintenance of human salivary gland-derived organoids. While the heterogeneous cellular composition of organoids derived from a single cell constitutes one of their major strengths, this same quality could represent a challenge when investigating gene co-expression regulation. Indeed, many variables are likely to influence the detection of a cell type-specific molecular signature from transcriptomic data. The representation of a given cell type and its quantitative relationships with other cell types within the sample, the number of unique genes expressed within this population, the sensitivity of the platform used, the number of samples and even the bioinformatic approaches used to identify gene-expression modules are all parameters which can influence cell type-specific transcriptomic signatures[38].

Here, by adding small molecules to the optimized expansion medium (CHIR99090 and valproic acid), we were able to enrich for specific cellular states, e.g. stem/progenitor cells-like state, and overcome the limitations imposed by the lack of a cellular surface marker in enriching for a specific cell type. This strategy, combined with a bulk-RNA sequencing strategy and a molecular network framework (WGCNA), allowed us to obtain an unbiased, wide overview of the complexity of the regulatory network responsible for organoid renewal and differentiation. Indeed, we show that the early inhibition, at a single cell stage, of GSK3B and the induction of chromatin remodeling, using the histone deacetylase inhibitor valproic acid, seems to promote a Wnt hyperactive transcription profile and a switch to a more pluripotent state. Under these conditions organoid-derived cells display a significant increase in proliferation, while at the same time they lose the ability to acquire a mature differentiation phenotype and salivary gland specification. This may indicate a more “regenerative” profile similar to what has been recently described for intestinal derived organoids[36,39]. While further investigation will be needed to confirm a metabolic role in self-renewal ability of salivary gland-derived cells, the high expression of Pparδ could suggest the activation of a Pparδ-driven FAO program upon CV treatment. Activation of FAO could be responsible for the increased fraction of proliferating cells able to give rise to organoids, as well as for the possible “rejuvenation” of aged salivary gland organoid-derived cells[40].

While manipulation of medium composition is a fundamental requirement to study and to understand the *in vitro* biological processes behind organoid formation, likewise, is the manipulation of the ECM in which the cells are cultured. Our gene co-expression analysis

provided evidence that the ability to give rise to organoids and the maintenance of salivary gland organoid culture could be dependent on integrin expression levels. Interestingly, the integrin-driven Yap activation program suggested here could enable the transition of stem-like cells (P1) to a higher proliferative TA-like state (P2-P4). These results could be used to identify critical gel components in organoid formation that could be used to create a well-defined, dynamic, synthetic matrix potentially suitable for GMP-compliant procedure.

Despite CV treatment seeming to enrich for a more pluripotent-like phenotype and increased passaging for a TA-like phenotype, these organoids seem to lose the salivary gland specification that characterizes the P1 organoids. The progressive decline of the acinar development profile within passages indicates that differently from mouse-derived salivary gland organoid culture [18], human-derived salivary gland culture conditions are not yet "permissive/tuned" to maintain long-term the heterogeneity and self-organizing potential that define mouse-derived salivary gland organoids, as well as intestinal organoids[41,42]. This could be due the fact that the enrichment provided by current culture conditions hinders human-derived salivary gland organoids to undergo symmetry breaking (Serra et al; 2018), while maintaining a more "hyperactivation-like state" or a more "regenerative-like state" [39]. While the bulk RNA sequencing approach represents more a screen-shot of the organoids' transcriptomic profile at the end of the culture, organoid single cell RNA sequencing could enable the identification of how the transcriptomic profile of single cells changes under different conditions and shed light on possible symmetry breaking mechanisms in salivary gland organoids. From the co-expression gene analysis presented here, P1 organoids are the only ones that retain a secretory acinar transcription profile, indicating that these organoids better resemble the complex multicellular structure of the salivary gland tissue of origin. Therefore, they are the ones that can potentially recapitulate first the regeneration of the epithelium and subsequently the re-establishment of tissue homeostasis[36,39,42]. Single cell sequencing analysis of these P1 human salivary gland-derived organoids could potentially allow the discovery of the equivalent of the intestinal Paneth cells, responsible for creating the niche environment and the correct formation of intestinal crypt in intestinal organoids, and shed light on the dynamics of salivary gland organoid development. The understanding of single cell trajectories, an integrated multiomic approach combined with time course experiments and genetics-based perturbation (e.g CRISPR-CAS) could allow further elucidation of cell-fate switches in salivary gland organoids. These switches could then be used to guarantee a long-term expansion of complex multicellular organoids that retain salivary gland specification.

Our study represents the first transcriptomic analysis of human-derived salivary gland organoids and a rich resource of information for the salivary gland community. The information gained by the co-expression gene analysis will open up new possibilities for the use of salivary

gland organoids, both in terms of tissue regeneration model as well as a model for the understanding the underlying biological pathways involved in the balance between tissue homeostasis and regeneration.

MATERIAL AND METHODS

Patients

Human non-malignant submandibular gland tissues were obtained from donors after informed consent and Institutional Review Board (IRB) approval during an elective head and neck dissection procedure for the removal of squamous cell carcinoma of the oral cavity at the University Medical Centre Groningen (UMCG) and Medical Centre Leuwaarden (MCL).

Isolation of human submandibular gland derived cells

Human submandibular gland biopsies were collected in the operating room and transferred to the lab in a 50 mL falcon tube containing HBSS 1% BSA on ice. The biopsy was weighted in a sterile petri dish and minced into small pieces using a sterile disposable scalpel. The minced tissue was transfer to GentleMACS C tubes and digested in Hank's Balanced Salt Solution (HBSS) containing 1% bovine serum albumin (BSA; Invitrogen) and supplemented with collagenase type II (0,63mg/mL; Gibco), hyaluronidase (0,5 mg/mL, Sigma-Aldrich) and $CaCl_2$ (6.25mM; Sigma-Aldrich).To obtain optimal digestion 20 mg of tissue was processed per 1 mL of digestion buffer volume, with a maximum of 100 mg of tissue per tube. Two rounds of mechanical digestion were performed using GentleMACS tissue dissociator. In between mechanical digestions, the tubes were incubated in a shaking water bath for 30 minutes at 37°C. At the end of the digestion, cells were collected by centrifugation at 400 G for 5 minutes, the cell pellets washed thoroughly with HBSS 1%BSA, filtered through a 100 μm cell strainers (BD Biosciences) and spun at 400G for 5 minutes. The pellet was resuspended in Dulbecco's modified Eagle's medium: F12 (DMEM F12) containing Pen/Strep antibiotics (Invitrogen), Glutamax, 20 ng/mL epidermal growth factor (EGF; Sigma Aldrich), 20 ng/mL fibroblast growth factor-2 (Sigma- Aldrich), N2 (Invitrogen), 10 μg/mL insulin (Sigma-Aldrich) and 1 μM dexamethasone (Sigma-Aldrich).and cell number counted with the use of Scepter Cell Counter. Only cells within t range size between 6,126 μm and 8,467 μm were taken in consideration. The cell clumps obtained were seeded at a density of $4x10^4$ cells per well in a 6-well plate and incubate at 37°C and 5% CO_2 for 3 days as floating primary culture.

Self-renewal assay of human salivary gland derived cells

Three days-old primary culture were harvested and dispersed to single cells suspension using 0,05% trypsin EDTA (Invitrogen). Single cells were counted and resuspended in culture media at a final concentration of or $0,8x10^6$ cells per mL. 25 μL of cell suspension was mix on ice with 50 μL of ice cold Matrigel and the 75 μL gel pipetted in the middle of a 12-well plate. Following polymerization of the Matrigel ®, 1mL of culture media was added. The culture media used in this study are described as follow. Enriched media (EM): EM; DMEM/F12,

pen/strep [1x; Invitrogen], glutamax [1x; Invitrogen], N2 [1x; Gibco], EGF [20ng/mL; Sigma Aldrich], FGF2 [20ng/nL;sigma Aldrich], insulin [10μg/mL;Sigma Aldrich], dexamethasone [1μM; Sigma Aldrich], Y27632 [10μM; Sigma Aldrich]. Wnt enriched media (WRY): DMEM/F12, pen/strep [1x; Invitrogen], glutamax [1x; Invitrogen], N2 [1x; Gibco], EGF [20ng/mL; Sigma Aldrich], FGF2 [20ng/nL;sigma Aldrich], insulin [10μg/mL;Sigma Aldrich], dexamethasone [1μM; Sigma Aldrich], Y27632 [10μM; Sigma Aldrich], 10% R-spondin1 conditioned medium and 50 % Wnt3a conditioned media. WRYTN: DMEM/F12, pen/strep [1x; Invitrogen], glutamax [1x; Invitrogen], N2 [1x; Gibco], EGF [20ng/mL; Sigma Aldrich], FGF2 [20ng/nL;sigma Aldrich], insulin [10μg/mL;Sigma Aldrich], dexamethasone [1μM; Sigma Aldrich], noggin[50ng/mL; Preprotech-Bioconnect], A8301[1μM Tocris], Y27632 [10μM; Sigma Aldrich], 10% R-spondin1 conditioned medium and 50 % Wnt3a conditioned media. One week after seeding (end of the passage), the media was replaced with Dispase enzyme (1 mg/mL in DEMEM F12 at 37°C for 30-45 minutes) to dissolve the gels. All the organoids released from the dissolved gels were processed to single cells using 0,05% trypsin-EDTA treatment to form single cell suspension. Organoids and cell number at the end of the passage were noted and the secondary organoid derived single cells re-seeded in Matrigel to start a new passage. Number of organoids and single cells at the end of each passage were used to calculate Organoid Formation Efficiency percentage (OFE%) and Population Doubling as follows:

$$Organoid\ Formation\ Efficiency\ (OFE\%) = \frac{Number\ of\ Organoid\ harvested\ at\ the\ end\ of\ the\ pasaage}{Number\ of\ single\ cells\ seeded\ at\ the\ beginning\ of\ the\ passage}\ x\ 100$$

$$Population\ Doubling = \frac{\ln(harvestes\ cells/seeded\ cells)}{ln2}$$

Treatment of human salivary gland derived organoid with CHIR99201 and valproic acid

For comparison of different culture conditions, small molecule as CHIR99021 [3μM] and valproic acid [1μM] were added to the WRYTN media. The cells were kept in culture for 7 days and the media was changed every two days. At the end of the passage the number of organoids and cells number were determined as described above. Organoid-derived single cells were re-seeded in the next passage at a density of $0{,}8x10^6$ cells per mL and culture in absence of CHIR99201 and valproic acid (washout experiment).

Differentiation assay

Human salivary gland-derived organoids were kept in culture for 7 days in WRYTN expansion media in presence or absence of CHIR99201 and valproic acid. At the end of the passage, the media was harvested and ice-cold PBS 1%BSA was added to the well to dissolve the

Matrigel® and release organoids. Organoids were harvested and spun at 400G for 5 minutes. The pellet was re-suspended in 1mL differentiation media and kept on ice. Organoids were counted and seeded at a final density of 20-30 organoids per 75 μL of gel (25 μL media + 50 μL Matrigel®) in a Matrigel ® pre-coated 96 well plate. Following polymerization of the gel at 37°C, 150 μL of differentiation media with/or without CHIR99201 and valproic acid was added on top of the gel. Organoid were harvested after 6 days for RNA sequencing analysis and after 30 days for immunofluorescence and immunohistochemistry analysis of salivary gland specific proteins. Differentiation media is described as follow: DMEM/F12, pen/strep [1x; Invitrogen], glutamax [1x; Invitrogen], HGF (Preprotech), FGF-10 (Preprotech), Heparin salt (Stem Cell Technology), DAPT (Sigma), FCS (Greiner).

Immunofluorescence and immunohistochemistry staining of human salivary gland-derived organoid.

Organoids cultured in Matrigel ® were harvested, washed and fixed by using 4%PFA for 10-30 minutes at room temperature. For whole mount staining Samples were wash with 0,2% BSA PBS and permeabilized with a blocking solution (0,5% triton, 1% BSA in PBS) for 1 hour 30 minutes at room temperature with gentle shaking. Sample were incubated with primary antibody staining in blocking buffer at 4 °C for 24-48 h. Secondary antibody (1:250) and DAPI staining were performed in 0,1%BSA PBS at room temperature over night with gentle shaking. Sample were thoroughly washed with 0,1% BSA PBS and mount on an object glass for imaging Images were acquired by using Leica SP8 confocal microscope. For AQP5, Amylase immunofluorescence staining on differentiated organoid, 4 μm paraffine section were deparaffinize and incubated at 4 °C overnight, after citrate-mediated antigen retrieval, with primary antibodies as follow: anti-Aqp5 (1:200, Abcam), anti-α amylase (1:200, Sigma). Section were washed and incubated with secondary antibody for 2h at room temperature in the dark. DAPI was used as nuclei counterstaining. Imaging were acquired using Leica DM6000 B and processed using Image J software. For immunohistochemistry detection of Mucin, paraffine section were processed as described above and incubated in Alcian Blue solution (Alcian blue 8GX Sigma, A5268) for 30 minutes at room temperature. Nuclei were visualized by using nuclear fast red counterstaining for 5 minutes at room temperature. Section were washed, rehydrate and mount using Eukit (Sigma).

Lentiviral production and lentiviral transduction of human salivary gland-derived cells.

HEK293T cells were plated in poly-L-lysin coated 10 cm dish at a density of $1,5x10^6$ and cultured in DMEM supplemented with 10% FBS, Pen/Strep [1x; Invitrogen], Glutamax [1x; Invitrogen] and incubated ON at 37°C and 5% CO_2. On the next day cells were transfected

with 3 μg of p-GAMA PPARδ, p-GAMA ELOVL1 (AddGene) [30] or empty p-GAMA 3 μg of the packaging plasmid PAX2, 0,7 μg of envelope plasmid VSV-G and 40 μL of PEI (1 μg/mL) as previously described [40]. On the next day medium was changed to DMEM F12. Two days after transfection the viruses were collected, filtered through a sterile syringe filter with a 0,45 μm pore size and hydrophilic PVDF membrane and frozen in 250 μL aliquots at -80 °C. We have tittered the virus-containing supernatant by transduction of mCherry gene. Viruses were always in the range of $5,0x10^6$ – $7,0x10^6$ transduction unit (TU)/mL.

At end of the passage culture media was removed and Dispase (Gibco) was added. After incubation at 37°C for 30 minutes, organoid were harvested, washed and dissociated to single cells by using 0.05% trypsin-EDTA (Invitrogen). Human salivary gland organoid-derived single cells were counted and resuspended in WRYTN media to a final concentration of $2.5x10^6$ cells per mL. For each 100 μL of cell suspension 250 μL of viral supernatant and polybrene (6 μg/mL) was added. The mixture was divided in 350 μL aliquots in a 24-well plate and incubated ON at 37°C and 5% CO_2. The day after transduction single cells were counted to adjust for dead cells, resuspended in media to a final concentration of $0,8x10^6$ cells per mL and seeded in Matrigel into 12-well plate. The cells were cultured for 7 to 10 days in WRYTN media at 37°C and 5% CO_2.

Flow Activate Cell Sorted (FACS) analysis

At day 7 cell culture media was removed Matrigel was dissolved with the use of Dispase (1 mg/mL; Gibco) and organoids dispersed to single cells with the use of 0.05% trypsin-EDTA. Cells were washed with 0.2% BSA in PBS and resuspended in 0.2% BSA with the viability dye (DAPI) in PBS. PPARδ and ELOVL1 overexpressing cells were isolated by fluorescence-activated cell sorting for mCherry-positive cells, seeded in Matrigel and cultured in EM. Organoid forming efficiency and cell number were assessed as described above.

Immunoblot

To monitor endogenous gene responses, mouse and human organoids were harvested and centrifuged pellets homogenized by sonication in 2x Laemnli buffer. Protein concentration of the lysates was determined using Bradford quantification method. Homogenates were then boiled at 99°C for 5 minutes and equal protein amounts were separated with 10 or 12% polyacrylamide gels and transfered to PVDF membranes using Trans Blot Turbo System (Bio-Rad). The membranes were blocked in 5% BSA in PBS-Teween-20 and incubated 1 h at RT. Incubation with primary antibodies was done ON at 4°C following by incubation with HRP-conjugated secondary antibodies. Membranes were developed using ECL reagent (Thermo Fisher Scientific) and the signal was detected using ChemiDoc imager (Biorad). Densiometric

analysis of western blots at non-saturated exposure were performed using Image J software and the values normalized against the one of GAPDH loading control. For immunoblots, the following primary antibodies at the indicated dilutions were used: rabbit anti-ELOVL1; mouse anti-GAPDH (Fitzgerald) 1:10000

RNA isolation and RNA sequencing data generation

Human salivary gland-derive organoids were harvested and stored in RNA later. Total RNA was isolated form individual samples was performed using Quigen RNeasy micro kit according to the manufacture instruction. RNA quality and quantity were assessed using Bioanalyzer assay and only sample with a concentration of > 10ng and RNA integrity scores (RIN) of > 8.5 were used to generate the libraries. NEXTflex™ Poly (A) Beads kit was used to isolate pure and intact messenger RNA (mRNA). RNA sequencing library were prepared using NETflex™ Rapid Directional qRNA-Seq ™ kit accordingly to manufacturer's protocol. FastQC (version 0.11.5) was utilized to perform quality control checks on the raw sequence data. Reads were aligned to the human genome using Spliced Transcripts Alignment to a Reference (STAR) (version 2.5.3a). Aligned reads were normalized excluding low abundance genes. Principal component analysis was performed on the 30 samples in order to detect extreme outlier.

Weighted gene co-expression network analysis (WGCNA)

Gene co-expression analysis was performed on the normalized RNA-Seq expression data (Log2 cpm), using the R package WGCNA [43]. All 30 samples were included in the analysis. Genes were clustered into modules by using the average linkage hierarchical algorithm [43].All cluster consisting of at least 30 genes were identified and summarized by their module eigengene[24]. Highly similar modules were merged together is their Pearson correlation coefficient exceed 0.25. At the end of the analysis 59 co-expression modules were identified. To identify key driver genes within the modules we determined the strength of module membership for each gene in the module. Module membership is determined by calculating the Pearson correlation of the expression profile of every gene in the module with the module eigengene. Genes that have had module membership of > 0.6 were genes that were considered highly connected within the module[24] (https://horvath.genetics.ucla.edu/html/CoexpressionNetwork/Rpackages/WGCNA/Tutorials/).

To identify possible stem cell related modules, we investigated the relationship of each module with known stem cells related traits: ability of self-renew and ability to differentiate. We performed Pearson correlation between the module eigengene of each module and the sample phenotypic trait (OFE, CV and P1). Modules that have a high correlation (value -1 to 1) and high significance of the correlation (P<0,05) with the module eigengene were selected.

Bayesian network structure learning to estimate the module-trait network

A Bayesian network are graphical models where nodes represent random variables and arrows represent probabilistic dependencies between them[25]. We create the Bayesian network using bnlearn package (version 4.2) using the hill climbing learning structure(https://www.bnlearn.com) to predict the directed acyclic graph (DAG) that describe the dependencies and relationship between two types of variable: modules stem cell phenotypic traits.

Pathway analysis

GO term enrichment analysis of modules driver genes was performed using Database for Annotation, Visualization and Integrated Discovery Functional Annotation Tool (DAVID v6.770) (www.david-d.ncifcrf.gov). Bubble plots representing most represented pathway were created with Excel based on the significance of the pathway given by DAVID and the number of gene enriched per pathway.

Statistical Analysis

All statistical analyses in this study were performed using GraphPad Prism8 software (GraphPad, La Jolla, CA, USA). The number of mice, patients or individual organoids analyzed (n), presented error bars (SEM), statistical analysis and p values are all stated in each figure or figure legend.

REFERENCES

1 Emmerson, E. & Knox, S. M. Salivary gland stem cells: A review of development, regeneration and cancer. *Genesis* **56**, e23211, doi:10.1002/dvg.23211 (2018).

2 Pringle, S., Van Os, R. & Coppes, R. P. Concise review: Adult salivary gland stem cells and a potential therapy for xerostomia. *Stem Cells* **31**, 613-619, doi:10.1002/stem.1327 (2013).

3 Tsai, W. L., Huang, T. L., Liao, K. C., Chuang, H. C., Lin, Y. T., Lee, T. F. *et al.* Impact of late toxicities on quality of life for survivors of nasopharyngeal carcinoma. *BMC Cancer* **14**, 856, doi:10.1186/1471-2407-14-856 (2014).

4 Rocchi, C. & Emmerson, E. Mouth-Watering Results: Clinical Need, Current Approaches, and Future Directions for Salivary Gland Regeneration. *Trends Mol Med* **26**, 649-669, doi:10.1016/j.molmed.2020.03.009 (2020).

5 Vissink, A., Jansma, J., Spijkervet, F. K., Burlage, F. R. & Coppes, R. P. Oral sequelae of head and neck radiotherapy. *Crit Rev Oral Biol Med* **14**, 199-212, doi:10.1177/154411130301400305 (2003).

6 Vissink, A., Mitchell, J. B., Baum, B. J., Limesand, K. H., Jensen, S. B., Fox, P. C. *et al.* Clinical management of salivary gland hypofunction and xerostomia in head-and-neck cancer patients: successes and barriers. *Int J Radiat Oncol Biol Phys* **78**, 983-991, doi:10.1016/j.ijrobp.2010.06.052 (2010).

7 Lombaert, I. M., Brunsting, J. F., Wierenga, P. K., Faber, H., Stokman, M. A., Kok, T. *et al.* Rescue of salivary gland function after stem cell transplantation in irradiated glands. *PLoS One* **3**, e2063, doi:10.1371/journal.pone.0002063 (2008).

8 Pringle, S., Maimets, M., van der Zwaag, M., Stokman, M. A., van Gosliga, D., Zwart, E. *et al.* Human Salivary Gland Stem Cells Functionally Restore Radiation Damaged Salivary Glands. *Stem Cells* **34**, 640-652, doi:10.1002/stem.2278 (2016).

9 Emmerson, E., May, A. J., Berthoin, L., Cruz-Pacheco, N., Nathan, S., Mattingly, A. J. *et al.* Salivary glands regenerate after radiation injury through SOX2-mediated secretory cell replacement. *EMBO Mol Med* **10**, doi:10.15252/emmm.201708051 (2018).

10 Peng, X., Wu, Y., Brouwer, U., van Vliet, T., Wang, B., Demaria, M. *et al.* Cellular senescence contributes to radiation-induced hyposalivation by affecting the stem/progenitor cell niche. *Cell Death Dis* **11**, 854, doi:10.1038/s41419-020-03074-9 (2020).

11 Baum, B. J., Alevizos, I., Zheng, C., Cotrim, A. P., Liu, S., McCullagh, L. *et al.* Early responses to adenoviral-mediated transfer of the aquaporin-1 cDNA for radiation-induced salivary hypofunction. *Proc Natl Acad Sci U S A* **109**, 19403-19407, doi:10.1073/pnas.1210662109 (2012).

12 Lombaert, I. M. A., Patel, V. N., Jones, C. E., Villier, D. C., Canada, A. E., Moore, M. R. *et al.* CERE-120 Prevents Irradiation-Induced Hypofunction and Restores Immune Homeostasis in Porcine Salivary Glands. *Mol Ther Methods Clin Dev* **18**, 839-855, doi:10.1016/j.omtm.2020.07.016 (2020).

13 Barker, N., van Es, J. H., Kuipers, J., Kujala, P., van den Born, M., Cozijnsen, M. *et al.* Identification of stem cells in small intestine and colon by marker gene Lgr5. *Nature* **449**, 1003-1007, doi:10.1038/nature06196 (2007).

14 May, A. J., Cruz-Pacheco, N., Emmerson, E., Gaylord, E. A., Seidel, K., Nathan, S. *et al.* Diverse progenitor cells preserve salivary gland ductal architecture after radiation-induced damage. *Development* **145**, doi:10.1242/dev.166363 (2018).

15 Weng, P. L., Aure, M. H., Maruyama, T. & Ovitt, C. E. Limited Regeneration of Adult Salivary Glands after Severe Injury Involves Cellular Plasticity. *Cell Rep* **24**, 1464-1470 e1463, doi:10.1016/j.celrep.2018.07.016 (2018).
16 Ninche, N., Kwak, M. & Ghazizadeh, S. Diverse epithelial cell populations contribute to the regeneration of secretory units in injured salivary glands. *Development* **147**, doi:10.1242/dev.192807 (2020).
17 Nanduri, L. S., Baanstra, M., Faber, H., Rocchi, C., Zwart, E., de Haan, G. *et al.* Purification and ex vivo expansion of fully functional salivary gland stem cells. *Stem Cell Reports* **3**, 957-964, doi:10.1016/j.stemcr.2014.09.015 (2014).
18 Maimets, M., Rocchi, C., Bron, R., Pringle, S., Kuipers, J., Giepmans, B. N. *et al.* Long-Term In Vitro Expansion of Salivary Gland Stem Cells Driven by Wnt Signals. *Stem Cell Reports* **6**, 150-162, doi:10.1016/j.stemcr.2015.11.009 (2016).
19 Zhang, B. & Horvath, S. A general framework for weighted gene co-expression network analysis. *Stat Appl Genet Mol Biol* **4**, Article17, doi:10.2202/1544-6115.1128 (2005).
20 Roccio, M., Hahnewald, S., Perny, M. & Senn, P. Cell cycle reactivation of cochlear progenitor cells in neonatal FUCCI mice by a GSK3 small molecule inhibitor. *Sci Rep* **5**, 17886, doi:10.1038/srep17886 (2015).
21 Roccio, M., Perny, M., Ealy, M., Widmer, H. R., Heller, S. & Senn, P. Molecular characterization and prospective isolation of human fetal cochlear hair cell progenitors. *Nat Commun* **9**, 4027, doi:10.1038/s41467-018-06334-7 (2018).
22 Yin, X., Farin, H. F., van Es, J. H., Clevers, H., Langer, R. & Karp, J. M. Niche-independent high-purity cultures of Lgr5+ intestinal stem cells and their progeny. *Nat Methods* **11**, 106-112, doi:10.1038/nmeth.2737 (2014).
23 McLean, W. J., Yin, X., Lu, L., Lenz, D. R., McLean, D., Langer, R. *et al.* Clonal Expansion of Lgr5-Positive Cells from Mammalian Cochlea and High-Purity Generation of Sensory Hair Cells. *Cell Rep* **18**, 1917-1929, doi:10.1016/j.celrep.2017.01.066 (2017).
24 Horvath, S. & Dong, J. Geometric interpretation of gene coexpression network analysis. *PLoS Comput Biol* **4**, e1000117, doi:10.1371/journal.pcbi.1000117 (2008).
25 Korb, K., Nicholson, A. *Bayesian Artificial Intelligence*. 2nd Edition edn, (CRC Press, 2011).
26 Cawley, A., Golding, S., Goulsbra, A., Hoptroff, M., Kumaran, S. & Marriott, R. Microbiology insights into boosting salivary defences through the use of enzymes and proteins. *J Dent* **80 Suppl 1**, S19-S25, doi:10.1016/j.jdent.2018.10.010 (2019).
27 Tanaka, J., Ogawa, M., Hojo, H., Kawashima, Y., Mabuchi, Y., Hata, K. *et al.* Generation of orthotopically functional salivary gland from embryonic stem cells. *Nat Commun* **9**, 4216, doi:10.1038/s41467-018-06469-7 (2018).
28 Landeira, D., Bagci, H., Malinowski, A. R., Brown, K. E., Soza-Ried, J., Feytout, A. *et al.* Jarid2 Coordinates Nanog Expression and PCP/Wnt Signaling Required for Efficient ESC Differentiation and Early Embryo Development. *Cell Rep* **12**, 573-586, doi:10.1016/j.celrep.2015.06.060 (2015).
29 Sperber, H., Mathieu, J., Wang, Y., Ferreccio, A., Hesson, J., Xu, Z. *et al.* The metabolome regulates the epigenetic landscape during naive-to-primed human embryonic stem cell transition. *Nat Cell Biol* **17**, 1523-1535, doi:10.1038/ncb3264 (2015).

30 Burridge, K. Focal adhesions: a personal perspective on a half century of progress. *FEBS J* **284**, 3355-3361, doi:10.1111/febs.14195 (2017).
31 Kim, N. G. & Gumbiner, B. M. Adhesion to fibronectin regulates Hippo signaling via the FAK-Src-PI3K pathway. *J Cell Biol* **210**, 503-515, doi:10.1083/jcb.201501025 (2015).
32 Hu, J. K., Du, W., Shelton, S. J., Oldham, M. C., DiPersio, C. M. & Klein, O. D. An FAK-YAP-mTOR Signaling Axis Regulates Stem Cell-Based Tissue Renewal in Mice. *Cell Stem Cell* **21**, 91-106 e106, doi:10.1016/j.stem.2017.03.023 (2017).
33 Bhandari, S., Lee, J. N., Kim, Y. I., Nam, I. K., Kim, S. J., Kim, S. J. *et al.* The fatty acid chain elongase, Elovl1, is required for kidney and swim bladder development during zebrafish embryogenesis. *Organogenesis* **12**, 78-93, doi:10.1080/15476278.2016.1172164 (2016).
34 Sassa, T., Tadaki, M., Kiyonari, H. & Kihara, A. Very long-chain tear film lipids produced by fatty acid elongase ELOVL1 prevent dry eye disease in mice. *FASEB J* **32**, 2966-2978, doi:10.1096/fj.201700947R (2018).
35 Zhao, Q., Zhang, L., Hai, B., Wang, J., Baetge, C. L., Deveau, M. A. *et al.* Transient activation of the Hedgehog-Gli pathway rescues radiotherapy-induced dry mouth via recovering salivary gland resident macrophages. *Cancer Res*, doi:10.1158/0008-5472.CAN-20-0503 (2020).
36 Serra, D., Mayr, U., Boni, A., Lukonin, I., Rempfler, M., Challet Meylan, L. *et al.* Self-organization and symmetry breaking in intestinal organoid development. *Nature* **569**, 66-72, doi:10.1038/s41586-019-1146-y (2019).
37 Huch, M., Gehart, H., van Boxtel, R., Hamer, K., Blokzijl, F., Verstegen, M. M. *et al.* Long-term culture of genome-stable bipotent stem cells from adult human liver. *Cell* **160**, 299-312, doi:10.1016/j.cell.2014.11.050 (2015).
38 Oldham, M. C. in *The OMICs: Applications in Neuroscience* (ed Coppola G.) Ch. 6, (Oxford University Press, 2013).
39 Lukonin, I., Serra, D., Challet Meylan, L., Volkmann, K., Baaten, J., Zhao, R. *et al.* Phenotypic landscape of intestinal organoid regeneration. *Nature* **586**, 275-280, doi:10.1038/s41586-020-2776-9 (2020).
40 Mihaylova, M. M., Cheng, C. W., Cao, A. Q., Tripathi, S., Mana, M. D., Bauer-Rowe, K. E. *et al.* Fasting Activates Fatty Acid Oxidation to Enhance Intestinal Stem Cell Function during Homeostasis and Aging. *Cell Stem Cell* **22**, 769-778 e764, doi:10.1016/j.stem.2018.04.001 (2018).
41 Sato, T., Vries, R. G., Snippert, H. J., van de Wetering, M., Barker, N., Stange, D. E. *et al.* Single Lgr5 stem cells build crypt-villus structures in vitro without a mesenchymal niche. *Nature* **459**, 262-265, doi:10.1038/nature07935 (2009).
42 Spence, J. R., Mayhew, C. N., Rankin, S. A., Kuhar, M. F., Vallance, J. E., Tolle, K. *et al.* Directed differentiation of human pluripotent stem cells into intestinal tissue in vitro. *Nature* **470**, 105-109, doi:10.1038/nature09691 (2011).
43 Langfelder, P. & Horvath, S. WGCNA: an R package for weighted correlation network analysis. *BMC Bioinformatics* **9**, 559, doi:10.1186/1471-2105-9-559 (2008).

CHAPTER 7

GMP COMPLIANT ISOLATION AND EXPANSION OF PRIMARY HUMAN-DERIVED SALIVARY GLAND ORGANOIDS FOR AUTOLOGOUS CELL-BASED THERAPY FOR XEROSTOMIA

Rocchi C., Jellema-de Bruin A., Baanstra A., van Rooij N., Brouwer U., van Os R., Jorritsma-Smit A., Barazzuol L., van Zanten J., Coppes RP.

In preparation

ABSTRACT

Radiotherapy treatment for head and neck cancer frequently results in irreversible xerostomia, which leads to a drastic decrease in the quality of life of the patient affected. Currently no long-term restorative treatment that aims to regenerate the salivary gland tissue exists. Here, we develop a GMP-compliant protocol for isolation and expansion of human-derived salivary gland organoids suitable for an autologous cell-based therapy to regenerate the lost functional tissue. This GMP-compliant protocol allows for the isolation as well as the expansion of human salivary gland cells derived from patient submandibular gland biopsies before radiotherapy treatment with an efficiency comparable to current non-GMP research-based protocols. We also show that functionality of salivary gland derived cells is maintained after cryopreservation allowing the protocol to be adapted to the radiotherapy treatment schedule of the patients. This protocol is conducted in well-defined conditions and accordingly to GMP-safety measures. The cells obtained are genetically stable and display a commitment to mature salivary gland functionality demonstrating the safety and feasibility of cell-based therapy for xerostomia to move towards clinical translation.

INTRODUCTION

Xerostomia may occur when salivary glands have been irreversibly damaged, as a result of ageing and autoimmune diseases (such as Sjögren's Syndrome) but also as a consequence of radiotherapy treatment for head and neck cancers (HNC)[1].Co-irradiation of healthy salivary gland during HNC treatment may induce a rapid and progressive decline of secretory function in patients[2]. The progressive functional decline of the saliva producing acinar units culminates in irreversible hyposalivation and the subsequent manifestation of the accompanying patho-physiological features of xerostomia, such as difficulty in mastication and swallowing, speech impairment and accelerated tooth decay, which drastically reduce the quality of life of the surviving patients[3-6].

Despite the beneficial effects of modern high precision radiotherapy technologies, such as intensity-modulated radiation therapy (IMRT) and proton therapy, to minimize the radiation dose administered to the parotid gland, still 40% of the patients experience xerostomia symptoms[7,8]. While parotid glands are responsible for 50% of stimulated saliva production, the discrepancy between sparing of the parotid gland and the severe xerostomia complication upon treatment could be explained by the fact that sparing of the parotid gland alone is not sufficient[9]. The submandibular glands are responsible for 65% of unstimulated saliva production and their ability to produce mucins is fundamental for maintaining a proper hydration of the mucosal membranes[10]. Due to their anatomical location in proximity to the neck nodes, such as the often-metastatic submandibular node (Ib) and II nodes[11,12], and the tumor volume coverage during radiotherapy treatment sparing of submandibular glands is very hard to achieve. Therefore, a regenerative approach could be a unique opportunity to restore the secretive function of the submandibular glands.

Cell-based therapies have been proposed with the aim of generating new functional acinar cells through the exogenous supply of stem and progenitor cells with the potential to either physically replace the lost tissue or re-activate the endogenous repair mechanisms. Although recent studies have shown an intrinsic regeneration potential of murine[13-15] and human[16] salivary gland driven by resident stem/progenitor-like cells[13,15,17], their spontaneous turnover rate cannot compensate for the massive loss of acinar cells that underlies the development of hyposalivation after radiotherapy[16]. None of the current treatments for radiation-induced xerostomia address the regenerative potential of the submandibular gland and its underlying mechanisms, but rather they focus on palliative treatments, such as saliva substitutes, that only aim to reduce the discomforts caused by the symptoms[1].

Proof of principle pre-clinical studies that support the success of a cell-based therapy aimed to generate new functional acinar cells through the transplantation of exogenous stem/progenitor-like cells possessing the ability to physically replace and repopulate lost tissue and to re-activate endogenous regeneration processes have been extensively

performed[17-20]. Mouse-into-mouse transplantation studies using selected cells based on known stem cell markers (c-Kit and CD24/CD29) have confirmed the presence of a stem-like cell population within the submandibular gland[18,19]. Furthermore, these studies showed the potential of salivary gland-derived cells to rescue radiation-induced hyposalivation. Unfortunately, the translation of these findings from mouse to human are limited by the lack of common markers to identify human salivary gland stem/progenitor cells[21]. Due to this bottleneck and the current lack of knowledge of human specific stem/progenitor cell markers, a deeper understanding of the complexity of the niche is crucial to allow the expansion of non-selected human salivary gland-derived cells and for the progression of a cell-based therapy for xerostomia.

The development of salivary gland organoid cultures allowed the identification of the Wnt pathway as a key signaling pathway, fundamental for salivary gland regeneration and for large-scale expansion of unselected murine salivary gland-derived cells[17]. These results paved the way for new transplantation studies based on unselected Wnt-enriched salivary gland-derived cells. Transplantation of cells derived from organoids cultured in Wnt-enriched conditions into irradiated salivary glands significantly increased cellular engraftment into the damaged gland, as well as the ability to restore salivary gland function, compared to previous transplantations performed using selected salivary gland-derived cells[17]. Although culturing of salivary gland cells from human salivary gland biopsies proved their ability to differentiate and rescue the hyposalivation phenotype[20], it was only by implementing and further optimizing the Wnt3a and R-spondin1 (RSPO1) enriched media developed using mouse cultures that it was possible to produce a clinically relevant yield of undifferentiated human salivary gland cells suitable for therapeutic application. Human salivary gland-derived organoid culture requires the addiction of Noggin to block the bone morphogenetic protein (BMP) signaling activity, shown to control differentiation in intestinal epithelium[22], and the inhibition of the Tgfβ pathway by the addition of the chemical inhibitor A83-01 (This thesis Chapter 6: ***A molecular network-based approach reveals human salivary gland stem cell features*****).**

In this work, we aimed to translate the salivary gland organoid technology into a GMP-compliant setting suitable for an autologous cell-based therapy for patients at risk for developing radiation-induced hyposalivation and consequential xerostomia. While further *in vivo* studies are required to confirm the ability of human-derived salivary gland organoids to functionally restore the hyposalivation phenotype upon transplantation, our procedure highlights the success in the development of a GMP-compliant protocol, inclusive of a cryopreservation step, which allows the isolation and expansion of genetically stable human-derived salivary gland organoids. Furthermore, the work here described, and performed at the ATMP-GMP facility of the University Medical Center Groningen, demonstrates the safety and

the feasibility of a standardized large-scale organoid production protocol for human-derived salivary gland organoids suitable for an autologous cell-based therapy for xerostomia patients.

EXPERIMENTAL DESIGN AND DEVELOPMENT OF THE PROTOCOL

The following procedure describes how to isolate and expand human primary salivary gland stem/progenitor-like cells following a GMP-compliant protocol. In this section we describe the results obtained, as well as the experimental set up considerations that need to be taken into account when performing the protocol.

The protocol presented here involves the following main steps **(Figure 1):**

Step 1 and 2: isolation and cryopreservation of primary human salivary gland cells.

Step 3: thawing of salivary gland-derived cell procedure.

Step 4: expansion of human salivary gland-derived organoids and quality control test.

Step 5: human salivary gland-derived stem/progenitor cell transplantation.

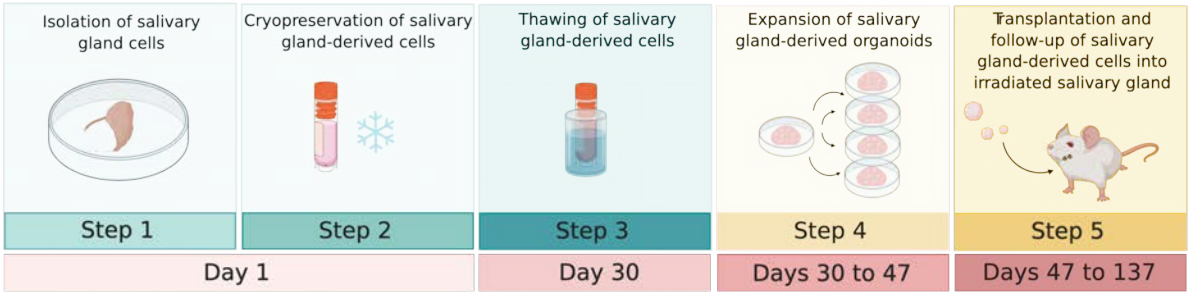

Figure 1: Overview of the protocol for salivary gland stem cells isolation and transplantation. In Step 1 the patient's biopsy is collected and the tissue processed for isolation of salivary gland-derived stem-like cells. The same day at the end of the isolation procedure the digested tissue is cryopreserved (Step 2). At day 30 (or when required) the cryovial will be thawed (Step 3) and the cells seeded in Matrigel for expansion (Step 4). In Step 5 the expanded salivary gland-derived cells are harvested and transplanted into immunocompromised mice previously subjected to 15 Gy irradiation of the salivary gland. Figure created with Biorender.

ANTICIPATED RESULTS

Isolation of human salivary gland stem/progenitor-like cells

Fresh human salivary gland biopsies are obtained from human non-malignant submandibular salivary gland tissue during the course of an elective or therapeutic ipsilateral neck dissection for the removal of squamous cell carcinomas of the oral cavity. Written informed consent is necessary in order to obtain donor tissue. Importantly, donor tissue viability decreases with time after surgical removal, therefore biopsies need to be immediately placed in cold collection solution on ice and processed as soon as possible. Tissue must be handled in a class II biological safety cabinet under aseptic conditions using sterile surgical tools.

In order to set up a large-scale strategy for GMP-compliant human-derived salivary gland organoid production, we adapted the protocol developed in (A molecular network-based approach identifies salivary gland stem cell signature, *manuscript in preparation Chapter 6 in this thesis)* to allow the isolation of human salivary gland-derived cells under GMP grade conditions (Figure 2A). To this purpose, it was required to find and test GMP-grade enzymes that could replace their research isolation counterparts without affecting the yield of primary salivary gland culture. Combination of Pulmozyme, Collagenase NB6 and $CaCl_2$ was tested and the yield per gram of tissue was compared with that obtained from the research isolation procedure (Figure 2B, C and D). At the end of the GMP-compliant isolation procedure, the yield and the morphological appearance of the tissue clumps obtained did not show any difference compared to the tissue clumps obtained following the research isolation protocol, showing that GMP-grade isolation had 100% efficacy.

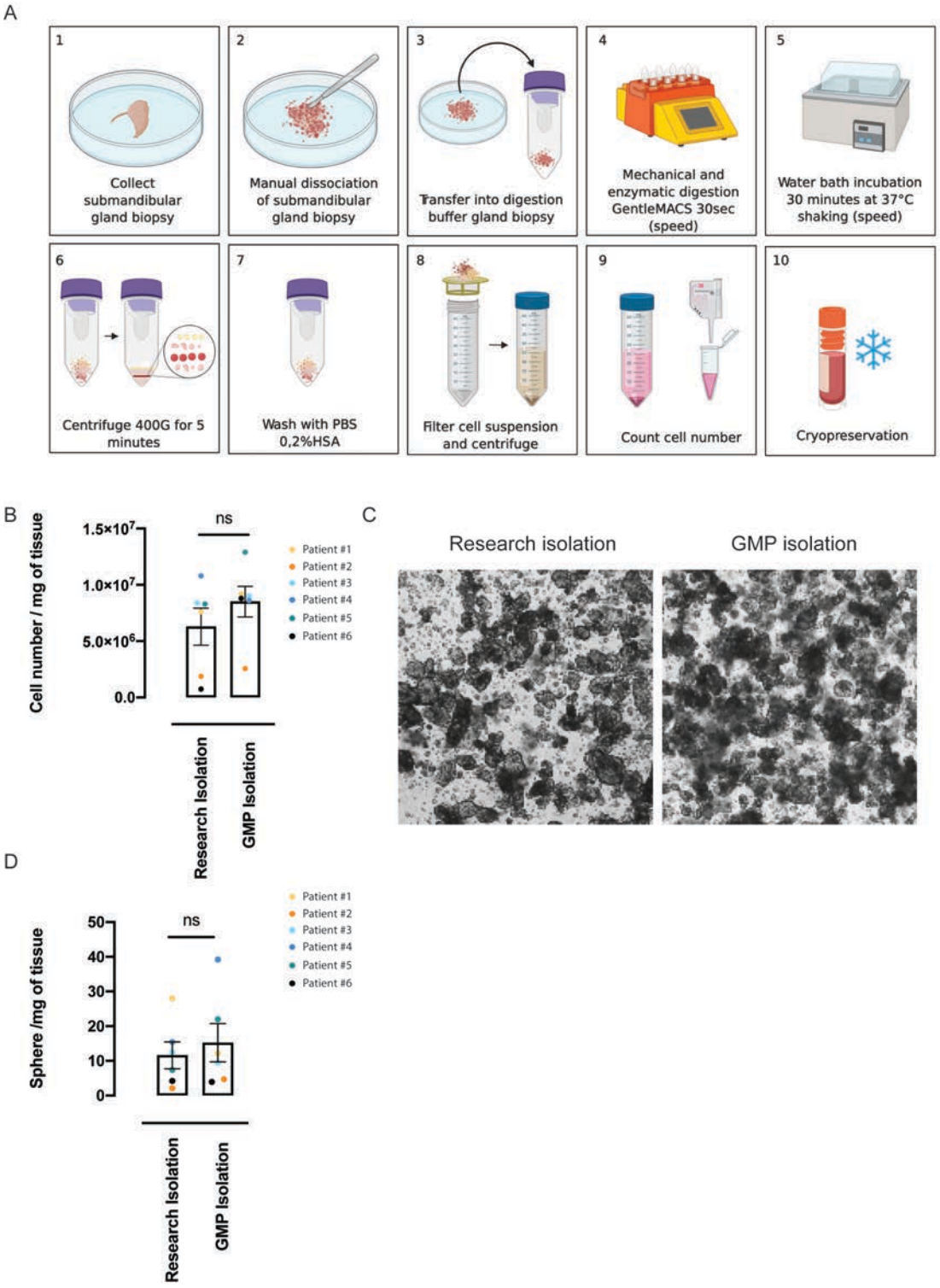

Figure 2: Isolation of salivary gland-derived cells. A) Schematic representation of key stages of the isolation of primary salivary gland-derived cells from patient's biopsy. **B)** Quantification of cell number/mg of tissue obtained at the end of the isolation procedure and comparing research isolation and GMP isolation. Each colour dot represents a separate patient. **C)** Representative bright-field images showing the comparison in the yield **(D)** of primary sphere after three days of floating culture between research isolation and GMP isolation. Data are represented as mean ± SEM. Each colour dot represents a separate patient. Statistical significance between the three groups was determined using one-way ANOVA ($p<0.05$). *$p<0.05$, **$p<0.01$, ***$p<0.001$, ****$p<0.0001$. Figure created with Biorender.

Validation of GMP-compliant human-derived salivary gland cells (hSG) freezing and thawing procedure

Human salivary gland-derived cell clumps were frozen at the end of the isolation procedure using a controlled-rate freezing device (details are provided in the Material section) to maximize reproducibility, minimize the risk of cell damage and improve viability after cryopreservation. After thawing 88% of human salivary gland derived cells were viable (Figure 3 A and B) and could be used for expansion of human salivary gland derived cells.

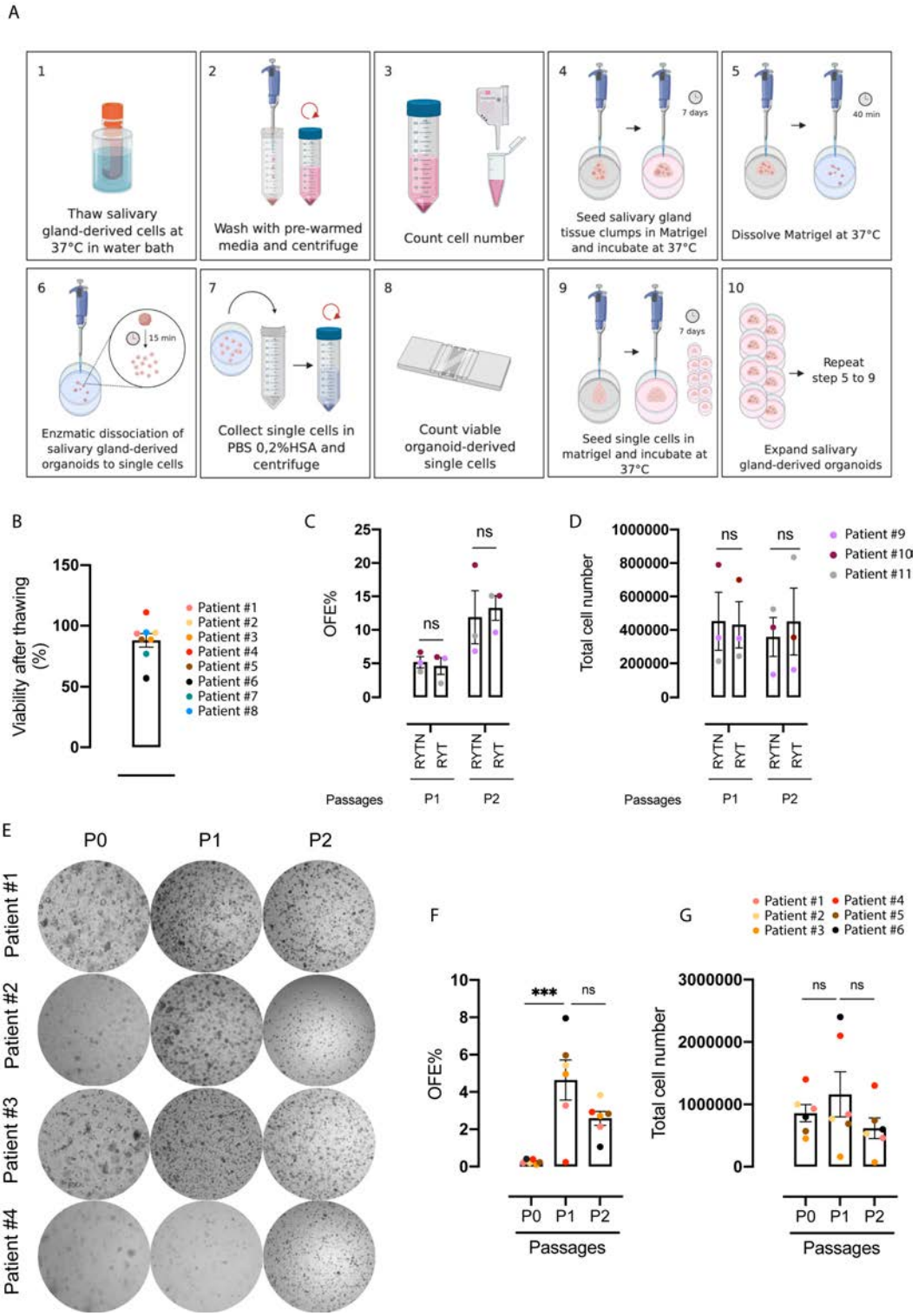
A
1
Thaw salivary gland-derived cells at 37°C in water bath
2
Wash with pre-warmed media and centrifuge
3
Count cell number
4
7 days
Seed salivary gland tissue clumps in Matrigel and incubate at 37°C
5
40 min
Dissolve Matrigel at 37°C
6
15 min
Enzmatic dissociation of salivary gland-derived organoids to single cells
7
Collect single cells in PBS 0,2%HSA and centrifuge
8
Count viable organoid-derived single cells
9
7 days
Seed single cells in matrigel and incubate at 37°C
10
Repeat step 5 to 9
Expand salivary gland-derived organoids
B
Viability after thawing (%)
150
100
50
0
Patient #1
Patient #2
Patient #3
Patient #4
Patient #5
Patient #6
Patient #7
Patient #8
C
OFE%
25
20
15
10
5
0
ns
ns
RYTN
RYT
RYTN
RYT
Passages
P1
P2
D
Total cell number
1000000
800000
600000
400000
200000
0
ns
ns
Patient #9
Patient #10
Patient #11
RYTN
RYT
RYTN
RYT
Passages
P1
P2
E
P0
P1
P2
Patient #1
Patient #2
Patient #3
Patient #4
F
OFE%
10
8
6
4
2
0
***
ns
P0
P1
P2
Passages
G
Patient #1
Patient #2
Patient #3
Patient #4
Patient #5
Patient #6
Total cell number
3000000
2000000
1000000
0
ns
ns
P0
P1
P2
Passages

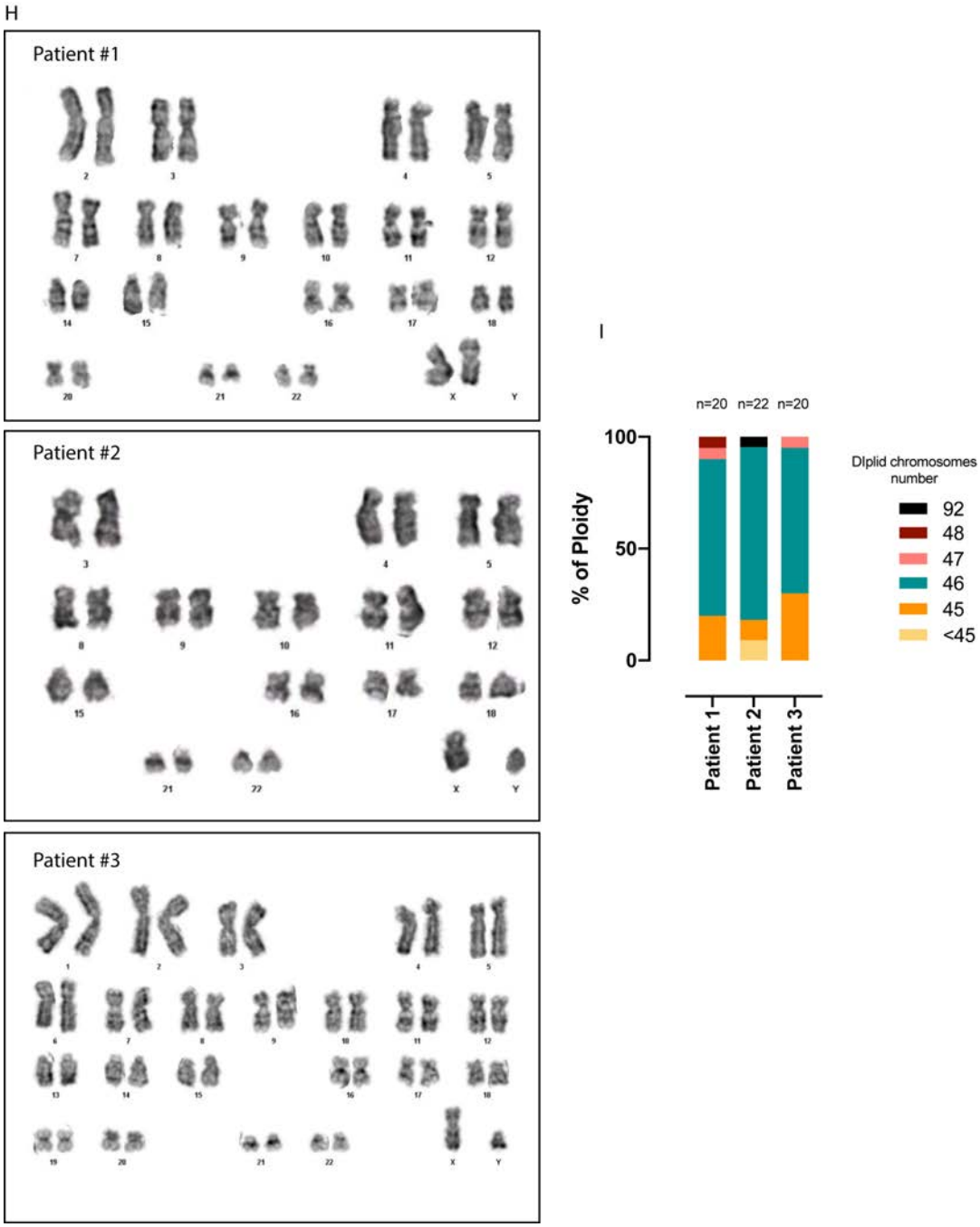

Figure 3: Expansion of salivary gland-derived stem-like cells. A) Schematic representation of key stages of the expansion protocol of salivary gland-derived stem-like cells. **B)** Viability of salivary gland-derived cells after thawing expressed as %. Each colour dot represents a patient. **C)** Organoid formation efficiency (OFE) and total cell number **(D)** of patient-derived salivary gland organoid at passage (P) 1 and 2 cultured in RYTN research media (R) and RYT-research media. Each colour dot represents a separate patient. **E)** Representative bright field images of 4 out 6 patients-derived salivary gland organoids that were culture at the GMP facility. **F)** Organoid formation efficiency (OFE) and **(G)** total cell number of patient-derived organoids culture in RYT media under GMP condition P0, P1 and P2. **H)** Representative karyotyping images of three patient-derived organoid culture at passage 2, illustrating a normal chromosomal count (n=46). **I)** Chromosome count on a total of 66 metaphases from 3 different patients. Data are represented as mean ± SEM (B, C, D, F and G). Statistical significance between the three groups was determined using one-way ANOVA ($p<0.05$). *$p<0.05$, **$p<0.01$, ***$p<0.001$, ****$p<0.0001$. Figure created with Biorender.

Expansion of human-derived salivary gland organoid and assessment of differentiation potential

In order to obtain a GMP-compliant cellular product, it is required that the expansion media in which the cells are grown has a well-defined composition. The risk assessment analysis on the expansion media components described in (A molecular network-based approach identifies salivary gland stem cell signature, *manuscript in preparation Chapter 6 in this thesis*), revealed that Wnt3a conditioned media, as well as RSPO1 conditioned media, and Noggin did not meet the requirements for therapeutic use. While Wnt3a is not yet available as a GMP-grade component, in view of replacing RSPO1 conditioned media we used a recombinant human R-spondin-1 protein supplemented in the media and compared the organoid formation ability between the "research" and GMP-grade expansion media. With respect to the ability of human-derived salivary gland cells to self-renew and expand, organoid formation efficiency (OFE) and population doublings RYTN and RYT didn't show any significance differences (Figure 3C and D). The organoids derived from the GMP-compliant expansion showed a significant increase in OFE% at P1 compared to P0 (Figure 3E and F), as well as an increase in cell number (Figure 3G). For the use of human salivary gland derived cells as cell a cell therapy, it is vital to provide evidence that the cells used do not accumulate any chromosomal aberrations in culture that could potentially lead to tumor formation in the recipient patients. Therefore, we analyzed the number of chromosomes in human salivary gland derived organoids at the end of passage 2 from 3 different patients and found that on average 71.7% of the cells exhibit a normal number of chromosomes and only a small percentage of cells exhibit chromosomal number greater (6.2%) or less (3.03%) than 46 (Figure 3H and I).

To assess the quality of patient-derived salivary gland organoid culturing, we tested their potential to differentiate and to produce mature salivary gland functional proteins.

The organoids formed at the end of each passage (P0, P1 and P2) from 3 different patients were transferred into a new gel in the presence of differentiation media (Figure 4A). The morphological and immunofluorescent analysis of the differentiated cultures showed that human-derived organoids isolated and expanded using a GMP-grade protocol are able to differentiate into both acinar and ductal lineages and are capable of expressing mature salivary gland functional proteins such as mucin and amylase (Figure 4B, C and D). Importantly from a "clinical" point of view, we were able to assess the differentiation potential of patient-derived salivary gland organoids originating from cultures showing different growth capacities.

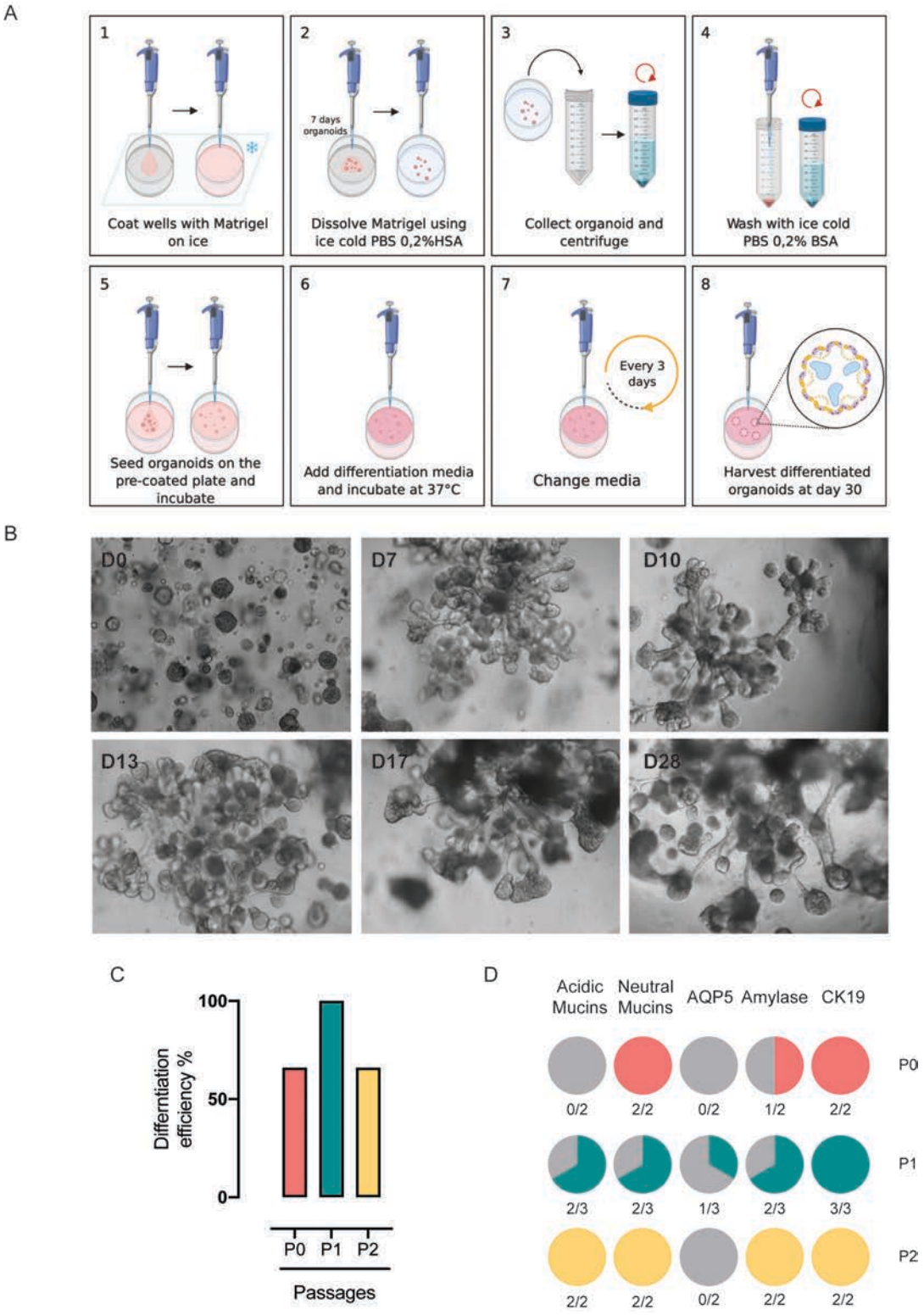

Figure 4: Differentiation of human salivary gland-derived organoids. A) Schematic representation of the key stages of the differentiation procedure of salivary gland organoids. **B)** Representative bright-field images of differentiating salivary gland-derived organoids at different time points. **C)** Differentiation efficiency of 3 different patient-derived salivary gland organoid culture under GMP condition, at passage 0 (P0), passage 1 (P1) and passage 2 (P2). **D)** Pie chart indicating the expression of key salivary gland functional proteins of differentiated organoids at P0 (pink), passage 1 (green) and at passage 2 (yellow) in 3 different patients. Figure created with Biorender.

Human-derived salivary gland transplantation

In order to assess the regeneration potential of patient-derived salivary gland organoids, the organoid-derived single cells obtained using the GMP expansion protocol were transplanted into locally irradiated salivary glands of Rag2-/- immunocompromised mice (Figure 5A). GMP-expanded organoid-derived single cells were extensively washed to remove any residual trace of Matrigel, as well as Gentamycin. An ELISA assay was performed to demonstrate that after 3 washes of cultured human-derived salivary gland cell suspensions the amount of laminin, which constitutes 60% of the Matrigel composition, detected in the supernatant was $1.643x10^{-6} \pm 3.638x10^{-7}$ mg/mL indicating a significant reduction in laminin concentration compared to the initial value of 8.2 mg/mL (Figure 5B). We considered these cells were usable for transplantation.

When working with small volumes of concentrated cells we recommend resuspending an excess of cells to reduce the risk of volume loss during transplantation as well as counting the remaining cells at the end of the transplantation procedure. $1x10^5$ cells were transplanted locally into each salivary gland with a sterile Hamilton syringe, being careful to homogeneously distribute the cells at multiple locations throughout the gland and to reduce possible leakage by decreasing the volume along the needle track. Both the saliva flow rate and the percentage of engraftment were assessed every month for three months following transplantation. A significant improvement in saliva flow rate was achieved upon transplantation at 15 days post-irradiation and the small percentage of cells that engrafted into the damaged tissue displayed the ability to organize into native ductal and acinar structures (figure 5C and D), indicating that organoid-derived cells from the GMP-grade expansion protocol retain the ability to “home” within the niche and that they are able to differentiate to acinar and ductal lineages.

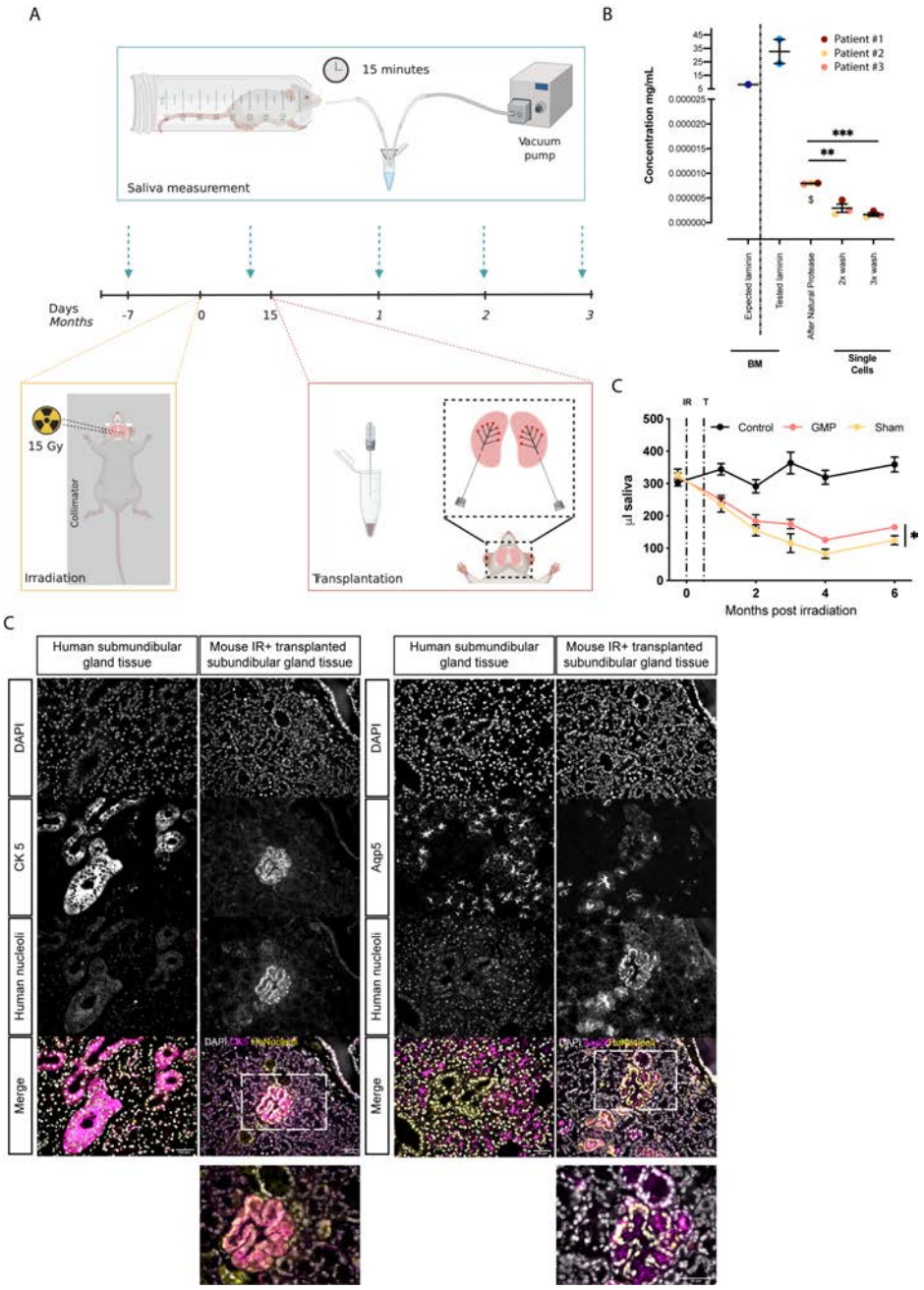

Figure 5: Transplantation of human salivary gland-derived organoids. A) Overview of the transplantation timeline into locally irradiated Rag2- γc- immunodeficient mice. **B)** Graph displays ELISA results of laminin level (mg/mL) in Basement Matrigel (BM) (Tested laminin), supernatant after Natural Protease step for dissolution of the gel ($= estimated concentration due to absorbance value above the limit of the standard curve), supernatant obtained as results of multiple consecutive washing step (2x wash and 3x wash) The resulted concentrations were compared to the concentration of laminin expected from the purchased batch of Matrigel (Expected laminin). Statistical significance for ELISA assay was determined using t-Test ($p<0.05$). *$p<0.05$, **$p<0.01$, ***$p<0.001$, ****$p<0.0001$. **C)** Time course analysis of relative saliva production of human salivary gland organoid-derived cells transplanted in 15Gy locally-irradiated mice in comparison to control and irradiated sham transplanted animals.IR= irradiation; T= transplantation. Statistical significance was determined using 2-way ANOVA($p<0.05$). *$p<0.05$, **$p<0.01$, ***$p<0.001$. **D)** immunofluorescence staining of ductal marker cytokeratin 5 (CK 5), acinar marker Aquaporin 5 (Aqp 5) and human anti nucleoli (HuNuc) in human salivary gland tissue (positive control) and in irradiated transplanted murine submandibular gland at day 134 post transplantation. Scale bar is 50 µm.

MATERIALS:

BIOLOGICAL MATERIAL

Human non-malignant submandibular gland tissues were obtained from donors after informed consent and Institutional Review Board (IRB) approval during an elective head and neck dissection procedure for the removal of squamous cell carcinoma of the oral cavity at the University Medical Centre Groningen (UMCG) and Medical Centre Leeuwarden (MCL).

EQUIPMENT

- NuncTM Cell Culture/Petri dishes (60x15 mm, Cat. No: 150288; Thermo Scientific)
- Costar 12 well plate, tissue culture treated (Cat.No: 3513; Corning)
- Costar 96 well plate, tissue culture treated (Cat.No: 3595; Corning)
- Disposable scalpel sterile (n.10A, Cat. No 233-5513 (0502); VWR Swann-Morton)
- Centrifuge tubes (15 and 50 mL; Cat.No: 188271 and 227261; Greiner Bio-One)
- Easystrainer, mesh for 50 ml tube (100 µm; Cat. No: 542000; Greiner)
- GentleMACS Octo Dissociator (Cat.No: 130-095-937; Milteny)
- C-tubes for GentleMACS (Cat. No: 130-093-237; Milteny)
- Disposable serological pipettes (5 mL; Cat.No: 7045; Corning)
- Disposable serological pipettes (10 mL; Cat.No: 7015; Corning)
- Disposable serological pipettes (25 mL; Cat.No: 7016; Corning)
- Graduated filter tips (P10; Cat.No: F171103; Gilson)
- Graduated filter tips (P30; Cat.No: F171303; Gilson)
- Graduated filter tips (P200; Cat.No: F171503; Gilson)
- Graduated filter tips (P1000; Cat.No: F171703; Gilson)
- Pipetteboy (Cat.No: 4910; Corning)
- Cryotube vials (1.8 mL; Cat.No: 377267; Nunc)
- Scepter™ 2.0 Handheld Automated Cell Counter (Merk Millipore)
- Scepter Cell Counter Sensor (40µm; Cat.No: PHCC40050; Merk Millipore)
- Storage bottle (500mL; Cat.No: 8393; Corning)
- Eppendorf (Cat No: 72.690.001; SARSTEDT)
- CO_2 incubator (37 °C, 5% CO_2; Cat.No: Forma 3111; Clean air)
- Centrifuge (Cat.No: 460RS; Rotanta)
- Bright Field microscope (Leica DM1L; Leica micro-system b.v)
- Hamilton syringe (Cat.No: 7636-01, Hamiltoncompany)
- 28G Hamilton syringe's needle (Cat.No:7803-02, Hamilton Company
- Suturing wire Safil 5-0 (Cat.No. C1048507, BBraun,)
- Vacuum-system

- Planer Freezing machine (Kryo 560-16; Cryo-Solutions)

REAGENTS

- HBSS w/o Ca/Mg/Phenol red (1x) (500mL; Cat.No: 14175053)
- HSA (100 mL; Cat.No: 15522636; Sanquin)
- $CaCl_2$ (Cat.No: G00115; Pharmacy UMCG)
- Albuman (50 mL bottle; Cat.No: 15522636; Pharmacy UMCG)
- Collagenase NB6 (1g; N0002779; Nordmark)
- Pulmozyme (6x 2,5 mL; Cat.No: RVG 16734; KFF/Roche)
- DMEMF12 w/o phenol red (500mL; Cat.No: 21041-025; Gibco)
- DMEMF12 Phenol red (500mL; Cat.No: 11320-074 Gibco)
- Neutral Protease AF GMP from Chlostridium histolyticum (> 100DMC-U; Cat.No: N0003553)
- D-PBS (1x) (500mL; Cat.no: 14190-144; Gibco)
- GMP Trypsin (1g (0,23M); Cat.No: 063698801; Roche)
- Basement Matrigel (10mL; Cat.No: 356237; Corning)
- Gentamycin (10mg/vial; Cat.no:RVG 57572; KFF/Centrafarm)
- Pen/Strep (100mL; Cat.No: 15140-122 Gibco)
- Glutamax-I CTS (100mL; Cat.no: A1286001; Thermo Fisher)
- Cryostore CS-10 (16mL/vial; Cat.No: 7931; Stem Cell Technology)
- Rho kinase inhibitor Y-27632 (10mg/vial; Cat.no: ab 120129; Abcam)
- Recombinant human R-spondin-1 (20 µg; Cat.No: SRP3292; Sigma)
- GMP recombinant human EGF (100µg/vial; Cat.no: 170-176-406; Milteny)
- GMP recombinant human FGF2 (25µg; Cat.No: GMP100-18E; Preprotech)
- Dexamethason (100gr; Cat.No: 14731231; Pharmacy UMCG)
- HGF (Cat.no: 100-39; Preprotech)
- FGF-10 (Cat.No: 100-26-A; Preprotech)
- Heparin salt 0.2% (Cat.No: 7980; Stem Cell Technology)
- DAPT (5mg; Cat.No: D5942-5MG; Sigma)
- Carbachol (1g; Cat. No:C4382; Sigma)
- FCS (Cat.No: 758085; Greiner)
- CTS ^{TM} N-2 Supplement (5mL; A1370701; Thermo Fisher)
- Recombinant human insulin (100mg; Cat.No:91077C; Sigma)
- A83-01 (10mg; Cat.No: 2939; Tocris bioscience)
- Water for injection (WFI)

- NaCl (Baxter)
- Isofluorane
- 70% Ethanol
- 0.5% Chlorohexidine (Cat.No:ROL 1652710, Addedpharma)
- Rimadyl/ carprofelican (Cat.No: 1172061; Dechra)
- Pilocarpine
- Mice: Rag2 mice (C;129S4-Rag2<tm1.1Flv> Il2rg<tm1.1Flv>/J)

REAGENT SET UP

- HBSS 1%HSA:
- HBSS 1% Albuman:
- Digestion solution: HBSS 1% albuman + collagenase NB6 and Pulmozyme
- Neutral Protease:
- PBS 0.2% HSA
- PBS 1% HSA
- Carbachol: Reconstitute in PBS and prepare a stock concentration of 100mM. Further dilute in media to a concentration of 100μM. Prepare aliquots and store at -20 °C. Add 2μL/mL of culture media for a final concentration of 100ng/mL
- Heparin sodium salt 0.2%: Dilute the 2mg/mL stock in PBS to a final concentration of 100 μg/mL. Store aliquots at 4 °C. Add 1 μL/mL for a final concentration of 100 ng/mL
- DAPT: Reconstitute in DMSO and prepare a stock concentration of 10mM. Further dilute in media to a concentration of 100 μM. Prepare aliquots and store at -20°C. Add 10 μL/mL of culture media for a final concentration of 1 μM.
- HGF: Reconstitute in PBS 0.1 %BSA to 5 μg/mL. Prepare aliquots and store them at -20 °C. Add 10 μ L/mL of culture media for a final concentration of 50ng/mL
- Dexamethasone: Reconstitute in medium to a final concentration of 1mM. Filter solution through a 0.2 μM filter. Prepare aliquots and store them at -20 °C.
- GMP recombinant human EGF: Reconstitute in 1mL of water for injection (WFI) to 0,1mg/mL. Dilute the stock 5x with PBS 0.1HSA% to a final concentration of 20μg/mL. Prepare 100 μL aliquots and store them at -20°C. Add 100μL to a 50mL medium to reach a final concentration of 40 ng/mL.
- GMP recombinant human FGF2: Reconstitute in 250 μL of WFI to a concentration of 0.1 mg/mL. Dilute 4x with PBS 0.1% HSA to reach a final concentration of 25 μg/mL. Prepare 40 μL aliquots and store them at -20°C.

Add 40μL to a 50mL medium to reach a final concentration of 20 ng/mL

- Rho kinase inhibitor Y-27632: Reconstitute in medium to a final concentration of 1mM. Filter the solution through a 0.2μm filter. Prepare 50μL aliquots and store them at -20°C. Use a final concentration of 10 μM (10μL/mL of media).
- R-spondin human recombinant: Reconstitute in sterilized H_2O to a final concentration of 100 μg/mL. Further dilute with PBS 0.1%HSA to 10 μg/mL. Filter through a 0.22 μM filter. Prepare 250 μL aliquots and store at -20 °C. Use 10μL/medium to reach a concentration of 100 ng/mL.
- CTS N2 (100x): thaw the vial and prepare 500 μL aliquots and store -20 °C.
- A83-01 (Tgfβ inhibitor): Reconstitute in DMSO to a concentration of 1mM.Prepare 50 μL aliquots and store at -20°C. Use 1 μL/mL for a final concentration of 1μM/mL.
- Recombinant human insulin: Reconstitute in WFI at pH 2-3 to a concentration of 2mg/mL. Filter through a 0.2 μm filter and prepare 250 μL aliquots and store at 4°C.
- GMP culture media: to prepare 50mL of GMP culture media, supplement DMEMF12 with 500 μL of Y-27632, 250 μL of insulin, 100 μL of EGF, 40 μL FGF, 50 μL dexamethasone, 500 μL of N2, 50 μL of A83-01 and 500 μL of R-spondin
- Differentiation media: to prepare 1mL of differentiation media, supplement DMEMF12 with 1 μ L of heparin sodium salt, 10 μL of DAPT, 10 μL of HGF,10 μL of FGF10, 2μL of Carbachol and 100 μL of FCS.
- Wash media: To prepare 100 ml of wash medium, supplement 90 ml of DMEM/F12 with 10 ml of 10% (wt/vol) HSA (final concentration = 1%).
- Pilocarpine solution

PROCEDURE

Isolation of human submandibular gland

Timing 4h

1. Transfer the material collected in the operating room in a 50 mL falcon tube containing (HBSS) supplemented with 1% (HSA) on ice.

CRITICAL STEP: Do not store resected material on ice for more than 24h prior starting the procedure. The prolonged storage on ice will result in a lower yield of primary spheres.

2. Weigh the resected piece of tissue in a sterile petri dish **(Figure 2a).**
3. Use a sterile disposable scalpel to mince the whole submandibular gland into small pieces (~1mm^3) in a 10-cm culture dish **(Figure 2b**).
4. Digest the submandibular gland in HBSS supplemented with 1% Albuman with Collagenase NB6 (0,00575 PZ U/mg of minced tissue of) and Pulmozyme (0.625

E/mg of minced tissue) in a gentleMACS C tube. Use 1 gentleMACS C tube every 100mg of minced tissue.

5. Place the C tube in the gentleMACS dissociator for 25 seconds at 143 rounds per run.
6. Incubate the gentleMACS C tubes for 30 minutes at 37°C in a shaking water-bath.
7. (vii) Repeat (5) and (6)
8. Centrifuge the gentleMACS C tubes at 400g for 5 minutes at 4°C.
9. Aspirate the supernatant and resuspend the pellet in 4mL of HBSS 1%HSA. Use a 5/10 mL pipette to ensure a proper wash and to provide further dissociation.
10. Centrifuge the gentleMACS C tubes at 400g for 5 minutes at 4°C.
11. (Aspirate the supernatant and resuspend the pellet in 2mL of HBSS 1%HSA. Use a 5/10 mL pipette to ensure a proper wash and to provide further dissociation.
12. Filter the cell suspension over a 100μm filter to remove any connective and adipose tissue.
13. Centrifuge the gentleMACS C tubes at 400g for 5 minutes at 4°C.
14. Aspirate supernatant and resuspend the pellet in 1mL DMEM f12.
15. With the use of Scepter Cell Counter, count the number of cells ranging between 6.126 μm and 8.467 μm in size in a 1:50 dilution of the resuspended cell pellet.

▲ **CRITICAL STEP:** take 100μL aliquot and check using a light microscope the presence of cells clumps. If no cells clumps are present at this isolation stage, no organoid culture will be possible

At this stage human salivary gland cell clumps can be cryopreserved

Cryopreservation of salivary gland derived cells clumps.

● **Timing: 30 minutes**

16. After having counted the cell clumps in step (xx), centrifuge the cell suspension at 400g for 5 minutes at 4°C.
17. Resuspend the pellet in 1mL of CS10 freezing medium supplemented with 10μM Rho-kinase inhibitor Y-27632. Add the freezing medium dropwise to the tube and pipette gently up and down using a P1000 pipette and transfer it to a 1.5 mL cryovial. Place cryotubes on ice.
18. Freeze the cells by using a CoolCell freezing container (BioCision)
19. Transfer the cryotube to a Controlled Rate Freezing Machine (Figure 3a [temperature cooling program).
20. Transfer the cryotube containing the cells to liquid nitrogen.

■ **PAUSE POINT:** Cells can be store in liquid nitrogen, where they are expected to have a shelf-life of several years.

Procedure for thawing salivary gland derived isolated cell clumps

Timing: 30 minutes

21. Prepare a 15mL tube with 10mL of wash medium and warm it at room temperature.
22. Bring the cells to the cell culture lab on ice, spray the cryotube with ethanol and place it in a 37°C water-bath until a small ice clump remain.
23. Add 1 mL of pre-warm wash media dropwise to the cell and transfer them to an empty 15 mL tube. Wash the cryotube with an additional mL of wash medium and transfer it to the 15 mL tube containing the cells. Add the remain 8 mL of wash medium dropwise to the same tube.
24. Centrifuge the 15 mL tube containing the cells at 250g for 10 minutes at room temperature.
25. Discard the supernatant and wash the pellet with 10 mL of pre-warmed GMP culture media
26. Aspirate the supernatant and resuspend the cell pellet in 1 mL of pre-warmed GMP culture media.
27. With the use of Scepter Cell Counter, count the number of cells ranging between 6.126 µm and 8.467 µm in size in a 1:50 dilution of the resuspended cell pellet.

CRITICAL STEP: Check availability of cells after thawing

28. Seed cell clumps at a density of 0.4 x 10^6 in a 75 µL Matrigel drop in the middle of one well of a 12-well tissue culture plate.

CRITICAL STEP: Work quickly to avoid that Matrigel solidify before plating

29. Place the tissue culture plate in the incubator (37°C and 5% CO_2) for 15 minutes to allow Matrigel to solidify.
30. Pre-warm the salivary gland GMP culture media at 37°C for 10 minutes before adding it to the seeded wells.
31. Add 1mL of GMP culture media to the seeded well and place the plate in the incubator (37°C and 5% CO_2).
32. Leave the plate in the incubator for 7 days

Expansion of human salivary gland derived organoid and quality control test Timing 17 days

33. At day 7(or 10) from the start of the culture, remove media from each well and replace it with 1 mL of Neutral Protease and incubate the plate for 30-40 minutes at 37°C and 5% CO_2.
34. Collect organoids in Neutral Protease in a 15 mL tube and wash each well with 1 mL PBS1x supplemented with 0.2%HSA.
35. Centrifuge the 15 mL collection tube containing organoid at 400g for 5 minutes at 4°C. Collect maximum 6 of 12 well plate per tube
36. Discard supernatant and add 1.5 mL of GMP Trypsin per collection tube and incubate max 15minutes in the incubator (37°C and 5% CO_2).

CRITICAL STEP: check the plate every 5 minutes and resuspend each well with the use of a P1000 to help the enzymatic dissociation of the organoid into single cells and to avoid over-digestion.

37. Inactivate the GMP trypsin by adding 2 mL of PBS1x supplemented with 1%HSA for each well.
38. Transfer up to 6 wells into a 15 mL collection tube and centrifuge the single cells suspension at 400g for 5 minutes at 4°C.
39. Discard supernatant and resuspend the pellet in GMP culture media.
40. Count organoid derived single cell availability using trypan blue (1:1)
41. Seed organoid derived single cells in the next culture passage at a final concertation of $0.8x10^6$ cells per mL. 25 µL of cell suspension mix on ice with 50 µL of ice cold Matrigel and the 75 µL gel pipetted in the middle of a 12-well plate.

CRITICAL STEP: Work quickly to avoid that Matrigel solidify before plating.

42. Place the plate in the incubator (37°C and 5% CO_2) for 15-20 minutes to allow Matrigel to solidify
43. Gently pipette 1 mL of prewarmed GMP culture media into each well and place the plate in the incubator (37°C and 5% CO_2) for 10 days.

BOX 1| Quality control: differentiation of salivary gland derived organoid

(A)Differentiation of human salivary gland derived organoid

(i) Before starting the differentiation assay, prepare an adequate volume of differentiation media

(ii) Dilute Matrigel 1:1 with ice cold media in a 15 mL collection tube.

(iii) Place a 96 well plate on ice and coat the bottom of each well with 40 μL of diluted ice cold Matrigel.

(iv) Rotate the plate so that the diluted Matrigel will form a uniform layer covering the complete bottom of the wells

(v) Let the Matrigel polymerize at 37°C for 30 minutes before proceeding.

(vi) At the end of Passage 1 after thawing human salivary gland derived cells, aspirate the media and add 1mL of ice cold 1x PBS 1%HSA to each well, without disturbing the gel.

(vi) Precoat the inside and outside of a 1 mL tip by dipping the full length of the tip in 1x PBS 1%HSA and resuspend in it 2x. This will avoid organoid from sticking to the tip.

After coating the tip, resuspend the content of each well

? TROUBLESHOOTING

(vii)Transfer the organoid to a 15 mL collection tube precoated with 1x PBS 1%HSA. This will prevent the organoid from sticking to the side of the tube.

(viii) Wash the well with 1 mL ice cold 1x PBS 1%HSA to collect all the organoids

(ix) Fill up the tube with 10 mL of ice cold PBS1x and centrifuge at 400g for 5 minutes at 4°C

(x) Remove the supernatant. The pellet should be strong and no Matrigel layer should be visible.

▲ **CRITICAL STEP:** Organoid recovery from Matrigel is essential for downstream assay. Remaining of Matrigel can modify their behavior in the new gel.

(xi) Resuspend the pellet in up to 1 mL of differentiation media and keep the tube on ice.

(xii) Mix properly the organoid suspension and use 100 uL to count with the use of bright field microscope the total number of organoids.

▲ **CRITICAL STEP:** It is important to count the total number of organoids in order to be able to resuspend them in differentiation media at a final concentration of 20-30 organoids per 25 uL of media. Higher or lower organoid concentration per well can impair their differentiation ability.

(xiii) Centrifuge the 15 mL collection tube contain the organoid at 400g for 5 minutes at 4°C.

(xv) Seed organoids at a final concentration of 20-30 organoids per 25 μL of media and mix on ice with 50 μL of ice cold Matrigel. Pipette a 75 μL gel in each well of a 96 well plate

▲ **CRITICAL STEP:** Work quickly to avoid that Matrigel solidify before plating.

(xvi) Place the plate in the incubator (37°C and 5% CO_2) for 30 minutes to allow Matrigel to solidify

(xvii) Add 150 μL of differentiation media per well and incubate at 37°C, 5% CO_2.

(xviii) Change media every 3 days.

(xviii) At day 30 harvest the structure and stain for salivary gland functional marker

Transplantation of human salivary gland organoid-derived cells into immunodeficient mice. ● **Timing: 20 minutes per mouse**

44. At the end of P1, remove media from each well and replace it with 1 mL of Neutral Protease and incubate the plate for 30-40 minutes at 37°C and 5% CO_2.
45. Collect organoids in Neutral Protease in a 15 mL tube and wash each well with 1 mL 1x PBS supplemented with 0.2%BSA.
46. Centrifuge the 15 mL collection tube containing organoid at 400g for 5 minutes at 4°C. Collect maximum 6 of 12 well plate per tube
47. Discard supernatant and add 1.5 mL of GMP Trypsin per collection tube and incubate max. 15 minutes in the incubator (37°C and 5% CO_2).

▲ **CRITICAL STEP:** check the plate every 5 minutes and resuspend each well with the use of a P1000 to help the enzymatic dissociation of the organoid into single cells and to avoid over-digestion.

48. Inactivate the GMP trypsin by adding 2 mL of 1x PBS supplemented with 1%HSA for each well.
49. Transfer up to 6 wells into a 15 mL collection tube and centrifuge the single cells suspension at 400g for 5 minutes at 4°C.
50. Wash the cell suspension with 10 mL 1x PBS 0.2%HSA in a 15 mL tube
51. Centrifuge the 15 mL tube collection containing the cell suspension at 400g for 5min at 4°C
52. Discard supernatant and repeat the washing step (51-52)
53. Count organoid derived single cell availability using trypan blue (1:1)
54. In a sterile eppendorf tube resuspend $5x10^5$ cells in a volume of 50 µL of NaCl
55. Under a downhood flow cabinet, anaesthetize a previously locally irradiated (15Gy) Rag2 mice (C;129S4-Rag2<tm1.1Flv> Il2rg<tm1.1Flv>/J) using isolfluoarane (0,5 L/min, 5% isofluorane) until non-reflexive to gentle pressure of the toe. Anesthesia is maintained throughout the operation at 0.5 L/min; 2% isoflurane.
56. With the mouse supine, shaved and clean the region of the neck with a solution containing 70% ethanol and 0.5% chlorohexidine
57. A 5 mm incision is made in the neck to expose the salivary gland
58. Draw 10 µL of cell suspension into a sterile 25 µL Hamilton syringe with a 28G needle
59. Position the syringe to the submandibular gland and move the needle 2-3 mm into the tissue
60. Inject 2 uL of cell suspension in 5 different spots within the submandibular gland tissue making sure that the cell suspension does not leak out the injection site
61. Repeat the same procedure for the remaining gland

62. Suture the incision in the neck using horizontal mattress stitches
63. Allow the animals to recover and monitor for 24 h providing 3mg of flunixin subcutaneously
64. Allow engraftment and regeneration for 3 months

Advantages compared to other methods

Advances in understanding how salivary gland tissue is organized and controlled by the surrounding niche[13,15,17,23], as well as developments in gene therapy [24-26] and bioengineering approaches[27], have revolutionized the salivary gland regeneration field and opened new possibilities for clinical treatment of xerostomia. However, considering the amount of salivary gland parenchymal damage induced by radiotherapy treatment for HNC patients, the replacement of the lost acinar compartment with exogenous cells requires a large-scale production of salivary gland committed cells. Although acinar cells have been proven to act as lineage-restricted progenitors to maintain the homeostasis of the acinar compartment, acinar cell-based transplantation strategies are currently limited by the challenges to maintain and expand acinar progenitor cells[28,29].

Culturing of human-derived salivary gland cells as a monolayer may cause a loss of acinar phenotype, resulting, instead, in an expansion of cells that exhibit a more striated duct phenotype[30]. Enrichment of culture media, as well as the introduction of the mechanical properties of an extracellular matrix (ECM) via the use of Matrigel and/or collagen, promotes the development of structures with a more acinar phenotype[30-32]. While the acinar phenotype seems to a certain extent be reproducible *in vitro*, these studies do not allow for expansion through sequential passaging and long-term maintenance of acinar cells. Without establishing expansion potential, no evidence is provided of a functional capability of salivary gland acini to maintain their phenotype after proliferation as well as to provide support for other salivary gland cell types such as ductal and myoepithelial cells[30,31]. Our model overcomes the current low scalability potential of acinar cells by taking advantage of submandibular gland-derived stem-like cells, which have the potential to self-organize into complex multicellular structures and to provide lineage segregation, mimicking the complexity of the tissue of origin[17,18].

As an alternative to adult stem cells, it has been shown that functional salivary gland organoids can be derived from pluripotent stem cells, such as embryonic stem cells (ESCs) and induced pluripotent stem cells (iPS cells)[33]. While their easily accessible source and their ability to differentiate to all adult cell types make them an exciting candidate with high therapeutic and translational potential, the high incidence of genetic and epigenetic variation occurring during reprogramming represents a limitation for their clinical application[34,35]. Although in the near future production of salivary gland committed cells might be achievable with the use of patient-

specific iPS cells, endogenous adult salivary gland-derived stem/progenitor-like cells are more compliant with regulatory requirements as they are considered to be less harmful (due to the abovementioned variation of iPS cells) and are also considered ethically more suitable.

Importantly, regardless of the lack of knowledge in terms of native homeostatic function, both bone-marrow-derived mesenchymal stem cells (BMCs) and adipose-derived mesenchymal stem cells (AdMSCs) have been proposed as experimental cell-based therapies for radiation-induced hyposalivation[36,37]. Despite being easy to isolate, culture and expand from readily accessible sources and volunteers, the mechanism of action of MSCs is still unclear, and thus poses questions about the initial enthusiasm of early-phase clinical trials[38]. AdMSCs are characterized by the expression of three surface markers, none of which are AdMSC-specific[37], and by their ability to differentiate into bone, adipose and chondrogenic lineages. Nonetheless, the repeated systemic injection of AdMSCs seems to improve the post-irradiation hyposalivation phenotype of mice[39,40]. While organoid-derived salivary gland cells[17,18,20] are able to rescue the hyposalivation phenotype by replacing and repopulating lost tissue in the damaged gland, transplanted AdMSCs seem to elicit a “hit and run” mechanism of action whereby the increase in flow rate, as well as the decrease in saliva secretion lag time, seems to be triggered by signaling of the AdMSCs without long-term engraftment of the cells[39,41,42]. Due to their secretory profile and paracrine effects on both adjacent and distal cells, AdMSCs have previously been described as “medicinal signaling cells”[43], as they are capable of modulating immune responses and stimulating endogenous processes. While, efforts in identifying these secreted factors could eliminate the need for injection of AdMSCs and remove the associated risks linked with the poor characterization of these cells[44] the possible systemic effect caused by known local distribution of these factors potentially stimulating tumor growth should be assessed. The relatively old age of patients diagnosed with HNC (63-65 years old on average), together with the natural functional decline of adult tissue stem cell with age, may pose a limit in the application of human salivary gland stem/progenitor cells for xerostomia treatment[21,45,46]. In accordance with studies performed in other slow-turnover tissues, such as the brain, the fraction of quiescent mouse salivary gland cells expressing stem cell enriched markers $CD24^{hi}CD29^{hi}$ increases in number in the salivary gland of aged mice, but the ability of these stem cells to form primary spheres seems to be drastically reduced[14]. This suggests that salivary gland quiescent stem cells from aged mice are more resistant to activation compared to salivary gland stem/progenitor cells from younger mice. Interestingly though, when salivary gland stem/progenitor cells from aged mice were cultured in the presence of enriched niche signalling, the *in vitro* growth and *in vivo* regeneration potential of these cells was restored and was comparable to their younger counterparts[14]. Contrary to those of the salivary gland adult stem cells, the *in vivo* functionality of MSCs seems to be dependent on factors related to the donor including age and disease.

These studies provided evidence that the quality of human derived-MSCs declines with increasing age, in part due to acquisition of senescence characteristics, and reduction in quantity and quality of secretome, influencing the ability of MSCs to improve tissue regeneration[47,48]. Considering the relatively old age of patients suffering from xerostomia, the age of the donor poses a strong limitation in autologous MSCs transplantation as a therapeutic approach to rescue radiation-induced xerostomia.

Limitations

We have shown that patient-derived salivary gland organoids can be expanded using a GMP-compliant approach. While replacing RSPO1-conditioned media with a human recombinant protein seems sufficient to create the necessary Wnt stimulation necessary to promote salivary gland-derived cells to proliferate and expand, the addition of GMP-grade Wnt3a to the current medium could potentially further increase the organoid forming efficiency but is regretfully not available yet. In order to expand salivary gland-derived stem cells as organoids the support of an extracellular matrix is required. While Matrigel resembles complex basement membrane environments of many tissues, its animal derivation could pose limitation for its clinical use. The Dutch Central Committee on Research Involving Human Subjects (CCMO) evaluated the risk assessment and provisionally suggested the use of Matrigel to expand salivary gland-derived stem-like cells for clinical use provided all animal traces have to be removed prior to transplantation. In this protocol we provide evidence that multiple washing steps prior to transplantation is effective in significantly reducing traces of laminin which contributes up to 60% of the extracellular matrix, and thus the use of Matrigel is being considered by the CCMO for Phase1/Phase2 clinical trials. Furthermore, artificial synthetic matrices are currently being tested in our group for their applicability to our protocol. A synthetic hydrogel would accommodate organoid growth, while providing a molecularly well-defined and dynamic matrix applicable to later Phase trials. Moreover, these hydrogels could potentially reduce functional variability following transplantation by generating a more homogeneous, reproducible, and clinically compatible organoid culture system where variation in size, shape and cell-type composition are reduced[49-52].

While transplantation of mouse salivary gland organoid-derived cells into salivary glands irradiated recipient mice resulted in engraftment and long-term survival of the transplanted cells[17,18], human salivary gland organoid-derived cells transplanted into immunodeficient recipient mice seem to transiently engraft and mainly act in a paracrine manner[20]. Although immune deficient mice such as NOD.Cg-PrkdcscidIl2rgtmlWjl/SzJ (NSG)[20] and C;129S4-Rag2<tm1.1Flv> Il2rg<tm1.1Flv>/J (Rag2- γc-) were used to generate a “humanized” mouse model for salivary gland generation, the transient engraftment of human cells into irradiated recipient mice could be explained by a rejection of the transplanted cells[20]. While these mouse

models lack B, T and NK (Natural Killer) cells, the remaining host innate immune cells, such as macrophages and dendritic cells, present in the human-transplanted immune deficient mice (FcγIVr, CCR5)[20] could represent an impediment to human cell engraftment[53-55]. The autologous nature of the cell-based therapy for xerostomia patients described here, will overcome the rejection of the transplanted cells and will remove the need for immunosuppression.

While the paracrine effect of human salivary gland organoid-derived cells seems to be sufficient to rescue the damage induced by 5 Gy local irradiation, increasing the radiation dose to the clinically relevant dose of 15 Gy[56] drastically reduces both engraftment capability and the potential paracrine mechanism of action and thus results in a poor functional output. Importantly, a consideration needs to be posed when comparing the radiotherapy treatment plan of a patient with the irradiation experimental set up used for mice *in vivo* studies. While in *in vivo* mice studies the irradiated salivary glands receive a homogenous 15 Gy radiation dose, in patients undergoing radiotherapy treatment for head and neck tumors salivary glands will receive a dose gradient that decreases with distance from the homogenous dose to the tumor. Therefore, the non-homogenous distribution of the dose within the salivary gland, may allow for better engraftment of transplanted cells at sites with lower radiation-induced damage. This may offer a double-edge sword effect, whereby stem cells may engraft more efficiently in the areas that have received lower doses of radiation and therefore increasing the chance of effective paracrine stimulation proposed in human into mouse studies[20]. An efficient regeneration in low dose regions could allow the re-establishment of niche homoeostasis and build up a “regeneration gradient” that could eventually rescue the areas that have received higher dose.

REFERENCES

1 Rocchi, C. & Emmerson, E. Mouth-Watering Results: Clinical Need, Current Approaches, and Future Directions for Salivary Gland Regeneration. *Trends Mol Med*, doi:10.1016/j.molmed.2020.03.009 (2020).

2 Burlage, F. R., Coppes, R. P., Meertens, H., Stokman, M. A. & Vissink, A. Parotid and submandibular/sublingual salivary flow during high dose radiotherapy. *Radiother Oncol* **61**, 271-274, doi:10.1016/s0167-8140(01)00427-3 (2001).

3 Langendijk, J. A., Doornaert, P., Verdonck-de Leeuw, I. M., Leemans, C. R., Aaronson, N. K. & Slotman, B. J. Impact of late treatment-related toxicity on quality of life among patients with head and neck cancer treated with radiotherapy. *J Clin Oncol* **26**, 3770-3776, doi:10.1200/JCO.2007.14.6647 (2008).

4 Vissink, A., Jansma, J., Spijkervet, F. K., Burlage, F. R. & Coppes, R. P. Oral sequelae of head and neck radiotherapy. *Crit Rev Oral Biol Med* **14**, 199-212, doi:10.1177/154411130301400305 (2003).

5 Konings, A. W., Coppes, R. P. & Vissink, A. On the mechanism of salivary gland radiosensitivity. *Int J Radiat Oncol Biol Phys* **62**, 1187-1194, doi:10.1016/j.ijrobp.2004.12.051 (2005).

6 Tsai, W. L., Huang, T. L., Liao, K. C., Chuang, H. C., Lin, Y. T., Lee, T. F. *et al.* Impact of late toxicities on quality of life for survivors of nasopharyngeal carcinoma. *BMC Cancer* **14**, 856, doi:10.1186/1471-2407-14-856 (2014).

7 Nutting, C. M., Morden, J. P., Harrington, K. J., Urbano, T. G., Bhide, S. A., Clark, C. *et al.* Parotid-sparing intensity modulated versus conventional radiotherapy in head and neck cancer (PARSPORT): a phase 3 multicentre randomised controlled trial. *Lancet Oncol* **12**, 127-136, doi:10.1016/S1470-2045(10)70290-4 (2011).

8 van Luijk, P., Pringle, S., Deasy, J. O., Moiseenko, V. V., Faber, H., Hovan, A. *et al.* Sparing the region of the salivary gland containing stem cells preserves saliva production after radiotherapy for head and neck cancer. *Sci Transl Med* **7**, 305ra147, doi:10.1126/scitranslmed.aac4441 (2015).

9 Murdoch-Kinch, C. A., Kim, H. M., Vineberg, K. A., Ship, J. A. & Eisbruch, A. Dose-effect relationships for the submandibular salivary glands and implications for their sparing by intensity modulated radiotherapy. *Int J Radiat Oncol Biol Phys* **72**, 373-382, doi:10.1016/j.ijrobp.2007.12.033 (2008).

10 Humphrey, S. P. & Williamson, R. T. A review of saliva: normal composition, flow, and function. *J Prosthet Dent* **85**, 162-169, doi:10.1067/mpr.2001.113778 (2001).

11 Chao, K. S., Wippold, F. J., Ozyigit, G., Tran, B. N. & Dempsey, J. F. Determination and delineation of nodal target volumes for head-and-neck cancer based on patterns of failure in patients receiving definitive and postoperative IMRT. *Int J Radiat Oncol Biol Phys* **53**, 1174-1184, doi:10.1016/s0360-3016(02)02881-x (2002).

12 Gregoire, V., Coche, E., Cosnard, G., Hamoir, M. & Reychler, H. Selection and delineation of lymph node target volumes in head and neck conformal radiotherapy. Proposal for standardizing terminology and procedure based on the surgical experience. *Radiother Oncol* **56**, 135-150, doi:10.1016/s0167-8140(00)00202-4 (2000).

13 Emmerson, E., May, A. J., Berthoin, L., Cruz-Pacheco, N., Nathan, S., Mattingly, A. J. *et al.* Salivary glands regenerate after radiation injury through SOX2-mediated secretory cell replacement. *EMBO Mol Med* **10**, doi:10.15252/emmm.201708051 (2018).

14 Maimets, M., Bron, R., de Haan, G., van Os, R. & Coppes, R. P. Similar ex vivo expansion and post-irradiation regenerative potential of juvenile and aged salivary gland stem cells. *Radiother Oncol* **116**, 443-448, doi:10.1016/j.radonc.2015.06.022 (2015).
15 May, A. J., Cruz-Pacheco, N., Emmerson, E., Gaylord, E. A., Seidel, K., Nathan, S. *et al.* Diverse progenitor cells preserve salivary gland ductal architecture after radiation-induced damage. *Development* **145**, doi:10.1242/dev.166363 (2018).
16 Luitje, M. E., Israel, A. K., Cummings, M. A., Giampoli, E. J., Allen, P. D., Newlands, S. D. *et al.* Long-Term Maintenance of Acinar Cells in Human Submandibular Glands After Radiation Therapy. *Int J Radiat Oncol Biol Phys*, doi:10.1016/j.ijrobp.2020.10.037 (2020).
17 Maimets, M., Rocchi, C., Bron, R., Pringle, S., Kuipers, J., Giepmans, B. N. *et al.* Long-Term In Vitro Expansion of Salivary Gland Stem Cells Driven by Wnt Signals. *Stem Cell Reports* **6**, 150-162, doi:10.1016/j.stemcr.2015.11.009 (2016).
18 Nanduri, L. S., Baanstra, M., Faber, H., Rocchi, C., Zwart, E., de Haan, G. *et al.* Purification and ex vivo expansion of fully functional salivary gland stem cells. *Stem Cell Reports* **3**, 957-964, doi:10.1016/j.stemcr.2014.09.015 (2014).
19 Lombaert, I. M., Brunsting, J. F., Wierenga, P. K., Faber, H., Stokman, M. A., Kok, T. *et al.* Rescue of salivary gland function after stem cell transplantation in irradiated glands. *PLoS One* **3**, e2063, doi:10.1371/journal.pone.0002063 (2008).
20 Pringle, S., Maimets, M., van der Zwaag, M., Stokman, M. A., van Gosliga, D., Zwart, E. *et al.* Human Salivary Gland Stem Cells Functionally Restore Radiation Damaged Salivary Glands. *Stem Cells* **34**, 640-652, doi:10.1002/stem.2278 (2016).
21 Pringle, S., Van Os, R. & Coppes, R. P. Concise review: Adult salivary gland stem cells and a potential therapy for xerostomia. *Stem Cells* **31**, 613-619, doi:10.1002/stem.1327 (2013).
22 Sato, T., Vries, R. G., Snippert, H. J., van de Wetering, M., Barker, N., Stange, D. E. *et al.* Single Lgr5 stem cells build crypt-villus structures in vitro without a mesenchymal niche. *Nature* **459**, 262-265, doi:10.1038/nature07935 (2009).
23 Aure, M. H., Konieczny, S. F. & Ovitt, C. E. Salivary gland homeostasis is maintained through acinar cell self-duplication. *Dev Cell* **33**, 231-237, doi:10.1016/j.devcel.2015.02.013 (2015).
24 Delporte, C., O'Connell, B. C., He, X., Lancaster, H. E., O'Connell, A. C., Agre, P. *et al.* Increased fluid secretion after adenoviral-mediated transfer of the aquaporin-1 cDNA to irradiated rat salivary glands. *Proc Natl Acad Sci U S A* **94**, 3268-3273, doi:10.1073/pnas.94.7.3268 (1997).
25 Baum, B. J., Alevizos, I., Zheng, C., Cotrim, A. P., Liu, S., McCullagh, L. *et al.* Early responses to adenoviral-mediated transfer of the aquaporin-1 cDNA for radiation-induced salivary hypofunction. *Proc Natl Acad Sci U S A* **109**, 19403-19407, doi:10.1073/pnas.1210662109 (2012).
26 Alevizos, I., Zheng, C., Cotrim, A. P., Liu, S., McCullagh, L., Billings, M. E. *et al.* Late responses to adenoviral-mediated transfer of the aquaporin-1 gene for radiation-induced salivary hypofunction. *Gene Ther* **24**, 176-186, doi:10.1038/gt.2016.87 (2017).
27 Gao, Z., Wu, T., Xu, J., Liu, G., Xie, Y., Zhang, C. *et al.* Generation of Bioartificial Salivary Gland Using Whole-Organ Decellularized Bioscaffold. *Cells Tissues Organs* **200**, 171-180, doi:10.1159/000371873 (2014).

28 Jang, S. I., Ong, H. L., Gallo, A., Liu, X., Illei, G. & Alevizos, I. Establishment of functional acinar-like cultures from human salivary glands. *J Dent Res* **94**, 304-311, doi:10.1177/0022034514559251 (2015).
29 Shubin, A. D., Sharipol, A., Felong, T. J., Weng, P. L., Schutrum, B. E., Joe, D. S. *et al.* Stress or injury induces cellular plasticity in salivary gland acinar cells. *Cell Tissue Res*, doi:10.1007/s00441-019-03157-w (2020).
30 Maria, O. M., Zeitouni, A., Gologan, O. & Tran, S. D. Matrigel improves functional properties of primary human salivary gland cells. *Tissue Eng Part A* **17**, 1229-1238, doi:10.1089/ten.TEA.2010.0297 (2011).
31 Pradhan-Bhatt, S., Harrington, D. A., Duncan, R. L., Jia, X., Witt, R. L. & Farach-Carson, M. C. Implantable three-dimensional salivary spheroid assemblies demonstrate fluid and protein secretory responses to neurotransmitters. *Tissue Eng Part A* **19**, 1610-1620, doi:10.1089/ten.TEA.2012.0301 (2013).
32 Joraku, A., Sullivan, C. A., Yoo, J. & Atala, A. In-vitro reconstitution of three-dimensional human salivary gland tissue structures. *Differentiation* **75**, 318-324, doi:10.1111/j.1432-0436.2006.00138.x (2007).
33 Tanaka, J., Ogawa, M., Hojo, H., Kawashima, Y., Mabuchi, Y., Hata, K. *et al.* Generation of orthotopically functional salivary gland from embryonic stem cells. *Nat Commun* **9**, 4216, doi:10.1038/s41467-018-06469-7 (2018).
34 Liang, G. & Zhang, Y. Genetic and epigenetic variations in iPSCs: potential causes and implications for application. *Cell Stem Cell* **13**, 149-159, doi:10.1016/j.stem.2013.07.001 (2013).
35 Ma, H., Morey, R., O'Neil, R. C., He, Y., Daughtry, B., Schultz, M. D. *et al.* Abnormalities in human pluripotent cells due to reprogramming mechanisms. *Nature* **511**, 177-183, doi:10.1038/nature13551 (2014).
36 Gronhoj, C., Jensen, D. H., Glovinski, P. V., Jensen, S. B., Bardow, A., Oliveri, R. S. *et al.* First-in-man mesenchymal stem cells for radiation-induced xerostomia (MESRIX): study protocol for a randomized controlled trial. *Trials* **18**, 108, doi:10.1186/s13063-017-1856-0 (2017).
37 Gronhoj, C., Jensen, D. H., Vester-Glowinski, P., Jensen, S. B., Bardow, A., Oliveri, R. S. *et al.* Safety and Efficacy of Mesenchymal Stem Cells for Radiation-Induced Xerostomia: A Randomized, Placebo-Controlled Phase 1/2 Trial (MESRIX). *Int J Radiat Oncol Biol Phys* **101**, 581-592, doi:10.1016/j.ijrobp.2018.02.034 (2018).
38 Galipeau, J. & Sensebe, L. Mesenchymal Stromal Cells: Clinical Challenges and Therapeutic Opportunities. *Cell Stem Cell* **22**, 824-833, doi:10.1016/j.stem.2018.05.004 (2018).
39 Lim, J. Y., Ra, J. C., Shin, I. S., Jang, Y. H., An, H. Y., Choi, J. S. *et al.* Systemic transplantation of human adipose tissue-derived mesenchymal stem cells for the regeneration of irradiation-induced salivary gland damage. *PLoS One* **8**, e71167, doi:10.1371/journal.pone.0071167 (2013).
40 Xiong, X., Shi, X. & Chen, F. Human adipose tissuederived stem cells alleviate radiationinduced xerostomia. *Int J Mol Med* **34**, 749-755, doi:10.3892/ijmm.2014.1837 (2014).
41 Prockop, D. J. The exciting prospects of new therapies with mesenchymal stromal cells. *Cytotherapy* **19**, 1-8, doi:10.1016/j.jcyt.2016.09.008 (2017).

42 Sumita, Y., Liu, Y., Khalili, S., Maria, O. M., Xia, D., Key, S. *et al.* Bone marrow-derived cells rescue salivary gland function in mice with head and neck irradiation. *Int J Biochem Cell Biol* **43**, 80-87, doi:10.1016/j.biocel.2010.09.023 (2011).
43 Caplan, A. I. & Correa, D. The MSC: an injury drugstore. *Cell Stem Cell* **9**, 11-15, doi:10.1016/j.stem.2011.06.008 (2011).
44 Robey, P. "Mesenchymal stem cells": fact or fiction, and implications in their therapeutic use. *F1000Res* **6**, doi:10.12688/f1000research.10955.1 (2017).
45 Kalamakis, G., Brune, D., Ravichandran, S., Bolz, J., Fan, W., Ziebell, F. *et al.* Quiescence Modulates Stem Cell Maintenance and Regenerative Capacity in the Aging Brain. *Cell* **176**, 1407-1419 e1414, doi:10.1016/j.cell.2019.01.040 (2019).
46 Stoyanov, G. S., Kitanova, M., Dzhenkov, D. L., Ghenev, P. & Sapundzhiev, N. Demographics of Head and Neck Cancer Patients: A Single Institution Experience. *Cureus* **9**, e1418, doi:10.7759/cureus.1418 (2017).
47 Liu, M., Lei, H., Dong, P., Fu, X., Yang, Z., Yang, Y. *et al.* Adipose-Derived Mesenchymal Stem Cells from the Elderly Exhibit Decreased Migration and Differentiation Abilities with Senescent Properties. *Cell Transplant* **26**, 1505-1519, doi:10.1177/0963689717721221 (2017).
48 Sarkar, P., Redondo, J., Kemp, K., Ginty, M., Wilkins, A., Scolding, N. J. *et al.* Reduced neuroprotective potential of the mesenchymal stromal cell secretome with ex vivo expansion, age and progressive multiple sclerosis. *Cytotherapy* **20**, 21-28, doi:10.1016/j.jcyt.2017.08.007 (2018).
49 Huch, M., Knoblich, J. A., Lutolf, M. P. & Martinez-Arias, A. The hope and the hype of organoid research. *Development* **144**, 938-941, doi:10.1242/dev.150201 (2017).
50 Cruz-Acuna, R., Quiros, M., Farkas, A. E., Dedhia, P. H., Huang, S., Siuda, D. *et al.* Synthetic hydrogels for human intestinal organoid generation and colonic wound repair. *Nat Cell Biol* **19**, 1326-1335, doi:10.1038/ncb3632 (2017).
51 Gjorevski, N. & Lutolf, M. P. Synthesis and characterization of well-defined hydrogel matrices and their application to intestinal stem cell and organoid culture. *Nat Protoc* **12**, 2263-2274, doi:10.1038/nprot.2017.095 (2017).
52 Gjorevski, N., Sachs, N., Manfrin, A., Giger, S., Bragina, M. E., Ordonez-Moran, P. *et al.* Designer matrices for intestinal stem cell and organoid culture. *Nature* **539**, 560-564, doi:10.1038/nature20168 (2016).
53 Brehm, M. A. & Shultz, L. D. Human allograft rejection in humanized mice: a historical perspective. *Cell Mol Immunol* **9**, 225-231, doi:10.1038/cmi.2011.64 (2012).
54 Kooreman, N. G., de Almeida, P. E., Stack, J. P., Nelakanti, R. V., Diecke, S., Shao, N. Y. *et al.* Alloimmune Responses of Humanized Mice to Human Pluripotent Stem Cell Therapeutics. *Cell Rep* **20**, 1978-1990, doi:10.1016/j.celrep.2017.08.003 (2017).
55 Shultz, L. D., Keck, J., Burzenski, L., Jangalwe, S., Vaidya, S., Greiner, D. L. *et al.* Humanized mouse models of immunological diseases and precision medicine. *Mamm Genome* **30**, 123-142, doi:10.1007/s00335-019-09796-2 (2019).
56 Coppes, R. P., Vissink, A. & Konings, A. W. Comparison of radiosensitivity of rat parotid and submandibular glands after different radiation schedules. *Radiother Oncol* **63**, 321-328, doi:10.1016/s0167-8140(02)00129-9 (2002).

CHAPTER 8

SUMMARY & DISCUSSION

SUMMARY

Irreversible hyposalivation and xerostomia (also known as dry mouth syndrome) are the main consequences of salivary gland dysfunction. Radiation-induced hyposalivation may lead to xerostomia and can be caused by radiotherapy of head and neck cancer patients. Inclusion of the salivary glands in the field of radiation during radiotherapy may lead to the disruption of the salivary gland cellular niches and to a progressive and irreversible decline of the progenitor-like acinar cells leading to a subsequential loss of homeostasis and ultimately to the permanent loss of acinar tissue responsible for saliva production and secretion. While xerostomia *per se* is not a life-threatening condition, of the 500,000 patients diagnosed every year with head and neck cancer 40% of those who receive radiotherapy, even the most modern forms, will experience a severe decrease in their quality of life. Although in the past two decades there has been a significant amount of research on the development of a means to overcome xerostomia, current clinical strategies approved by the Food and Drug Administration (FDA) provide only temporary relief from the discomfort caused by xerostomia-related symptoms. Therefore, novel approaches such as those derived from regenerative medicine are needed. Understanding the regenerative potential of the adult salivary gland is essential for progressing our knowledge on salivary gland biology and for the development of new regenerative therapeutic strategies aimed at a long-term restoration of the damaged salivary gland. Although it has been shown that salivary glands retain, to a certain extent, the ability to regenerate, current regenerative approaches for radiation-induced salivary gland dysfunction have been curtailed by the lack of identity/knowledge of both the key cellular players and the signalling pathways regulating the tissue integrity of salivary glands.

By connecting preclinical and clinical research, the work described in this thesis shows how combining murine-injury models with both mouse and human salivary gland-derived organoid technologies can be used to identify cell sources relevant for salivary gland homeostasis and regeneration as well as the underlying regulatory mechanisms. Thereby this work aids the development of potential clinically relevant regenerative therapy approaches to treat radiation-induced hyposalivation.

Chapter 2 reflects on how over the last 30 years changes in adult stem cell definition have influenced the way salivary gland tissue integrity has been investigated and perceived. The hardwired professional stem cell paradigm based on the hematopoietic

stem cell system is introduced and by providing an overview of the available data on salivary gland stem/progenitor cells, the applicability of such a paradigm as a template for salivary gland biology (and other rapidly dividing tissues) is questioned. Next it is discussed how the stem cell function in the salivary gland can be executed by cells of different nature either under homeostasis or during repair of damaged tissue. It is speculated that more than a well-defined, rare, quiescent cell that resides at the apex of a hierarchical tree, dynamic mechanisms of plasticity within the gland epithelium might be responsible for the renewal of salivary glands. Furthermore, it is hypothesised that in order to replace lost or damaged tissue it is the environment, in terms of the signals provided by the niche, rather than cell specific surface phenotypic characteristics (such as cell surface marker expression), which shapes a stem cell-like function. Speculation is cast on how understanding the dynamic of cell-cell interactions through time and taking advantage of integrative multi-omic approaches could be a unique opportunity to unravel which pathways regulate cell-fate specification in salivary gland regeneration. Finally, how the knowledge from these integrative multi-omic approaches could open up possibilities for new therapeutic strategies to rescue radiation-induced hyposalivation is discussed.

In **Chapter 3**, the identification of the Wnt pathway as an essential component of the complex signalling network that regulates salivary gland tissue integrity during homeostasis and regeneration is described. Immunofluorescent co-staining for the general ductal epithelial marker EpCAM and the Wnt-reporter gene β-catenin was used to visualize Wnt-responsive cells within the salivary gland epithelium. EpCAM+ cells were isolated using Fluorescent Activate Cell Sorting (FACS), and subsequently cultured in Matrigel and media supplemented with Wnt3a and Rspo1, both well-known stimulators of the Wnt pathway. Only $EpCAM^{high}$ cells under Wnt stimulation generated organoid cultures capable of long-term expansion while maintaining the ability to give rise to all salivary gland cell lineages. Notably, the addition of Wnt inhibitors to EpCAM-derived organoid cultures led to a reduction in organoid formation efficiency confirming the essentiality of ectopic Wnt source in the renewal of salivary gland-derived organoids. Finally, transplantation of cells derived from Wnt-driven salivary gland derived organoids into locally irradiated mouse salivary glands was shown to rescue the radiation-induced hyposalivation phenotype to a greater extent than using the cells obtained from organoids cultured in medium devoid of Wnt.

In **Chapter 4**, evidence is provided that the Hippo pathway regulator YAP functions as a sensor of tissue integrity in response to salivary gland damage. Following severe local damage, induced *in vivo* via ligation of the salivary gland, the normally quiescent ductal compartment activates a YAP-driven tissue response characterized by high levels of nuclear YAP and increased proliferation of ductal cells in close proximity to the damage site, suggesting that YAP nuclear activity is required during regeneration. This local-injury response indicates that differentiated epithelial cells can function as a source of stem-like cells for tissue regeneration. Using a well-established salivary gland organoid culture system, chemical and genetic modulation of YAP nuclear activity was shown to impact the self-renewal ability of both mouse and human salivary gland-derived cells. Inhibition of YAP nuclear activity led to a reduction in organoid formation efficiency, while stimulation of YAP nuclear translocation increased organoid forming efficiency and promoted long-term expansion of salivary gland-derived cells. Finally, using organoids as a regenerative model, pharmacological inhibition of Mst1/2 kinases, and consequent activation of YAP nuclear activity after irradiation, was demonstrated to significantly improve the regenerative response after irradiation of human salivary gland-derived cells.

In **Chapter 5**, it is reported that autophagy is a key pathway for self-renewal activation of salivary gland organoids and that its pharmacological manipulation has the potential to promote tissue regeneration. Utilising organoid formation as a regeneration process, an increase in autophagy flux within the stem-like cell population, reflected by the ability to form secondary and tertiary organoids, is identified. Evidence that such self-renewal ability requires a constant “fuel of energy” from the autophagy machinery is provided. Furthermore, inhibition of both early and late steps of autophagy, as well as the knockout of the autophagy related gene 5 (*Atg5*), led to a significant reduction of self-renewal ability and therefore regenerative capacity of salivary gland-derived cells. Furthermore, it was shown that the levels of LC3, p62 and ATG16L1, all of which reflect autophagic activity, remain constantly low in the acinar compartment before and after injury, while they significantly increase in the normally quiescent ductal compartment in response to injury. Based on the expression of surface markers, stem-like cells ($CD24^{hi}/CD29^{hi}$) and a progenitor-like cell population ($CD24^{med/hi}/CD29^{med/hi}$) that reside in the ductal compartment were isolated and their basal autophagy activities were compared. Interestingly, the stem-like cell population showed a low autophagic flux compared to progenitor-like cells, reflecting the difference in the basal

autophagic activity of these cells *in vivo* as well as their potentially different roles during homeostasis and regeneration.

In Chapter 6, the potential mechanisms that could drive cell fate specification during human salivary gland regeneration were investigated. Using submandibular salivary gland-derived organoids as a model for regeneration and an unbiased molecular network-based analysis approach, gene activity patterns, which indicate differential cell states, were identified. Gene co-expression analysis revealed that passage 1 (P1) salivary gland-derived organoids are characterized by a transcriptomic profile that closely resembles the SOX2-driven acinar development responsible for homeostasis maintenance in the mouse sublingual gland. This transcriptomic profile is downregulated in human salivary gland-derived organoids enriched for stem cells by treatment with the GSK3 inhibitor and Wnt pathway activator, CHIR, and the histone deacetylase inhibitor, valproic acid. The co-expression gene pattern of these enriched organoids points towards the integration of several biological pathways to maintain a proliferative, non-differentiated phenotype resembling a potentially more pluripotent cell-like state. Interestingly, the high expression of peroxisome proliferator activated receptor δ (PPARδ), a nutrient sensor and enzyme involved in lipid metabolism and fatty acid oxidation (FAO), indicate a potential role for a PPARδ-driven FAO program in the formation of organoids. This was emphasised by an increased organoid forming efficiency of human salivary gland-derived cells with PPARδ overexpression. Finally, when looking at the pathways and genes active during long-term culture, it was revealed that maintenance of salivary gland organoids could be dependent on integrin levels and potentially on the activation of the *ITGA3-SRC-RAC2* axis leading to a LATS1/2-independent YAP-activation program. This gene expression pattern could be responsible for the transition from a stem-like cell state (P1) to a more proliferative transient amplifying (TA)-like state (P2-P4). The expression of the fatty acid elongase ELOVL1 in adult human salivary gland biopsies could confirm a role of metabolic pathways in salivary gland organoid self-renewal, a hypothesis which is strengthened by an increased organoid formation efficiency upon overexpression of ELOVL1. The transcriptomic information gained in this chapter will allow for the exploration and understanding of new biological mechanisms potentially involved in maintaining the balance between tissue homeostasis and regeneration in adult salivary gland.

In Chapter 7, the development of a good manufacturing practice (GMP)-compliant protocol for the isolation and the expansion of human-derived salivary gland organoids is described. This protocol is potentially suitable for an autologous cell-based therapy to regenerate the lost functionality of the tissue after radiotherapy. The proposed GMP-compliant protocol allows for the isolation and the expansion of human salivary gland-derived cells from patient biopsies maintaining an efficiency that is comparable to the current non-GMP research-based protocol. The viability and the maintained commitment towards salivary gland function displayed by the cells after cryopreservation allows this procedure to be adapted to the patient's radiotherapy treatment schedule. Finally, the cells obtained are genetically stable and displayed encouraging results when transplanted into a murine *in vivo* regenerative model for salivary gland. By placing our newly developed protocol in the context of currently available treatment options for radiation-induced hyposalivation, the strengths, limitations, and future challenges of such an approach are highlighted.

DISCUSSION AND FUTURE PERSPECTIVES

Despite the recent progress in the salivary gland regeneration field, there is still little known about the processes regulating tissue homeostasis and regeneration. The work described in this thesis focused on two main aspects. Firstly, we aimed to bridge the gap in knowledge of regenerative processes gained recently with the use of both *in vivo* and *in vitro* mouse, and human *in vitro* models. We explored the potential of human salivary gland organoids as a model of regeneration and provide future perspectives that could help the design and development of new organoid-based experimental approaches. Secondly, we aimed to utilize the human salivary gland-derived organoid system to develop a GMP-compliant protocol with the goal of taking the research from "bench to the bedside" and open up to new cell-based therapies for the long-term treatment of radiation-induced hyposalivation. Furthermore, we examined the advances made, and consider potential future developments in the field.

Modelling salivary gland regeneration using organoids

In the salivary glands, as well as other adult tissues, homeostasis is the result of a tightly controlled signalling process that maintains the balance between proliferation and differentiation. Decades of research in embryonic salivary gland development, as well as the development of genetic lineage-tracing models, have set a basis to explore homeostasis and regenerative processes in adult salivary glands. The emerging model for salivary gland maintenance, discussed in Chapter 2, is that salivary glands rely on lineage-restricted progenitor cells for homeostatic-renewal while showing an intrinsic degree of plasticity upon damage that confers a temporary stem-like state to mature differentiated and post-mitotic cells. The stemness of salivary gland cells therefore appears to be a bidirectional dynamic cell state[1,2] that is imposed on cells by the microenvironment where the cells reside through a spatial and temporal regulation[3]. This intrinsic plasticity of salivary gland cells can be recapitulated *in vitro* when exogenous Wnt and R-spondin signalling are provided (Chapter 3). The ability of Wnt-responsive cells to generate asymmetric, self-organized 3D structures (known as organoids) containing all salivary gland cell lineages (Chapter 3) recapitulates the self-organization and branching morphogenesis of salivary gland epithelial cells[4]. This *in vitro* behaviour indicates a context-dependent functionality of salivary gland-derived cells that can potentially be adopted in response to changes within the microenvironment to fulfil regenerative purposes. It appears therefore that, similar to

what has been shown for intestinal organoids, salivary gland-derived organoid formation recapitulates a cycle of repair and homeostasis typical of the regeneration process[5,6] and therefore can be used to model salivary gland regeneration. While the derivation of certain organoids (such as those derived from pluripotent stem cells) relies uniquely on endogenous signalling, it is demonstrated in Chapter 3 that salivary gland-derived organoids require specific exogenous signals from the niche to drive a first cell expansion phase. This is then followed by a second self-patterning and morphogenetic rearrangement phase that leads to the final organoid architecture, similar to what has been shown in intestinal organoids[7]. While it is shown that Wnt stimulation is fundamental to orchestrate the generation of "mature", self-organized organoids, it is established in Chapter 4 that the activation of nuclear YAP rather than Wnt seems to be the signal required to drive the first phase in both salivary gland regeneration response upon injury *in vivo* and salivary gland-derived organoid formation. Sensing morphogens (such as Wnt) and tissue integrity via cellular mechanosensors (such as YAP) are two of the many ways a cell can sense the microenvironment. In the last decade, a growing body of evidence has highlighted how the central dogma of molecular biology, from DNA to protein, has evolved and how cell metabolism, before thought to be a passive player, has gained a central role in regulating cell fate decision[6,8,9]. The results obtained in Chapter 5 and Chapter 6, shed light on the importance of "metabolic reprogramming" and the energy substrates provided by the environment, such as fatty acids and long chain fatty acids, in regulating salivary gland-derived cell self-renewal ability (Chapter 6). This, together with the role of the autophagy pathway described in Chapter 5, highlights the importance of metabolic plasticity, as well as catabolic processes, in choosing and maintaining the appropriate metabolite levels to support the bioenergetic needs required by specific cells, such as those able to exert plasticity to respond to changes in homeostasis.

While the "deconstructive approach" taken in Chapters 3, 4 and 5 aimed at dissecting the niche signalling has led to the recognition of Wnt, YAP and autophagy as important key players during the regeneration process and potential targets for regenerative-based therapy, individual elements of a much bigger picture were studied in isolation. Starting from the assumption of Aristotle that "the whole is greater than the sum of its parts", the complexity of the salivary gland regenerative process itself cannot be completely explained by the sum of each single pathway without taking into

consideration the possible interplay between them, as well as the cell variability generated through cell collective behaviour (cell-cell interactions and feedback loops). The cellular state enrichment approach, combined with a co-expression gene analysis described in Chapter 6, moves towards this direction: understanding the system as a whole instead of reporting a list of individual parts, providing an unbiased, broad overview of the complexity of the regulatory network responsible for human salivary gland organoid formation and expansion. Chapter 6 shows how exposure to different environments (different morphogens in this case) increases the propensity of a cell towards a specific organoid state. This indicates that the initial conditions, in terms of morphogens, extrinsic physical cues and metabolic flux, to which the single cells are subjected affect the final characteristics of the organoids and, as a direct consequence, their range of applicability. The multicellular dynamics interaction which governs salivary gland regeneration processes is perhaps "the elephant in the room". Therefore, how can the transient spatiotemporal activation of these factors, which cells sense and dynamically respond to in order to orchestrate the regenerative response, be mapped? Considering the interplay between YAP with Wnt and YAP and autophagy[10], can YAP therefore be the hub for integration of other signalling pathways within the salivary gland regeneration process and thus responsible for the switch between the regenerative and homeostatic state?

To answer these questions an approach similar to the one recently taken in intestinal organoids[5,6] and new born skin organoids[11] could pave the way to unravel the molecular mechanisms and the morphological dynamics of salivary gland organoid formation and potentially open up new regenerative strategies. Using technologies that allow resolution of the transcriptome (single cell sequencing) and the proteome (image-based technology) at a single cell level and taking advantage of computational modelling to integrate spatiotemporal information of cells within its "society" will allow researchers to unravel cell-fate decisions of salivary gland cells and the pathways by which they are specified. Finally, it would be interesting to validate if the knowledge gained from the proposed approach could be used to manipulate the *in vivo* phases of salivary gland tissue regeneration, as well as to answer the remaining unanswered questions in the salivary gland field. What are the sources of the morphogens required for epithelial tissue maintenance and their plasticity activation upon (radiation-induced) injury? Can we extend the concept of plasticity to the salivary gland niche? Or is it the loss of niche plasticity upon damage that impedes (or drastically reduces) the

activation of mechanisms responsible in guiding epithelial plasticity and therefore affect regeneration?

While the time may be ripe for the salivary gland (organoids) field to embrace this approach, some challenging points remain. 1) The scarcity of reliable landmark genes that identify specific cell types within salivary gland-derived organoids will potentially pose an issue in mapping single cell RNA sequencing (scRNAseq)-derived transcriptomic data onto spatial reference maps[12].This step is fundamental to maintain the spatial context of the single cells in terms of local environment and cell-to-cell interactions, that otherwise would be lost considering that scRNAseq approaches require the dissociation of organoids to single cells. Combining scRNAseq with laser microdissection[13] or the use of photoactivable reporter in combination with scRNAseq[14] could potentially allow the identification of a salivary gland landmark gene landscape. Once obtained, the use of multiplex cell approaches that combine scRNAseq data with sequential high-throughput imaging techniques and segmentation algorithm, will allow an understanding of how gene expression and the subcellular distribution of the proteome are responsible for cell fate determination[6,15,16]. 2) The phenotypic variability of salivary gland organoid culture could pose an issue in terms of reproducibility of spatial organization of landmark genes. 3) Beside the transcriptome, proteome and metabolome, there is increased evidence highlighting how perturbation of the microenvironment can lead to changes at the chromatin level and how these changes could be responsible for the transcriptomic switches that determine cell fate decisions[9]. Therefore, epigenetic marks, such as DNA methylation or histone modifications, should be traced through space and time, and integrated within the multiscale approach. 4) While organoids have already reached a certain degree of complexity, both in terms of cell heterogeneity and spatial self-organization, when compared to the complex macro physiology of their tissue counterparts, they lack important aspects such as a vasculature system, a parasympathetic nervous system and an immune system. Recent advances have enabled the vascularisation of liver[17] organoids, which improved their maturation and graft survival upon transplantation. Furthermore, the co-culturing of organoids with immune cells possessing the potential to recapitulate the tumour immune microenvironment has opened up new avenues for immuno-oncology and auto-immune disease research[18]. However, the degree of complexity of

the organoid system should be chosen and weighted based on the research question at hand.

Resolving the salivary gland organoid formation process and its spatiotemporal dynamics as a whole will offer unprecedented opportunities to map the regeneration process and potentially establish a blueprint for targeted control of cell fate. Can we find a “switch point” within the self-organization process that can be targeted, or stabilized to increase the regeneration potential? In this way, we could use intrinsic cellular properties to develop drugs that will not be targeting a single specific gene, but rather complex multicellular processes, such as self-organization as a means that leads to a specific cellular state and not to a cell type.

Salivary gland regeneration: the road ahead

As the population rapidly ages, the natural decay of tissues and organs together with an increased propensity for infection and cancer have placed the need for developing regenerative medicine strategies as high priority. Head and neck cancers affect worldwide 500,000 patients annually, with 40% of the patients receiving radiation treatment facing “the challenges of living beyond”: the consequences of the radiotherapy treatment and the chronic and progressive decline of salivary gland function, ultimately leading to the onset of xerostomia[19]. Despite increased investments in cell-based preclinical research and clinical trials for xerostomia treatment, the number of proven therapies is relatively small (7%)[20].

Clinical trials for salivary gland regenerative therapies, based on the replacement of lost epithelial tissue with exogenous cells may need to consider three main points: 1) a large-scale production of salivary gland committed cells, 2) a strategy to increase the survival and the engraftment of the transplanted cells, and 3) a means to induce proliferation of transplanted cells *in vivo*. In Chapter 7, we have described the potential of a GMP-compliant protocol for the isolation and the expansion of human salivary gland organoid-derived cells to be used in the treatment of radiation-induced hyposalivation. Heterologous transplantation of human salivary gland organoid-derived cells has proven the potential, safety, and beneficial effect of this approach in *in vivo* pre-clinical studies providing significant rescue of saliva production compared to irradiated non-transplanted control animals[21]. The preserved functionality and the commitment towards salivary gland mature lineage of cryopreserved human salivary gland-derived cells, as well as their genetic stability, make the proposed GMP-compliant protocol a suitable, and currently unique, autologous organoid-based

treatment for xerostomia. Currently among internationally registered clinical trials there are none which focus on the potential of adult salivary gland tissue-resident stem cells. The formulation of a robust mechanistic hypothesis (such as cell replacement and/or paracrine effects of the transplanted cells) and the selection of the most appropriate cell source are only the first two major steps to ensure the success of future clinical trials of salivary gland cell-based regenerative therapies. The first one strongly influencing the second one and therefore the design of the trial itself.

Establishing well-defined standards for *ex vivo* processing that guarantee the quality, reproducibility, and potency of the cell source, required for international regulation and implementation[22] is essential for any proposed cell-based regenerative therapy. In Chapter 2, we have documented the growing evidence that plasticity mechanisms, rather than a single defined cell entity, are potentially responsible for salivary gland renewal. Therefore, instead of looking for potential predictive stem cell surface markers as identifier for salivary gland stem-like cells, we should look at the response patterns that characterize the newly acquired stem-like cell state (or regenerative state), and which are thus able to drive at first a regenerative response and subsequently reinstating tissue homeostasis[5,6]. The transcriptomic approach conducted in Chapter 6 suggests that cells giving rise to P1 organoids could possess these characteristics and therefore could be used as potential cell source for the Phase I/II clinical trial planned to be performed at the University Medical Center Groningen (UMCG). In this way the source of cells for clinical application could be chosen based on their therapeutic (or regenerative) potential rather than on a single characteristic, such as the presence of a surface marker. A surface marker-based selection could lead to “false positives and false negatives” in the identification of optimal cell source candidates since different cells within the tissue with diverse potentials could present the same surface markers.

Besides understanding the signals which regulate cell fate specification to allow for the selection and expansion of the optimal cell source for transplantation, it is also necessary to understand how radiation can affect the recipient tissue. An increased understanding of how the recipient environment is altered upon injury could have an impact on the success of any transplantation, both in terms of promoting endogenous cell repair and efficient engraftment of transplanted cells. Cellular senescence has recently been suggested as a contributor to the development of radiation-induced hyposalivation[23], as well as an early feature of primary Sjogren’s syndrome[24], an

autoimmune disease that causes dry mouth. It remains unclear as to whether cellular senescence is the driver of the pathology or solely a consequence of radiation-induced DNA damage. However, the presence of senescent cells within the acinar[23] and ductal compartments[24,25], as well as their SASP expression profile, could be responsible for the deterioration of the microenvironment[26] also in irradiated salivary glands. This, in turn, could potentially not only lead to an impaired endogenous regeneration response of salivary glands, but also create a hostile microenvironment for the engraftment and proliferation of transplanted cells. Recently, studies on aged mouse models showed that the genetic and pharmacological removal of senescent cells significantly improved the age-related phenotype[27] and mitigated the radiation-induced senescent phenotype in hematopoietic stem cells[28] and in salivary glands[25] . Thus, there is increasing numbers of early phase clinical trials addressing safety, target engagement and efficacy of senolytics in disease treatment. Furthermore, the improved secretory functionality of irradiated glands upon senolytic treatment[25] could open up to the use of senolytics

as a “priming” (or preconditioning) strategy to improve the engraftment potential of transplanted cells and consequent repopulation of the salivary gland epithelium. Moreover, the evidence showing that YAP functions as a sensor of salivary gland tissue integrity *in vivo* and promotes the initiation of a regenerative response similar to what has been described in intestinal organoids, reported in Chapter 4[6], may provide new potential targets within the Hippo signaling cascade to promote proliferation of transplanted cells.

At the point of diagnosis and treatment, head and neck cancer patients are often of a progressed age and thus may already exhibit underlying xerostomia due to age-related microenvironmental changes. The additive effect of age-induced xerostomia and radiation-induced xerostomia could further inhibit the repair ability of salivary gland. While the success of mouse transplantation of salivary gland organoid-derived cells from young donors into young recipients (described in Chapter 3) is relevant as a proof of principle and emphasizes the potential of such an approach, the age of patients necessitates proof of successful applicability in aged mouse models. Transplantation of salivary gland organoid-derived cells from old mice into young recipient mice showed that the young microenvironment, although injured, sustained the engraftment and proliferation of old-transplanted salivary gland-derived cells[29]. Future experiments should include transplantation of patient-derived cells into aged

irradiated salivary glands in order to highlight potential differences, pitfall and variables in response to transplantation that could be crucial for the development and the improvement of new cell-based regenerative strategies for older patients.

The bench-to-bedside approach proposed here will benefit from a combined reverse translational research approach (bedside-to-bench approach). Currently the primary endpoints to describe/quantify the success of transplanted salivary gland-derived cells in treating radiation-induced hyposalivation include increased saliva production. The post-mortem analysis of the transplanted gland via scRNA seq could be used to identify predictive markers of successful graft outcome. Such markers and the involved cues could be used to improve the *in vitro* generation and selection of salivary gland-derived organoids with an increased capacity for engraftment, which subsequently could increase the efficiency of the transplant and the success of a clinical trial. Furthermore, the use of imaging technique such as magnetic resonance imaging (MRI) or positron emission tomography/computed tomography (PET/CT) to map the irradiated gland in combination with labelling and tracing of transplanted cells, for example with superparamagnetic iron oxide nanoparticles[30,31] or prostate specific membrane antigen ligand[32,33], could help to monitor in real time the behavior of the transplanted cells. The identification of a migratory path, as well as a homing preference, of the transplanted cells could be a unique opportunity to detect a receptive niche within the irradiated gland that may be better suitable for the transplanted cells. The characterization of the molecular signature of these regions could pave the way to the discovery of biomarkers that could be used to predict the responsiveness of the tissue and therefore the patient transplantation outcome. It should be kept in mind that perhaps the presence of transplanted cells itself could not be enough to produce a functional therapeutic outcome, but that a receptive environment should also be present.

While the GMP protocol, developed in Chapter 7, will be used to test the safety and feasibility of salivary gland organoid-derived cells in a clinical setting, it is necessary to keep in mind that other mechanistic hypotheses beyond long-term cell replacement, such as the recently suggested paracrine effect of transplanted salivary gland-derived cells[21,34,35] could be (co)-responsible for tissue regeneration. This hypothesis will lead to new potential therapeutic approaches and to clinical trials aimed at leveraging the effect of exogenously supplied cells to initiate the activation of endogenous regeneration responses of surviving cells (if still present) that will ultimately lead to

improved functionality of the tissue. Consequently, different standards for the characterization of the cell source should be considered. In contrast to the selection of cells for long-term replacement strategies based on the self-renewal and the regenerative cellular state that support appropriate cell fate decisions, the focus of choosing cells for paracrine stimulation should be based on the secretory profiles of the cells. Therefore, characterization of the secretome of human salivary gland organoids by stable isotope-labeling with amino acids in cell culture-coupled mass spectrometry (SILAC-MS) would potentially provide insights in the secreted factors that are likely to contribute to the regeneration process and organoid formation. Furthermore, the targets of the secreted factors should be considered. Are the secreted factors targeted towards epithelial cells or other components of the salivary gland niche? Do they contribute to the induction of intrinsic cell plasticity of salivary gland epithelial cells or are they acting on the reactivation of the receptive niche?

We could therefore speculate that the “best” therapeutic options to rescue radiation-induced hyposalivation would be a combination of priming strategies to allow better engraftment, transplantation of cells with regenerative properties for long term tissue replacement and transplantation of cells with paracrine stimulatory functions that could support both the endogenous receptive niche and the transplanted cells for an enhanced and prolonged regeneration and subsequent functionality.

REFERENCES

1 Ninche, N., Kwak, M. & Ghazizadeh, S. Diverse epithelial cell populations contribute to the regeneration of secretory units in injured salivary glands. *Development* **147**, doi:10.1242/dev.192807 (2020).

2 Weng, P. L., Aure, M. H., Maruyama, T. & Ovitt, C. E. Limited Regeneration of Adult Salivary Glands after Severe Injury Involves Cellular Plasticity. *Cell Rep* **24**, 1464-1470 e1463, doi:10.1016/j.celrep.2018.07.016 (2018).

3 Chacon-Martinez, C. A., Koester, J. & Wickstrom, S. A. Signaling in the stem cell niche: regulating cell fate, function and plasticity. *Development* **145**, doi:10.1242/dev.165399 (2018).

4 Wei, C., Larsen, M., Hoffman, M. P. & Yamada, K. M. Self-organization and branching morphogenesis of primary salivary epithelial cells. *Tissue Eng* **13**, 721-735, doi:10.1089/ten.2006.0123 (2007).

5 Lukonin, I., Serra, D., Challet Meylan, L., Volkmann, K., Baaten, J., Zhao, R. *et al.* Phenotypic landscape of intestinal organoid regeneration. *Nature* **586**, 275-280, doi:10.1038/s41586-020-2776-9 (2020).

6 Serra, D., Mayr, U., Boni, A., Lukonin, I., Rempfler, M., Challet Meylan, L. *et al.* Self-organization and symmetry breaking in intestinal organoid development. *Nature* **569**, 66-72, doi:10.1038/s41586-019-1146-y (2019).

7 Sasai, Y. Cytosystems dynamics in self-organization of tissue architecture. *Nature* **493**, 318-326, doi:10.1038/nature11859 (2013).

8 Ito, K., Carracedo, A., Weiss, D., Arai, F., Ala, U., Avigan, D. E. *et al.* A PML-PPAR-delta pathway for fatty acid oxidation regulates hematopoietic stem cell maintenance. *Nat Med* **18**, 1350-1358, doi:10.1038/nm.2882 (2012).

9 Ly, C. H., Lynch, G. S. & Ryall, J. G. A Metabolic Roadmap for Somatic Stem Cell Fate. *Cell Metab* **31**, 1052-1067, doi:10.1016/j.cmet.2020.04.022 (2020).

10 Totaro, A., Zhuang, Q., Panciera, T., Battilana, G., Azzolin, L., Brumana, G. *et al.* Cell phenotypic plasticity requires autophagic flux driven by YAP/TAZ mechanotransduction. *Proc Natl Acad Sci U S A* **116**, 17848-17857, doi:10.1073/pnas.1908228116 (2019).

11 Lei, M., Schumacher, L. J., Lai, Y. C., Juan, W. T., Yeh, C. Y., Wu, P. *et al.* Self-organization process in newborn skin organoid formation inspires strategy to restore hair regeneration of adult cells. *Proc Natl Acad Sci U S A* **114**, E7101-E7110, doi:10.1073/pnas.1700475114 (2017).

12 Mayr, U., Serra, D. & Liberali, P. Exploring single cells in space and time during tissue development, homeostasis and regeneration. *Development* **146**, doi:10.1242/dev.176727 (2019).

13 Moor, A. E., Harnik, Y., Ben-Moshe, S., Massasa, E. E., Rozenberg, M., Eilam, R. *et al.* Spatial Reconstruction of Single Enterocytes Uncovers Broad Zonation along the Intestinal Villus Axis. *Cell* **175**, 1156-1167 e1115, doi:10.1016/j.cell.2018.08.063 (2018).

14 Medaglia, C., Giladi, A., Stoler-Barak, L., De Giovanni, M., Salame, T. M., Biram, A. *et al.* Spatial reconstruction of immune niches by combining photoactivatable reporters and scRNA-seq. *Science* **358**, 1622-1626, doi:10.1126/science.aao4277 (2017).

15 Gut, G., Herrmann, M. D. & Pelkmans, L. Multiplexed protein maps link subcellular organization to cellular states. *Science* **361**, doi:10.1126/science.aar7042 (2018).

16 Zhu, Q., Shah, S., Dries, R., Cai, L. & Yuan, G. C. Identification of spatially associated subpopulations by combining scRNAseq and sequential fluorescence in situ hybridization data. *Nat Biotechnol*, doi:10.1038/nbt.4260 (2018).
17 Takebe, T., Sekine, K., Enomura, M., Koike, H., Kimura, M., Ogaeri, T. *et al.* Vascularized and functional human liver from an iPSC-derived organ bud transplant. *Nature* **499**, 481-484, doi:10.1038/nature12271 (2013).
18 Yuki, K., Cheng, N., Nakano, M. & Kuo, C. J. Organoid Models of Tumor Immunology. *Trends Immunol* **41**, 652-664, doi:10.1016/j.it.2020.06.010 (2020).
19 Tsai, W. L., Huang, T. L., Liao, K. C., Chuang, H. C., Lin, Y. T., Lee, T. F. *et al.* Impact of late toxicities on quality of life for survivors of nasopharyngeal carcinoma. *BMC Cancer* **14**, 856, doi:10.1186/1471-2407-14-856 (2014).
20 Rocchi, C. & Emmerson, E. Mouth-Watering Results: Clinical Need, Current Approaches, and Future Directions for Salivary Gland Regeneration. *Trends Mol Med* **26**, 649-669, doi:10.1016/j.molmed.2020.03.009 (2020).
21 Pringle, S., Maimets, M., van der Zwaag, M., Stokman, M. A., van Gosliga, D., Zwart, E. *et al.* Human Salivary Gland Stem Cells Functionally Restore Radiation Damaged Salivary Glands. *Stem Cells* **34**, 640-652, doi:10.1002/stem.2278 (2016).
22 Pellegrini, G., Rama, P., Matuska, S., Lambiase, A., Bonini, S., Pocobelli, A. *et al.* Biological parameters determining the clinical outcome of autologous cultures of limbal stem cells. *Regen Med* **8**, 553-567, doi:10.2217/rme.13.43 (2013).
23 Marmary, Y., Adar, R., Gaska, S., Wygoda, A., Maly, A., Cohen, J. *et al.* Radiation-Induced Loss of Salivary Gland Function Is Driven by Cellular Senescence and Prevented by IL6 Modulation. *Cancer Res* **76**, 1170-1180, doi:10.1158/0008-5472.CAN-15-1671 (2016).
24 Wang, X., Bootsma, H., Terpstra, J., Vissink, A., van der Vegt, B., Spijkervet, F. K. L. *et al.* Progenitor cell niche senescence reflects pathology of the parotid salivary gland in primary Sjogren's syndrome. *Rheumatology (Oxford)* **59**, 3003-3013, doi:10.1093/rheumatology/keaa012 (2020).
25 Peng, X., Wu, Y., Brouwer, U., van Vliet, T., Wang, B., Demaria, M. *et al.* Cellular senescence contributes to radiation-induced hyposalivation by affecting the stem/progenitor cell niche. *Cell Death Dis* **11**, 854, doi:10.1038/s41419-020-03074-9 (2020).
26 Ferreira-Gonzalez, S., Lu, W. Y., Raven, A., Dwyer, B., Man, T. Y., O'Duibhir, E. *et al.* Paracrine cellular senescence exacerbates biliary injury and impairs regeneration. *Nat Commun* **9**, 1020, doi:10.1038/s41467-018-03299-5 (2018).
27 Xu, M., Pirtskhalava, T., Farr, J. N., Weigand, B. M., Palmer, A. K., Weivoda, M. M. *et al.* Senolytics improve physical function and increase lifespan in old age. *Nat Med* **24**, 1246-1256, doi:10.1038/s41591-018-0092-9 (2018).
28 Chang, J., Wang, Y., Shao, L., Laberge, R. M., Demaria, M., Campisi, J. *et al.* Clearance of senescent cells by ABT263 rejuvenates aged hematopoietic stem cells in mice. *Nat Med* **22**, 78-83, doi:10.1038/nm.4010 (2016).
29 Maimets, M., Rocchi, C., Bron, R., Pringle, S., Kuipers, J., Giepmans, B. N. *et al.* Long-Term In Vitro Expansion of Salivary Gland Stem Cells Driven by Wnt Signals. *Stem Cell Reports* **6**, 150-162, doi:10.1016/j.stemcr.2015.11.009 (2016).
30 de Vries, I. J., Lesterhuis, W. J., Barentsz, J. O., Verdijk, P., van Krieken, J. H., Boerman, O. C. *et al.* Magnetic resonance tracking of dendritic cells in melanoma

patients for monitoring of cellular therapy. *Nat Biotechnol* **23**, 1407-1413, doi:10.1038/nbt1154 (2005).
31 Hartman, R. E., Nathan, N. H., Ghosh, N., Pernia, C. D., Law, J., Nuryyev, R. *et al.* A Biomarker for Predicting Responsiveness to Stem Cell Therapy Based on Mechanism-of-Action: Evidence from Cerebral Injury. *Cell Rep* **31**, 107622, doi:10.1016/j.celrep.2020.107622 (2020).
32 Klein Nulent, T. J. W., Valstar, M. H., de Keizer, B., Willems, S. M., Smit, L. A., Al-Mamgani, A. *et al.* Physiologic distribution of PSMA-ligand in salivary glands and seromucous glands of the head and neck on PET/CT. *Oral Surg Oral Med Oral Pathol Oral Radiol* **125**, 478-486, doi:10.1016/j.oooo.2018.01.011 (2018).
33 Valstar, M. H., de Bakker, B. S., Steenbakkers, R., de Jong, K. H., Smit, L. A., Klein Nulent, T. J. W. *et al.* The tubarial salivary glands: A potential new organ at risk for radiotherapy. *Radiother Oncol*, doi:10.1016/j.radonc.2020.09.034 (2020).
34 Gronhoj, C., Jensen, D. H., Glovinski, P. V., Jensen, S. B., Bardow, A., Oliveri, R. S. *et al.* First-in-man mesenchymal stem cells for radiation-induced xerostomia (MESRIX): study protocol for a randomized controlled trial. *Trials* **18**, 108, doi:10.1186/s13063-017-1856-0 (2017).
35 Gronhoj, C., Jensen, D. H., Vester-Glowinski, P., Jensen, S. B., Bardow, A., Oliveri, R. S. *et al.* Safety and Efficacy of Mesenchymal Stem Cells for Radiation-Induced Xerostomia: A Randomized, Placebo-Controlled Phase 1/2 Trial (MESRIX). *Int J Radiat Oncol Biol Phys* **101**, 581-592, doi:10.1016/j.ijrobp.2018.02.034 (2018).

CHAPTER 9

APPENDICES

Nederlandse Samenvatting

Disfunctie van de speekselklieren en de daarmee gepaard gaande onomkeerbare afname van de speekselproductie (hyposalivatie) kan leiden tot het droge mondsyndroom (Xerostomie). Xerostomie kan veroorzaakt worden door straling geïnduceerde hyposalivatie, zoals kan optreden bij patiënten met hoofd-halskanker na radiotherapie. Wanneer de speekselklieren tijdens radiotherapie in het bestraalde gebied liggen kan dit leiden tot verstoring van de micro-omgeving, de cellulaire niche, van de in het weefsel aanwezige speekselklier cellen. Een verlies van balans tussen cel verlies en cel vorming (homeostase) kan vervolgens leiden tot een progressieve en onomkeerbare achteruitgang van het aantal acinaire voorlopercellen. Dit resulteerd vervolgens in een afname van acinair weefsel dat verantwoordelijk is voor de productie met hyposalivatie als gevolg. Hoewel xerostomie op zich geen levensbedreigende aandoening is, zullen van de 500.000 patiënten bij wie elk jaar hoofd-halskanker wordt vastgesteld en die met moderne radiotherapie behandeld worden, 40% een ernstige vermindering van hun kwaliteit van leven ervaren.

In de afgelopen twee decennia is er veel onderzoek gedaan naar de ontwikkeling van middelen om xerostomie te behandelen. De huidige beschikbare, door de Amerikaanse “Food and Drug Administration (FDA)” goedgekeurde, klinische strategieën zorgen echter alleen voor een tijdelijke verlichting van de ongemakken veroorzaakt door aan xerostomie gerelateerde symptomen. Er zijn dus compleet nieuwe benaderingen, zoals die afgeleid van regeneratieve geneeskunde, nodig om deze aandoening afdoende te behandelen. Het verkrijgen en verbeteren van inzichten in speekselklierbiologie, de mechanismen betrokken bij regeneratie en de mate waarin de volwassen speekselklieren kunnen regenereren, is daarom essentieel voor de ontwikkeling van nieuwe regeneratieve therapeutische strategieën gericht op een langdurig herstel van de beschadigde speekselklier.

Het is bekend dat de speekselklieren tot op zekere hoogte het vermogen behouden om te kunnen regenereren. Echter wordt de mogelijkheid om gebruik te maken van regeneratieve geneeskunde voor de behandeling van door straling beschadigde speekselklieren beperkt door het gebrek aan kennis over de identiteit van de betrokken cellen en signaalroutes die verantwoordelijk zijn voor regulatie van de weefselintegriteit van de speekselklieren.

Het werk in dit proefschrift beschreven laat zien dat pre-klinisch en klinisch onderzoek, gebruik makend van een diermodel voor stralingsschade aan de speekselklieren en muizen en humane speekselklier organoïden technologieën, gecombineerd kunnen worden om de cel types betrokken bij speekselklier homeostase en regeneratie na schade en de betrokken onderliggende regulatoren te identificeren.
Dit werk draagt daarom bij aan de ontwikkeling van potentiële klinisch relevante regeneratieve therapie om door straling geïnduceerde hyposalivatie te behandelen.

Hoofdstuk 2 beschrijft hoe de definitie van adulte stamcellen over de afgelopen 30 jaar veranderd is en hoe dit de manier waarop het behoudt van weefsel integriteit van de speekselklier onderzocht en begrepen wordt heeft beïnvloed heeft.
Het professionele dogma over stamcellen die gebaseerd is op het hematopoëtische stamcelsysteem wordt geïntroduceerd en vergeleken met de beschikbare gegevens over speekselklierstam en/of voorlopercellen, waarbij de toepasbaarheid van een dergelijk paradigma als sjabloon voor speekselklierbiologie (en andere snel delende weefsels) in twijfel getrokken wordt. Vervolgens wordt besproken welke speekselklier stamcelfuncties uitgevoerd kunnen worden door verschillende cellen onder verschillende omstandigheden, zoals tijdens homeostase of herstel van schade. Er wordt gespeculeerd dat wellicht niet een goed gedefinieerde zeldzame cel in rust zich aan de top van de hiërarchie bevindt, zoals in het hematopoëtische systeem, maar dat een dynamisch mechanisme van plasticiteit van cellen in het klierepitheel verantwoordelijk zou kunnen zijn voor de regeneratie van speekselklieren.

Verder wordt gesuggereerd dat om verloren of beschadigd weefsel te vervangen omgevingssignalen uit de niche een rol spelen bij een het induceren van een stamcelachtige functie van cellen tijdens regeneratie, in plaats van dat op het celoppervlak aanwezige fenotypische factoren bij specifieke cellen de stamcelfunctie bepalen. Tevens wordt er gespeculeerd over hoe het begrijpen van de tijdsafhankelijke cel-cel interactie dynamieken kunnen helpen bij het ontrafelen van signaal routes die betrokken zijn bij de regulatie van het lot van een cel tijdens speekselklier regeneratie en hoe een integratieve “multi-omic” benaderingen hierbij gebruikt kan worden. Ten slotte wordt besproken hoe de kennis verkregen met deze integratieve “multi-omic” aanpak mogelijkheden zou kunnen bieden om nieuwe

therapeutische strategieën voor door straling geïnduceerde hyposalivatie te ontwikkelen.

In **Hoofdstuk 3** wordt de Wnt-signaal route geïdentificeerd als een essentieel onderdeel van het complexe signaalnetwerk dat de integriteit van het speekselklierweefsel tijdens homeostase en regeneratie reguleert. Door het immunofluorescentie co-labelen van de algemene epitheliale cel marker EpCAM met de Wnt-reporter β-catenin op de speekselklier afvoergangcellen hebben we laten zien dat voornamelijk speekselklier afvoergangcellen (ducten) ontvankelijk zijn voor Wnt geïnduceerde activatie. Vervolgens werden EpCAM positieve cellen met behulp van "Fluorescent Activate Cell Sorting (FACS)" geïsoleerd en vervolgens gekweekt in Matrigel en een specifiek media aangevuld met Wnt3a en Rspo1, beide bekende stimulatoren van de Wnt-signaal route. Hieruit bleek dat alleen hoog positieve EpCAM cellen na kweken onder Wnt-stimulatie organoïden konden genereren die instaat waren om zichzelf langdurig te vernieuwen (zelfvernieuwing, een eigenschap van stamcellen die asymmetrisch delen in een nieuwe stamcel en in een vaak meer gedifferentieerde cel) en alle cel types van de speekselklier konden vormen. Toevoeging van remmers van de Wnt-signaal route aan het medium, leidde tot een sterke vermindering van de efficiëntie waarin organoïden gevormd werden. Dit resultaat bevestigt de belangrijke rol die van buiten toegevoegde Wnt speelt bij de vorming en in stand houden bij van speekselklier-afkomstige organoïden. Ten slotte werd aangetoond dat transplantatie van cellen verkregen uit deze door Wnt-aangedreven speekselklier organoïden, in muizen speekselklieren die lokaal bestaald waren, de door straling geïnduceerde hyposalivatie in grotere mate kon verminderen dan wanneer cellen gebruikt werden die afkomstig waren uit organoïden die gekweekt waren in medium zonder Wnt.

Vervolgens wordt in **Hoofdstuk 4** aangetoond dat de Hippo signaal route regulator YAP functioneert als een sensor van weefselintegriteit in reactie op speekselklierschade.
Na het toebrengen van schade aan de speekselklieren, door een gedeelte daarvan af te binden waardoor dit degenereert, worden normaal in rust zijnde ductale cellen geactiveerd via een door YAP aangedreven weefsel reactie. Deze reactie wordt gekenmerkt door hoge mate van translocatie van Yap van het cytoplasma naar de

celkern en een gerelateerde verhoogde proliferatie deze cellen in de nabijheid van de plek van schade. Dus het lijkt erop dat YAP activiteit in de celkern vereist is voor de aanzet tot regeneratie. Deze reactie op lokaal letsel suggereert ook dat gedifferentieerde epitheelcellen kunnen functioneren als een bron van stamachtige cellen ter regeneratie van het weefsel. Met behulp van het boven beschreven speekselklier organoïden kweeksysteem, werd vervolgens aangetoond dat moleculaire en genetische modulatie van translocatie van YAP naar de celkern invloed heeft op het vermogen tot zelfvernieuwing van zowel muis- als menselijke speekselkliercellen. Inderdaad leidde remming van deze nucleaire activiteit van YAP vervolgens tot een vermindering van de mate waarin organoïden gevormd werden, terwijl stimulatie van de nucleaire translocatie van YAP de efficiëntie van vorming van organoïden verhoogde en de tevens de lange termijn expansie (zelfvernieuwing) van de speekselklier afkomstige cellen bevorderde. Ten slotte werd gebruik makend van organoïden als model voor regeneratie, aangetoond dat farmacologische remming van Mst1/2-kinasen en de daaruit voortvloeiende activering van YAP-nucleaire activiteit, de regeneratieve respons van menselijke speekselkliercellen na bestraling significant verbeterde.

In **Hoofdstuk 5** wordt gerapporteerd dat autofagie een belangrijke rol speelt bij de zelfvernieuwing van organoïden van de speekselklier en dat de farmacologische manipulatie van autofagie in potentie weefselregeneratie kan bevorderen. Door organoïden te gebruiken als model voor regeneratie, werd gevonden dat een toename van de autofagie-flux binnen de stamcelachtige cel populatie het vermogen om secundaire en tertiaire organoïden te vormen reflecteert. Tevens werd aangetoond dat voor een dergelijk zelf vernieuwend vermogen van stamcellen een constante aanvoer van energie, gedreven door autofagie, vereist. Het remmen van zowel de vroege als late stappen in het autofagy proces en het uitschakelen van het autofagie-gerelateerde gen 5 (Atg5), leidde tot een significante vermindering van het zelf vernieuwingsvermogen en dus regeneratieve potentieel van speekselkliercellen. Verder werd aangetoond dat voor en na schade de niveaus van autofagische activiteit weerspiegelde eiwitten LC3, p62 en ATG16L1 allemaal constant laag blijven in gedifferentieerde acinaire cellen, terwijl deze juist significant toenemen in normaal in rust zijnde ductale, alwaar de stamcellen zouden zitten. Op basis van de expressie van cel oppervlakte markers werden in de afvoerkanaal aanwezige vermeende

stamcellen ($CD24^{hi}/CD29^{hi}$) en voorlopercellen ($CD24^{med/hi}/CD29^{med/hi}$) geïsoleerd en werd hun basale autofagie-activiteiten vergeleken. Het bleek dat $CD24^{hi}/CD29^{hi}$ cellen een lage autofagische flux vertoonde in vergelijking met $CD24^{med/hi}/CD29^{med/hi}$ cellen, hetgeen een reflectie is van het verschil in de basale autofagische activiteit van deze cellen *in vivo*, evenals de mogelijk verschillende rol die deze spelen tijdens homeostase en regeneratie.

In **Hoofdstuk 6** werden de mogelijke mechanismen onderzocht die de lotsbestemming van cellen tijdens regeneratie van de menselijke speekselklier zouden kunnen sturen. Met behulp van submandibulaire speekselklier organoïden als een model voor regeneratie en een onbevooroordeelde analyse gebaseerd op moleculaire netwerken, werden genexpressie patronen die gedifferentieerde cel stadia aangeven, geïdentificeerd. Gen co-expressie analyse onthulde dat vroege van speekselklier afkomstige organoïden gekenmerkt worden door een transcriptomisch profiel dat sterk lijkt op door SOX2 aangestuurde acinaire cel ontwikkeling. Acinaire cellen worden verantwoordelijk gehouden voor het onderhoud van de speekselklieren van de muis gedurende homeostase. Dit gen transcriptie profiel wordt echter negatief reguleert in van menselijke speekselklier afkomstige organoïden die zijn verrijkt met stamcellen door een behandeling met de GSK3-remmer en Wnt-pathway-activator, CHIR, en de histondeacetylase-remmer, valproïnezuur. Het gen co-expressie patroon van deze met stamcellen verrijkte organoïden wijst richting de integratie van verschillende biologische routes die erop sturen om een proliferatief, ongedifferentieerd fenotype te behouden die meer lijkt op het fenotype van een pluripotente cel. Interessant is dat er een hoge expressie van een nutriëntensensor en enzym dat betrokken is bij lipiden metabolisme en vetzuuroxidatie (FAO) “peroxisome proliferator activated receptor δ (PPARδ)” gevonden werd. Dit gen speelt mogelijke rol bij processen betrokken bij de vorming van organoïden hetgeen verder benadrukt wordt door de bevinding dat na overexpressie van het PPARδ gen er een verhoogde efficiëntie van menselijke speekselklier afkomstige organoïden vorming werd gevonden. Ten slotte, als we kijken naar de signaal routes en genen die actief zijn tijdens het langdurig kweken van speekselklier organoïden, zien we deze mogelijk afhankelijk zijn van integrine niveaus en mogelijk van de activering van de ITGA3-SRC-RAC2-signaal as die leidt tot een LATS1/2 onafhankelijke YAP-activering. Dit genexpressiepatroon zou

verantwoordelijk kunnen zijn voor de overgang van een stamcel achtige cel stadium bij vroege organoïden kweek naar een meer proliferatieve “transient amplifying” toestand van organoïden die we zien nadat ze meerdere keren gepasseerd zijn. De expressie van het vetzuur elongase ELOVL1 in biopsieën van volwassen menselijke speekselklieren bevestigd een mogelijke rol van metabole routes in de zelfvernieuwing van organoïden van de speekselklier. Deze hypothese die wordt versterkt door de waarneming dat overexpressie van ELOVL1 een verhoogde efficiëntie van organoïden vorming induceert. De informatie van gen transcriptie patronen die in dit hoofdstuk verkregen werd, zal helpen bij het onderzoeken en begrijpen van nieuwe biologische mechanismen die mogelijk betrokken zijn bij de handhaven van het evenwicht tussen weefselhomeostase en regeneratie in de volwassen speekselklier.

In **Hoofdstuk 7** wordt de ontwikkeling van een “good manufacturing practice” (GMP) -conform protocol voor de isolatie en expansie van menselijke speekselklier organoïden beschreven. Dit protocol zou geschikt kunnen zijn voor een autologe celtherapie ter herstel van de functionaliteit van de speekselklier na radiotherapie. Het voorgestelde GMP-conforme protocol maakt de isolatie en vermeerdering van patiënten speekselklier biopsieën afkomstige cellen met een vergelijkbare efficiëntie van huidige niet-GMP-onderzoeksprotocol mogelijk. Doordat de cellen na cryopreservatie levensvatbaar blijven en instaat zijn om speekselkliercellen te vormen die deelnemen aan de klierfunctie, kan deze procedure worden aangepast aan het radiotherapie behandelschema van de patiënt. Ten slotte blijken de verkregen cellen genetisch stabiel te zijn en vertoonden ze bemoedigende resultaten wanneer ze werden (xeno-)getransplanteerd in een muizen speekselklier regeneratie model. Door ons nieuw ontwikkelde protocol te vergelijken met de huidige beschikbare behandelingsopties voor door straling geïnduceerde hyposalivatie, kunnen de sterke punten, beperkingen en toekomstige uitdagingen van een dergelijke benadering bestudeerd worden.

Acknowledgements

Edinburgh, March 2021

Some might say it is about time! And indeed, it is. After many years in Groningen and after moving country this book is finally completed. It might be true that I have written the majority of this thesis being alone in front of my computer, but the truth is that it took a whole lot of people to shape it and complete it. A whole lot of people who have taught me, challenged me, inspired me, guided me, and cheered me up throughout my time in Groningen.

To **Rob**, who hired me knowing that I held a pipette for the first time only six months prior to meeting him, and who believed in me before I believed in myself. Thank you for guiding me throughout all these years, for giving me the opportunity to explore, to risk and to fail; for being brutally honest sometimes, and extremely comprehensive during a difficult moment in my life; for the many animated discussions, but most of all thank you for nurturing my love for science. Thank you to you and **Monicque** also for the nice lab bbqs and the many late beers drunk around the fire in good company. Trips back home by bike on those evenings were always an adventure.
To **Ronald,** thank you for all the input and the help you gave me during my PhD meetings throughout the years. Your knowledge in stem cells as well as your always positive and peaceful vibe were fundamental for my scientific growth and helped to "buffer" the animated discussions with Rob ☺.
To **Prof. Gerald de Haan** for having recommended me for the job that led to the completion of this thesis and for always being available for discussions, thank you.

To the reading committee, **Prof. Gerald de Haan, Prof. Cathrine Ovitt and Prof.Marcel Verheij,** for taking your time to read and correct my thesis. It was an honour to have you to approve my dissertation.

To **Greetje** and **Lies**, who were always ready to help with documents and emails and did a great job to patch up my not so perfect organization, thank you. If this thesis is here it is also because of you.

To **Prof. Arjan Vissink**, to the **oral and maxillofacial surgery teams at the UMCG and at the MCL**, **Monique**, **Nienke**, and **the Pharmacy department at the UMCG**, that made the “human salivary gland project” possible, thanks. And to **all the patients who participated in the studies**, who may never read this, this literally wouldn’t have been possible without you so thank you.

The work in this thesis would not have been possible without the core facilities at the UMCG. Thank you to **Klaas** from the imaging facility, for all the time spent in front of the SP8 with me; to **Geert, Hank, Roelof-Jan** and **Theo** from the FACS facility for all their help with sorters and analysers. To **Catriene, Miriam** and **Michelle**, from the CDP for their patience and help with CCD applications and animal experiments, thank you.

To all the people that made the 5th floor of the building 3215 a great, stimulating, inspiring and friendly environment to work in. To **Prof. Harrie Kampinga**, **Prof. Ody Sibon**, **Steven and Peter van Luijk, thanks** for your support and critical, yet constructive, discussion during meetings and for the great fun during lab days.
Hein, we met a long time ago, but only in the last few years I have gotten to know you and I am thankful for everything I learned from you, part of the job in this thesis would not have been successful without your help. **Nico,** thank you for teaching me the ABC of illustrating.

There is one office that I could never thank enough on the 5th floor and it’s the technicians’ office, or “the confessional”. For the many coffees (maybe too many), the laughs, the tears, the complaining after a bad day, that was always my favourite place. To the people who made that office **Marianne, Anne, Mirjam, Uilke, Jeanette, Pauline, Fleur, Maria, Ellie and Bart** thank you! To **Jeanette** for all your help, even now that I am away, for all the last-minute order requests and the “Jeanette hugs” when I was down (I could still use one of those sometimes). To **Mirjam, Anne** and **Uilke**, the three pillars of Rob’s group, without your work this thesis would not be here today. I will always be grateful for what you have taught me, for what you have done and what are still doing for me. The infinite number of hours spent in cell culture or collecting saliva would have been terribly slow without a good laugh.

To you, gone too soon, terribly missed but never forgotten, **Hette.** I wish I could say thank you knowing that we will be soon celebrating together. There is no staining I do without thinking of you and sometimes I can still hear you saying "DAUGH!!". I wish you could see that I am not fighting anymore with paraffine or cryo blocks, and you'll be happy to know that I didn't chase any more mice across the floor of the CDP room. Everything I know about staining and my confidence in working with animals is because you. To **Tekla**, whose energy and positive vibes are contagious, thank you for always be so thoughtful and caring, looking forward for a day at the famous beach house. To **Reinier,** to whom I will always be grateful for pointing out I was wearing two different boots and that became a really good friend. Looking forward to having you, **Maren** and the boys up here in Edinburgh.

I was lucky enough to have shared a big part of my PhD with a bunch of great people. **Despina, Yixian, Wonde (Mr. "It's OK"), Francesco, Matteo, Gabriel and Eduardo.** Thank you for all the take away dinner eaten in the kitchen of the 5th floor while waiting western blot or staining to be finished, for all the fun in and outside work. Our journey might have taken different paths, but I will cherish those moments forever. **Vaishali, Melanie, Anita, Roald, Yu Yi, Els, Niels, Suzanne, Wouter**, **Abhi, Daisy, Luc, Yi** and **Julie,** it was nice to share a part of my journey with you.

Thank you also to **Prof. Fulvio Reggiori** and his group for "adopting" me on the 7th floor during my virus work and introducing me to the autophagy world. **Mario, Pauline, Ralph and Yingying**, thank you for your help in the lab and for the many many many many beers drunk during the beer festival. To **Idil**, beside the many beers, I could not have asked for a better partner to deal with the joy and sorrows of the autophagy-salivary gland paper and with endless evening hours in an oversized fireman sweater waiting to go back to our experiment. It was great fun learning from and with you. Looking forward to seeing you again. To **Muriel,** that like me suffered from the endless grey season in Groningen and dreamed about the blue seas, you always had a smile, good advice and a word of encouragement for me, thank you.

I considered myself lucky to have started my journey in Rob's group with people that inspired me and guided me throughout the years. To **Yamini,** the first time my name was on a paper was thanks to you. To **Martti,** your determination and passion for

science and your drive to explore new techniques were an inspiration for me. Hope to meet you, **Sara** and the little ones somewhere soon. Thank you both for always being there. **Nynke,** for all the help in the lab and for all the fun outside work, looking forward to see you, **Jurjen** and the babies again.

To all the students I had the opportunity to supervise during my PhD thank you because I have learned something from each of you. **Margherita (Mago), Cinthya, Laura, Ijsbrand** and **Victor** thank you for all your work, I wish you all the best for your future careers.

Pao, Vivian, Danielle, and **Andries,** I will always remember our trip to Hilderbergh and the "highlight" of sharing a room with all of you. Thank you for making the office and the lab a nice place to work in. **Pao,** I miss our early morning "dates" every second Friday before the work in progress meetings. Sharing the office with you was great fun. Thank you for being not only a colleague, but also a great friend. **Davide**, we met only once (in person, at least) while I was leaving, but I want to thank you for the work done with the YAP revisions, I really appreciate it.

To **Elaine** for being a great role model, for giving me all the support needed in this new journey as a Post Doc in Edinburgh, thank you. To my new colleagues **John**, **Ella and Sonia** for have warmly welcoming me into the group. A special thanks to **John** and **Andrea** who, besides being good friends, always make sure to provide me with my daily intake of sugar and carbohydrates. To **Emily,** who draw the cover of this book and who's enthusiasm for putting science into art is contagious, thank you.

Then there are those people, that brought out the best of me and that kept reminding me why it's all worth it. To **Marianne**, because besides having taught me a lot in the lab, you have become a really good friend. Your honesty, loyalty and sense of humour were fundamentals to survive the ups and down of the PhD journey. One thing only: we need to work on your wine selection. To **Peter** that turned my world upside-down and yet it never felt more right. For all the missing "s" and "ed" that you had to correct in all these pages; for all the time I said "I can't" and you say "Yes you can", thank you. Without your help, your support and your love I could not have done it. To **Lara,** for the fresh air you brought to the lab, for your optimism and support during the meetings

and experiments, but most of all for choosing me as a friend and be always by my side. I wish we would have had more time to spend together in Groningen. To **Brian**, for making sure I would never forget again the capital of Canada and for being always ready to help. To **Sarah**, for guiding my first steps into my PhD, for always having my back and whose company it's never boring. To **Giulia,** with **Marten**, **Ale and Leo**, because beside me possibly swapping your cat and crashing your car against the only pole in an empty carpark you kept me as a friend, and my journey in Groningen would have not be the same without you. To **Caterina, Francesco** and my two favourite girls **Rosa** and **Sara,** for making me part of your crazy life, for sharing all the important moments with me, for the many lunches and dinners, but most of all for all your love and affection. I miss you a lot. To **Eloisa,** for being one of the greatest people I met in Groningen and by who's side I know it is possible to get out of any bad situation including being stuck with a car in a sand dune.

To **Annemieke**, **Kevin, Fred** and **John,** thank you for welcoming me with open arms into their family and showing me all their support in these years.

Alle mie amiche di sempre **Linda e Silvia,** perche' anche a distanza di anni e centinaia di kilometri ci sono sempre.

Alla mia **mamma** e al mio **papà** che durante tutti questi anni mi hanno supportato e sopportato; mi hanno ascoltato e capito anche quando per loro era tutto incomprensibile e che nonostante la distanza continuano a dimostrarmi il loro amore incondizionatamente, grazie. Questa tesi è dedicate a voi.

To **Nora,** that filled up a place in my heart I didn't know I had and that motivates me every day to be better than the day before, love you unconditionally.

Curriculum vitae

Cecilia Rocchi

Research experience

2019- to present	**Postdoctoral fellow** Laboratory of Dr. Elaine Emmerson, Institute for Regeneration and Repair, Center for Regenerative Medicine, Edinburgh, United Kingdom
2013-2019	**Doctoral candidate** Laboratory of Prof. Rob Coppes, Department of Biomedical Science and System, University Medical Centre Groningen, Groningen, the Netherlands
2012	**Intern** Under the supervision of Prof. F.Foijer at the European Research Institute for the Biology of Ageing (ERIBA), Groningen, the Netherlands.
2011-2012	**Erasmus exchange program** Under the supervision of Dr. P. Meerlo at the Department of Behavioral Physiology, University of Groningen (RUG), Groningen, the Netherlands

Education

2009-2012	**Master student** University of Parma, Parma, Italy
2004-2009	**Undergraduate student** University of Parma, Parma, Italy

Conference oral presentations

2015	3rd Annual PhD Student Meeting of the Cancer Research Centre Groningen, (Groningen, The Netherlands).
2017	Gordon Research Conference Salivary Gland and Exocrine Biology (Galveston, Texas, USA).
2017	10th Annual Meeting of the Dutch Society for Stem Cell Research (DSSCR) (Utrecht, The Netherlands).
2018	EMBO|EMBL Symposium: Organoids: Modelling Organ Development and Disease in 3D Culture (Heidelberg, Germany).
2018	6th Annual PhD Student Meeting of the Cancer Research Centre Groningen, (Groningen, The Netherlands).
2018	NVRB Annual fall meeting (Utrecht, The Netherland).
2020	IRR Early Career Innovator 2020 (Edinburgh, UK). Pitch Finalist.

Awards

2015	NVRB Klaas Breur Travel Award (Utrecht, The Netherlands)
2015	Fellowship for Hydra XI: European Summer School on Stem Cells & Regenerative Medicine (Hydra, Greece).
2018	EMBO|EMBL Symposium Travel Grant 2018 (Heidelberg, Germany)

List of Publications

Nanduri L.S, Baanstra M, Faber H, **Rocchi C**, Zwart E, de Haan G, van Os R, Coppes R.P. Purification and ex-vivo expansion of fully functional salivary gland stem cells. **Stem Cell Reports** 2014 3(6):957-64

Maimets M, **Rocchi C**, Bron R, Pringle S, Kuipers J, Giepmans BN, Vries RG, Clevers H, de Haan G, van Os R, Coppes RP. Long-Term In Vitro Expansion of Salivary Gland Stem Cells Driven by Wnt Signals. **Stem Cell Reports** 2016 6(1):150-62

Mauthe M, Orhon I *, **Rocchi C***, Zhou X*, Luhr M, Hijlkema KL, Coppes RP, Engedal N, Mari M, Reggiori F. Chloroquine inhibits autophagic flux by decresing autophagosome-lysosome fusion. **Autophagy** 2018 14(8):1435-1455 (* equal contribution)

Rocchi C and Emmerson E. Mouth-Watering Results: Clinical Need, Current Approaches, and Future Directions for Salivary Gland Regeneration. **Trends Molecular Medicine** 2020 May 1;S1471-4914(20)30089-7.

Rocchi C, Barazzuol L, Coppes R.P. The evolving definition of salivary gland stem cells. **npj Regenerative Medicine** 6, 4 (2021)

Orhon I., **Rocchi C**., Villarejo-Zori B., Serrano Martinez P., Baanstra M., Brouwer U., Boya P., Coppes RP.,Reggiorl F.Autophagy induction during stem cell activation plays a key role in salivary gland self-renewal. **Autophagy** 2021 *(in press)*